THE EFFECTS OF IONISING RADIATION ON POLYPROPYLENE

GRAHAM F. BODEN M.Sc.

A thesis submitted for the degree of Doctor of Philosophy of the University of Aston in Birmingham.

JULY 1973

S U M M A R Y

The interaction of ionising radiation with polymers is described and the literature relating to the effects on polypropylene is reviewed. Oxidative and free radical reactions are discussed with particular reference to post-irradiation effects.

Isotactic and atactic polypropylene were γ and electron irradiated to doses of up to 20 megarad. Irradiations were mainly made in air. A series of other polymers were also irradiated in a preliminary survey.

Molar mass measurements are used to measure the radiation yield for chain scission G (s). Irradiation at room temperature causes significantly more chain scission than at 195 K. Additional chain scission occurs on storage following irradiation at 195 K.

Free radical concentrations are determined by electron spin resonance, and the decay rates measured. The radical formed in air is a peroxy radical and in vacuo is a hydrocarbon radical. At 77 K in vacuo the radical is $- CH_2 - C^{\bullet} (CH_3) - CH_2 -$ but additional radicals are produced on warming to room temperature. The effects of increasing temperature on radicals formed in air are described. Electron spin resonance studies on atactic polypropylene, and isotactic polypropylene in hydrogen, sulphur dioxide and nitric oxide are reported.

The melting temperatures, spherulite growth rates, and isothermal crystallisation rates of irradiated polypropylene are compared to those of the non-irradiated polymer. Crystallisation is found to proceed with an Avrami integer n = 2. At a given

crystallisation temperature, the overall crystallisation rate of irradiated polymer is less than the non-irradiated, but spherulite growth rates are identical.

Thermogravimetric analysis is used to assess the thermal stability of irradiated polypropylene in nitrogen, air and oxygen. Hydroperoxide analysis is used to show that several molecules of oxygen are absorbed for each initial radical, and that hydroperoxides continue to be formed for a long period following irradiation.

Possible solutions for minimising irradiation and post-irradiation degradation are suggested, together with some problems for further study.

I N D E X

INTRODUCTION TO THE PROBLEM

High energy radiation, at relatively low doses, is widely used as a method of sterilisation of medical equipment and supplies. The irradiation in air of disposable syringes made from unstabilised polypropylene has caused problems of embrittlement which become more serious on storage. For this reason an examination of the effects of electron and γ-radiation on polypropylene with and without air was carried out.

The irradiation of polypropylene in vacuo has been studied quite widely, but relatively few studies of the irradiation effects in air have been made. In addition, little has been published on the effects of radiation on the crystallisation process and thermal stability of polypropylene.

The work described in this thesis has mainly concentrated on changes that may be described as post-irradiation effects. To minimise the effects of diffusion-controlled reactions, most studies have been made using polypropylene in the form of finely divided powder, although work on solid polypropylene is also described. The main physical properties chosen for investigation were, molar mass, the formation of free radicals and measurement of their concentrations, melting points and crystallinity, and thermal stability.

CHAPTER ONE : INTRODUCTION

1.1 High Energy Radiation.

High energy radiation causes ionising effects in materials and is often termed ionising radiation. Radiation chemistry is the study of the chemical effects caused by such radiation. In contrast, photochemistry is concerned with the chemical effects of visible and ultra-violet radiation of much lower energy, insufficient to cause general ionisation.

1.1.1 Sources and Characteristics of High Energy Radiation

(i) Electromagnetic Radiation

X-radiation is electromagnetic radiation similar to light, but of shorter wavelength (< 5 nm) and higher energy (> 25 MJ mol^{-1} or > 10 keV). X-radiation was used for much of the earlier studies in radiation chemistry but suffers from low penetration, low dose rates, a range of energies and imprecise doses. X-radiation is produced from machine sources in which a stream of electrons bombards a target material from which the rays emanate.

γ-radiation is of even shorter wavelength and greater energy (typically >1 MeV) than x-radiation. γ-rays are produced from radioactive disintegrations and are either monoenergetic or have a limited number of discrete energies. γ-rays do not have a finite limit of penetration but the intensity decreases logarithmically within the material irradiated. The penetration of electromagnetic radiation and neutrons is characterised by a half-value thickness (hvt)

which is the thickness of material that reduces the radiation intensity by 50%. For γ-rays from a cobalt-60 source the hvt in water is 10 cm and 70m in air. Cobalt-60 is a convenient source that can be used with suitable shielding to provide high dose rates. The physical arrangement of isotope radiation sources are of various types. For small-scale work, a lead-shielded well-type source is used in which cobalt-60 rods are arranged around a cylindrical cavity into which the sample is introduced. Where more space is required a concrete room or cave is constructed around the retractable source, with labyrinth access to minimise the escape of stray radiation. Another method uses spent nuclear fuel rods stored at the bottom of a deep pond containing water, which acts as the shielding. The samples are lowered into the pond in water-tight containers.

(ii) Charged Particles.

Charged particles, other than electrons, have only a small and finite range of penetration into materials. Thus the range of 1 MeV accelerated protons is approximately 0.02 mm in water whilethat of α-particles is even less. For this reason heavy charged particles are not widely used in radiation studies.

High energy electrons can be obtained from isotope or machine sources. Electrons from radioactive decay are called β-particles or β-radiation and have a distribution of energies up to a characteristic maximum energy. Strontium-90 is a widely used source of β-radiation but for bulk irradiation, the energy and intensity are too small and machine sources are preferred.

The Van de Graaff generator is a convenient source of high-energy and high intensity electron beams. This source is constructed with a moving belt to transfer the charge from a low-voltage supply to an insulated hollow spherical electrode. A potential of up to 20 MV can be built up and used to produce a focussed beam of mono-energetic electrons by means of an accelerating tube along which the potential is regularly decreased. Other machine sources, including the betatron, cyclotron, synchrotron and linear accelerators have been developed for very high energy studies but are extremely expensive and not readily available.

(iii) Neutrons

Neutron-irradiation produces quite different effects from the previous types of high-energy radiation considered. Since they are uncharged, neutrons interact by direct collision with atomic nuclei. Neutron-irradiation frequently induces radioactivity in the samples, whereas electromagnetic and electron-irradiation of less than 1.56 MeV never causes this. Because of this potential radiation hazard and the complex chemical effects produced, neutron-irradiation is not suitable for basic studies.

1.1.2 Historical

Radiation chemical effects were first observed by Roentgen[1] in 1895 and Becquerel[2] in 1896, by exposing photographic plates to x-rays and natural radioactivity respectively. Amongst other early studies Mund[3] showed that polymerisation could be initiated with high energy radiation. A rapid development of interest in

radiation chemistry occurred during and after the Second World War when the first nuclear reactors and accelerating machines were developed. Techniques of observation of the reactive species produced also developed rapidly at this time.

Early studies of the effects of radiation on polymers were initiated by the work of Dole and Rose[4] in 1948 on low density polyethylene. In 1952, Charlesby and co-workers[5] published the first of many important papers [6] on radiation polymer chemistry since which time there has been an accelerating interest in this field.

1.1.3 Definitions and Units

The amount of energy absorbed by a system is referred to as the dose. The unit of radiation dose is the rad, which corresponds to the absorption of 10 μJ per gram of material irradiated. For solids, irradiation doses are usually given in megarads (M rad) corresponding to 10 J g^{-1} . The unit of radiation exposure, the roentgen (R), is the amount of incident radiation which produces a total of 2.58×10^{-4} coulomb of electrical charge on all the ions of one sign in one kilogram of air.

The radiation chemical yield is expressed as a G-value. This is the number of molecules changed for each 16×10^{-18} J (100 eV) of radiation energy absorbed by the system. In radiation chemistry the electron volt (eV) is commonly used as a unit of energy. It is the amount of energy possessed by an electron accelerated by a potential of 1 volt. Since the charge on an electron is (approx.)

1.6×10^{-19} C,

$$1 \text{ eV} = 1.6 \times 10^{-19} \text{ J}$$

Other conversions are

$$1 \text{ eV} = 96.49 \text{ kJ mol}^{-1}$$

$$1 \text{ rad} = 6.24 \times 10^{13} \text{ eV g}^{-1}$$

1.2 Interaction of Radiation with Matter

The following outline of the interaction of radiation with matter, is restricted to the effects of moderately energetic γ-rays and electrons, on condensed organic systems, in particular on solid polymers. For this purpose, changes in the nuclear structure and in ionic and gaseous systems will be excluded.

1.2.1 Comparison of Electrons and γ-rays

The first stage in the production of chemical effects by high energy radiation is the interaction with the orbital electrons of the substrate. If the radiation is an electron beam, the primary electron is deviated and the bound electron either gains sufficient energy to leave its parent molecule completely (ionisation) or is excited to a higher energy level (excitation) :

$$A \longrightarrow A^{\cdot +} + e^{-} \quad \text{(Ionisation)} \quad \text{(See footnote)}$$

in which $A^{\cdot +}$ is the parent radical ion.

$$A \longrightarrow A^{*} \quad \text{(Excitation)}$$

The loss of energy of γ-radiation in passing through matter is mainly caused through collision with the orbital electrons (Compton effect) or by absorption (photoelectric effect).

The Compton effect is the main process by which 1 MeV γ-photons lose energy. In this process part of the photon energy is used to eject an orbital electron with considerable kinetic energy. The rest

---

Footnote: $\longrightarrow$ represents the action of a high energy photon or electron

of the energy continues in the scattered photon which now has lower energy and longer wavelength. The ejected electron can have energies ranging from 0 to $2h\nu / (mc^2 + 2h\nu)$ of the energy of the incident photon, where $h\nu$ is the energy of the photon and mc^2 is the rest energy of the electron. The average energy of the electron is approximately half the maximum energy. The average energy fraction transferred to the electron is 40% for a 1 MeV photon, 24% for a 0.5 MeV photon and 14% for a 0.1 MeV photon.

The photoelectric effect becomes important at energies below 60 keV. All the energy of the photon is used in ejecting an electron, usually from an inner (K) shell. The energy of the electron equals that of the incident photon, less the binding energy of the electron which is usually only a few hundred electron volts. The filling of the vacant inner orbital from an outer orbital provides further energy, either in the form of x-ray emission or by ejection of a further electron (Auger effect).

The passage of a γ-photon through a substance thus gives rise to a number of electrons of fairly high energy which can also produce the effects of ionisation and excitation as already stated for an incident electron beam. γ-rays may therefore be considered as internal sources of electron irradiation, and in many systems the effects of both types of radiation are indistinguishable for a given dose.

1.2.2 Ionisation, Excitation and Free Radical Formation

The probability of ionisation (and excitation) depends on the velocity of the electron and increases rapidly as the electron slows down towards the end of its path. For each ionisation

probably two or more groups are excited to non-ionic excited states.

The secondary electron ejected during ionisation is known as as a δ-electron. The number of δ-electrons is considerably greater than the number in the incident beam (perhaps as many as ten for each incident electron). The δ-electron is estimated [7] to have an average energy of about 75 eV and a mean path of about 100 nm. Because of its relatively low velocity the δ-electron causes many more ionisations per unit path length than does the incident electron. During the first 3 nm radius, called a spur, the secondary electron will probably create 2 or 3 ion-pairs and 4 or 5 electronically excited species. The time scale for these events is about 10^{-15} second but within about 10^{-13} second the energy of the electron is less than about 0.025 eV (2.4 kJ mol^{-1}) and it is attracted back to a positive radical ion :

$$A^{\bullet +} + e^{-} = A^{*}$$

This releases an amount of energy equal to the ionisation energy which leaves the polymer in an energy-rich condition from which further reaction may ensue. The probability of escape of the ejected electron from the field of its parent ion is fairly low in condensed organic media because of their relatively low dielectric constant. Probably 97% of the ejected electrons are recaptured by the parent ion as measured by the radiation yield of electrons[8]. The return of the electron may be delayed by the presence of electron traps, such as double bonds. The lifetime of ionic or excited states is usually very brief and such species are not normally involved in post-irradiation effects.

Free radicals, species containing an unpaired electron, are produced in polymers and take part in reactions both during and following irradiation. They may be produced from neutral molecules, ions and excited species. Radical reactions tend to be unselective and form a mixture of products. Abstraction reactions frequently occur, producing a new radical capable of repeating the reaction, i.e. cause a chain reaction. Many free radicals react readily with oxygen to form peroxy radicals

$$R^{\bullet} + O_2 \longrightarrow RO_2^{\bullet}$$

Free radicals are normally removed from a system by combination or disproportionation reactions.

1.2.3 Radiolysis of Alkanes

As an example of the effect of high energy radiation on a specific system, the behaviour of liquid n-hexane may be considered. The products resulting from this system are given in table 1.1. This system was chosen by Dewhurst[9] and is suitable as a model for the behaviour of polymers such as polyethylene and polypropylene.

Kevan and Libby[10] found the dimerisation products to be n-dodecane (resulting from 1.1 combination), 5-methyl undecane (1,2 combination), 5,6-dimethyl decane (2,2), 4-ethyl 5-methyl nonane (2,3), and 4,5-diethyl octane (3,3).

Similar behaviour is found with other condensed alkanes and in general the main effects are found to be:

1) production of H_2,
2) formation of dimers,
3) production of fragments from C_1 to C_n and combination of these fragments,
4) unsaturation.

TABLE 1.1

Radiolysis Products of Liquid n-hexane C_6H_{14}

Product	G-value
H_2	5.0
CH_4	0.1
C_2H_4	0.3
C_2H_6	0.3
C_3H_6	0.1
C_3H_8	0.4
C_4H_{10}	0.5
C_5H_{12}	0.3
C_6H_{12}	1.2
C_7	0.2
C_8	0.5
C_9	0.5
C_{10}	0.4
C_{12}	2.0

The radiation behaviour can be explained by either radical or ionic reactions, and studies of the effects of both free radical and ionic scavengers[11] indicate that both mechanisms are involved. Radical reactions are to be expected because of the small (3%) escape of electrons from the parent ion. However, the time interval before electron-parent ion recombination (10^{-7} second) is sufficient for ion-molecule reactions to occur and products of radiolysis are frequently found to correlate more closely with bond strengths measured on ions by mass spectrometry, than with those obtained from thermal measurements.

Radical Reactions

$$RH \rightsquigarrow RH^{+\bullet} + e^- \rightarrow RH^{*} \rightarrow R^\bullet + H^\bullet$$
$$\searrow R^\bullet + R^\bullet$$

$$H^\bullet + H^\bullet \rightarrow H_2$$

$$R^\bullet + R'H \rightarrow RH + R'^\bullet$$

$$R^\bullet + R'^\bullet \rightarrow RR'$$

Unsaturated species may be produced by either disproportionation or by elimination of molecular hydrogen as a primary process.

$$C_2H_5^\bullet + C_6H_{13}^\bullet \rightarrow C_2H_4 + C_6H_{14}$$

$$C_6H_{14} \rightsquigarrow C_6H_{12} + H_2$$

Ionic Reactions

$$C_6H_{14}^{+\bullet} \rightarrow C_2H_5^+ + C_2H_4 + C_2H_5^\bullet$$

$$C_6H_{14}^{+\bullet} \rightarrow C_4H_8 + C_2H_6$$

$$C_6H_{14}^{+\bullet} \rightarrow C_6H_{12}^{+\bullet} + H_2$$

Other ion-molecule reactions involve transfer of atomic hydrogen, molecular hydrogen and protons.

In long-chain linear hydrocarbons such as dodecane, it is found[12] that C-C scission is favoured 2 to 4 atoms from the chain end, and it is also found that branched chains are more readily ruptured than linear ones, since tertiary C atoms appear to be particularly sensitive to radiation.

1.2.4 Summary of Chemical Events Observed in Polymers

The chief effects of high energy radiation on polymers, during and post-irradiation, can be categorised as degradation, cross-link formation, unsaturation, free radical effects and changes in physical structure and properties.

Degradation

1) Chain degradation (scission).

2) Production of hydrogen and other molecular fragments.

3) Surface oxidation in the presence of air.

4) Peroxide and hydroperoxide formation.

Cross-link Formation

1) Formation of intermolecular cross-links.

2) Formation of intramolecular cross-links (rings).

3) Formation of insoluble gel.

Unsaturation

1) Production of vinyl and vinylene saturation.

2) Formation of conjugated double bond sequences.

3) Decay of unsaturation.

Free Radicals

1) Formation and decay of trapped free radicals.

2) Isomerisation of radicals.

3) Isotope exchange with deuterium and back reaction with molecular hydrogen.

4) Surface polymerisation (graft) in the presence of monomers.

Physical Structure and Properties

1) Reduction of crystallinity.

2) Change in crystallisation rate from the melt.

3) Change in properties such as viscosity, tensile strength, electrical conductivity and colour.

Some effects are not readily categorised, and include the phenomenon of oxy-luminescence and energy transfer processes within the polymer or involving additives. Chain scission, cross-linking and oxidation probably have the most important consequences on the

properties of the irradiated polymer and these will be considered in more detail in the following sections.

1.2.5 Chain Scission

Some polymers show a progressive decrease in molar mass after high energy irradiation. This is due to the permanent fracture of the main chain with a rearrangement of the atoms near the point of fracture to stabilise the end groups, usually accompanied by the liberation of small molecular species. It is probable that the majority of chain scissions are temporary, because the long chain fragments are held in place by the solid polymer matrix. Chain scission is essentially different from thermal depolymerisation which proceeds by a chain mechanism. In radiation degradation absorption of energy is equally likely at any of the repeat units of the chain, and normally each unit is equally likely to fracture. In radiation degradation there is little monomer produced even after high doses.

The probability of the C-C bond reforming does however appear to be related to the heat of polymerisation. Wall[13] has shown that in polymers having heats of polymerisation in excess of 70 kJ mol^{-1}, such as polyethylene, poly(methyl acrylate), polyacrylic acid and polystyrene, cross-linking predominates. Polymers with lower heats of polymerisation such as poly (α-methyl styrene), polyisobutylene poly(methyl methacrylate) and polymethacrylic acid, chiefly degrade as a result of irradiation. Polypropylene with a heat of polymerisation of 69 kJ mol^{-1}, takes part in both cross-linking and chain scission processes.

The G-values for chain scission, G(s), can be obtained from molar mass determinations, if the fracture density is proportional to the dose. Charlesby[14] has derived the relationship :

$$\frac{1}{\bar{M}_n} = \frac{1}{\bar{M}_n^o} + \frac{R\,G(s)}{100\,N_a} \qquad \ldots\ldots (1.1)$$

in which $\bar{M}_n$ and $\bar{M}_n^o$ are the number average molar masses before and after irradiation. R is the dose in eV g^{-1} and N_a is Avogadro's constant. Alternatively :

$$\frac{1}{\bar{M}_n} = \frac{1}{\bar{M}_n^o} + 1.04 \times 10^{-6}\, r\, G(S) \qquad \ldots\ldots (1.2)$$

where r is the dose expressed in megarad. In the absence of cross-linking, plots of $1/\bar{M}_n$ vs. dose normally give a straight line from the slope of which, G (s) may be found. In general only number-average molar masses may be used in equation 1.1 and plots derived from it. However, if the distribution was originally a random one, then further random scission will maintain a random distribution and other average values of molar mass, such as viscosity-average $\bar{M}_v$ and weight-average $\bar{M}_w$ are applicable since their ratios to $\bar{M}_n$ will maintain cnstant values. For non-random initial distributions, plots of $1/\bar{M}_v$ and $1/\bar{M}_w$ vs. dose are curved at low doses, but it is found [6] that the distribution approaches a random one when as few as 4 or 5 fractures in each intial molecule have occurred. This explains the approach to linearity of such plots at higher doses.

1.2.6 Cross-Linking

Cross-linking feactions lead to the formation of three-dimensional molecular networks and these can be investigated by changes in molar mass, solubility, swelling and mechanical properties. Some of the reactions leading to the formation of cross-linked structures include :

Free Radical Combination

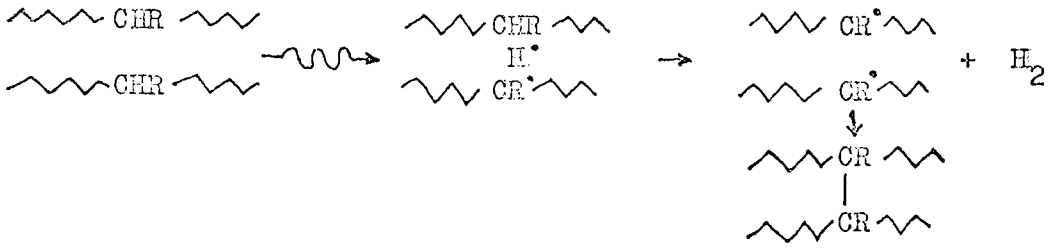

The crosslinking reaction may involve migration of the radical along the polymer chain until it is adjacent to another radical where it reacts. The extent of crosslinking is frequently increased by annealing after irradiation, which suggests that radical migration is taking place.

Ion Molecule Reactions

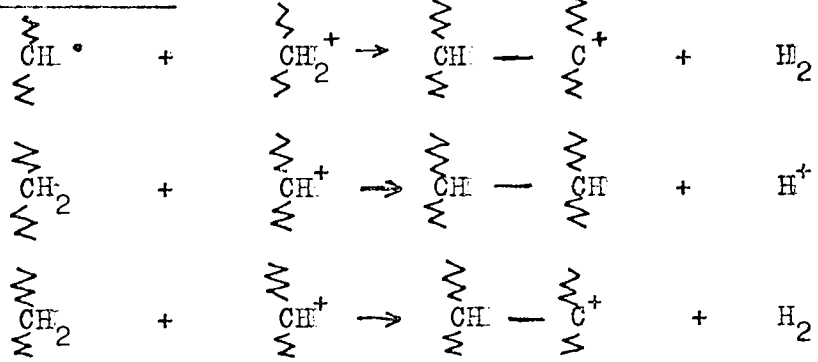

The first of these reactions is very favourable energetically[15].

Crosslinking Through Double Bonds

This may be through either vinylene

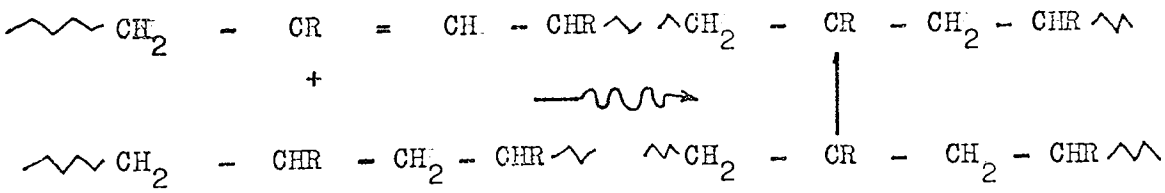

or vinylidene unsaturation

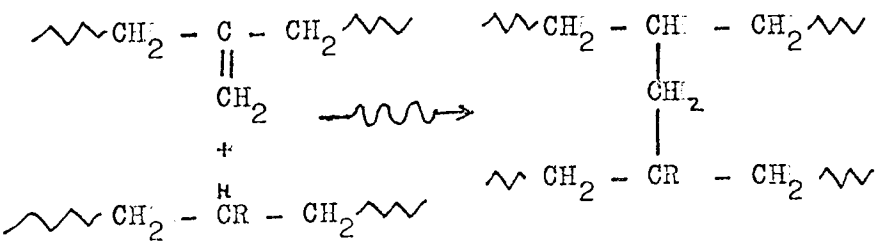

In polyethylene however, more unsaturation is destroyed than cross-links formed (the respective G-values being 3.7 and 0.8)[16]. The reason for this may be the formation of intra-molecular crosslinks.

The fundamental theory of crosslinking of polymers by irradiation is similar to that of crosslinked systems formed by polymerisation, and the statistical consequences have been developed by Charlesby[6]. The extent of crosslinking in a polymer is measured by $\overline{M}_c$, the number-average molar mass between crosslinks and this may be related to the G-value for crosslinking G(x) by the relationship :

$$\overline{M}_c = \frac{0.48 \times 10^6}{G(x)\ r} \qquad \ldots\ldots (1.3)$$

in which r is the dose in megarad. $\overline{M}_c$ determines the elastic and swelling characteristics of the crosslinked network, from which G(x) may be found. The crosslink yield may also be found from the dose that causes the onset of partial insolubility, the gel-formation dose.

1.2.7 Simultaneous Chain Scission and Crosslinking

In polypropylene crosslinking is normally accompanied by chain scission and it is found that at low doses the effects of scission are predominant. The degradation may be considered to occur in two stages:

1. scission without crosslinking,
2. crosslinking without scission.

Also in the presence of oxygen, crosslinking processes are interrupted and degradation alone is observed.

Charlesby and Pinner[17] have derived a relationship which enables the calculation of G(x) and G(s) from gel measurements when

both processes occur simultaneously :

$$S + S^{\frac{1}{2}} = \frac{G(s)}{2G(x)} + \frac{0.48 \times 10^6}{r \bar{M}_n G(x)} \quad \ldots\ldots (1.4)$$

in which S is the soluble fraction of polymer of intial number-average molarmass $\bar{M}_n$ after a dose of r megarad This equation assumes :

1. an intially random molar mass distribution,
2. random crosslinking and degradation,
3. constant values of G(s) and G(x) with dose.

From equation 1.4 plots of $S + S^{\frac{1}{2}}$ vs. $1/r$ should yield a straight line with an intercept of $G(s)/2G(x)$. For non-random initial distributions the plots are curved, but equation 1.4 is found to apply at high doses, suggesting that random distributions of molar mass are eventually produced. Exact modifications of the Charlesby-Pinner equation have been derived for various initial distributions by Inokuti[18]. For polymers of uncertain distribution the ratio $G(s)/2G(x)$ can be accurately established although the individual radiation yields may be uncertain.

1.2.8 Irradiation in Oxygen

The photochemical and thermal oxidation of hydrocarbons has been reviewed widely [19, 20, 21] and the most generally accepted mechanism is one originally proposed by Bolland[22]. High energy radiation in the presence of oxygen initiates a similar process in many hydrocarbon polymers. The detailed mechanism varies with each polymer and in addition, diffusion and matrix processes for solid polymers may become rate-determining, particularly in radical transfer and termination processes.

The basic mechanism is as follows :

Initiation

$$RH \xrightarrow{\sim\sim} R^{\bullet} + H^{\bullet}$$

Propagation

$$R^{\bullet} + O_2 \longrightarrow RO_2^{\bullet}$$

$$RO_2^{\bullet} + RH \longrightarrow ROOH + R^{\bullet}$$

Termination

$$RO_2^{\bullet} + RO_2^{\bullet} \longrightarrow RO_2R + O_2$$

$$RO_2^{\bullet} + R^{\bullet} \longrightarrow ROOR$$

$$RO_2^{\bullet} + H^{\bullet} \longrightarrow ROOH$$

$$R^{\bullet} + R^{\bullet} \longrightarrow RR$$

In addition the hydroperoxides may decompose

$$ROOH \longrightarrow RO^{\bullet} + OH^{\bullet}$$

$$ROOH + RH \longrightarrow RO^{\bullet} + H_2O + R^{\bullet}$$

and the radicals formed can initiate chain branching

$$RO^{\bullet} + RH \longrightarrow ROH + R^{\bullet}$$

$$HO^{\bullet} + RH \longrightarrow HOH + R^{\bullet}$$

A number of volatile reaction products are usually observed, such as H_2O, CO_2, aldehydes and ketones, while C=O and OH groups appear in the spectrum of the polymer when it is irradiated in oxygen. These products result from the decomposition of peroxy compounds and some of their reactions include :

$$R - \underset{\underset{O_2^{\bullet}}{|}}{CH} - R' \longrightarrow R - \underset{\underset{O}{\|}}{C} - R' + OH^{\bullet}$$

$$R - \underset{\underset{O_2^{\bullet}}{|}}{CH} - R' + R'' - \underset{\underset{O_2^{\bullet}}{|}}{CH} - R''' \longrightarrow RR'C{=}O + R'' - \underset{\underset{OH}{|}}{CH} - R''' + O_2$$

$$R - \underset{\underset{O_2H}{|}}{CH} - R' \longrightarrow R - \underset{\underset{O}{\|}}{C} - R' + H_2O$$

$$R - \underset{\underset{OOH}{|}}{CH} - CH_2 - R' \longrightarrow RCHO + R'CH_2OH$$

The latter reaction accounts for some of the additional chain scission observed in oxidative degradation.

The radical $HO_2^{\bullet}$ may play an important part in oxidative reaction and could arise from

$$RH + O_2 \longrightarrow R^{\bullet} + HO_2^{\bullet}$$

or by $RH + O_3 \longrightarrow RO^{\bullet} + HO_2^{\bullet}$

since ozone is produced by the irradiation of oxygen.

Radiation oxidative degradation has been studies by mass spectroscopic studies of the decomposition fragments, infra-red spectroscopy, oxygen absorption and molar mass determinations. Oxidation ractions also occur when the irradiation is carried out in vacuo and the polymer is then exposed to air or oxygen.

1.3 Irradiation of Polypropylene and Related Polymers

1.3.1 Molecular Structure

In general vinyl polymers, in which each carbon atom of the main chain carries at least one hydrogen atom, such as polyethylene or polystyrene, tend to crosslink when irradiated. Polymers containing tetra-substituted carbon atoms, such as poly (methyl methacrylate) or polyisobutylene tend to degrade[23]. Polypropylene is found to be intermediate in behaviour, and both degradation and crosslinking

take place.

(i) Scission and Crosslinking

Black and Lyons[24] have observed a progressive decrease of intrinsic viscosity $[\eta]$ up to a gel-formation dose of 50 Mrad. When polypropylene is irradiated to doses above this, crosslinking predominates over scission to a small extent. Similar behaviour has been observed by other workers and Table 1.2 summarises the values of G(s) and G(x) reported. The most likely value for G(s)/2G(x) appears to be 0.75 for isotactic and 0.37for atactic polypropylene.

Veselovskiii et al.[37] have investigated the cause of the divergencies in G(x) and G(s) values and gel-formation doses found by different authors,and they have shown that the irradiation behaviour depends on the molar mass, the mobility of the chain segments, vinylidene double-bond and oxygen content,and the physical state of the polymer. The gel-formation dose is least for polymers of high initial molar mass; thus, a sample of $[\eta]$ = 2.2 had a gel-dose of 100 Mrad while one of $[\eta]$ = 5.3 required only 6.5 Mrad. Between these extremes there is a regular decrease in gel-dose as the molar mass increases.

The results of Black and Lyons[38] using an isotactic polymer of initially random molar mass distribution, show that a rapid decrease in molar mass(G(s) = 4.95) occurs at low doses. The molar masses were measured by intrinsic viscosities and the number of chain breaks calculated assuming random scission.

Equation 1.2 ought to apply under these conditions when $\overline{M}_n$ is replaced by $\overline{M}_v$, giving a linear plot of $1/\overline{M}_v$ vs. r. The authors however,obtained a linear plot between $1/\overline{M}_v$ and $r^{\frac{1}{2}}$. Jellinek[39] has pointed out however, there is a change of slope at a dose of about 5 Mrad and that only below this dose is $1/\overline{M}_v$ linear with $r^{\frac{1}{2}}$. Above 10 Mrad $1/\overline{M}_v$ is linear with r. He suggests that in the early stages

Table 1.2

Scission and Crosslinking Yields in Polypropylene

Polymer I = Isotactic A = Atactic	Gel Dose / megarad	G(s)	G(x)	G(s)/2G(x)	Reference
I	50	0.96	0.6	0.75	24
I	–	1.0	1.3	0.40	25
I	–	0.28	0.14	1.0	26
I	15	0.10(min) 0.21(max)	0.07(min) 0.14(max)	0.73	27
A	14	0.10(min) 0.24(max)	0.12(min) 0.27(max)	0.44	27
A	30	0.30	0.19	0.80	28
I	10	0.62	0.50	0.62	29
I	–	0.17	0.11	0.78	30
I	–	0.32	0.20	0.80	31
I	–	1.20	0.80	0.75	31
I(quenched)	–	0.10	0.061	0.8	32
I(annealed)	–	0.16	0.11	0.7	32
I	14	0.17	0.16	0.55	33
A	28	0.13	0.17	0.37	33
I (α-rad.)	25	0.73	0.50	0.73	34
I (α-rad.)	25	0.55	0.31	0.90	34
I	–	–	–	0.75	35
A	–	–	–	0.40	35
I(annealed)	25	–	–	0.75	36
I(quenched)	18	–	–	0.43	36

of degradation random scission is predominant, but at later stages scission and crosslinking occur simultaneously but compensate one another.

Schnabel and Dole[27] found that although G(s)/2G(x) values were between 0.45 and 0.75 an intial decrease in $\overline{M}_v$ occurred. The analysis of their results was complicated by starting with an initially broad distribution of $\overline{M}_w/\overline{M}_n = 5$ but they calculated that this is reduced to a nearly random distribtution of $\overline{M}_w/\overline{M}_n = 2.7$ when 2 bond ruptures occur in each original chain. The range of values of G(s) and G(x) given them in Table 1.2 correspond to the assumption of random and pseudo-random distributions which would lead to respective maximum and minimum G-values.

The possible errors involved in using $[\eta]$ to characterise molar molar mass in polymers that may crosslink or branch has been pointed out by Dole et al.[40] and also by Salovey and Dammont[28] who, using atactic polypropylene obtained a decrease in $[\eta]$ while $\overline{M}_n$ was unaffected up to the gel-formation dose. Dole[41] has shown that if A represents the change of $[\eta]$ with dose then it can be shown that

$$A = \frac{a}{b}\frac{db}{dr} + \ln \overline{M}_w \frac{da}{dr} + \frac{a\overline{M}_w}{N_a}\left\{q - \frac{p}{b}\right\} \quad ...(1.5)$$

where $b = \overline{M}_w/\overline{M}_n$ (initial), a is the exponent of the Mark-Houwink equation, while q and p are the probabilities of crosslinking and scission. Thus a negative value of A may occur from negative $\frac{db}{dr}$ and $\frac{da}{dr}$ values as well as resulting from p/b exceeding q.

Keyser, Clegg and Dole[40] have investigated the intrinsic viscosities of isotactic and atactic polypropylene as a function of radiation dose and found the relationship:

$$\ln [\eta]_r / [\eta]_o = Ar^{\frac{1}{2}} + Br \quad \ldots\ldots\ldots \quad 1.6$$

in which $[\eta]_o$ and $[\eta]_r$ are the intrinsic viscosities before and after irradiation, and A and B are empirical constants. Such a relationship can be derived from theoretical principles. For atactic polypropylene B=0 but is found to be -8×10^{-16} for the isotactic polymer. When $1/[\eta]_r$ is plotted vs. r straight lines are found at low doses. At higher doses the slopes decrease and then become linear again before gelation. The initially rapid decrease in molar mass may be caused by the presence of weak bonds in the polymer, or may result from the initially broad distribution.

The G(s) and G(x) values given in Table 1.2 are based on the assumption that they are constant throughout the irradiation. This is probably true at doses higher than the gel-point, but at lower doses may not be correct.

Keyser, Clegg and Dole[40] have obtained an apparent intial value of G(s) = 1.2 which drops to 0.27 at the gel dose, while the G(x) value was found to be constant at 0.18. Black and Lyons[38] have also suggested that scission and crosslinking are not directly proportional to dose but that scission is initially high and tends to decrease, while the reverse is true for crosslinking. This is attributed to competitive reactions in which radiolytically formed unsaturated species produce end-links and cross-links with excited or ionised species which would otherwise cause main chain fracture. Lyons[42] has suggested that under these conditions the Charlesby-Pinner relationship (equation 1.4) should be replaced by the empirical relationship

$$s + s^{\frac{1}{2}} = kr^{-k} \quad \ldots\ldots (1.7)$$

Using existing data, he has found that the values of k between 0.4 and 0.6 give a substantial improvement to the linearity of the

of the appropriate plots. Marans and Zapas[43] however, have used polypropylenes of various molar mass distribution and found that G(s) and G(x) values are constant, and that the apparent variations are due to distribution changes.

Influence of Physical State

The lower G(s)/2G(x) ratio in atactic polypropylene compared to isotactic, shows that more crosslinking occurs in the amorphous state. An increase in the extent of crosslinking occurs in isotactic polypropylene, if it is heated after irradiation[32] or is irradiated just below the melting point[44, 45]. Sobue and Tajima[32] found thatthe percentage gel increased from 0% to 34% after 13 Mrad, as a result of heating to 453K, following irradiation at 298 K. Isotactic polymers of high crystallinity, as a result of pre-irradiation annealing, gave larger G(s)/2G(x) ratios and gel-formation doses, than quenched samples of low crystallinity[36]. In contrast, Charlesby, Von Arnim and Callaghan[46], found the G(x) values of polyethylene to be unaffected by the degree of crystallinity.

(ii) Unsaturation

Following irradiation, the infra-red spectra of polypropylene show new absorption bands. Absorption at 886 cm^{-1} and 1642 cm^{-1} has been reported by Black and Lyons[38] and confirmed by Slovhokotova[47] and Sobue[48]. These bands are considered to be caused by the vinylidene group, which appears to be the main change in the infra-red spectrum, particularly at low doses. Slovhokotova also reports an absorption band at 735-740 cm^{-1} due to propyl branches, and she and Black and Lyons suggest that the process taking place is

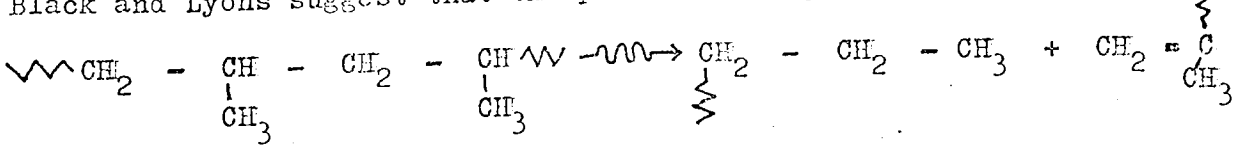

Infra-red measurments at temperatures high enough (438 - 453 K) to avoid crystalline absorption bands, have enabled Black and Lyons to calculate a one-to-one scission to vinylidene group ratio. These results have been questioned by Dole and co-workers, but Slovhokhotova has found equal concentrations of propyl and vinylidene groups in atactic polypropylene, while in isotactic the lower proportion of vinylidene groups is explained by a partial disappearance as a result of free radical reaction.

The vinylidene group is considered by Veselovskii et al.[37] to play a fundamental part in the crosslinking process. They have shown that if vinylidene bonds are present in polypropylene before irradiation the gel-formation dose is reduced. A sample was pyrolysed to produce vinylidene unsaturation and then irradiated. The gel-formation dose fell from 50 Mrad to 35 Mrad despite the reduction in $[\eta]$ from 3.25 to 1.17, which in itself would have caused an increase in the gel-dose.

Above 350 Mrad, Alexander, Black and Charlesby[50] report absorption at 910 cm^{-1} due to vinyl unsaturation. The reaction

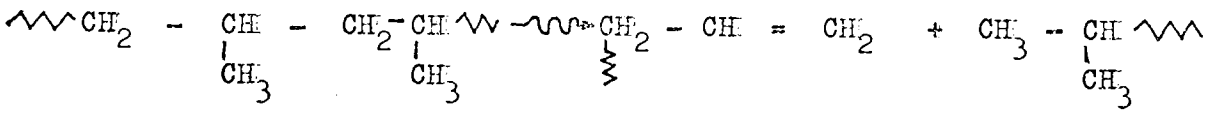

may occur infrequently. Unsaturation as a result of direct hydrogen removal may also be expected to occur. At high doses (> 1000 Mrad) conjugated sequences of double bonds have been observed.[47]

The irradiation of polypropylene produces hydrogen gas and Dole has suggested[49], based on the biradical theory of Schultz[51], that

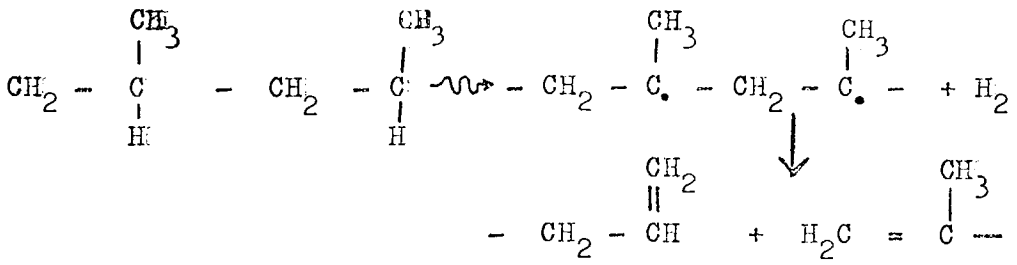

This reaction is however unlikely, since vinyl unsaturation is not

common.

An alternative mechanism has been proposed by Williams[52] based upon the decomposition of the primary ion formed :

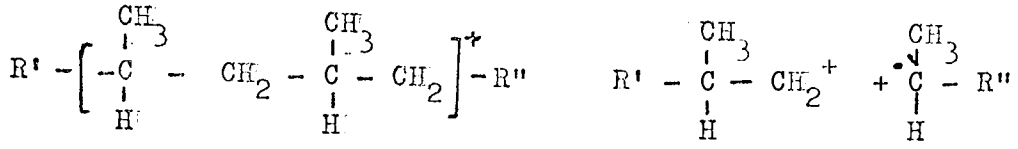

(A) (B)

The ionic fragment A then rearranges the more stable tert-butyl carbonium ion

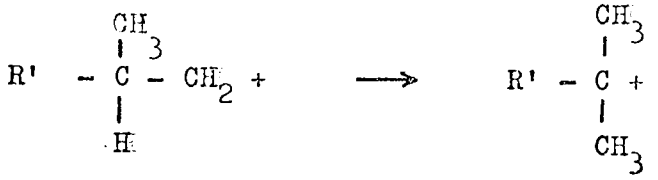

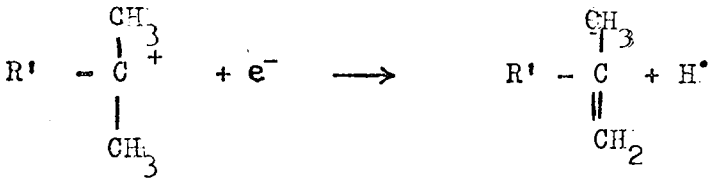

the hydrogen atom may then react with B, to produce a saturated species.

(iii) Gas Yields

The irradiation of polypropylene produces gases and Dole[49] has carried out analyses and radiation yields of the products. The main product is found to be hydrogen following γ-irradiation in vacuo. At room temperature, isotactic polypropylene produces 97.2% H_2 (G = 2.8) and 2.5% CH_4 (G = 0.07) and 0.3% of other hydrocarbons (ethane, propane and isobutane). Atactic polypropylene produces 95.7% H_2 (G = 2.3), 3.9% CH_4 (G = 0.10) and small amounts of ethane (0.1%). Irradiation at 77 K has little effect on the composition or yields of these gases.

The large excess of hydrogen partly results from its greater ability to leave the reaction site. There is a slightly greater yield of methane from the atactic polymer which reflects the increased mobility of the polymer matrix, allowing the gas to escape. The gas yields show that permanent scission occurs in the side branches as well as chain scission and dehydrogenation. The low yield of ethane suggests that methyl radicals, produced by C - CH_3 scission, abstract hydrogen from the polymer chains rather than combining with other methyl radicals. The gas yield from linear polyethylene is 99.7% H_2 (G = 3.8).

1.3.2 Free Radicals

Studies of the free radicals produced in polypropylene by high energy radiation have been reviewed by Campbell[53]. There is considerable disagreement over the radical structure and frequently mixtures of radicals have been observed [54 - 64]. There appear to be four main conclusions reached :

1. The radicals observed at low temperature is the alkyl radical R1; - CH_2 - $^{\bullet}C(CH_3)$ - CH_2 -
2. On warming theradical becomes more complex.
3. A quartet of lines of uncertain assignment is occasionally observed.
4. A broad singlet, probably due to a fairly stable polyenyl radical is found at high doses.

There appear to be two main interpretations of the room temperature spectrum of polypropylene.

(i) Fischer and Hellwege[59] have assigned the spectrum to an allyl radical R2;- CH_2 - $CH(CH_3)$ - $CH = C(CH_3)$ - $CH^{\bullet}$ - $CH(CH_3)$ - Measurements on orientated samples showed that those irradiated and

measured at low temperature, gave the same spectrum as the non-orientated sample and was assigned to R1. For $\theta = 0^{\circ}$ the spectrum was symmetrical with 17 equally spaced lines (10.5 G). For $\theta \neq 0^{\circ}$, a symmetrical spectrum of 7 equivalent (21G) lines with doublet substructure was found. The spectra were complicated by the presence of some peroxy radicals. Theoretical consideration of the allyl radical R2 showed that this anisotropy could be caused by this species. Milinchuk[65] has demonstrated the interconversion of radicals R1 and R2 both thermally and photochemically.

(ii) An alternative suggestion by Ayscough and Munari[66] is that the alkyl radical R1 is responsible for the room temperature as well as the low temperature spectrum.

They consider that the spectrum is due to 4 β protons equivalent in pairs, and asymmetric to the C - CH_3 bond. Evidence given for alkyl rather than allyl radicals is

(a) G values are much too high for allyl radicals (G = 1.0, while G = 0.1 for allyl radicals in polyethylene)

(b) The radical obtained is much less stable than the allyl radical in polyethylene

(c) The allyl radical CH_3 $CH^{\bullet}$ (CH_3) CH = CH (CH_3) $CH^{\bullet}$ CH_2 CH_3 obtained by irradiation of the model hydrocarbon 2,4 dimethyl hept - 3 - ene produced a very different spectrum.

Theoretical considerations shows also that the anisotropy and spin densities agree more closely with alkyl rather than allyl radicals. At high doses however the allyl radical is thought to be formed.

1.3.3. Radical Decay

The rate at which free radicals decay in polymer media has been the subject of recent reviews by Butyiagin[67]. The build-up and

decay of radicals in polypropylene is found to depend markedly on the physical state of the polymer. Ohnishi[57] and Loy[61] found that decay was faster in less crystalline samples. Milinchuk[63] has compared the kinetics of formation and decay in atactic and isotactic polypropylene. He found that at 77 K the radical concentration was nearly 10 times as large in the atactic polymer. At increasing temperature, the radical concentrations in each sample, were found to decrease but the relative rate in the atactic polymer was much more rapid, especially near the glass transition temperature 255 K. His data show a finite concentration of radicals in the atactic sample at room temperature, which suggests that it was partially crystalline. Milinchuk[63] and Forrestal and Hodgson[62] found on rapidly increasing the temperature of isotactic polypropylene irradiated at 77 K that 70% of the original radicals disappeared by 283 K. These radicals were probably heldin the amorphous regions of the polymer. Radical decay did not commence until 170 K. Nara et al [68] observed two regions of the second-order decay of the alkyl radical Rl; one commencing at 170 K with an activation energy of 70 kJ and another at 270 K with an activation energy of 210 kJ. He ascribed these observations to two different conformations of the radical and found that the decay constants were similar to those of dynamical studies of molecular motion in the polymer. Kusimoto [69] has studied the effects of temperature increase on irradiated atactic, syndiotactic and isotactic polypropylene. In each case he found that one radical producing a 6 - line spectrum, disappeared at 230 K. The radical in the atactic polymer disappeared completely at 263 K.

The decay of free radicals is normally a second order process, at least over a considerable part of the decay. Some authors [70] favour

interpretation by first-order kinetics, but usually the decay curve needs to be divided, somewhat arbitrarily, into several sections each with a different rate constant. Since two free radicals must meet for decay to occur, a first-order process is only likely under conditions where the radicals are not evenly distributed, as in the decay of radical pairs, or by reaction with photostimulation. The choice of first or second-order decay in polyethylene has been reviewed by Geymer and Wagner[71].

Klimshport et al.[72] have observed a stepwise decay of radicals in polypropylene, that is second-order in the absence of light, and first-order when light-stimulated. Stepwise decay has also been observed by Sohma[73] and Milinchuk and Pshezetshii[74] who found that the activation energy of decay increased from 21 kJ at 193 K, to 110 kJ at 323 K. Kusumoto[69] however, obtained second-order decay with a single activation energy for each polymer. He quotes the following parameters :

Atactic (259 K) $k_2 = 3.4 \times 10^{-1}$ dm^3 mol^{-1} s^{-1}; $E_A = 130$ kJ mol^{-1}

Isotactic (313 K) $k_2 = 1.1 \times 10^{-2}$ dm^3 mol^{-1} s^{-1} ; $E_A = 92$ kJ mol^{-1}

Syndiotactic (313 K) $k_2 = 3.0 \times 10^{-2}$ dm^3 mol^{-1} s^{-1} ; $E_A = 92$ kJ mol^{-1}

There are several theories that have been developed to account for free radical decay. In Waite's 'cage' theory[75] the radicals are considered to be constrained within an elementary structural volume, in which reaction takes place. At low diffusion rate and high reaction probability the radical decay rate is given by

$$\frac{-dC}{dt} = K_D \left(1 + \tau^{\frac{1}{2}} / t^{\frac{1}{2}} \right) C^2 \qquad \ldots\ldots (1.9)$$

where C is the radical concentration, K_D is the diffusion rate constant, τ is the fifetime of the radicals in the cage and t is the time.

Further : $$K_D = 4 \pi r_o D$$

and $$\tau = r_o^2 / \pi D$$

where D is the diffusion coefficient of the reacting species and r_o the effective cage radius.

Equation 1.9 is second-order with respect to concentration but has a time - dependent rate constant K_{Dt}

$$K_{Dt} = 4 \pi r_o D \left[1 + \left(r_o^2 / \pi D \right)^{\frac{1}{2}} t^{-\frac{1}{2}} \right] \ldots\ldots (1.10)$$

Thus the rate constant is initially high, but decreases to a constant value when $t \gg \tau$.

Lebedev[76] has similarly shown that the rate is relatively high when most of the cages are occupied, but that at low concentrations the reaction is a normal second-order process. The explanation of Waite and Lebedev, of the decreasing rate of decay, is much more convincing than the arbitrary division into two sections, fast and slow, with separate rate constants. These sections are frequently attributed to reactions in the amorphous and crystalline phases.

According to equation 1.10, analysis of the initial stages of decay by plotting K_{Dt} vs $t^{-\frac{1}{2}}$, gives an intercept of $4 \pi r_o D$ and slope $4 (\pi r_o^4 D)^{\frac{1}{2}}$, which allows evaluation of D and r_o. For polyethylene the cage radius at 343 K is 6.7 nm after 0.057 Mrad and 4.3 nm after 27.4 Mrad[67]. The cage radius at 120 K is found to be 0.53 nm. The effective cage radius cannot be simply correlated with the unit cell dimensions or the interchain distance, although at low temperatures, the cage radius of 0.53 nm is probably the distance separating radical pairs. It may be concluded for polypropylene,

that at temperatures below 170 K, only decay of radical pairs takes place.

Smith and Jacobs[77] have interpreted the kinetics of radical decay in terms of a non-uniform distribution of radicals. The radicals are assumed to be in isolated spherical spurs, within which there is a rapid attainment of uniform concentration. The overall concentration then decreases with time, due to a second-order recombination accompanied by expansion of the spur in a diffusion like process. The number of radicals in each spur is not thought to increase with dose, but there is an increase in the fraction of volume occupied by the spurs. After 6.4 Mrad the volume fraction in polypropylene was found to be 0.03. Ohnishi[78] has calculated that the spur overlap becomes an important factor above 50 Mrad.

In the above theories, the mechanism of radical migration, whether by simple diffusion or chemical reaction, is not considered. Originally it was thought that the combination of radicals is due to the mobility of polymer segments, since the activitation energy of rotation is similar to that of radical recombination[79]. Lebedev[80] has suggested that the physical properties of the polymer-matrix are the important factor and not the chemical structure of the radical. However, Bresler[81] has shown that for polymers in the glassy state, the extent of diffusion would be too small to allow radical recombination, and that the presence of oxygen, transforming the radical into a peroxy radical, often affects the rate of radical decay.

Bresler suggests that migration of the radical takes places by a series of hydrogen atom abstractions. Recent work by Pudov[82] has shown that the migration rate of free valence in polypropylene is several orders of magnitude greater than the chain migration rate.

The hydrogen atom abstraction is more likely to occur along a polymer chain than between chains. When two radicals become in close proximity (0.5 nm) they will normally recombine. The activation energy of radical decay, which is typically of the order of 80 - 120 kJ mol^{-1} (77) is thought to be the sum of three processes.

1. Activation energy of migration; (this will approximately equal the energy of diffusion of low molar mass species in polymers, typically 55 - 65 kJ mol^{-1})
2. Activation energy of hydrogen abstraction;(probably similar to the energy of chain transfer, 40 - 60 kJ mol^{-1})
3. Activation energy of recombination; by difference, this value must be small and is probably less than 4 kJ mol^{-1} (67).

Milinchuk (83) has kinetically analysed the changes of radical structure of irradiated polypropylene, in the temperature range 273 K - 323 K. The change of radical alkyl → allyl is found to have an activation energy of 25 kJ mol^{-1} and a rate constant of 10^{-22} cm^3 $radical^{-1}$ s^{-1}, which are similar to those of radical recombination. Similar results were found at higher doses for the conversion, alkyl → polyenyl. He concludes that both radical transformation and recombination proceed by free valence migration along the polymer chain. When two radicals meet, they recombine to form a double bond (in same chain) or a cross-link (radicals in adjacent chains). When a migrating radical encounters an existing double bond an allyl radical is formed, and when it meets

a conjugated sequence, a polyenyl radical is produced. A recent study [158] based on the kinetics of grafting reactions on irradiated polypropylene has shown that reactivity decreases in the series of radicals, allyl > polyenyl > peroxy.

1.3.4 Effects in Oxygen and Other Gases

Molecular Structure

When polypropylene is irradiated in the presence of oxygen, chain scission is the predominant reaction and crosslinking is not observed except at high doses with relatively thick samples, where the supply of oxygen is limited by its rate of diffusion. Oxidative degradation is more important in the surface layers and Sobue[31] has noted the different behaviour of films, powders and pellets. The extent of degradation is found to increase with the crystallinity of the samples[45] which suggests that the reaction involves radicals trapped in the crystalline regions. After irradiation in air, Sobue found strong absorption in the infra-red regions at 1720 cm^{-1} (due to C = O) and 3360 cm^{-1} (due to - OH). G(s) values in air do not appear to have been quoted in the literature, but the data of Wale [84] corresponds to a value of 3.3. This may be compared to the much smaller values in vacuo, given in Table 1.2. A similar effect is also found in poly(tetrafluoroethylene) with G(s) = 5.6 in air, and 0.17 in vacuo[85].

Isotactic samples irradiated in vacuo and then exposed to air also show oxidative degradation[29]. Matveev et el[86] measured the C = O group concentration and tan δ for irradiated polypropylene as a function of both dose and time after irradiation. Rapid initial increases in C = O and tan δ were attributed to absorbed oxygen.

The curves of C = O and tan δ show strong similarities which indicate that the extent of oxidation is reflected in the mechanical properties of the polymer. Matveer observed a gradual increase in tan δ for samples irradiated in vacuo, and then exposed to air. He concluded that a slow oxidation occurring over several months took place following irradiation, even when the samples were heated at 360 K, before exposure to air. Geymer[29] found an unusual change in apparent G(s) when post irradiation oxidation occurred. The initial value of 12.6, at doses $<$ 0.8 Mrad, decreased to 0.36 at doses between 9.5 and 22 Mrad (in vacuo). Treatment with methyl mercaptan following irradiation gave normal scission/crosslinking behaviour. This procedure destroyed the free radicals, which otherwise caused oxidative degradation when exposed to air, and accordingly, the gel formation dose fell from 32 Mrad to 10.4 Mrad.

The rate at which oxygen diffuses into semi-crystalline polymers is influenced by the morphology and surface/volume ratio. Mathematical theories based on diffusion equations have been developed by Bohm[87] and Matsuo and Dole[88] for the post irradiation oxidation of polyethylene. It was noted [88] that post-irradiation oxidation is greater in the more crystalline linear polyethylene than in branched polyethylene and is negligible for samples irradiated in the molten state.

Peroxy Radicals

The rapid conversion of alkyl or allyl radicals to peroxy radicals when exposed to air, has been frequently observed in polypropylene [58, 65, 89]. The conformation of this radical has been described in detail [89, 90] and the effect of orientation on

the E.S.R. spectrum analysed. The radical is axially symmetrical but the chain structure attached to the oxygen cannot be identified, since the electron always resides on the O_2 group and no hyperfine splitting is seen. For this reason, the E.S.R. spectra of peroxy radicals in other polymers e.g. polytetrafluoroethylene [91] are almost identical to those in polypropylene.

The line - shape and decay of the peroxy radicals have been studied by Eda et al [92]. Slightly different spectra are found when the irradiation is carried out in vacuo and then exposed to air, when compared to those irradiated in air. These differences, however, appear to originate in the different thermal treatments given which suggests that the rigidity of the polymer matrix containing the radicals, affects the resolution of the spectra. The decay curves have been interpreted in terms of successive first order reactions, although when their graphs are redrawn, they appear to follow reasonable second-order kinetics with a single rate constant. Since only relative values of radical concentration were given, the second-order rate constants cannot be evaluated. The decay curves were measured at low pressure (10^{-3} torr) and during the decay, the appearance of hyperfine splitting due to hydrocarbon radicals was observed. This was also noted by Fischer et al [89].

The reaction

$$R^{\cdot} + O_2 = RO_2$$

is therefore consideredat least partially reversible. The decay reaction is found to occur more slowly in the presence of stabilisers[93], and in some cases even an increase in radical concentration over a period of several days has been observed. The line shape of the

E.S.R spectrum is also changed due to the reaction

$$ROO^{\bullet} + AH \rightarrow ROOH + A^{\bullet}$$

as a result of which radicals of the stabiliser accumulate in the specimen.

The effect of ultra-violet light on the peroxy radicals has been studied by Milinchuk and Pshezetskii (65). The radicals were formed by the action of oxygen on allyl radicals, and ultra-violet irradiation at 77 K gave rise to the appearance of a four-line spectrum(measured at 77 K). On heating to 300 K a complex spectrum resulted and these changes were attributed to the following reactions:

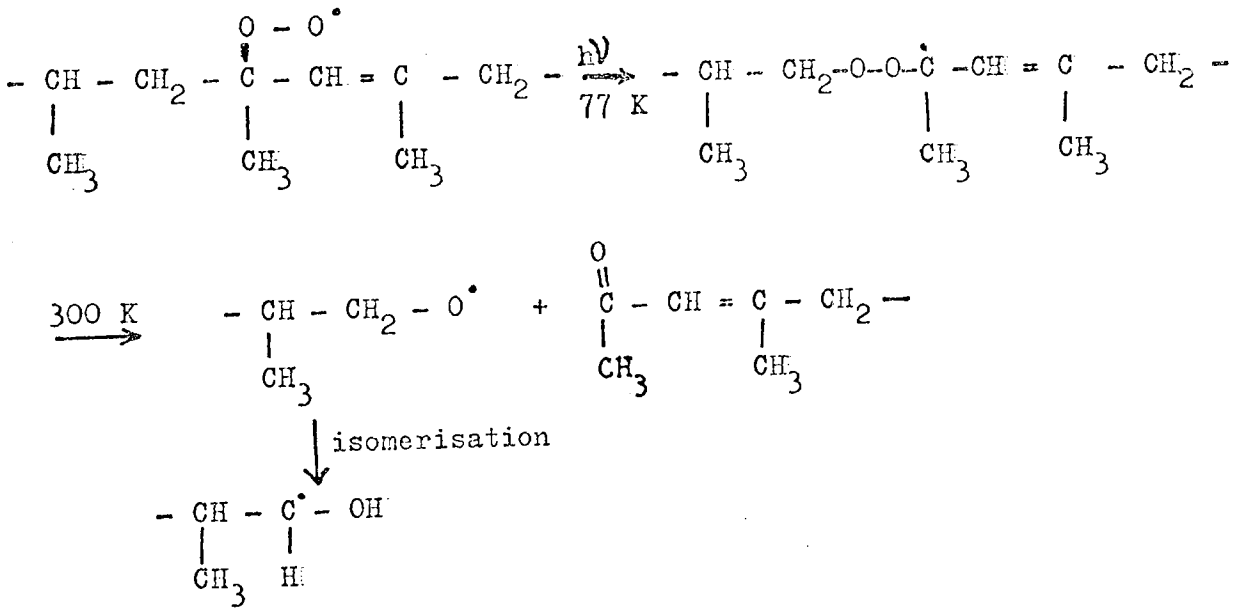

The absorption of oxygen during peroxy radical recombination has been measured by Neudorfl (94). The oxidation is considered to be a radical chain reaction in which several oxygen molecules are absorbed for each radical initially present. The following equation was deduced :

$$\frac{-d\left[O_2\right]}{d\left[R^{\bullet}\right]} = \frac{1}{\rho a^3} \cdot \frac{1}{\left[R^{\bullet}\right]} \quad \ldots\ldots 1.10$$

in which ρ is the density and a^3 the 'cage' volume of the radical. Equation 1.10 may be rearranged to :

$$[O_2] = \frac{1}{\rho a^3} \cdot \frac{[R^\cdot]_o}{[R^\cdot]} \quad \ldots\ldots 1.11$$

in which $[R^\cdot]_o$ is the initial radical concentration. The value of the cage radius at 323 K was found to be 3.7 nm. Fischer et al[88] found that 3 - 6 oxygen molecules were consumed during the decay of each original radical in polypropylene.

Hydroperoxides

Hydroperoxides are formed during the decay reaction of the peroxy radical by repeated hydrogen abstraction, as described in 1.2.9. The hydroperoxides may then decompose thermally[95] or photochemically[96]. The decomposition reactions of polypropylene hydroperoxide have been reviewed by Neiman [97]. When the hydroperoxide is heated, the infra-red absorption at 3360 cm^{-1} disappears, but the strong absorption at 1720 cm^{-1} (C = O) remains. A number of volatile products of decomposition are formed including water, formaldehyde, acetaldehyde, acetone, methanol, hydrogen peroxide, carbon monoxide, carbon dioxide and hydrogen [98]. Chien [99] has shown that sequences of hydroperoxides on the same polymer chain are frequently present. The analysis of hydroperoxides has been made iodometrically[96] colorimetrically by oxidation of ferrous ions[100] and by infra-red spectroscopy[99].

Nechitailo[93] has found that polypropylene stabilised with Ionol (2.6 di - tert butyl 4 methyl phenol) shows reduced chain scission and carbonyl formation compared to unstabilised polymer, when irradiated in air. It appears that Ionol is able to stabilise any radical formed before oxygen has time to diffuse in, and react with them. It is significant that irradiation in vacuo in the

presence of 2% Ionol did not cause gel formation at doses up to 200 Mrad. Other experiments [101] showed that di - tert butyl pyrocatechol was also effective in reducing radiation degradation in air, but that β - phenylnapthylamine was not. Geymer[29] has investigated the effect of Ionox 330 (1,3,5 - trimethyl 2,4,6 3,5 di tert. butyl - 4 - hydroxy benzyl benzene) on post-irradiation degradation, by irradiating in vacuo and then exposing to air 1 day later. The instrinsic viscosity in decalin at 150°C fell from 6.2 to 1.1 after 0.8 Mrad, while that of the stabilised sample decreased to only 3.7

Other gases and Liquids

A comprehensive investigation of the scission and crosslinking changes in polypropylene, irradiated in the presence of various substances has been made by Geymer [102]. In an earlier study [29] he found that exposure of irradiated samples to methyl mercaptan was an effective method of destroying free radicals and preventing post-irradiation effects. Methyl mercaptan was by far the most effective substance in preventing crosslinking during irradiation, even at concentrations as low as 0.1%. The reaction is considered to be :

$$R^{\bullet} + CH_3SH \rightarrow RH + CH_3S^{\bullet}$$

$$2CH_3S^{\bullet} \rightarrow CH_3S - S\,CH_3$$

Of the other wide range of substances tested by Geymer only ammonia was effective in increasing the extent of crosslinking. Sulphur monochloride has also been reported [103] as being very effective in increasing the crosslinking yield. ($G(x) = > 100$)

Ayscough et al [104] and Kuri and Ueda [105] have irradiated polypropylene in sulphur dioxide. The E.S.R. spectrum is a narrow asymmetric singlet considered to be due to the sulphinyl radical $RS^{\bullet}O_2$ in which the free electron is considered to reside chiefly on the sulphur atom. The radical is stable when exposed to air, but the formation process

$$R^{\bullet} + SO_2 \rightarrow RS^{\bullet}O_2$$

can be reversed by prolonged evacuation.

Irradiation in monomers such as allyl methacrylate [30] causes graft polymerisation and increased extent of crosslinking, compared to that in vacuo. Filippov et al.[106] have reported an extremely large G ($-Cl_2$) value in the range $10^4 - 10^6$, when irradiation takes place in chlorine. This value indicates that a chain reaction is taking place and this has been the subject of a U.S. patent [107] for the preparation of chlorinated polypropylene.

1.3.5 Crystallinity Changes

At very large radiation doses, Kozlov et al [108] have reported that fast electrons cause the degradation and eventual disappearance of polypropylene spherulites. At lower doses, using γ - radiation, Rybnikar et al [109] found no change in the spherulitic structure and spherulite growth rates in polypropylene, although there was an overall decrease in crystallinity. Tikhomirov et al [110] have measured the crystallinity decrease at doses up to 1000 Mrad. A density decrease from 0.92 to 0.88 corresponded to a crystallinity decrease from 82% to 43%. X-ray measurements showed corresponding results with overall levels of crystallinity much lower

The α-crystalline modification was found to be more resistant to degradation than the β- form.

Nechitailo [111] has measured (by D.T.A.) the melting points of stabilised and unstabilised polypropylene irradiated in air and in vacuo. For unstabilised polymer the melting points and heats of fusion decreased with radiation dose, and an exothermic degradation reaction occurred at about 470 K. The melting point decreased from an initial value of 433 K to 398 K after 200 Mrad in vacuo, and to 393 K after the same dose in air. The stabilised polymer, containing 2% Ionol, gave a reduction from 428 K to a melting range of 408 - 416 K after 200 Mrad (in air and in vacuo). The exothermic degradation reaction was not observed with the stabilised polymer.

In a recent investigation, Kusy and Turner [112] found an approximately linear decrease of melting point with radiation dose in vacuo, of 0.2 K / Mrad. They applied the Flory equation [113]

$$\frac{1}{T} - \frac{1}{T^{o}} = \frac{-R}{\Delta H_u} \ln X \quad \ldots\ldots 1.12$$

to the decrease of melting point caused by irradiation. In equation 1.12, T^{o} is the original melting point, T is the melting point after irradiation, ΔH_u is the heat of fusion per mole of crystalline repeat unit and X is the fraction of polymer in the crystalline state after irradiation, compared to that before (X = 1). G - values for the loss of crystalline units, G (- cr) may be calculated from

$$G(-cr) = \frac{(1 - X)}{M} \times \frac{0.962 \times 10^{6}}{r} \quad \ldots\ldots 1.13$$

in which M is the molar mass of the crystalline unit (3 x 42 g mol^{-1} for polypropylene) and r is the radiation dose in megarad . The application of equation 1.13 appeared to give sensible results for 6.6

Nylon and poly(ethylene terephthalate) in approximate agreement with G-values for gas evolution, chain scission, etc., For polypropylene however, an apparent G(-cr) of 47 was not explicable, although the authors suggested that the G-values for gas evolution, radical formation, etc., were likely to be underestimates, since they do not take into account changes in tacticity.

1.3.6 Mechanical Properties.

The changes in molecular and crystalline structure previously considered will affect the physical and mechanical properties of irradiated polypropylene depending to a large extent on whether the irradiation is carried out in air or in vacuo. Only a few studies of changes in mechanical properties have been reported. Irradiation in vacuo, to doses only of a few megarads, leads to an improvement in some mechanical properties, such as flexural modulus and melt flow index; the tensile strength, Vicat softening point and density are only slightly affected; the elongation at break, impact strength and tear resistance are all markedly diminished [114,115]. Irradiation in air usually has a deleterious effect on all of these properties, although the incorporation of antioxidants reduces the extent of deterioration.

At higher doses in vacuo, Sauer Merrill and Woodward [116] have shown by dynamic mechanical studies that there is an initial decrease in modulus caused by destruction of crystallites, but eventually the modulus becomes greater than the starting material. These observations were also confirmed by N.M.R. studies [45].

The mechanical properties of polypropylene change on storage following irradiation [117]. Little has been published on such

changes but Matveev et al.[85] has correlated the post-irradiation increase of tan δ with increase of carbonyl content.

1.3.7 Aim and Scope of Present Work

Although much work has been published on irradiation effects in polypropylene in vacuo and at high doses, relatively little has been done at low doses and in the presence of oxygen. These however, are the conditions under which polypropylene articles, e.g. hypodermic syringes, are likely to be irradiated for sterilisation purposes. The recent development of techniques capable of investigating thermal and crystallisation properties has produced additional methods for the investigation of irradiated polymers. In particular, the reasons for post-irradiation degradation appear to need to be sought in the changes in solid structure following irradiation.

After an initial investigation on a range of polymers for possible post-irradiation effects, polypropylene was selected as the polymer on which further investigation was to be concentrated. Both γ and electron irradiations up to doses of 20 megarads were carried out. Since irradiation facilities outside the University were used, wide variation in conditions of irradiation were not possible. Also measurements during and immediately after irradation could not normally be made. To a certain extent, these limitations directed attention towards post-irradiation effects. The physical and chemical properties investigated include molar mass, free radical concentrations and their decay rates, melting points and crystallisation processes, hydroperoxide concentrations and thermal stability.

CHAPTER TWO : MATERIALS AND IRRADIATION FACILITIES

2.1 POLYPROPYLENE

2.1.1 Polypropylene Powder

An unstabilised polypropylene powder, Carlona HM, supplied by Shell Chemical Company was used for most of the work described in this thesis. The polypropylene was used as supplied except where this is specifically stated. The particle size was 0.010 to 0.10 mm diameter. The infra-red spectrum of this material in a potassium bromide disc, showed that it was 100% isotactic, since the peaks at 995 cm^{-1} and 974^{-1} were of equal size (118). The powder was stored in a dark bottle in a cupboard when not in use.

An additional sample of unstabilised isotactic polypropylene also supplied by Shell, Carlona KM, was used mainly for the preparation of solid specimens. The particle size of this sample was 0.05 to 0.15 mm.

2.1.2 Polypropylene Film

A sample of polypropylene film, supplied by the Shell Chemical Company prepared from Carlona W 5520 FKS was used for mechanical testing and some other studies. This material contained a small concentration of undisclosed antioxidants. The thickness of the film was 0.25 mm.

2.1.3 Polypropylene Pellets

Stabilised polypropylene in pellet form, 3mm diameter, was supplied by Shell Chemical Company (Code FE 61) and was used for melt

flow index determinations.

2.1.4 Atactic Polypropylene

A sample of atactic polypropylene was supplied by Shell Chemical Company. This material was soxhlet extracted with diethyl ether under nitrogen for several hours. The polymer was precipitated by pouring the extract into excess methanol. The solvent mixture was decanted and the amorphous polymer dried under vacuum at 50°C for 48 hours.

An additional sample of slightly higher molar mass supplied by Hercules Chemical Company (Code 54 - 6 - 1 XA) was used without further treatment.

2.1.5 Stereoblock Polypropylene

A sample of stereoblock polypropylene was supplied by Montecatini, Milan. This had been obtained by extraction with n-heptane, following extraction with diethyl ether, and was in the form of a semi-crystalline powder. The molar mass of this sample was fairly low ($\overline{M}_v$ = 8000). The tacticity estimated from infra-red spectrum measurements was 70 ± 5% isotactic. This was found by comparison of the heights of the absorption peaks at 995 cm^{-1} (sensitive to tacticity) and 974 cm^{-1}. A solid sample of stereoblock polypropylene of higher molar mass ($\overline{M}_v$ = 1.9 x 10^5) and lower isotacticity (55 ± 5%) was supplied by Hercules Chemical Company.

2.1.6 Injection Moulded Test-pieces

Test-pieces were preared by injection moulding of the Carlona KM powder, using a Florin manumold machine. The specimens used

in the molar mass and E.S.R. measurements (4.3.7) were disc-shaped, with a dimater of 57 mm and a thickness of 1.8 mm. The following moulding conditions were used :

Melt temperature :	200°C.
Mould temperature :	60°C.
Mould pressure (max) :	1000 p.s.i. (7 MNm^{-2}).
'Dwell' time :	15 seconds.
Cycle time :	60 seconds (approx).

Tensile test-pieces were also repared from polypropylene film (2.1.2) using a hand-operated cutting die (A.S.T.M. D - 638 - 68 type IV).

2.2 Other Polymers

2.2.1 Poly (methyl methacrylate)

A sample of poly(methyl methacrylate) was supplied by I.C.I. Plastics Division. The polymer was produced by A.Z.B.N. initiation and was in a finely divided physical state, with an average particle diameter of 0.2 mm.

2.2.2 Poly(vinyl chloride)

Emulsion-polymerised poly(vinyl chloride) powder was supplied by British Geon Limited. The polymer did not contain stabilisers and had an average particle diameter of 0.03 mm.

2.2.3 Cis-polyisoprene

A synthetic cis 1.4 polyisoprene 'Natsyn' was supplied by Goodyear Limited. This polymer was extracted with acetone to remove any antioxidants and was then dried under vacuum at 50°C to remove any residual solvent.

2.2.4 Trans-polyisoprene

The polymer used was milled balata; this was extracted with acetone for 60 hours and then dried under vacuum.

2.2.5 Poly(propylene oxide)

A sample of this polymer was supplied by Fort Dunlop (Research Centre). This had been produced with a ferric chloride catalyst system.

2.2.6 Nylon 6.6

Nylon 6.6 fibres of 0.635 mm diamter (bristle) were supplied by I.C.I. (Pontypool).

2.2.7 Poly(ethylene terephthalate)

'Melinex polyester film of thickness 0.254 mm was supplied by I.C.I. (Plastics Division).

2.3 Solvents and Antioxidants

2.3.1 Solvents

After some preliminary surveys of solvent efficiency, using decalin, tetralin and xylene, it was decided to use decalin as the solvent for isotactic polypropylene, for solution viscosity measurements. The best available grade was a mixture of cis and trans isomers, and this was purified by drying over anhydrous calcium chloride, followed by distillation under reduced pressure (40 torr), the fraction boiling between 80.0 and 80.5°C being collected.

Other solvents were used normally of 'Analar' grade and

were not further purified before use. Wherever 'Analar' grade solvents were not available, the solvents were dried and distilled prior to use.

2.3.2 Antioxidant

Since isotactic polypropylene is only soluble at temperatures in excess of 100°C, an antioxidant was added to the decalin solvent to minimise degradation during viscosity measurements. An antioxidant suitable for polyolefin stabilisation [119], Ionox 330, manufactured by the Shell Chemical Company, was used at a concentration of 0.5% w/v. Ionox 330 is 1, 3, 5-trimethyl - 2,4,6-tris (3,5-di-tert.butyl-4-hydroxy benzyl)benzene.

1,3,5-trimethyl-2,4,6-tris(3,5-di-tert. butyl-4-hydroxybenzyl) benzene

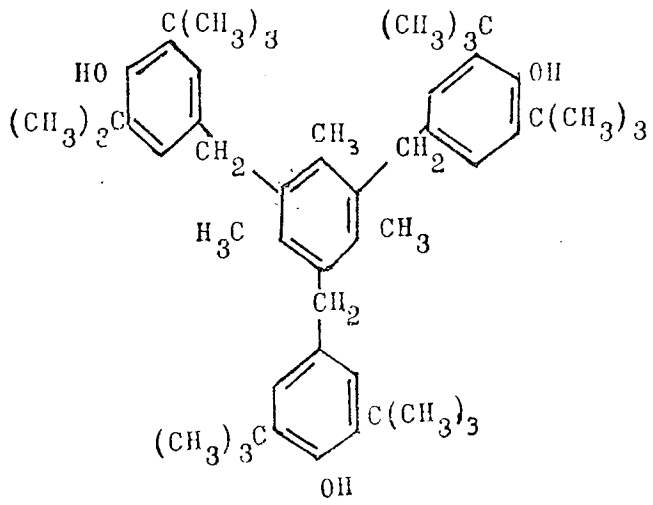

Ionox 330 is considered to function as an antioxidant by interrupting the chain reaction

$$R^{\bullet} + O_2 \longrightarrow RO_2^{\bullet}$$

$$RO_2^{\bullet} + RH \longrightarrow RO_2H + R^{\bullet}$$

Representing the antioxidant as AH, the above reaction is minimised, by transfer of hydrogen atoms from the antioxidant to the polymer radical :

$$R^{\bullet} + RH \longrightarrow RH + A^{\bullet}$$

The free radical A is relatively stable in hindered phenolic structures such as Ionox 330.

2.4 Irradiation Facilities

During the period over which this work was carried out, high energy irradiation sources of suitable size were not available at the University and irradiations were made at various establishments.

Initially, samples were sent to the Radiation Pond, Building 466, Harwell. Because of the problems of delay in receiving the samples after irradiation, other sources were used for most of the work described here.

A Van de Graaff accelerator at Southall's Limited, Birmingham, was most frequently used, but some γ-irradiations were also made at the Physical Chemistry Department, Leicester University.

2.4.1 γ-irradiation, Harwell

Spent fuel elements are used as the γ-source in a large water-shielded irradiation unit. The energy of the γ-rays resulting from fission covered a range and some typical irradiation conditions are given below :

Dose rate	0.425 - 0.409 M rad / hour
Mean energy	0.8 MeV
Maximum energy	3.0 MeV
Temperature	22°C

A variation in dose rate was usually stated, because of the rapid decay of some of the species in the fuel elements. It was not

possible to control the temperature during the irradiation.

2.4.2 Electron-irradation, Southalls, Birmingham.

High-energy electrons from a Van de Graaff accelerator were used. The voltage applied in the acceleration process was 4×10^6 volts. The electrons were focussed into a beam approximately 40 cm by 1 cm.

The samples were presented to this beam by a conveyor belt system, the speed of the belt movement being used to control the dose received. The conveyor speed was usually such that any part of the sample was in the electron beam for less than one second. For high doses, multiple passes beneath the beam were used in preference to slow belt speed which would cause a large rise in sample temperature.

The normal dose received for each pass was 2.5 M rad, which corresponds to an energy absorption of 25 J g^{-1}. The temperature rise so caused may be calculated to be 13°C assuming a specific heat capacity of 1.93 J K^{-1} g^{-1} (120). To minimise the effect of temperature increase, most irradiations were made with the samples surrounded with crushed solid carbon dioxide (195 K). Crushed ice (273 K) was used to surround the samples when irradiations were made in chlorine and sulphur dioxide.

2.4.3 γ-irradiation, Leicester University.

A well-type unit (Vickrad) was used with cobalt-60 rods as the γ-ray source. The irradiation unit is within a barrel of lead and the samples are introduced and removed by means of a simple pneumatic

device. Although only small volumes could be irradiated, irradiation at liquid nitrogen temperature (77 K) could be conveniently made in a small dewar flask.

The dose received was calculated from the dose rate and length of time of irradiation. The dose rate itself was calculated from the known half-life of cobalt-60 (5.26 years) and the initial dose rate quoted when the irradiation unit was supplied. At the time of use, the dose rate was in the range of 3-4 M rad/hour.

2.4.4 Ultra-violet Irradiation

For ultra-violet irradiation of the samples, both on its own and following high energy radiation, a 'Hanovia' lamp - 80 watt - was used with the main filter removed. The samples were normally thinly spread on a filter paper immediately below the lamp, at a distance of 30 cm. Film samples were also irradiated with the same source.

2.5 Vacuum Line and Procedure

2.5.1 Vacuum Line

The vacuum line used and described by Henson [121] was used for evacuation when this was necessary. This line was not normally capable of producing pressures lower than 5×10^{-4} torr.

2.5.2 Procedure

Pressures of 10^{-3} torr or better were used when samples were evacuated. For irradiations in vacuo, alternate flushings

with white-spot nitrogen and evacuation were used to minimise the amount of oxygen present. At leat three flushings with nitrogen were made before the final evacuation. For the preparation of samples in gases other than air alternate evacuation and introduction of the gas was used. At least two evacuations were made before the final introduction of the gas.

CHAPTER THREE : INITIAL STUDIES AND MOLAR MASS DETERMINATION

3.1 Initial Studies on Various Polymers

3.1.1 Introduction

Some irradiation and post-irradiation effects in a range of polymers of industrial importance, were studied in a preliminary survey. The polymers used were selected to cover a range of physical properties and chemical features and are listed below :

1. Poly (methyl methacrylate)	–	Amorphous, glassy.
2. Poly (vinyl chloride)	–	Partially crystalline; high m.pt.
3. Poly (propylene oxide)	–	Low melting point; variable tacticity.
4. Cis polyisoprene	–	Rubbery } Steric effect and influence of unsaturation
5. Trans polyisoprene	–	Crystalline }
6. Nylon 6.6	–	High m.pt. High crystallinity; fibre.
7. Poly(ethyleneterephthalate)	–	High m.p.t, low crystallinity; film.

The main aim of this survey was to find out if post-irradiation changes occurred widely, and if possible to select a system that could be conveniently characterised in solution at room temperature.

3.1.2 Results

The polymers were γ-irradiated to a dose of 10 megarads in air. The irradiations were made at Harwell and measurements of the irradiation effects were made as soon as possible after their return. This was

usually less than 1 week after irradiation.

In the following list of results the intrinsic viscosity $[\eta]$ and the viscosity-average molar mass, $\bar{M}_v$, were obtained by the methods detailed in section 3.3.1 for atactic polypropylene. The units of $[\eta]$ are 100 $cm^3\ g^{-1}$.

Irradiation Effects	Post Irradiation Effects
Polymethyl methacrylate $[\eta]$ in toluene at 25°C decreased from 1.275, ($\bar{M}_v$ = 6.72×10^5) to 0.246 ($\bar{M}_v = 0.71 \times 10^5$) (ref.122). Polymer becomes yellow.	No further decrease in molar mass up to 6 months after irradiation.
Poly(vinyl chloride) $[\eta]$ in T.H.F. at 25°C was unchanged (1.12). Turbidimetric titrations in tetrahydrofuran/water showed slight broadening of distribution. Polymer became brown and strong smell of HCl was present.	No further changes on storage up to 3 months.
Poly(propylene oxide) $[\eta]$ in toluene at 25°C decreased from 0.66 ($\bar{M}_v$ = 8.8 $\times 10^4$) to 0.24 ($\bar{M}_v = 2.3 \times 10^4$).(123) Polymer became greasy and gave odour of burnt sugar.	No further decrease in $\bar{M}_v$ after 6 months storage.
Cis polyisoprene. Polymer became crosslinked and only swelled in solvents. (Before irradiation was readily soluble). with $[\eta]$ = 1.80 in toluene at 25°C, and $\bar{M}_v$ = 6.96×10^4 (124)	Became soluble in toluene, with rapidly decreasing viscosity on storage over a period of 3-4 weeks. (A similar reduction in viscosity was also observed for the non-irradiated polymer).

contd. Irradiation Effects	Post-irradiation Effects
Trans polyisoprene. Polymer became insoluble in toluene with swelling ratio = 5.58 w/w. (Before irradiation was soluble with $[\eta]$ = 0.73 in toluene at 25°C).	3 months after irradiation polymer was still insoluble with unchanged swelling ratio.
6.6 Nylon and poly(ethylene terephthalate)	
No significant changes in stress-strain curves or breaking strength.	No changes observed up to 10 months after irradiation.

3.1.3 Conclusions.

It was concluded that no true post-irradiation effects were taking place, with the possible exception of cis polyisoprene. In this case, however, a similar degradation was also observed in the non-irradiated polymer when dissolved in toluene. The chief effects of irradiation were:

Poly(methyl methacrylate)	–	Chain scission.
Poly(propylene oxide)	–	Chain scission.
Poly(vinyl chloride)	–	Dehydrochlorination, and polyene formation.
Cis polyisoprene	–	Crosslinking.
Trans polyisoprene	–	Crosslinking.
Nylon 6.6	–	Unaffected at low doses.
Poly(ethylene terephthalate)	–	Unaffected at low doses.

The possible presence of free radicals in these irradiated polymers was not confirmed, since E.S.R. facilities were not then available. Following this initial survey of polymers, further investigation was limited to polypropylene.

3.1.4 Tensile Testing of Polypropylene Film.

In the early stages of this work it was hoped to verify by mechanical testing that post-irradiation embrittlement of polypropylene took place.

Several series of mechanical tests on tensile test-pieces cut from polypropylene film (2.1.2) were made using a Hounsfield tensometer, Type E. A wide range of testing rates were used but the differences between irradiated and non-irradiated polypropylene were negligible compared to the variation found in each set of results. No significant changes occurred with samples stored for several months after irradiation. The one conclusive result obtained was that whereas both high energy radiation and ultra-violet radiation individually caused no change in elongation at break and final strength, when high energy radiation was followed by ultra-violet photolysis, the film samples became brittle and ruptured immediately the yield point was reached.

3.2 Introduction.- (molar mass measurements.)

Attempts to measure number average molar masses of isotactic polypropylene by osmotic pressure at 130°C using a Mechrolab Model 502 high speed membrane osmometer were unsuccessful because of degradation of the semi-permeable membranes. The problems of modifying and operating a light-scattering apparatus at elevated temperatures to obtain weight average molar masses, were considered to be prohibitive.

For these reasons molar masses of isotactic polypropylene were determined by viscometry, although the limitations of this method (1.2.6) were considered. The viscosity average molar mass $\overline{M}_v$ is defined by the relationship :

$$\bar{M}_v = \left[\frac{\sum n_i M_i^{1+a}}{\sum n_i M_i} \right]^{\frac{1}{a}} \quad \ldots\ldots 3.1$$

in which n_i is the number of species of molar mass M_i, and a is the exponent in the Mark-Houwink equation.

$$[\eta] = K \bar{M}_v^{a} \quad \ldots\ldots 3.2$$

The value of $\bar{M}_v$ will normally lie between $\bar{M}_n$ and $\bar{M}_w$, the ratio $\bar{M}_v/\bar{M}_n$ being determined by the nature of the distribution and the value of a. For a most probable distribution $\bar{M}_v/\bar{M}_n = \left\{ 1 + a \Gamma (1 + a) \right\}^{1/a}$ (121) where $\Gamma(1 + a)$ is the Γ function of $1 + a$. Using the value of $a = 0.74$[125], $\bar{M}_v/\bar{M}_n = 1.88$. However, polypropylene normally has a wider molar mass distribution than that found in a most probable distribution[126].

Number average molar mass determination on atactic polypropylene was possible, since it is soluble at low temperatures and the molar mass was sufficiently low for vapour pressure osmometry to be used. Some measurements were also made of the melt flow index which although only an empirical measure of molar mass, can be related to weight average molar mass.

3.3 Experimental

3.3.1 Viscometry

Viscometry measurements were made with an Ubbelohde suspended level viscometer at 130°C using filtered stabilised decalin as solvent. The viscometer was fitted with ground glass joints at the tube ends to

facilitate high temperature usage. It was found that measurements of viscosity using a range of concentrations at high temperatures was not convenient by internal dilution, and time-consuming when separate solutions were prepared. Single point determinations at 0.1% w/v were found to give acceptable accuracy and reproducibility. Measurements were repeated until flow times agreed to within 0.2 second.

In order to calculate the intrinsic viscosity $[\eta]$, the Huggins constant k' in the relationship (127)

$$\frac{\eta_{sp}}{c} = [\eta] + k' [\eta]^2 c \quad \ldots\ldots 3.1$$

was found in a separate determination.

The viscosity number $\eta sp/c$ was found from the flow times t and t_o, of the solution and solvent ;

$$\frac{\eta_{sp}}{c} = \frac{t - t_o}{t_o c} \quad \ldots\ldots 3.2$$

It is assumed in equation 3.2 that the flow times are relatively long, so that end corrections can be ignored. This was found to be so for the viscometer and solvents used. The intrinsic viscosity of isotactic polypropylene is related to the viscosity average molar mass by (125)

$$[\eta] = 1.93 \times 10^{-4} \bar{M}_v^{0.74} \quad \ldots\ldots 3.3$$

Equations 3.1 and 3.3 were combined to prepare calibration graphs directly relating $\eta sp/c$ to $\bar{M}_v$ at 0.1% concentration. Measurements made on atactic polypropylene in toluene at 25°C were made in the usual manner by dilution within the viscometer to produce a range of concentrations, (usually 1.00, 0.714, 0.500, 0.333 and 0.200 % w/v).

$[\eta]$ was then found from the intercept of a graph of η_{sp}/c vs. c and related to molar mass by [128]

$$[\eta] = 2.18 \times 10^{-4} \bar{M}_v^{0.725}$$

3.3.2 Vapour Pressure Osmometry

Number average molar masses of atactic polypropylene were measured on a Mechrolab vapour pressure osmometer (Model 301A). The theory and operation of this instrument is given elsewhere [129, 130]. The measurements were made in toluene with a range of concentrations up to 4% w/v. The instrument was calibrated with benzil (di-benzoyl) using concentrations up to 0.05 mol dm^{-3} and the accuracy of the calibration was confirmed using pure triphenyl methyl chloride. Constant readings were obtained 7 minutes after the introduction of the sample, and this was taken as the normal operating time. Measurements were normally made in duplicate, starting with the weakest solutions.

3.3.3 Melt Flow Index

Measurements were made using a Davenport Polythene Grader (No 985). The apparatus consists of a heated barrel at the end of which is a tungsten carbide die. The polymer is extruded through the die using a piston to which a weight can be attached.

The melt flow index is empirically related to the molar mass of the polymer and is defined as the mass extruded in 10 minutes through a standard die (0.1994 cm diameter). A high value of melt flow index corresponds to a low molar mass. For low molar mass polymers, a special die (0.1181 cm diameter) can be used, which reduces the rate of extrusion to 0.1 of the original value. This was used for measurements on irradiated polymers. The measurements were normally made at 190°C using a standard piston weight of 2.16 kg. Measurements made on unstabilised polypropylene

proved unsatisfactory since the melt flow index was too large. Measurements at temperatures only 1° C above the melting point were attempted but the polymer again extruded rapidly from the die, even before the weight was attached.

3.4 Isotactic Polypropylene

3.4.1 Evaluation of Huggins' Constant k'

Table 3.1 gives the results obtained in decalin at 130° C, using non-irradiated unstabilised polypropylene and the same polymer γ-irradiated to a dose of 2.5 Mrad.

Table 3.1 Viscosity Date for Polypropylene in Decalin at 130° C

Concentration / g 100 cm^{-3}	η sp/c Unirradiated	η sp/c 2.5 Mrad
0.1	2.80	1.11
0.2	3.05	1.15
0.3	3.27	1.195
0.4	3.58	1.265
0.5	3.79	1.28

The plots of ηsp/c vs c are shown in Figure 3.1. The following values were obtained for the intrinsic viscosity and Huggins constant k' (equation 3.1)

Unirradiated polymer $[\eta] = 2.54$, $k' = 0.391$

2.5 Mrad polymer $[\eta] = 1.06$, $k' = 0.402$

The value of $k' = 0.40$ was used in evaluating $[\eta]$ from the single point viscosity measurements given in the following sections.

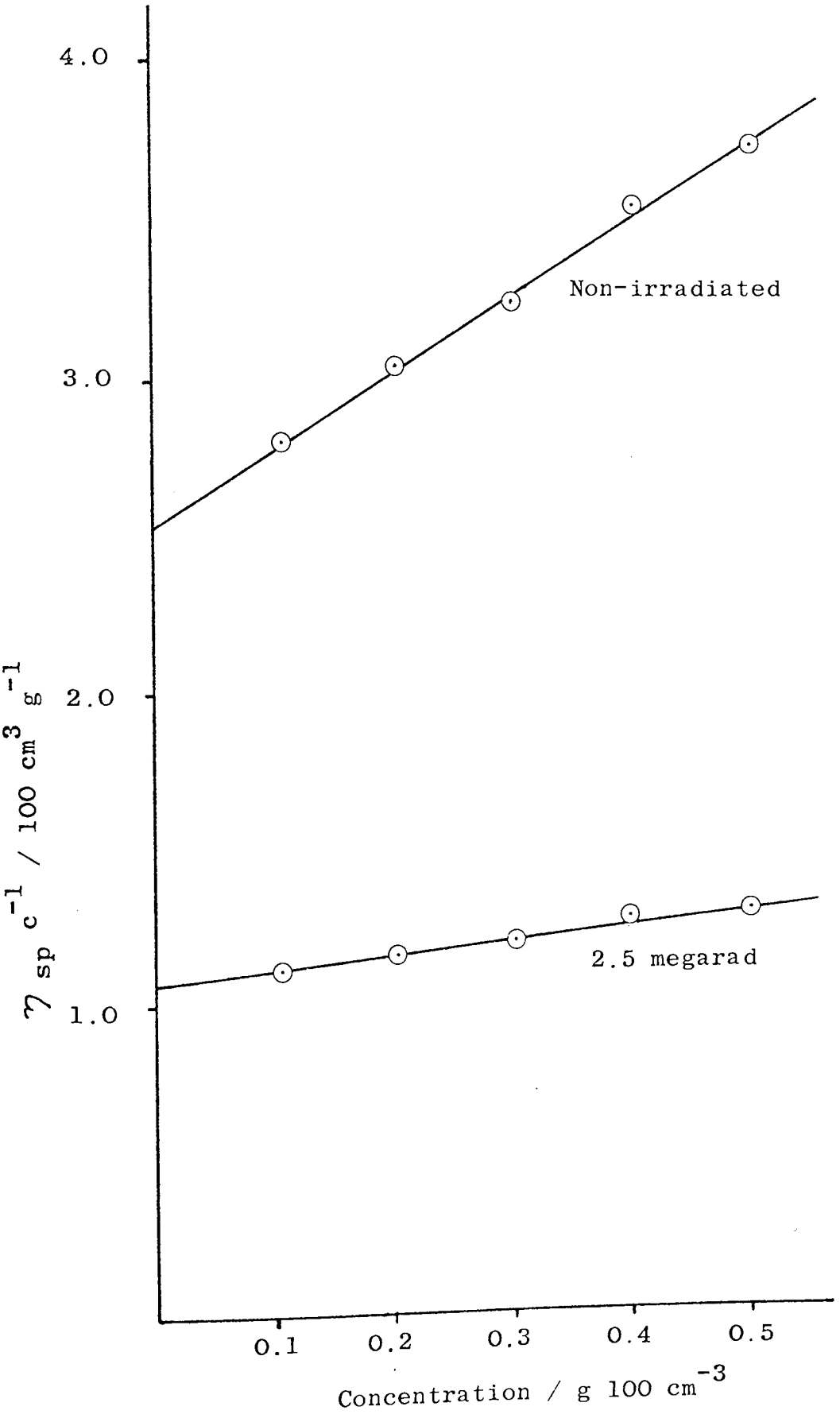

Fig. 3.1 Plots of $\eta_{sp}\, c^{-1}$ vs. c used to find k' for polypropylene in decalin at 130°C.

The units in which $[\eta]$ and $\eta_{sp/c}$ are given is 100 $cm^3\ g^{-1}$, quoted to the nearest 0.005 100$cm^3\ g^{-1}$. The accuracy of the determination of $\bar{M}_v$ from single point measurement is estimated to be $\pm$ 3%.

3.4.2 Results of γ and electron irradiation of unstabilised polypropylene in air.

	Dose/Megarad	$\eta_{sp}\ c^{-1}$ /100$cm^3 g^{-1}$	$[\eta]$/100 $cm^3\ g^{-1}$	$\bar{M}_v \times 10^{-4}$
Source: γ (Harwell) Temperature : 295 K Storage 7 - 10 days (ambient)	0	2.800	2.54	36.8
	1.0	1.415	1.35	15.5
	2.5	0.945	0.91	9.25
	5.0	0.62	0.605	5.50
	7.5	0.445	0.44	3.90
	10.0	0.35	0.345	2.80
Source : electron Temperature: 308 K Storage : 10days (ambient)	1 x 2.5	0.935	0.90	9.10
	2 x 2.5	0.715	0.695	6.40
	4 x 2.5	0.415	0.41	3.10
Source : electron Temperature : 312 K Storage : 24 hours at 195 K	1 x 3.25	1.18	1.13	12.35
	2 x 3.25	0.880	0.85	8.45
	3 x 3.25	0.63	0.615	5.40
	4 x 3.25	0.55	0.54	4.50
	5 x 3.25	0.45	0.44	3.50
	6 x 3.25	0.395	0.390	2.90
Source : electron Temperature : 195 K Storage : 4-6 hours at 195 K	1 x 3.25	1.33	1.27	14.20
	2 x 3.25	0.955	0.92	9.35
	3 x 3.25	0.80	0.775	7.40
	4 x 3.25	0.685	0.665	6.05
	5 x 3.25	0.585	0.57	4.90
	6 x 3.25	0.525	0.515	4.20

3.4.2 continued .....

	Dose/Megarad	$\eta_{sp}\ c^{-1}$ /100cm^{3}g^{-1}	$[\eta]$/100 cm^{3}g^{-1}	$\bar{M}_v$ x 10^{-4}
Source: γ(Leics)	1.20	1.74	1.62	20.50
Temperature : 195 K	2.49	1.42	1.34	15.70
Storage : 24 hours	3.48	1.185	1.135	12.40
at 195 K	5.52	1.14	1.09	11.75
	9.12	0.915	0.88	8.85

These results are illlustrated in Figure 3.2 in which $1/\bar{M}_v$ is plotted vs. dose.

3.4.3 Effect of Storage on $\bar{M}_v$.

A further smaller decrease in $\bar{M}_v$ was observed on storage following irradiation at 195 K. While kept at 195 K no decrease in $\bar{M}_v$ occurred, but when the samples were warmed to room temperature a decrease occurred over a period of several days, following which $\bar{M}_v$ became constant. This change occurred over less than 20 hours at 313 K. Some typical results are given in Table 3.3.

Table 3.3 Change of molar mass $\bar{M}_v$ with storage at room temperature following electron irradiation at 195 K.

	2.5 Mrad	5.0 Mrad	10.0 Mrad
Initially	164,000	121,000	72,600
After 1 day	130,000	100,000	69,500
After 7 days	101,000	69,000	58,000
After 3 months	102,000	69,000	54,000
After 6 months	102,000	67,000	57,000

Samples irradiated at room temperature and then cooled to

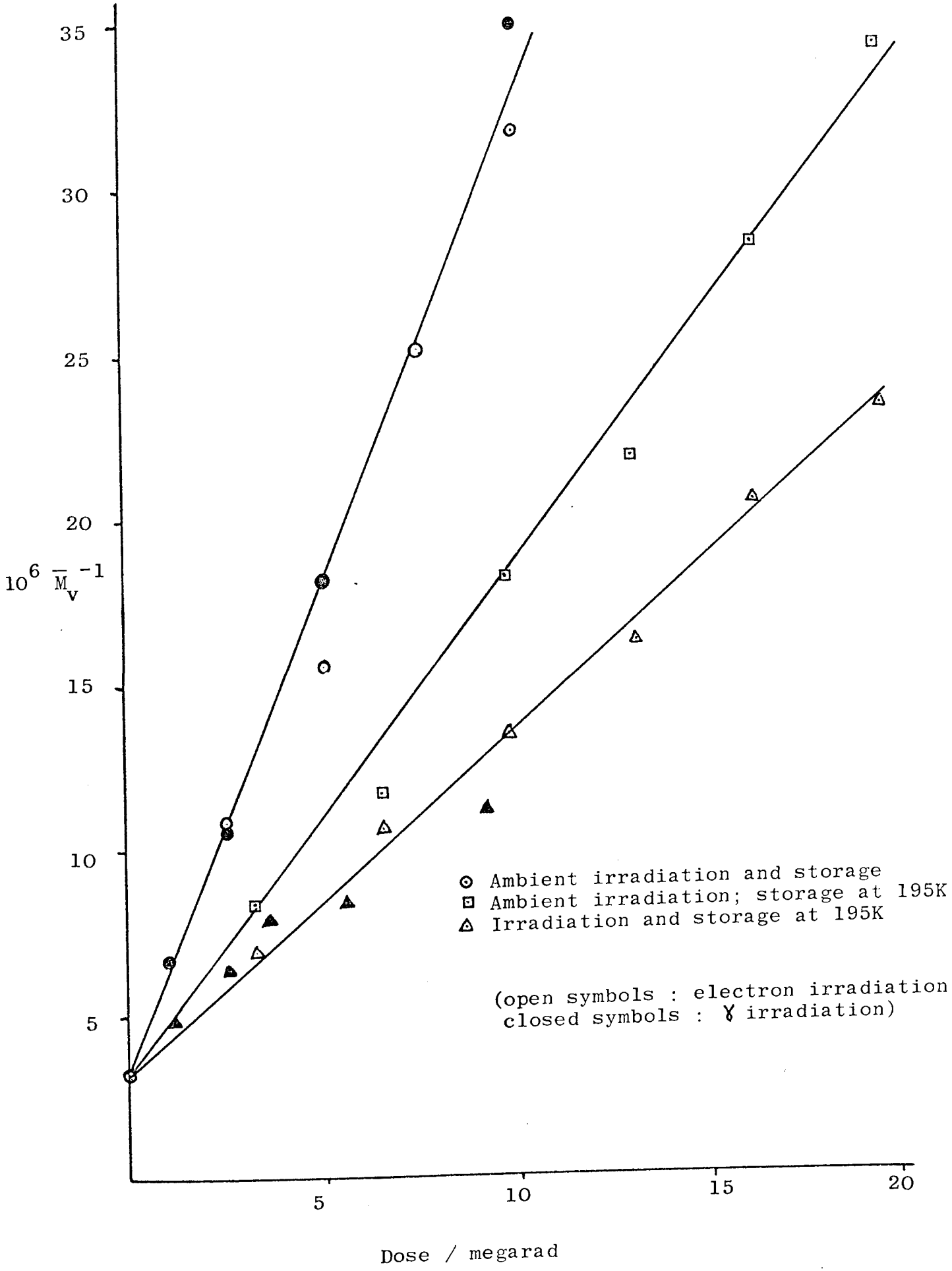

Fig. 3.2 Plots of $10^6 \overline{M}_v^{-1}$ vs. radiation dose under different conditions for isotactic polypropylene in air.

195 K until measurements were made, showed similar but smaller decreases in $\bar{M}_v$. When irradiated and stored at room temperature the changes in $\bar{M}_v$ over a prolonged period (up to 22 months), were found to be negligible.

3.4.4 Miscellaneous Molar Mass Results.

In this section are collected the results obtained under various irradiation conditions and pre-irradiation treatments. Unless stated otherwise the polymer was unstabilised polypropylene powder and the irradiation dose was 2.5 megarad (electron) at 195 K.

Table 3.4 Molar mass data of irradiated polypropylene.

Sample / Conditions / Dose	η_{sp}/c	$[\eta]$	$\bar{M}_v \times 10^{-4}$	G(s)
Vacuum	2.07	1.92	25.1	0.92
Vacuum; 3.48 Mrad(γ)	1.82	1.705	21.6	0.98
Nitrogen	1.99	1.855	24.0	1.04
Hydrogen	1.62	1.53	18.7	1.90
Nitric oxide	1.79	1.675	21.1	1.46
Sulphur dioxide (273 K)	1.25	1.205	13.3	3.47
Vacuum, then SO_2	1.68	1.58	19.5	1.74
Oxygen	1.60	1.51	18.3	1.96
Air	1.62	1.53	18.7	1.90
Chlorine (273 K)	0.89	0.86	8.5	5.77
Vacuum (pre-irrad. in air 2.5 Mrad)	0.955	0.92	9.35	0.68
Air (pre-irrad. in air 2.5Mrad)	0.795	0.77	7.35	2.74
Air (pre-irrad. in air 10Mrad)	0.51	0.50	4.05	4.94
Air (pre-irrad. in SO_2 2.5Mrad)	0.92	0.89	8.9	2.70
Stereoblock polypropylene unirradiated (Hercules Chem.)	1.645	1.55	19.0	-
Stereoblock polypropylene irradiated 2.5 Mrad	0.71	0.69	6.35	7.57

3.4.5 Ultra Violet Irradiation

Ultra-violet irradiations were made as described in 2.4.4 on non-irradiated poylmers and on samples that had previously been γ-irradiated to a dose of 2.5 megarad. The pre-irradiated polymers had been stored for 6 months to allow decay of any free radical species. Measurements were made on both unstabilised powder and on lightly-stabilised films (2.1.2).

Table 3.5 Molar mass changes caused by ultra-violet irradiation of non-irradiated and pre-irradiated (γ) polypropylene.

Unstabilised powder	Non-irradiated		Pre-irradiated	
Duration of u.v.	$\eta sp/c$	$\bar{M}_v \times 10^{-4}$	$\eta sp/c$	$\bar{M}_v \times 10^{-4}$
0 hour	2.80	36.8	1.055	10.65
1 hour	2.60	33.3	1.02	10.20
3 hours	2.49	31.7	1.00	9.95
6 hours	2.27	28.2	0.955	9.35
18 hours	1.92	23.0	0.855	8.05
30 hours	1.845	21.9	-	-
66 hours	1.75	20.5	0.865	8.20
Stabilised film				
0 min	2.33	28.4	0.93	9.05
2 min	2.32	28.2	-	-
6 min	2.19	27.0	-	-
24 min	1.94	23.3	-	-
40 min	1.675	19.5	-	-
60 min	1.67	19.4	0.885	8.45
180 min	1.62	18.6	0.94	9.15
360 min	1.63	18.8	0.87	8.25

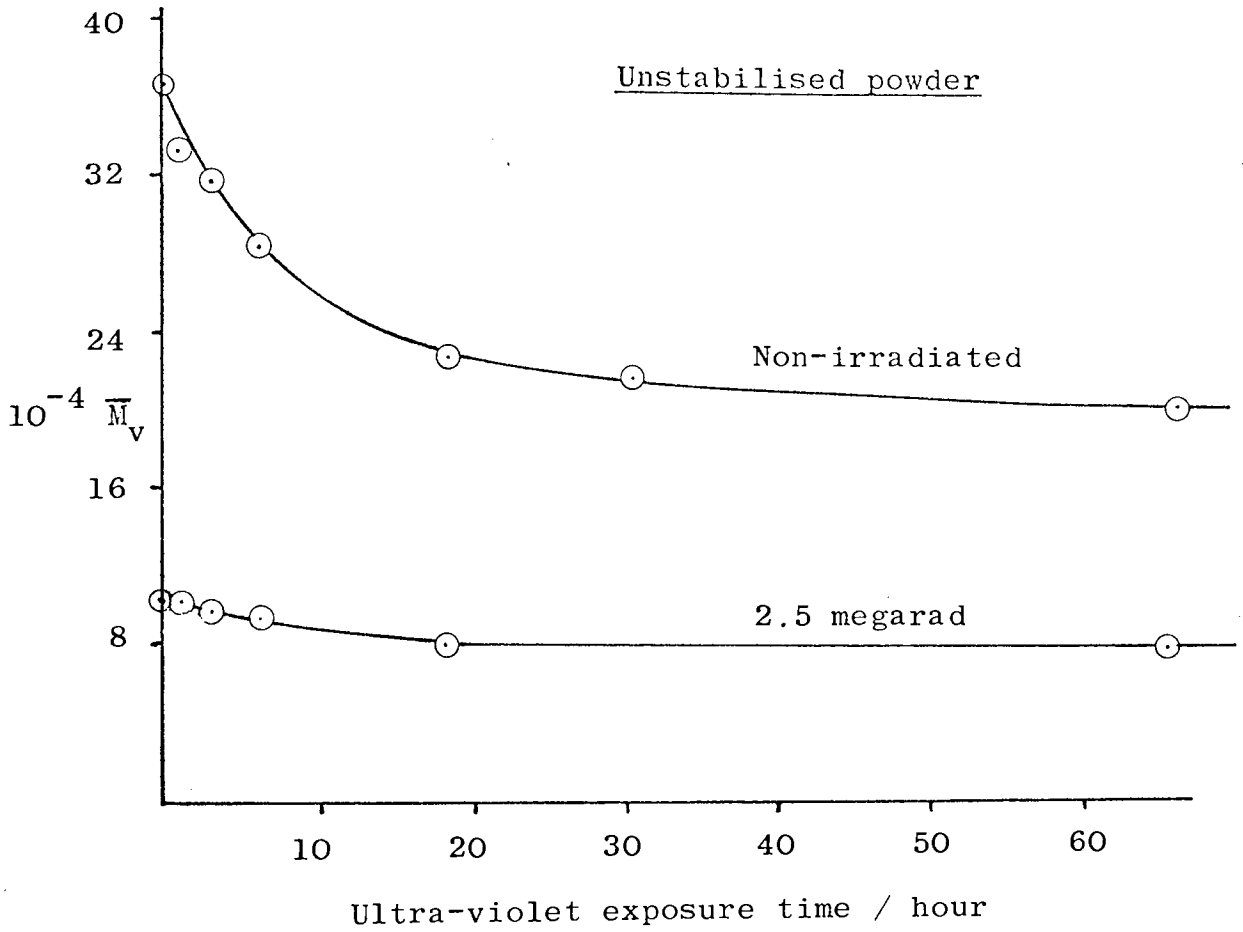

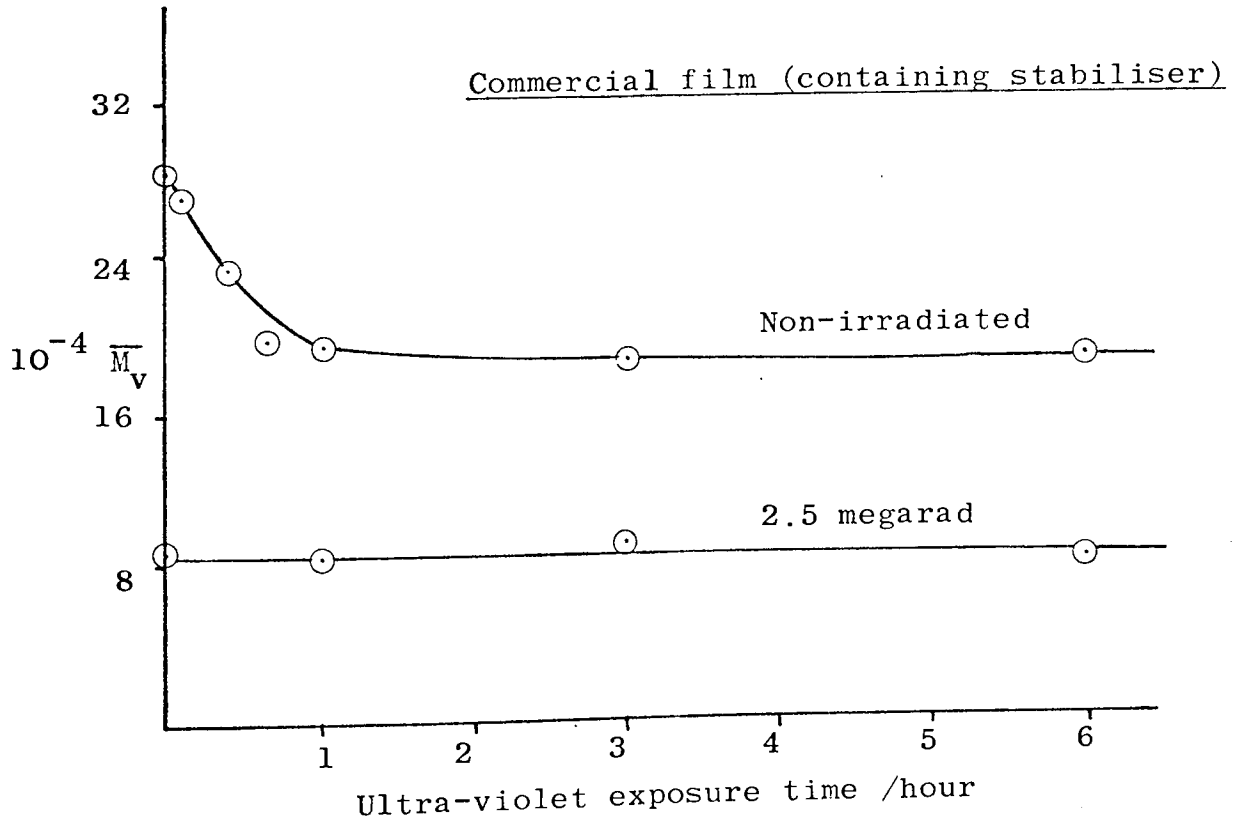

Fig. 3.3 Plots of $\overline{M}_v$ vs. ultra-violet exposure time for non-irradiated and pre-irradiated (γ) polypropylene.

Figure 3.3 is a plot of $\eta sp/c$ vs. duration of ultra-violet radiation. Plots of $1/\bar{M}_v$ vs. duration were not linear indicating that the scission process is non-random. Tensile testing of the pre-irradiated and photolysed film showed that greatly increased embrittlement occurred compared to the effect of either individual process. (Section 3.1.4).

3.4.6 Melt Flow Index.

The melt flow index of irradiated unstabilised polypropylene powder was found to be too large to be accurately measured. Measurements were made on stabilised polypropylene pellets (F E 61) that had been γ-irradiated to a dose of 2.5 megarad at 295 K. The results are given below together with corresponding measurements of $\eta sp/c$ and $\bar{M}_v$.

Table 3.6 Comparison of melt flow index and solution viscosity data.

Polymer	M.F.I	$\eta sp/c$	$\bar{M}_v \times 10^{-4}$	$\log_{10}\frac{600}{MFI}$
Non-irradiated powder	0.98	2.80	36.8	2.79
2.5 Mrad irradiated powder	-	0.945	9.3	-
FE 61 Unirradiated	0.78	2.96	39.4	2.92
Irradiated FE 61 (4 days)	10.85	1.61	18.4	1.72
Irradiated FE 61 (6 months)	11.60	1.68	19.5	1.71
Irradiated FE 61 (12 months)	13.14	1.62	18.5	1.66
Irradiated FE 61 (18 months)	9.95	1.70	20.0	1.76
Irradiated FE 61 (21 months)	12.50	1.65	19.1	1.65

The time in brackets is the time of storage after irradiation.

The values of solution and melt viscosity are seen to be approximately related by the empirical equation

$$\eta sp/c = \log_{10} (600 / MFI)$$

Assuming that this relationship applied to the unstabilised irradiated powder a melt flow index of 68 may be calculated, which value accounts for the experimental difficulties in its measurement.

3.5 Atactic Polypropylene.

Two samples of atactic polypropylene were used. Sample A was obtained by ether extraction (section 2.1.4) and Sample B was used as supplied (by Hercules Chemical Company). The radiation dose was 2.5 megarad (γ) in air at 295 K. The number average molar mass $\overline{M}_n$ was determined by vapour pressure osmometry, as illustrated by the results for sample A (non-irradiated).

Table 3.7 Calibration data for vapour pressure osmometer (V.P.O.)

Benzil concentration c /10^{-3} mol dm^{-3}	Δ R / ohm	$\Delta R\ c^{-1}$ / ohm dm^3 mol^{-1}
0.64	0.16	250
1.60	0.40	250
4.00	0.985	246
10.00	2.38	238
25.0	5.60	224
50.0	10.60	212

A graph of $\Delta R/c$ vs. c was drawn from which the apparent molar concentration and apparent molar mass of the polymer solutions could then be calculated.

Table 3.8 V.P.O. data obtained with non-irradiated atactic polypropylene (Sample A)

Polymer Concentration /g dm^{-3}	ΔR /ohm	$\Delta R\ c^{-1}$ /ohm dm^3 mol^{-1}	Apparent Molar Conc^n /10^{-3} mol dm^{-3}	$10^6/\bar{M}_n$ (apparent)	$\bar{M}_n$ (apparent)
40	2.99	235	12.72	318	3144
30	2.20	238	9.24	308	3245
20	1.40	243	5.76	288	3471
10	0.67	247	2.71	271	3694
6	0.40	249	1.61	267.6	3735
0 (by extrapolation)				258.4	3870

The true molar mass was then found by extrapolation of the linear plot of $1/M_n$ (app) vs. concentration to zero concentration. The values obtained together with the results of the solution viscosity measurements (3.3.1) are given below :

Table 3.9 Molar mass data for atactic polypropylene

Sample A	$\bar{M}_n$	$[\eta]$	k'	$\bar{M}_v$	$\bar{M}_v/M_n$
Non-irradiated	3870	0.250	0.420	16 600	4.29
Irradiated	3600	0.232	0.428	15 000	4.18
Sample B					
Non-irradiated	5980	0.307	0.438	22 000	3.68
Irradiated	5320	0.266	0.435	18 110	3.40

Measurements on both samples stored in solution and in the solid state

for up to 18 months, showed that no post-irradiation changes in molar mass occurred.

3.6 Discussion.

3.6.1 Effect of Radiation Dose ; G-values.

The single point method of $\bar{M}_v$ determination afforded a convenient if limited measure of the extent of chain scission. The Huggins constant k' was found to be unaffected by irradiation for both isotactic (3.4.1) and atactic (3.5) polymers. The plots of $1/\bar{M}_v$ vs. dose (Figure 3.2) are seen to be linear over the dose range studied. This indicates that a random scission process is taking place. The ratios of $\bar{M}_v/\bar{M}_n$ for the atactic polymer and results previously recorded in the literature [126] suggest that a broad initial molar mass distribution is present. From the argument presented in 1.2.6 curved plots of $\bar{M}_v^{-1}$ vs. dose might be expected at low doses but this is not apparent. Keyser Clegg and Dole[40] have similarly found linear plots using samples with a broad initial distribution.

The exact relationship between $\bar{M}_v$ and $\bar{M}_n$ is necessary to calculate the number of chain scissions and hence G(s). The G(s) values in Table 3.10 are those calculated for various assumed initial and final distributions, using equation 1.2 to find the radiation yields. Both γ and electron irradiation produce the same molar mass changes under identical temperature and storage conditions.

Table 3.10 G(s) values for isotactic polypropylene having various assumed molar mass distributions (irradiations in air).

$\overline{M}_v/\overline{M}_n$ ratio		G - value (scission)		
Initial	Final	A	B	C
1.88	1.88	2.00	2.93	5.52
3.00	1.88	1.67	2.61	5.19
5.00	1.88	1.18	2.13	4.70
3.00	3.00	3.16	4.66	8.76
5.00	5.00	5.33	7.85	14.66

A ; Irradiation at 195 K, storage at 195 K.

B ; Irradiation at 312 K, storage at 195 K.

C : Irradiation at 295 K, storage at 295 K (several days).

N.B. $\overline{M}_v/\overline{M}_n$ = 1.88 for a random distribution.

Since random scission will lead to a random molar mass distribution most likely G (s) values are in the following ranges

G(s) = 1.20 - 2.00 for irradiation and storage at 195 K.

G(s) = 2.13 - 2.93 for irradiation at 312 K, storage at 195 K.

G(s) = 4.70 - 5.52 for room temperature irradiation and storage.

These results are further discussed in section 3.6.2.

The results for atactic and stereoblock polypropylene show that although the changes of molar mass are small, the calculated G-values for scission are slightly higher than for isotactic polypropylene. The G(s) values for irradiation at room temperature are given below.

Table 3.11 G(s) values for atactic and stereoblock polypropylene.

Polymer	From $\overline{M}_n$	From $\overline{M}_v$ (assuming random distribution)
Sample A	7.5	4.7
Sample B	8.1	7.0
Stereoblock	-	7.6

These results should only be regarded as approximate since they were obtained in a region of molar mass measurement where neither vapour pressure osmometry or solution viscometry is particularly accurate. The results were also calculated for a single radiation dose only (2.5 megarad). The results do however show that considerable scission also occurs in systems that are not capable of trapping free radicals.

3.6.2 Effects of Radiation Temperature and Storage.

Table 3.3 shows that more chain scission occurs at higher irradiation temperatures and that the final extent of scission is affected by the storage temperature and time before measurement. It is probable that equal chain scission occurs initially in each case. However at low temperatures during and following irradiation the movement of chain fragments away from one another is reduced, and recombination can occur, and thus less permanent scission is observed.

The dissolution process in stabilised decalin does not appear to cause further chain scission and flow times were normally found to be stable for several hours at 130°C. It is possible that the chain fragments of irradiated polymers were in fact stabilised by hydrogen abstraction from either the solvent or antioxidant during measurement.

The decrease in molar mass of samples irradiated at 195 K and measured at intervals during room temperature storage (3.4.3) shows an approach towards the molar mass obtained by irradiation and storage at 295 K. The results below illustrate that the increase in G(s) decreases with irradiation dose.

Table 3.12 Effect of storage at room temperature on polypropylene irradiated to various doses at 195 K.

	2.5 Mrad	5.0 Mrad	10.0 Mrad
Initial G(s)	2.32	2.10	2.01
Final G(s)	5.15	4.25	2.80

The smaller increase of samples irradiated to higher doses may be caused by the second-order process of radical recombination. This will produce a proportionately larger decrease in radical concentration in samples having greater initial concentrations.

3.6.3 Irradiations in Various Gases and Effects of Pre-Irradiation.

The results given in section 3.4.4 allow calculation of G(s) for the various systems studied. The G(s) valuesgiven in 3.4.4 can only be regarded as approximate since they were in each case obtained at a single irradiation dose and calculated by assuming random distributions before and after irradiation.

The values of G(s) in vacuum and nitrogen are similar. In hydrogen, the G(s) is twice that in inert atmospheres, and is similar to that found in oxygen and air. It is probable that polymer radicals

abstract hydrogen atoms from the hydrogen atmosphere before recombination of chain fragments takes place. This would encourage permanent chain scission. Within experimental error, equal chain scission occurs in pure oxygen and air.

In sulphur dioxide and chlorine increased chain scission is encountered, but this may be caused partly by the higher irradiation temperature (273 K) which is above the glass transition temperature. Irradiation in vacuo, followed by exposure to sulphur dioxide, produces more chain scission than exposure to air following vacuum irradiation.

Pre-irradiation whether in air or in sulphur dioxide, produces an increase in G(s) when irradiated again. This probably results from decomposition of RO_2H and RSO_2H groups that have formed from previous radical decay in the polymer. The G(s) values for the pre-irradiated polymers were calculated from the additional scission caused by the second irradiation.

3.6.4 Ultra-violet Irradiation.

The reduction in molar mass caused by ultra-violet radiation is much greater in non-irradiated polypropylene than in pre-irradiated (γ) samples. This was observed for both powder and film samples (Figure 3.3). The shorter time to cause molar mass changes in the film samples probably results from the more even absorption of the ultra-violet radiation. The presence of ozone during photolysis was evident and may have some bearing on the results obtained.

Degradation of pre-irradiated polymer through photolytic decomposition of hydroperoxide groups causing reactions such as

$$-CH_2-\underset{\underset{O_2H}{|}}{\overset{\overset{CH_3}{|}}{C}}-CH_2- \xrightarrow{h\nu} -CH_2-\underset{\underset{O}{||}}{\overset{\overset{CH_3}{|}}{C}} + HO-CH_2-$$

might have been expected to produce considerable chain scission. E.S.R results (4.3.6) suggest however that partial reformation of peroxy radicals is the predominant reaction.

The relatively large decrease in molar mass of the non-irradiated polymer may be caused by the presence of 'weak'bonds in the backbone of the polymer molecule, and this suggestion is favoured by the non-random nature of the scission process. The molar mass of the polymer appears to reach a stable value following the rupture of these bonds. Pre-irradiated polymers are unlikely to possess any remaining weak bonds in the main polymer chain.

3.6.5 Melt Viscosity.

The melt flow index (and melt viscosity) is affected more by high energy irradiation and chain scission than any other single physical property. Even polypropylene in solid pellets and containing stabilisers showed a 15X increase in melt flow index following an irradiation dose of 2.5 megarad. This results from the strong molar mass dependence of melt viscosity, which Fox [131] has shown is related to $\overline{M}_w$ raised to a power 3.4. The molecular mobility of the polymer in the bulk (melt) state is clearly greatly increased by irradiation, and it is probable that a similar increase of mobility is also present in the solid state.

CHAPTER FOUR : ELECTRON SPIN RESONANCE

4.1 Introduction.

4.1.1. Basic Theory.

Whenever there are unpaired electrons in an atom or molecule, then they will act as magnetic dipoles and will align themselves in the direction of the applied magnetic field. The material is said to exhibit paramagnetism. Paramagnetic properties are exhibited most widely by free radicals and the ions of transition metals. One method of studying paramagnetic materials is the resonance method termed electric spin resonance (E.S.R.) or electron paramagnetic resonance (E.P.R.).

In the presence of an applied magnetic field there are only two allowed orientations of the spin and magnetic moments - parallel and antiparallel to the field direction. The electron has a spin $S = \frac{1}{2}$ and in accordance with quantization rules its energy level is split into $2S + 1 = 2$ sublevels (Zeeman effect). The energy difference between the two levels in a magnetic field strength H is given by

$$\Delta E = g\beta H \qquad \ldots\ldots (4.1)$$

in which g is the spectroscopic splitting factor, which for a free electron has the value 2.00232 and β the Bohr magneton, given by

$$\beta = \frac{eh}{4\pi mc} = 0.927 \times 10^{-27} \text{ J gauss}^{-1} \quad \ldots(4.2)$$

All of the electrons are divided between the two sublevels as indicated in Figure 4.1.

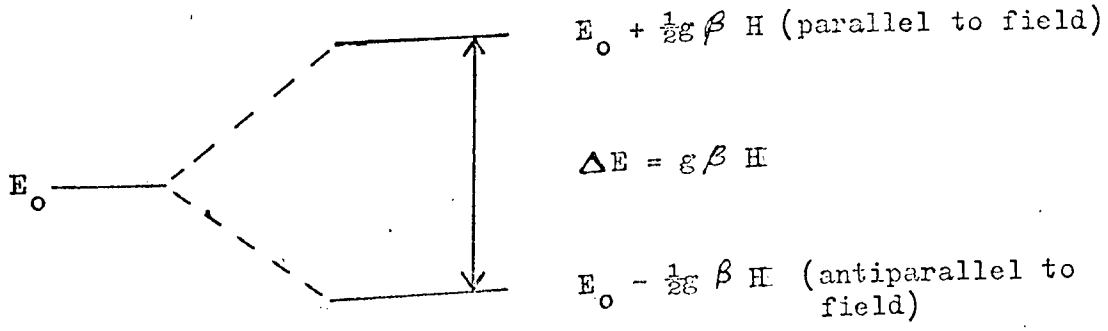

Figure 4.1 Splitting of electron energy levels in magnetic field.

The populations, n_1 and n_2, of the two energy levels is given by

$$\frac{n_1}{n_2} = e^{-\frac{\Delta E}{RT}} \qquad \ldots\ldots (4.3)$$

Transitions between these levels may be induced by interaction with high frequency electromagnetic radiation in a direction normal to the applied magnetic field. There is a net absorption of energy, and maximum absorption will occur when the quantum condition

$$\Delta E = h\nu = g\beta H \qquad \ldots\ldots (4.4)$$

is satisfied in which ν is the frequency of the applied radiation and h the Planck constant. In principle any combination of magnetic field strength and frequency of radiation satisfying Equation 4.4 should produce E.S.R. absorption. In practice most E.S.R. work uses microwave radiation of frequency 9000 - 10,000 MHz (X-band); the magnetic field corresponding to this frequency is about 3200 to 3600 gauss for a free electron. Usually, the microwave frequency is held constant while the magnetic field sweeps through the resonant condition. The dependence of the power absorbed as a function of magnetic field strength generally called an E.S.R. spectrum is shown in Figure 4.2. The E.S.R. spectrum is characterised by the following quantities : g-factor, width and shape of the lines, and the intensity.

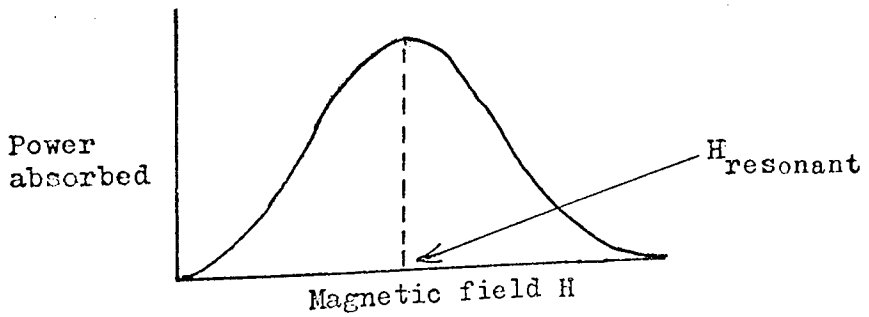

Figure 4.2 E.S.R. singlet spectrum.

In order to increase sensitivity, the absorption signal is not usually measured directly, but the first derivative is obtained, by modulation of the applied magnetic field. In this case the d.c. magnetic field sweeps slowly across the resonant value while a simultaneous low-amplitude radio frequency magnetic field is applied. The effect of this is shown in Figure 4.3.

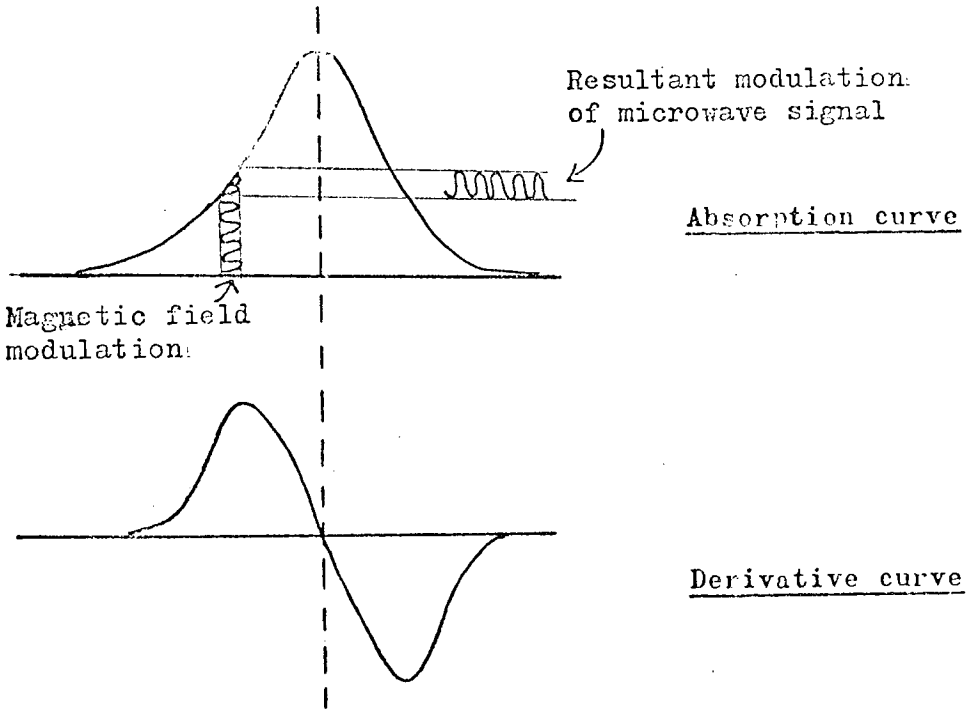

Figure 4.3 First derivative E.S.R. curve from modulation of absorption curve.

The alternating voltage with the modulation frequency is then amplified and rectified by a phase-sensitive rectifier before the signal is fed on to a recorder as the first derivative of the absorption line.

4.1.2 Qualitative Uses of E.S.R.

The spectroscopic splitting factor g, is a measure of the interaction between the spin and orbital motion of the unpaired electron. For

weak interactions, the g-value diverges little from that of the free electron (g = 2.0023). The value of the g-factor can be determined with great accuracy and its measurement is useful both for radical identification and for estimation of the amount of spin-orbit coupling. The width of the E.S.R. spectrum line is determined by the lifetime of the unpaired electrons in the excited state. This lifetime is determined by three processes:

(1) spin-lattice interaction.

(2) spin-spin interaction and

(3) exchange interaction.

Hyperfine structure of E.S.R. spectra results from the interaction of paramagnetic nuclei with an unpaired electron, which produces multiple transitions. Each electronic sub-level is split into $2I + 1$ equally spaced nuclear sub-levels of nuclear spin I. For a hydrogen atom $I = \frac{1}{2}$, and this results in 2 nuclear sub-levels for each electronic level. In practice the unpaired electron often interacts equally with several identical nuclei, producing $2nI + 1$ equally spaced lines. For interaction with n equivalent protons, $n + 1$ lines are observed, whose relative intensities are given by the coefficients of the binomial expansion of n. Interaction with n non-equivalent protons results in 2^n equally spaced lines.

4.1.3 Quantitative Measurements.

Spin concentrations can be measured by E.S.R., since the area beneath the absorption curve is proportional to the number of unpaired electrons. The actual area under the absorption curve depends on many instrumental factors and thus it is usual to compare the area with that of a standard of known concentration measured under identical conditions. Since in most spectrometers the derivative of the

absorption curve is obtained, this must first be integrated before quantitative measurements are made. This allows calculation of the factor relating E.S.R. signal area to concentration of unpaired spins. For a given free radical, the peak-to-peak height on the derivative curve will be directly related to its absorption area and this too can be related to spin concentration.

4.1.4 Radicals in Polymers.

The applications of E.S.R. techniques to polymer systems have been reviewed recently.(53) Applications have included the detection and identification of free radicals during polymerisation. The most common use however has been concerned with the detection, identification and measurement of macroradicals produced by the action of high energy radiation, by photodegradation, or by mechanical degradation of polymers.

4.2. Experimental.

The objectives of the E.S.R. measurements were to identify the radicals produced in irradiated polypropylene and to measure their concentrations following irradiation to obtain information on post-irradiation radical feactions. Radicals produced by irradiation in air and in vacuo were studied, together with some measurements in other gases. The effect of ultra-violet light on mechanical properties has been mentioned (3.1.4) and the radicals produced by photolysis of non-irradiated and pre-irradiated polypropylene were therefore also examined. Atactic and stereoblock polypropylene were studied to observe the effects of tacticity on free radicals, and measurements were also made on solid samples to observe the effects of diffusion controlled reaction with oxygen.

4.2.1 Description of Intruments Used.

Two instruments were used for the E.S.R studies :

(A) A Hilger and Watts 'Microspin' spectrometer, at the University of Aston. The instrument was used in the X-band microwave region together with an automatic frequency control accessory (W 956). A block diagram of the spectrometer is shown in Figure 4.4.[161]

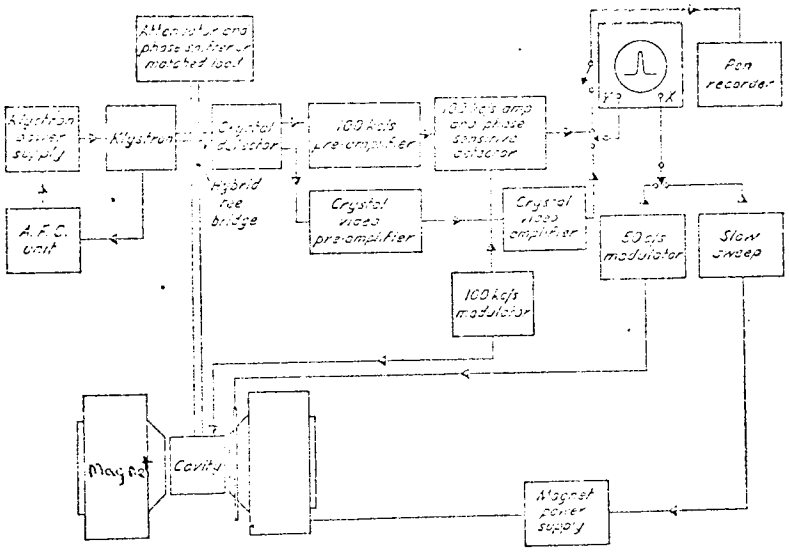

Figure 4.4 Block diagram of a high frequency modulation E.S.R. spectrometer.

The followinginstrumental settings were most frequently used :

Magnetic field sweep	:	500 Gauss
Scan time	:	600 seconds
Time constant	:	6 seconds
Magnet setting	:	270 (approx.)
Modulation current	:	0.24 amp. (max.)

(B) A Varian Associates E-3 E.P.R. spectrometer, in the Department of Physical Chemistry, University of Leicester. This instrument was also operated in the X-band and was fitted with automatic temperature control. The following settings were used for this spectrometer :

Magnetic field sweep	:	500 Gauss
Field setting	:	3200 Gauss
Modulation amplitude	:	1 Gauss
Microwave frequency	:	9.5 GHz
Time constant	:	0.3 second
Scan time	:	240 seconds.

4.2.2 Measurements in air.

E.S.R measurements on samples open to the atmosphere were usually made on approximately 60 mg of irradiated polymer in a thin quartz tube sealed at one end with an overall diameter of 6 mm. It was found for quantitative measurements that a reference standard was necessary and after some initial attempts with D.P.P.H. and Co^{3+}, the most convenient standard was found to be Cu^{2+}. This was introduced by using standard M/1 or M/10 solutions of $CuSO_4 . 5H_2O$ in deionised water. A few milligrams of the selected solution were introduced into a capillary (melting point) tube, weighed, sealed and placed in the centre of the polymer sample. Measurements at low temperatures on the E.3 spectrometer required the use of quartz tubes of maximum diameter 4 mm.

4.2.3 Measurements in Other Environments.

For samples irradiated in vacuo and gases other than air, the procedure described in 2.5.2 was used. The tube containing the sample

was designed so that during the irradiation the measuring portion could be screened by a heavy metal shield. The weighed amount of polymer was contained in an exposed portion of the tube. After irradiation the measuring section of the quartz tube was placed in the spectrometer and examined for the presence of free radicals in the irradiated quartz. If radicals were found to be present they were removed by cautious heating; if not, the tube was inverted to bring the polymer into the measuring region, before inserting into the cavity of the spectrometer.

4.2.4 Radical Decay Rates.

Since no temperature control facilities were available on the Microspin instrument the following technique was used to measure the rates of radical decay. The polymer sample with calibrating standard, was measured initially and then quickly transferred to a separate thermostat, usually in the temperature range 25 - 55°C, and a stopwatch started. After a known time interval the sample was removed and the reaction slowed by immediately transferring to a beaker containing ice and water. After allowing to cool, the sample was then transferred to the instrument and a reading quickly taken. Further measurements were then made in a similar manner at increasing time intervals.

4.3. Isotactic Polypropylene : Results and Discussion.

4.3.1 Electron and γ-radiation in Air.

Electron and γ-radiation produce identical effects, for a given radiation dose in the type of radical produced and its concentration. Immediate effects however could not be observed with the Harwell samples and thus the following refers, in the main, to the Southall (electron) and Leicester (γ) irradiated samples.

The derivative curve (solid line) infigure 4.5 shows a typical result obtained using the procedure in 4.2.4.(B). The broad signal at low field values corresponds to the copper ions introduced as a standard. The signal caused by the polymer is an asymmetric triplet than can be identified as a peroxy radical $RO_2^{\bullet}$. The lack of hyperfine structure in the spectrum prevents a detailed assignment of the nature of R in the $RO_2^{\bullet}$ radical. The parallel and perpendicular components of the triplet are indicated by the symbols $g_{\parallel}$ and $g_{\perp}$ in Figure 4.5.

Maximum structural detail is observable at low scan speed, time constant and modulation current (Figure 4.6) but these conditions could not be used for quantitative measurments since a wide magnetic field range is necessary to include the copper ion spectrum. Overlap of the two adjacent peaks in the $RO_2^{\bullet}$ spectrum was frequently observed immediately after irradiation, but they became more clearly resolved with time and this is shown in Figure 4.7. This change in spectrum shape is probably caused by alterations in the polymer matrix holding the radical, rather than changes in the chemical nature of R in the $RO_2^{\bullet}$ radical.

g-values.

The spectroscopic splitting factor g, for the three peaks in the $RO_2^{\bullet}$ radical spectrum were measured on the 'microspin' instrument. The slowest scan speed (200 gauss / 20 min) and the smallest time constant (Ext. Cap.) were used for these measurements. The spectrum conditions were calibrated using Fremy's salt, potassium peroxylamine disulphonate, which produces a spectrum of evenly spaced lines at accurately known intervals. The g-values were then found by introducing D.P.P.H. (diphenyl picryl hydrazyl) in a capillary tube into the polymer sample. The D.P.P.H. has a known g-value (2.0036) and for this substance the frequency at which absorption occurred

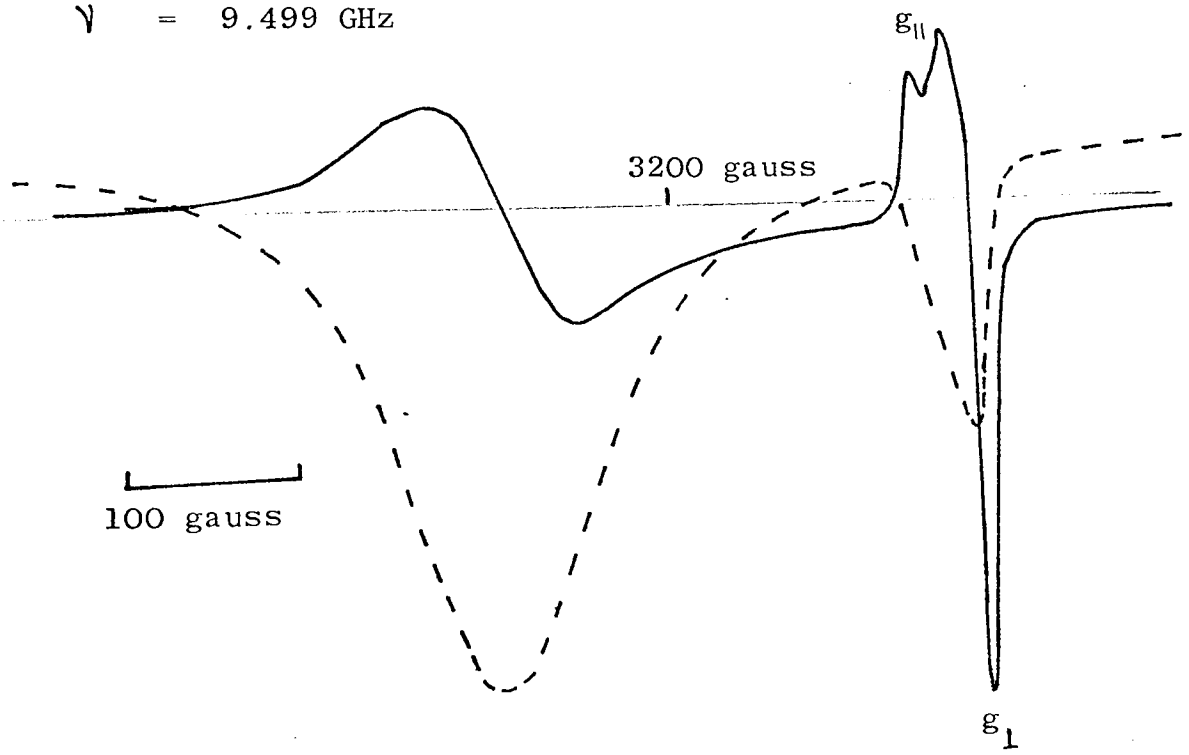

(Scan conditions as in 4.2.1 B).

Fig. 4.5 Derivative and absorption E.S.R. spectra of $RO_2^{\cdot}$ and copper ion standard.

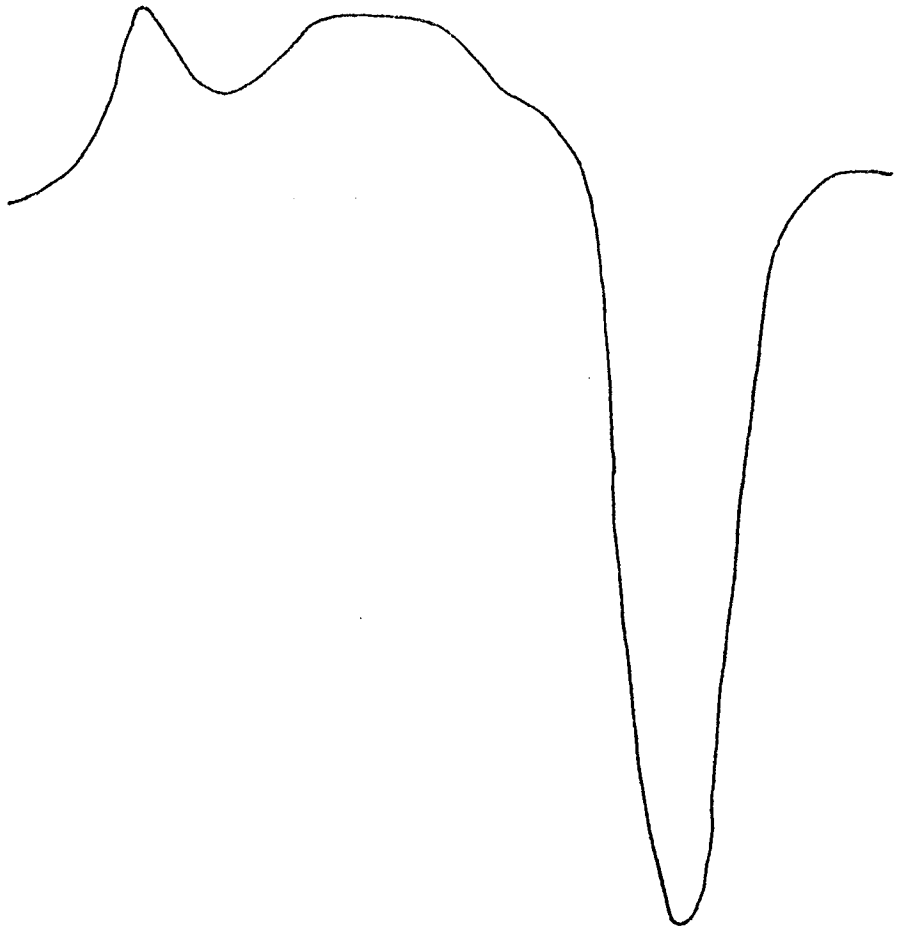

Fig 4.6 E.S.R. spectrum of $RO_2^{\bullet}$ radical in polypropylene measured at 100 gauss / 10 min.

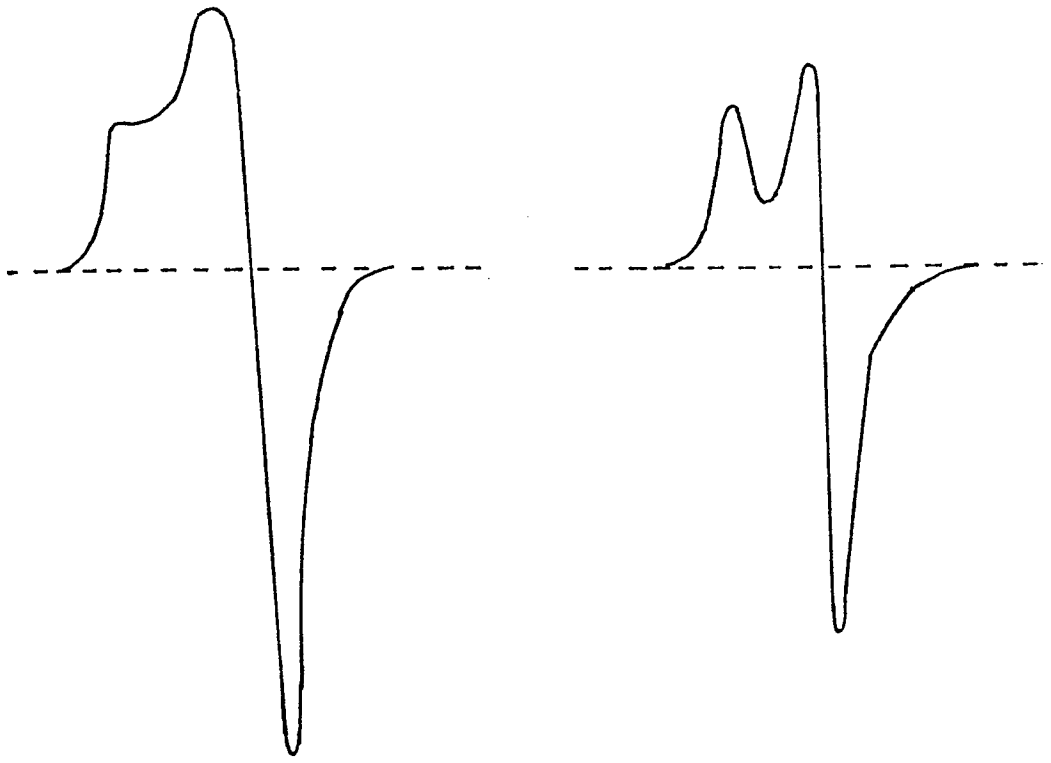

(Scan conditions as in 4.2.1 A)

Fig.4.7 E.S.R. spectrum of $RO_2^{\bullet}$ radical

(a) immediately after irradiation,

(b) after 4 days at room temperature.

was measured accurately. Thus from the relationship in equation 4.4 the magnetic field for the D.P.P.H., $H_{(D.P.P.H.)}$, may be found. The separation on the chart between the polymer peaks and the D.P.P.H. peak was then accurately measured, and using the relationship between chart length and magnetic field for the Fremy's salt, the values of the magnetic field for the polymer was found. The g-values were then calculated, since for a constant frequency

$$g_{(D.P.P.H.)} \; H_{(D.P.P.H.)} = g_{(RO_2^{\bullet})} \; H_{(RO_2^{\bullet})}$$

The following values were found :

$g_{\perp} = 2.0039$

$g_{\parallel} = 2.0268$

$g = 2.0091$ (for the central peak)

Radical concentrations

As described in 4.1.3 the peak-to-peak height was used as a measure of the polymer free radical concentrations. Integration of the derivative peak was carried out instrumentally on the Varian intrument and the absorption curves are shown as dotted lines in Figure 4.5.

For measurments made on the 'Microspin' instrument. no automatic integrator was incorporated and the derivative curves were numerically integrated in a manner similar to that described by Ayscough[132]. The areas under the absorption curves of the polymer radical and copper ions were measured and related to the derivative signal heights by a factor Z;

$$Z = \frac{A_p \; / \; d_p}{A_{cu} \; / \; d_{cu}}$$

where A_p and A_{cu} are the areas under the absorption curves of the polymer and copper ions while d_p and d_{cu} represent the peak-to-peak differential signal heights. When $d_p = d_{cu}$, the factor Z measures the ratio of the polymer radical area to that of the copper ions.

The factor obtained for the peroxy radical under conditions 4.2.2 (A) was

$$z = 0.041 + 0.01$$

and with conditions 4.2.2 (B) was

$$z = 0.035 + 0.01$$

The smaller value obtained using the Varian instrument is probably due to the faster scan conditions for both the derivative and absorption curves, failing to respond to the fine detail of the sharper polymer signal.

The number of radicals in one gram of polymer was calculated as follows :

$$\text{Radicals / gram} = \frac{6.02 \times 10^{23}\ d_p\ m_{cu}\ M_{cu}\ Z}{10^3\ d_{cu}\ m_p}$$

in which m_{cu} and m_p are the mases of copper ion solution and polymer respectively, and M_{cu} is the molarity of the copper ion solution. The values of the initial radical concentrations of samples irradiated in air are given in Table 4.1.

Table 4.1 Initial peroxy radical concentrations produced by irradiation of isotactic polypropylene in air.

Dose/ Megarad	Irrad. Temp/°C	10^{-18} x [Radical] g^{-1}	[Radical] 10^{-18} x g^{-1} Megarad^{-1}	μmoles $RO_2^\cdot$ / mole polymer repeat unit	$G(RO_2^\cdot)$
(a) Accelerated electrons					
2.5	"35"	0.95	0.38	66.4	0.608
2.5	"35"	1.00	0.40	70.0	0.640
2.5	-78	1.17	0.468	81.9	0.749
2.5	-78	1.27	0.508	88.9	0.813
2.5*	-78	1.31	0.524	91.7	0.838
2.5**	-78	1.365	0.546	95.6	0.874
3.25	-78	1.52	0.467	106.2	0.747
2 x 2.5	"35"	1.87	0.373	130.6	0.597
5.0	"48"	1.70	0.343	118.2	0.549
2 x 2.5	-78	2.15	0.430	150.5	0.688
5.0	-78	2.18	0.436	152.7	0.698
2 x 3.25	"39"	2.11	0.325	147.7	0.520
2 x 3.25	-78	2.66	0.410	186.3	0.656
3 x 3.25	-78	3.60	0.369	252	0.590
4 x 3.25	-78	4.81	0.370	337	0.592
4 x 3.25	"39"	3.59	0.276	251	0.442
6 x 3.25	"39"	4.63	0.244	324	0.390
6 x 3.25	-78	6.15	0.324	431	0.518
8 x 2.5	-78	6.56	0.328	459	0.524
(b) γ - radiation (Leicester)					
1.2	-196	0.735	0.613	51.5	0.981
2.49	-196	1.08	0.436	75.6	0.698
3.48	-196	2.14	0.615	150	0.984
5.52	-196	2.96	0.536	207	0.858
9.12	-196	4.64	0.55	326	0.880

The results marked * and ** were obtained with samples that had been previously irradiated to doses of 2.5 to 10.0 megarad respectively, more than 12 months prior to the second irradiation. The 'ambient' temperatures indicated ' ' in Table 4.1 were the estimated ones reached in the irradiation unit when the samples were not cooled, higher dose rates producing more heating of the sample. Plots of initial radical concentration vs. dose are shown in Figure 4.8.

The values of the radical concentrations were reproducible to approximately 10% accuracy. The results show that the radical concentrations increase with radiation dose. There is a downward curvature of the plot in Figure 4.8 when the irradiation was carried out at higher temperatures. The curvature is only slight when samples areheld at a constant low temperature to minimise any radical decay before measurement. The curvature is not apparent in the samples irradiated and measured at -196°C. The samples of polypropylene that had been pre-irradiated, showed slightly higher radical concentrations, on a second irradiation. This increase results from decomposition of hydroperoxide groups.

4.3.2 Effect of increasing temperature on polypropylene irradiated in air at 77 K.

A stoppered tube containing polypropylene powder in air was irradiated to a dose of 2.10 megarad at 77 K and using the variable temperature control facility was measured at intervals of approximately 20 K in the range 95 to 230 K. Some of the spectra obtained using 2 minute scan times, are shown in Figure 4.9. At 95 K the spectrum shows as the principal feature an 8-line entity.

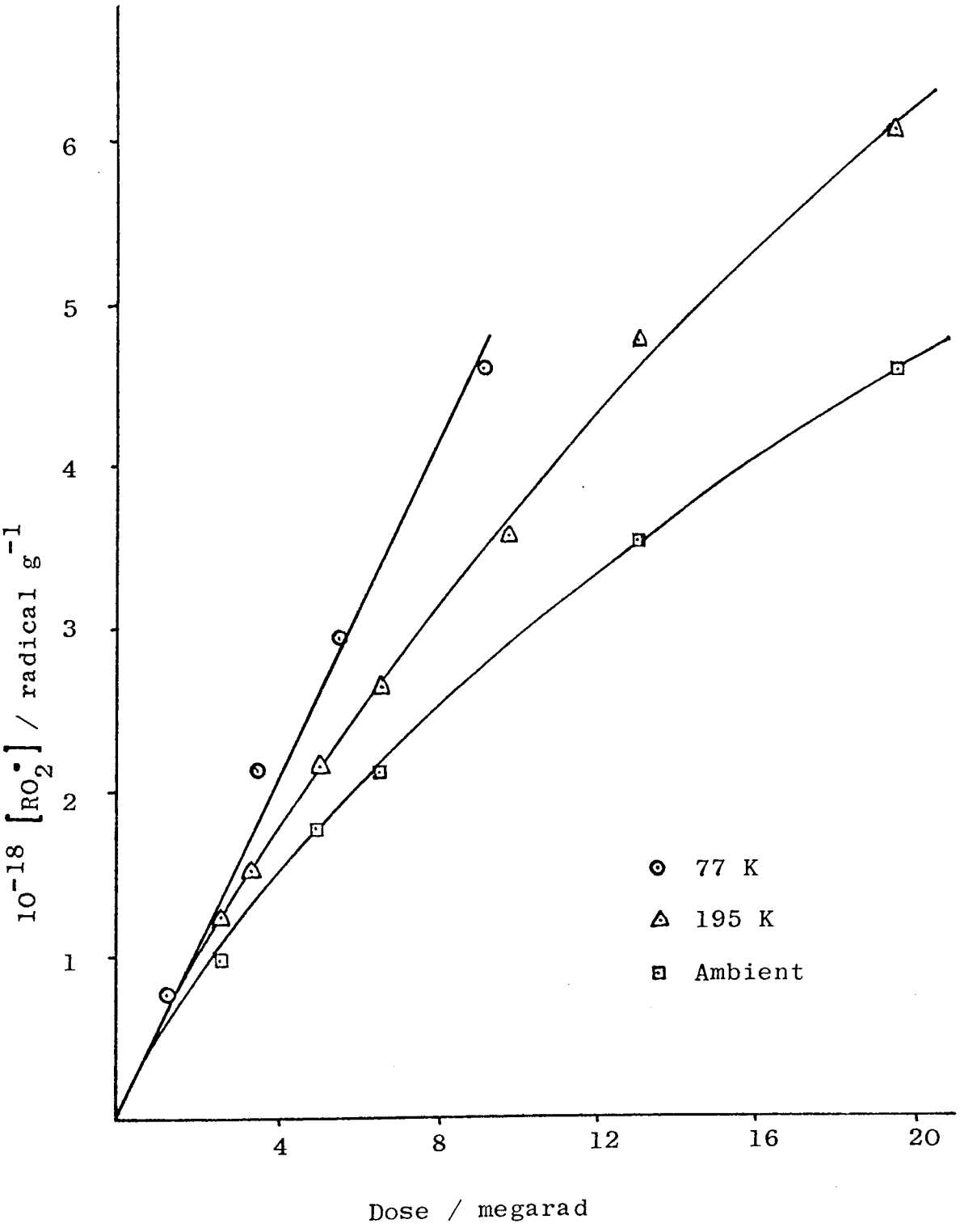

Fig. 4.8 Initial peroxy radical concentration as a function of irradiation dose, showing the effect of irradiation temperature.

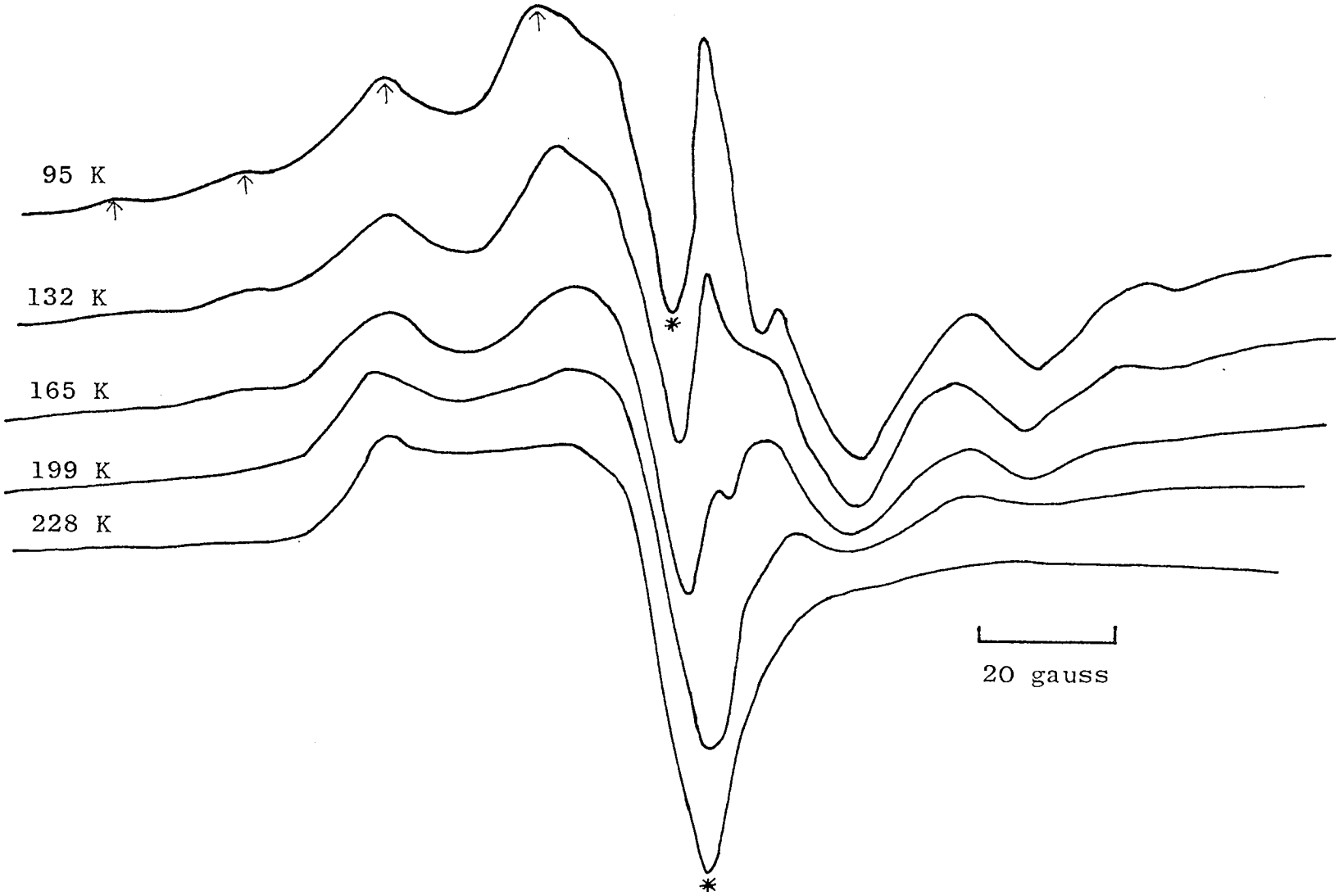

Fig. 4.9 Effect of increasing temperature on the E.S.R. spectra of isotactic polypropylene irradiated in air at 77 K.

This octet is also observed when irradiated in vacuo (4.3.4) and probably corresponds to the radical

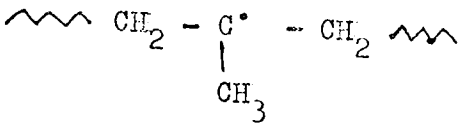

As the temperature increases the octet diminishes in intensity while the asymmetric peak marked * grows. By 199 K the radical is almost completely converted to the peroxy radical $RO_2^{\bullet}$. At 228 K there is no trace of any remaining hydrocarbon radical and the reaction cannot be reversed by lowering the temperature.

Similar experiments (4.3.7) with bulk specimens show that the peroxy radical is only formed slowly, and thus it appears that diffusion of oxygen into the sample after irradiation is necessary for the production of this radical. With the powder sample this diffusion occurs rapidly even at temperatures well below the glass-transition temperature.

The most probable structure of the peroxy radical initially formed can be deduced by assuming that that oxygen becomes attached at the site of the free electron;

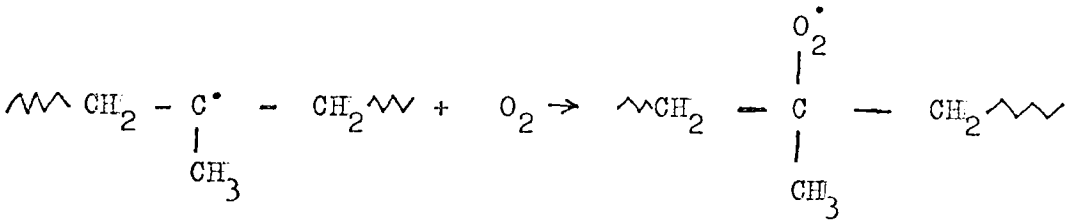

However this structure cannot be confirmed from its own E.S.R. spectrum due to lack of hyperfine splitting.

4.3.3 Decay Rates in Air.

Preliminary observations showed that a few minutes heating at 100°C was sufficient to remove all traces of the peroxy radical but at room temperature some were still present several months after irradiation.

Decay rates were measured as described in 4.2.4. The rates of decay were found to follow second-order kinetics, with a single rate constant over the period observed. The data given in Table 4.2 were obtained with a sample γ-irradiated at Harwell to a dose of 5.0 megarad.

Table 4.2 Radical decay rate data at 25, 40 and 55°C.

	Time/min	$10^{-17} \times [\text{Radical}]\, g^{-1}$	$10^{18} [RO_2^{\cdot}]^{-1}$ / g radical^{-1}
25°C	0	2.06	4.85
	1,440	1.59	6.29
	2,880	1.27	7.86
	5,760	1.05	9.56
	7,200	0.972	10.4
	10,080	0.779	12.8
	11,520	0.779	12.8
	14,400	0.599	16.7
	18,720	0.520	19.2
	20,160	0.461	21.7
40°C	0.0	1.04	9.62
	120	0.867	11.5
	390	0.693	15.9
	1,350	0.629	21.3
	2,940	0.332	30.1
	5,720	0.211	47.4
	6,150	0.197	50.8
	7,130	0.162	62.0
	8,560	0.144	69.3
55°C	0	0.373	26.8
	120	0.296	33.8
	240	0.232	43.1
	330	0.215	46.5
	420	0.194	51.6
	540	0.177	59.9

The second-order plots of $1/\left[RO_2^{\bullet}\right]$ vs. time are shown in Figures 4.10 - 12. The rate constants were found as follows :

$k_2 = 8.0 \times 10^{-22}$ (radical / g)$^{-1}$ min^{-1} (25°C)

$k_2 = 6.73 \times 10^{-21}$ (radical / g)$^{-1}$ min^{-1} (40°C)

$k_2 = 6.20 \times 10^{-20}$ (radical / g)$^{-1}$ min^{-1} (55°C)

Decay rates measured on samples irradiated with accelerated electrons were in agreement to within 10%.

An Arrhenius plot of log k_2 vs. 1/T for these data gave a good straight line (Figure 4.13) from which the Activation Energy = 114.1 kJ mol^{-1} and the pre-exponential factor A = 8.32×10^{-2} (radical /g)$^{-1}$ min^{-1} were obtained.

The rate constant of the decay reaction is given by :

$$k_2 = 8.32 \times 10^{-2}\, e^{-13,700/T} \text{(radical / g)}^{-1}\ \text{min}^{-1}$$

The pre-exponential factor may be more conventionally expressed as $A = 9.24 \times 10^{17}$ (mol dm^{-3})$^{-1}$ s^{-1} assuming a polymer density of 0.9 g cm^{-3}.

Because polypropylene is highly crystalline, and peroxy radicals are considered to be trapped in the crystalline regions, long-range migration of polymer segments is not considered responsible for the decay process. A sequence of hydrogen abstractions according to the chain process

$$RO_2^{\bullet} + RH \rightarrow R^{\bullet} + RO_2H$$

$$R^{\bullet} + O_2 \rightarrow RO_2^{\bullet}$$

will allow movement of the radicals until two radicals were sufficiently close to combine. The approach of the radicals would be controlled by local movements of segments of the polymer chains.

The radicals combining could be any combination of $R^{\bullet}$ and $RO_2^{\bullet}$, viz.

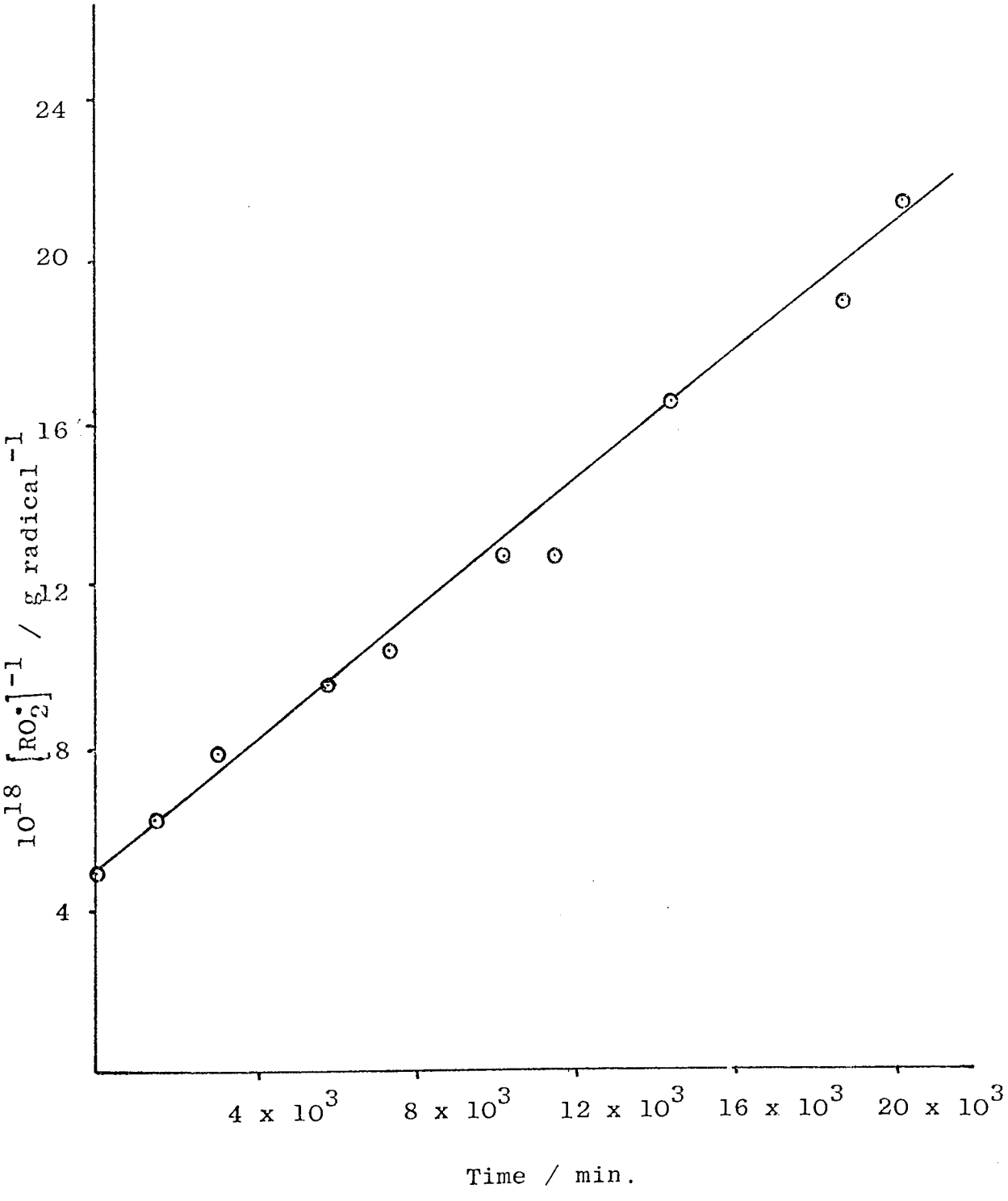

Fig. 4.10 Second-order plot of $RO_2^{\cdot}$ radical decay at 25°C

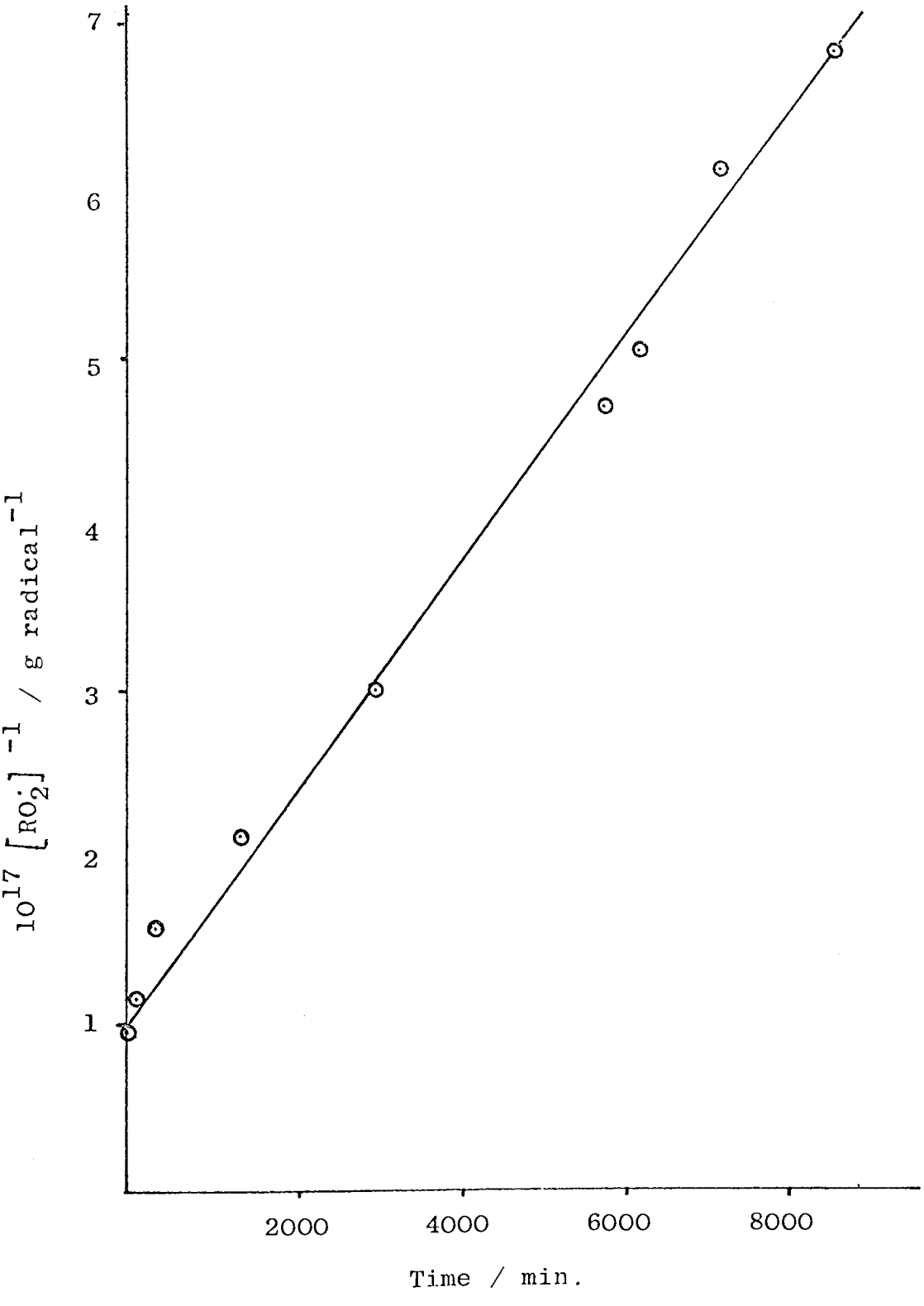

Fig. 4.11 Second-order plot of $RO_2^{\cdot}$ radical decay at 40°C

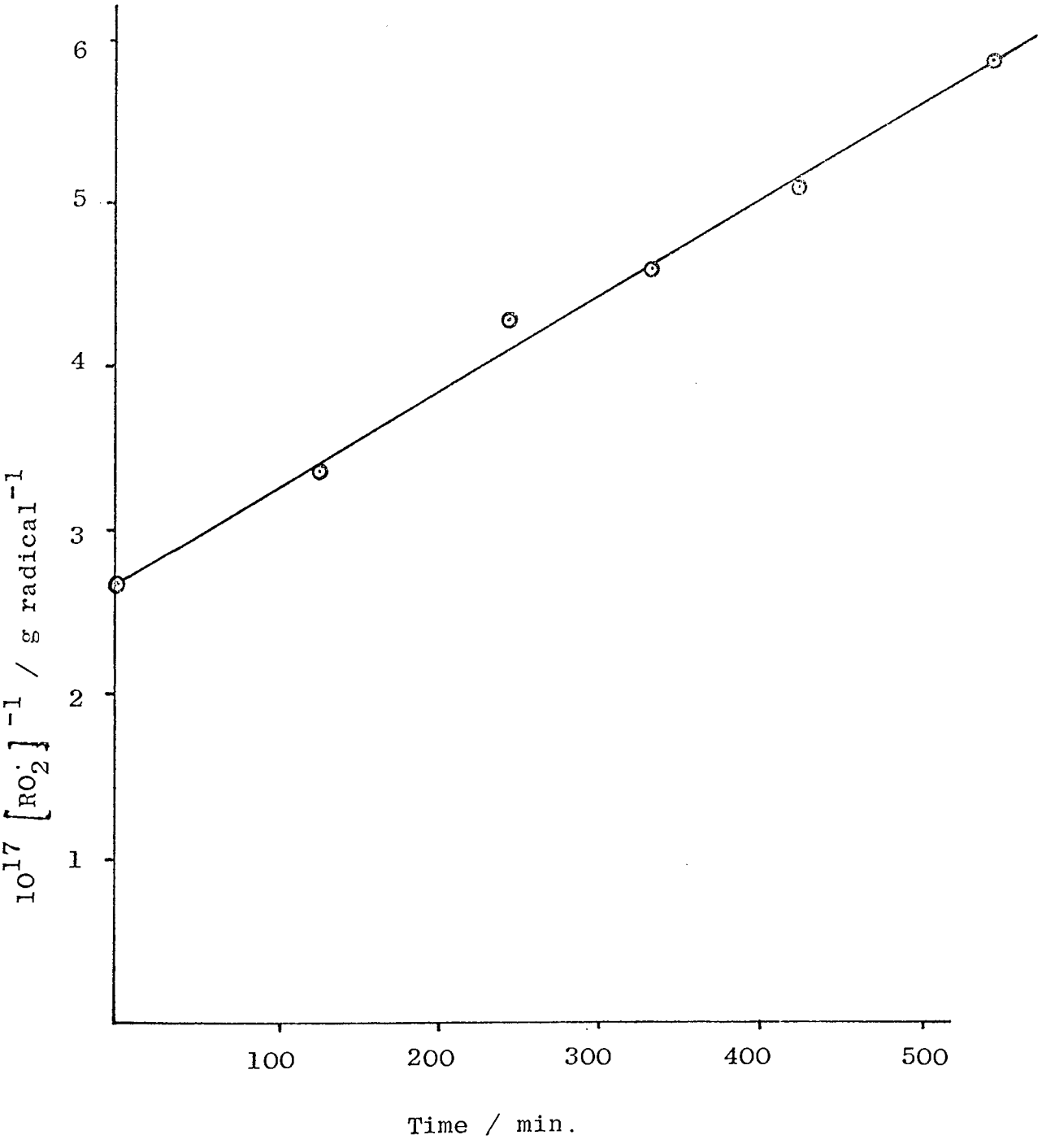

Fig. 4.12 Second-order plot of $RO_2^{\cdot}$ radical decay at 55°C.

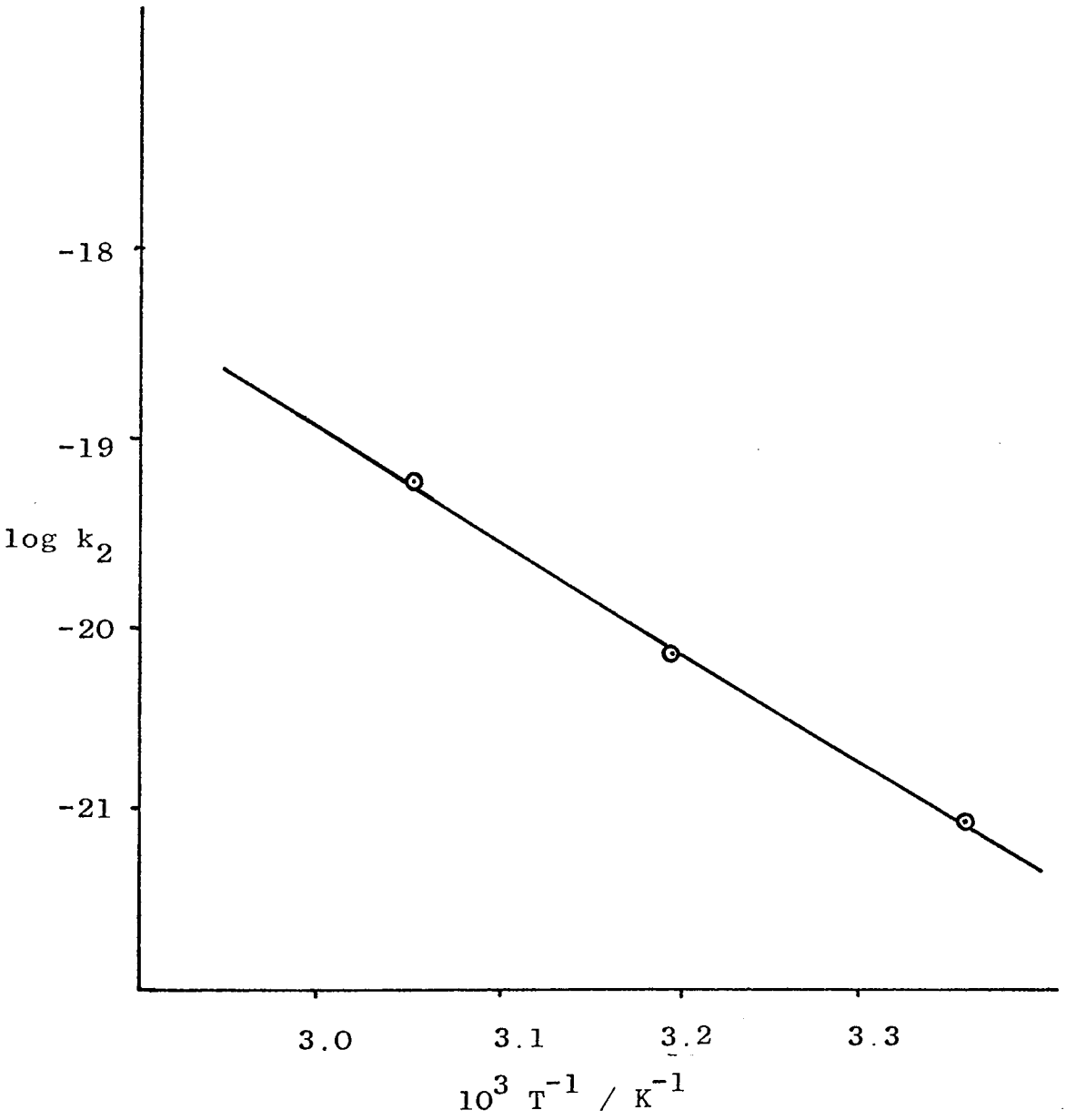

Fig 4.13 Arrhenius plot of log k_2 vs. 10^3 T^{-1} for $RO_2^{\bullet}$ radical decay.

$$RO_2^{\bullet} + R^{\bullet} \rightarrow RO_2R$$

$$RO_2^{\bullet} + RO_2^{\bullet} \rightarrow RO_2R + O_2$$

$$R^{\bullet} + R^{\bullet} \rightarrow RR$$

The rapid diffusion of oxygen in the finely divided polymer would explain the non-appearance of $R^{\bullet}$ in the E.S.R. spectrum. Thus the peroxy radicals decay observed is only an overall decrease caused by removal of free radicals by the reactions given above. This sequential process is confirmed by the large hydroperoxide concentrations that are eventually produced in the polymer (Section 6.2) and which show that several oxygen molecules are absorbed for each radical intially present.

4.3.4 Irradiation in vacuo.

When a suitable evacuation procedure was used (2.5.2), no traces of the peroxy radical were observed after irradiation in vacuo, and thus the amount of dissolved or absorbed oxygen was insufficient to cause detectable peroxy radical formation. At liquid nitrogen temperatures (77 K) the E.S.R. spectrum shown in Figure 4.14 was produced. In the centre of the spectrum there is a signal from the irradiated quartz tube and this is shown dotted, while the dashed line shows the probable spectrum without this contribution. The 'wing' lines of the spectrum are only recognisable as shoulders and are indicated with arrows in Figure 4.14. The splitting of the lines is approximately 23 gauss which corresponds to that expected for interaction with β - protons.[53]

The basic spectrum is an 8-line one which would result from interaction with the 7 near-equivalent protons in the radical

$$\sim CH_2 - \underset{\displaystyle CH_3}{\overset{\displaystyle C^{\bullet}}{|}} - CH_2 \sim \quad .$$

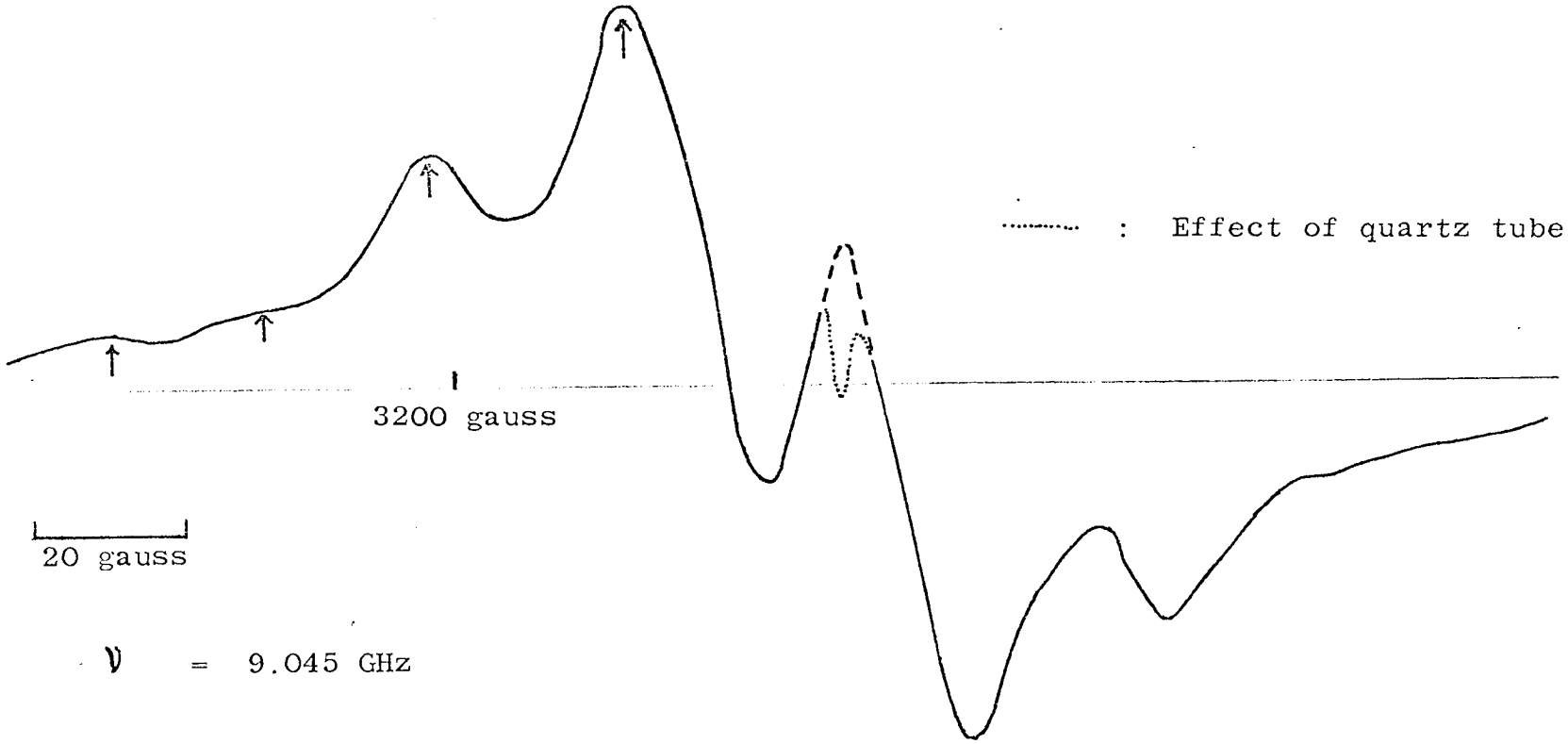

Fig. 4.14 E.S.R. spectrum of γ-irradiated isotactic polypropylene at 77 K in vacuo.

The intensities of the lines are not in the expected binomial distribution (1,7,21,35,35,21,7,1,), because of overlap of the lines.

On warming to room temperature the spectrum becomes more complex (Figure 4.15). The octet can still be identified (with arrows in Figure 4.16) while the additional lines include a series (marked o), again with a line separation of about 23 gauss. This 9-line series may correspond to the radical

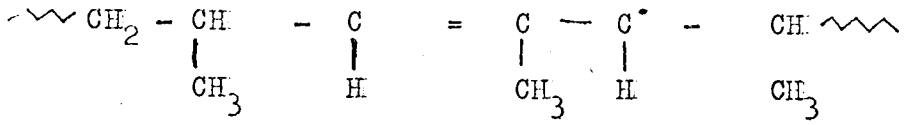

in which there would be interaction with 8 protons. The slight asymmetry in the centre of the spectrum may be due to the presence of some peroxy radicals, in addition to the effect of the irradiated quartz tube. In general, the central portions of E.S.R. spectra are somewhat complex and difficult to interpret.

When the irradiation and measurement is made at room temperature the octet is the major feature (Figure 4.16) although the contribution of the allyl radical can again be observed. The interpretation that it is an unsaturated radical that produces the nine-line series is supported by the observation that in an atmosphere of hydrogen (4.6.5.) the E.S.R. spectrum is unaffected by increase of temperature.

The radical produced by irradiation at room temperature was also measured with copper ions present as an internal standard, so that quantitative measurements could be made. The integrated (absorption) signal was obtained instrumentally and a Z-factor for this radical obtained as described previously, the value being found

$$Z = 0.083 + 0.02$$

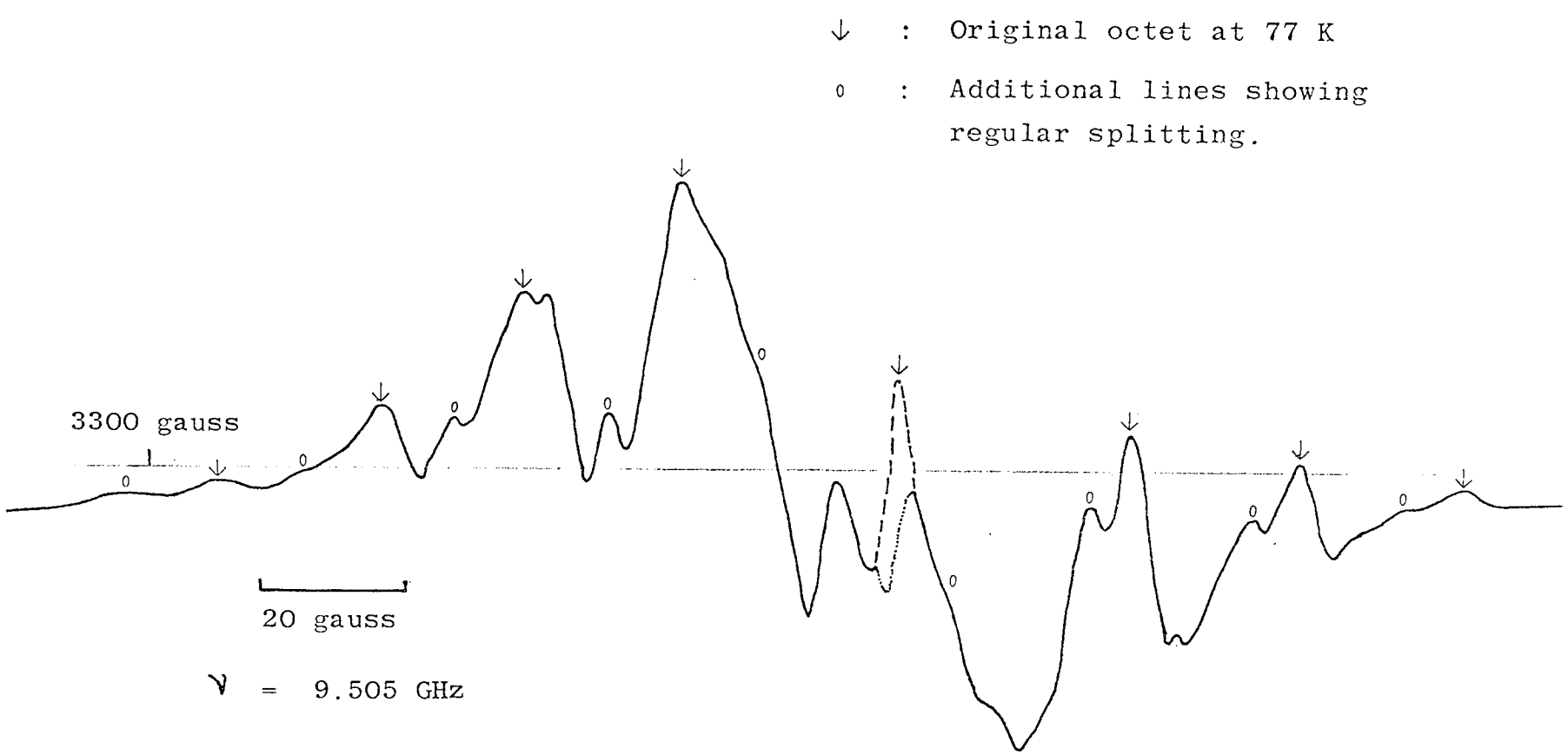

Fig. 4.15 E.S.R. spectrum of polypropylene at room temperature following γ-irradiation at 77 K in vacuo.

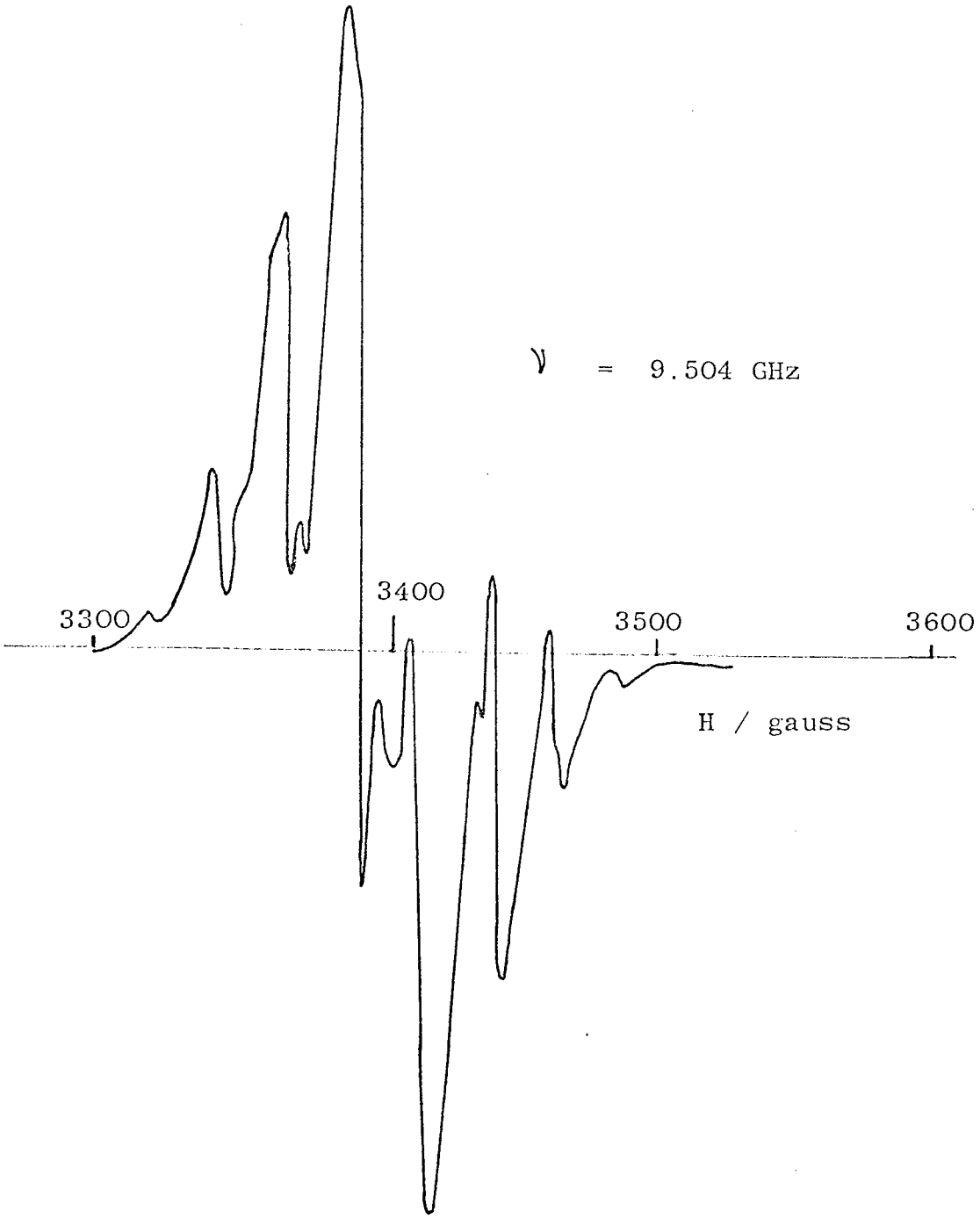

Fig. 4.16 E.S.R. spectrum of polypropylene in vacuo, irradiated and measured at room temperature.

The initial radical concentration found at a dose of 3.48 megarad was 2.25×10^{18} radical g^{-1} giving a G-value of 1.03 (of 0.984 for $RO_2^{\bullet}$). After 30 minutes at 55°C (Section 4.3.4) when the radical concentration was 0.747×10^{18} radical g^{-1}, the vacuum was broken and the E.S.R. spectrum immediately changed to that of the $RO_2^{\bullet}$ radical, the concentration of which was found to be 0.862×10^{18} radical g^{-1}. Within the experimental error of quantitiative E.S.R. measurements, this shows that complete and quantitative conversion of the hydrocarbon radicals to peroxy radicals occurs on exposure to air. The slight difference may be caused by the increasing complexity of the spectrum (Figure 4.19) which would modify the value of the Z-factor given above.

Irradiation in vacuo of samples that had been previously irradiated in air and then stored to allow all of the peroxy radicals to decay produced a complex E.S.R. spectrum. This was considered to be caused by a mixture of hydrocarbon and peroxy radicals, the concentration being approximately 7×10^{17} radical g^{-1} for a dose of 2.5 megarad. (G value = 0.45).

4.3.5 Decay Rates in Vacuo

The decay rate of the hydrocarbon radical at 55°C was measured giving the results in Table 4.3.

Table 4.3 Radical decay data in vacuo at 55°C.

Time/min	Radical $g^{-1} \times 10^{-18}$	$1/[R^{\bullet}] \times 10^{19}$
0	2.25	4.44
4	1.285	7.78
8	0.998	10.02
15	0.836	12.60
30	0.747	13.40

Figure 4.17 is a second-order kinetic plot of these results ($1/R^{\bullet}$ vs. time) which shows that in this case the reaction is not occurring by a simple second-order process. The change from essentially an alkyl radical (8 lines) to a mixture of alkyl and allyl radicals (8 plus 9 lines) described in 4.3.4 as the temperature increased, was again observed. The change of spectrum when the sample is held at 55°C is shown in Figure 4.18.

A probable explanation of the decreasing rate of decay is that if a small quantity of oxygen is present then an enhanced rate of decay would be observed until this is used up. The initial rate of decay is in fact very similar to that obtained in air for $RO_2^{\bullet}$ decay at the same temperature, shown by the solid line in Figure 4.18, while at later stages the $R^{\bullet}$ radical decay rate is considerably slower and similar to $RO_2^{\bullet}$ decay rate in vacuo (see Figure 4.19). It is postulated that the amount of any oxygen present is too small to produce detectable amounts of peroxy radicals.

Decay rates of the $RO_2^{\bullet}$ radical in vacuo were also measured. A sample of polypropylene was irradiated to 2.5 megarad in air with high energy electrons at 195 K and divided

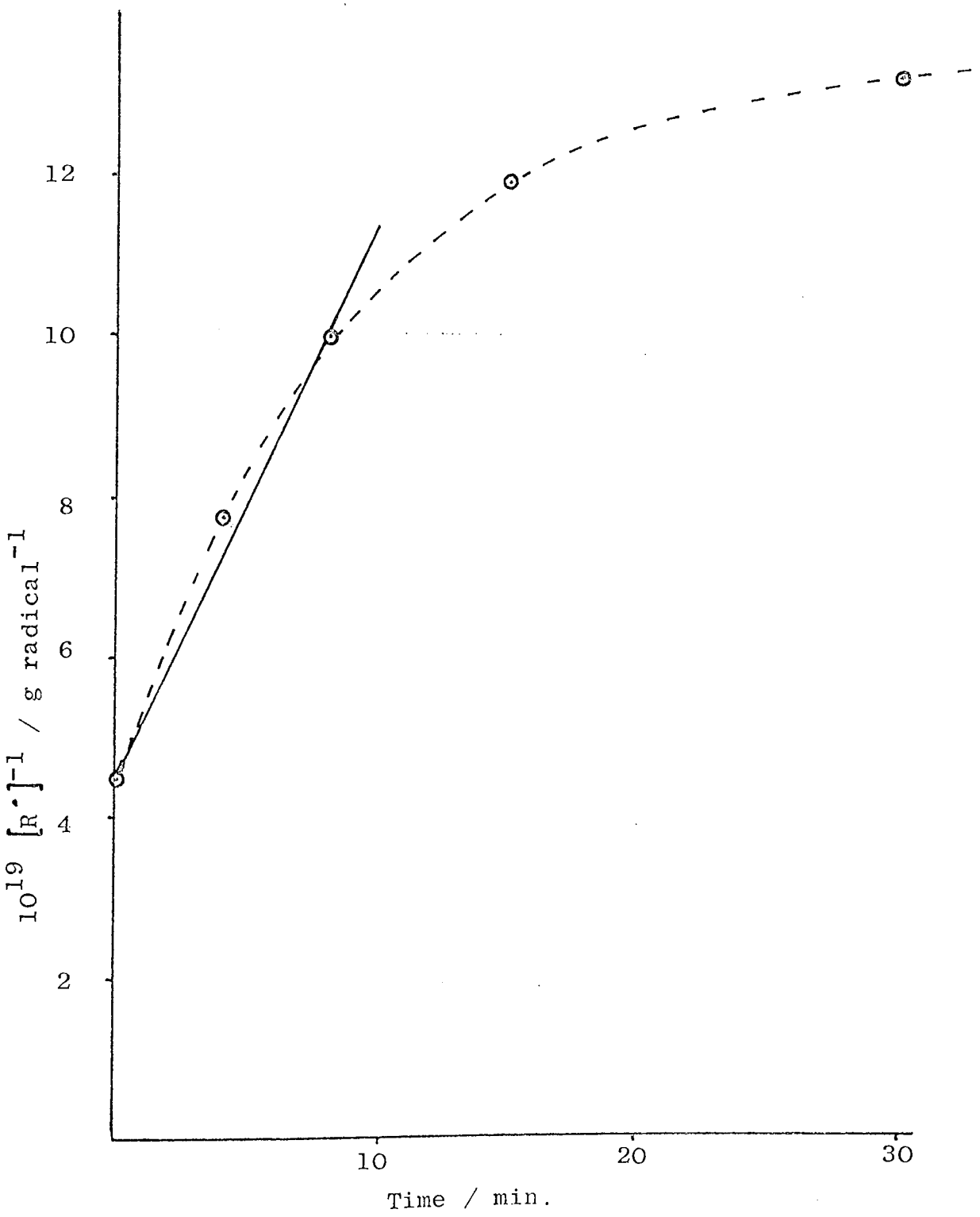

Fig. 4.17 Decay of radical R· in vacuo at 55°C

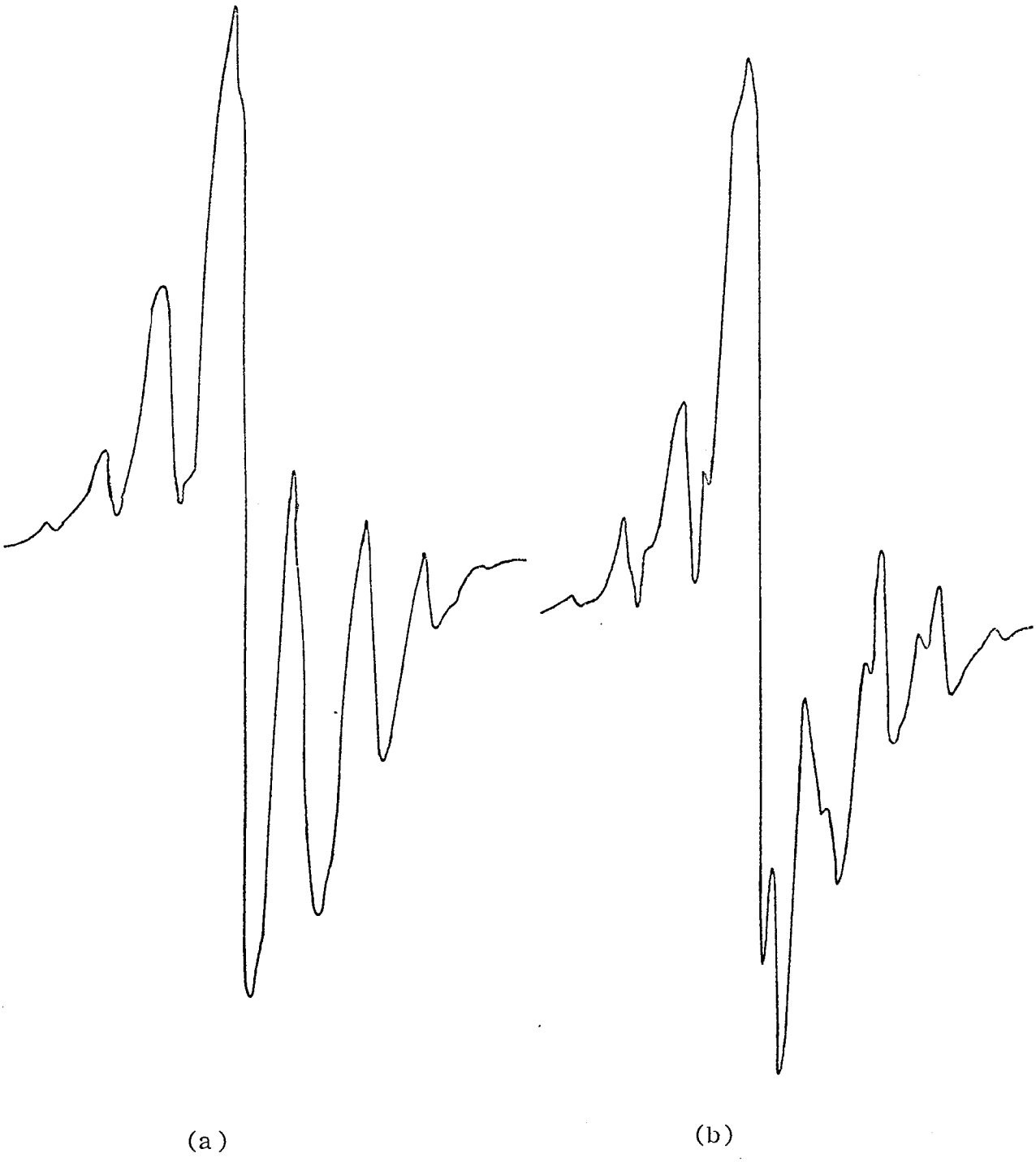

(a) (b)

Fig 4.18 Change of E.S.R. spectrum during radical decay of γ-irradiated polypropylene in vacuo at $55^{o}C$.

(a) Initial shape.

(b) After 15 minutes.

into two parts; one was measured in an open tube as in 4.2.2 (A); the other was sealed in a quartz tube as in 2.5.2. The results of the decay rates at 55°C are given in Table 4.4.

Table 4.4 Decay of $RO_2^\bullet$ radical in air and vacuo at 55°C

	Time/min	10^{-18} x Radical g^{-1}	$10^{18}\left[RO_2^\bullet\right]^{-1}$ /g radical^{-1}
In air	0	1.094	0.916
	43	0.272	3.68
	70	0.233	4.30
	120	0.155	6.47
	171	0.118	8.43
In vacuo	0	1.27	0.792
	22	1.00	0.987
	77	0.654	1.53
	135	0.438	2.30

The second-order plots of these data are shown in Figure 4.19 giving rate constants :

$$k_2 = 1.12 \times 10^{-20} (\text{spin/g})^{-1} \text{min}^{-1} \quad \text{(in vacuo)}$$

$$k_2 = 4.75 \times 10^{-20} (\text{spin/g})^{-1} \text{min}^{-1} \quad \text{(in air)}$$

The rate of decay is therefore less in vacuo, this observation being consistent with a hydrogen abstraction process followed by further oxygen absorption, when this is available. Further evidence of this explanation is that when a less efficient evacuation procedure was used an initial decay rate similar to that found in air was obtained, followed by a slower rate,

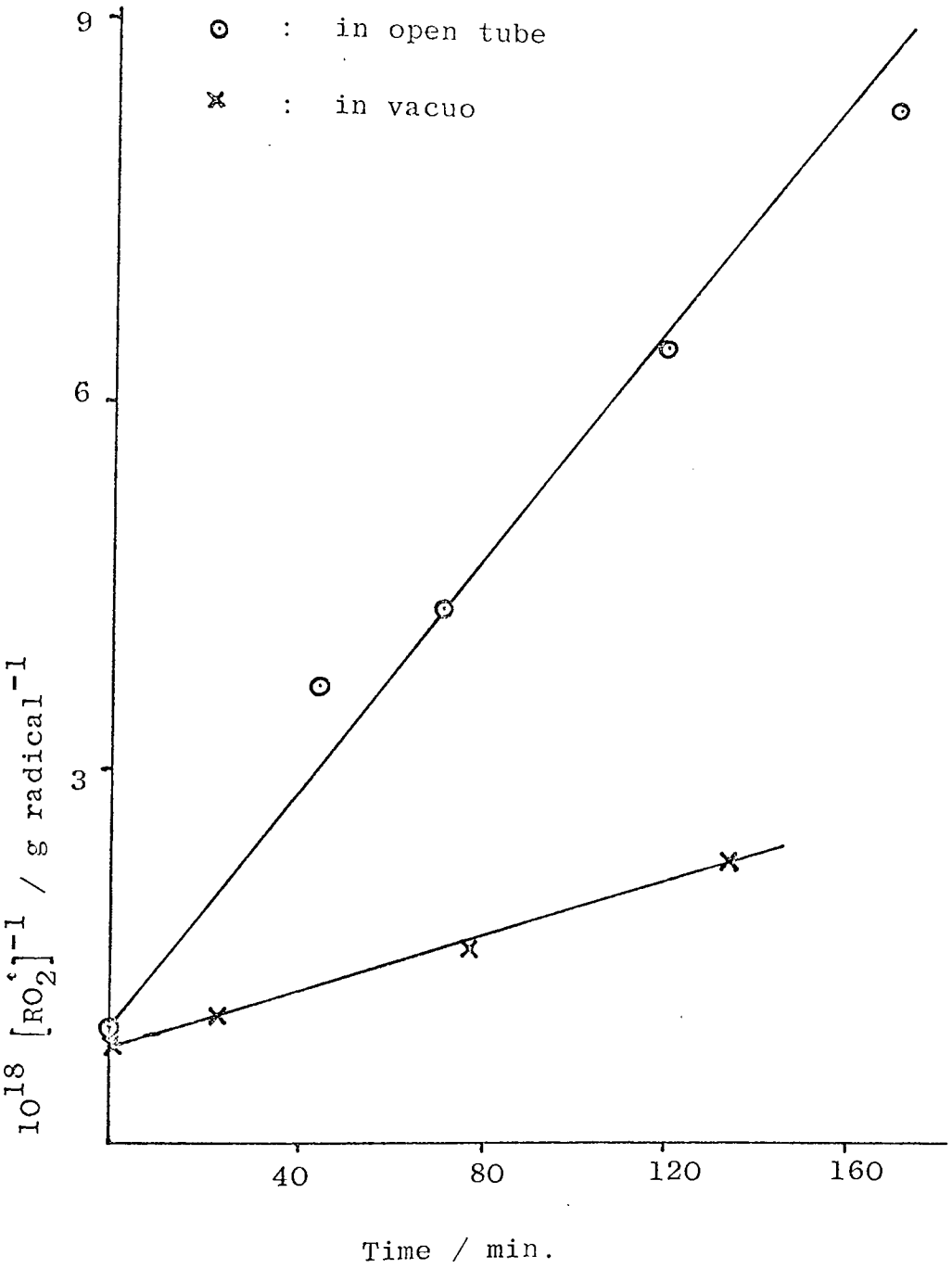

Fig. 4.19 Second-order plots of $RO_2^{\cdot}$ radical decay rates in vacuo and in air at 55°C.

similar to the effect observed in the decay of the vacuum radical (Figure 4.18).

4.3.6 Effects of Ultra-violet Radiation.

When the polypropylene was irradiated as described in 2.4.4 free radicals were detected and the E.S.R. spectrum obtained is shown in Figure 4.20 . The same radical was also found with a sample of commercially produced polypropylene film. Acetone extraction of the polymer removed a small amount of oily material, that appeared to be responsible for the formation of this radical. The infra-red spectrum of the extract suggested that it was a form of low molar mass polypropylene (largely atactic) with a high carbonyl content, since there was a strong absorption at 1740 cm^{-1}, but this may have been partially caused by remaining acetone. The carbonyl group in the polymer would probably be the cause of the radicals produced and indeed following extraction no radicals were produced by ultra-violet radiation.

The integrated signal for the radical is considerably asymmetric and could not be identified. The E.S.R. spectrum decayed by a second-order process without any change in line-shape. The integrated signal for the radical measured under conditions 4.2.2. (A) was obtained manually and the Z-factor found to be

$$z = 0.067 + 0.04$$

The concentrations of free radicals produced in a typical series of ultra-violet irradiations are given in Table 4.5 and illustrated as a function of irradiation time in Figure 4.21.

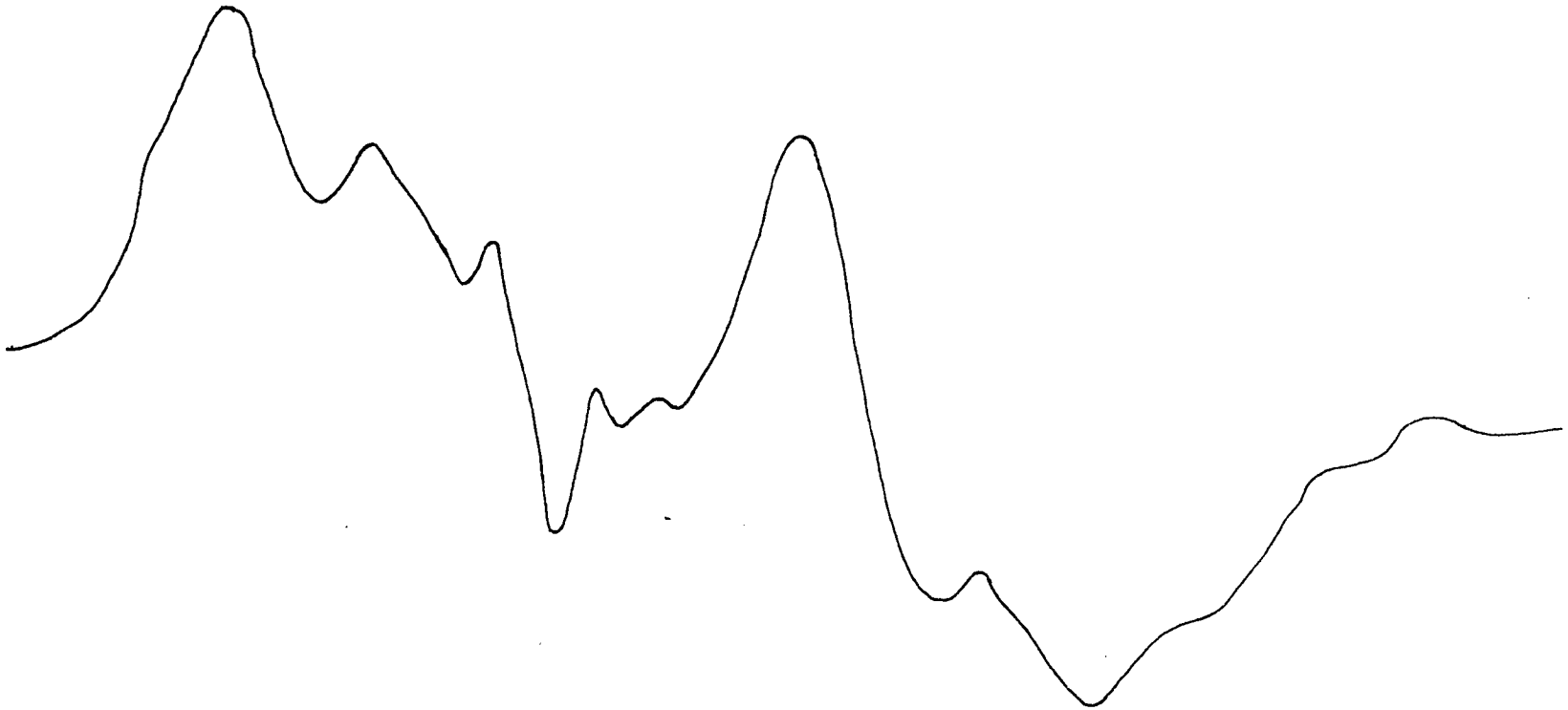

Fig. 4.20 E.S.R. spectrum of radical produced by ultra-violet irradiation of isotactic polypropylene at room temperature, measured at 100 gauss / 10 min.

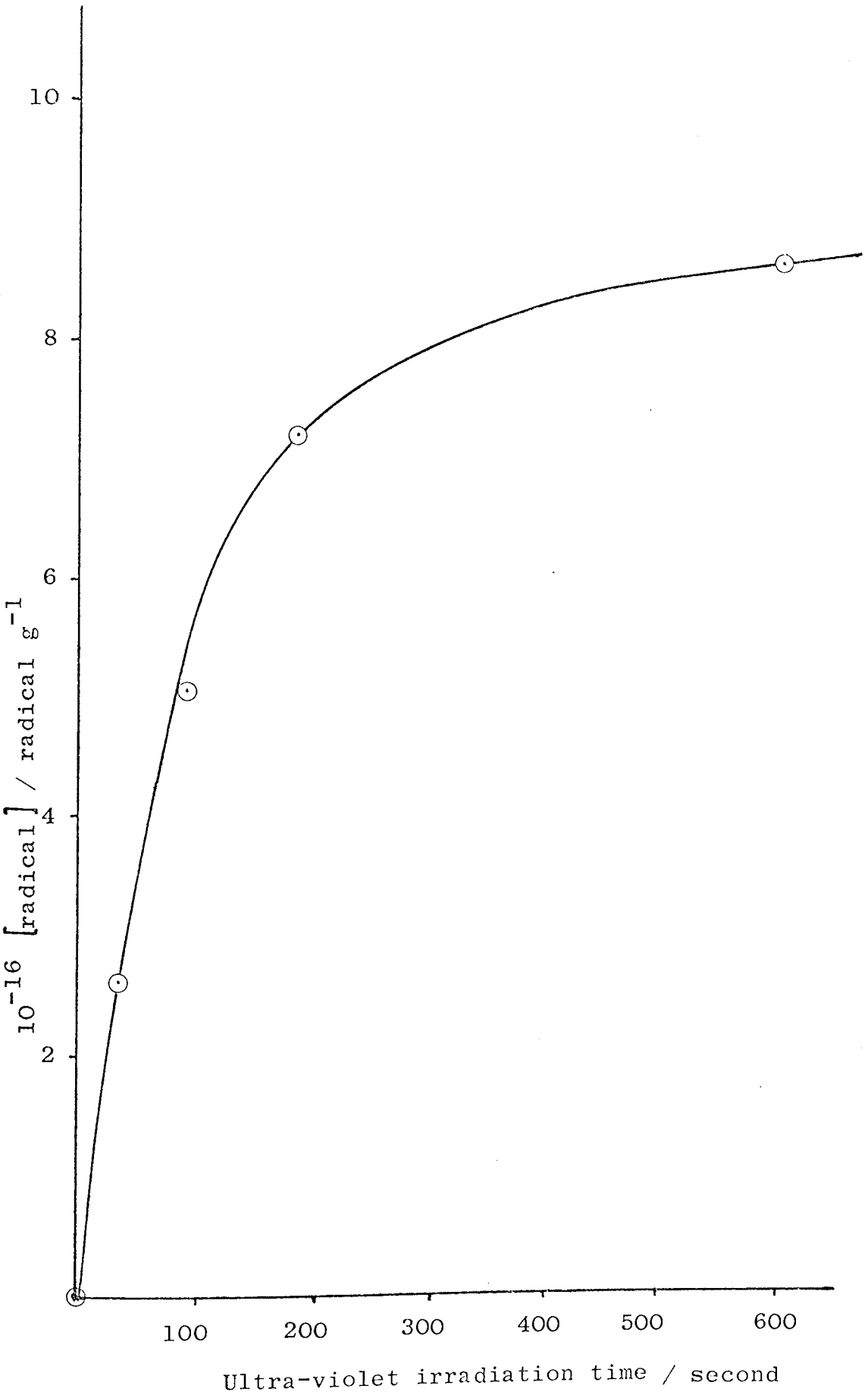

Fig. 4.21 Free radical concentration in isotactic polypropylene as a function of ultra-violet irradiation time.

Table 4.5 Concentration of free radical produced in polypropylene by ultra-violet irradiation.

Irradiation time/sec.	10^{-16} x Radical g^{-1}
30	2.63
90	5.08
180	7.21
600	8.75

These concentrations were reproducible to about ± 15%. The radical concentration was found to become constant after 600 seconds irradiation, and this was the usual time selected for radical production in the decay experiments. The E.S.R. spectrum was unaffected by evacuation or by treatment with sulphur dioxide.

The decay rates were measured at 23, 40, 50°C and the data obtained is given in Table 4.6. The second-order plots are given in Figures 4.22 - 4.24. The following rate constants (reproducible to ±10%) were obtained :

$$k_2 = 0.484 \times 10^{-19} \text{ (radical/g)}^{-1}\text{min}^{-1} \quad (23^\circ\text{C})$$

$$k_2 = 5.26 \times 10^{-19} \text{ (radical/g)}^{-1}\text{min}^{-1} \quad (40^\circ\text{C})$$

$$k_2 = 18.40 \times 10^{-19} \text{ (radical/g)}^{-1}\text{min}^{-1} \quad (50^\circ\text{C})$$

An Arrhenius plot of log k_2 vs. 1/T for these data, shown in Figure 4.25, shows good linearity and provides an activation energy of 106 kJ mol^{-1} and pre-exponential factor A = 3.55 $(\text{radical/g})^{-1}$ min^{-1}. The rate constant of this decay reaction is therefore given by :

$$k_2 = 3.55\, e^{-12719/T} (\text{radical/g})^{-1}\ \text{min}^{-1}.$$

Table 4.6 Radical decay rate data at 23, 40 and 50°C for polypropylene irradiated with ultra-violet light.

	Time/min	10^{-16} x radical g^{-1}	10^{17} g radical^{-1}
23°C			
	0	8.46	1.18
	15	7.94	1.26
	40	7.41	1.35
	70	6.45	1.55
	120	6.06	1.66
	180	4.61	2.17
40°C			
	0	3.76	2.66
	5	3.49	2.86
	10	3.22	3.11
	16	2.68	3.73
	36	2.35	4.26
	60	1.65	6.05
	80	1.27	7.89
50°C			
	0	8.20	1.22
	3	5.72	1.73
	6.5	3.87	2.58
	10	3.17	3.16
	15	2.38	4.20
	22	1.90	5.26

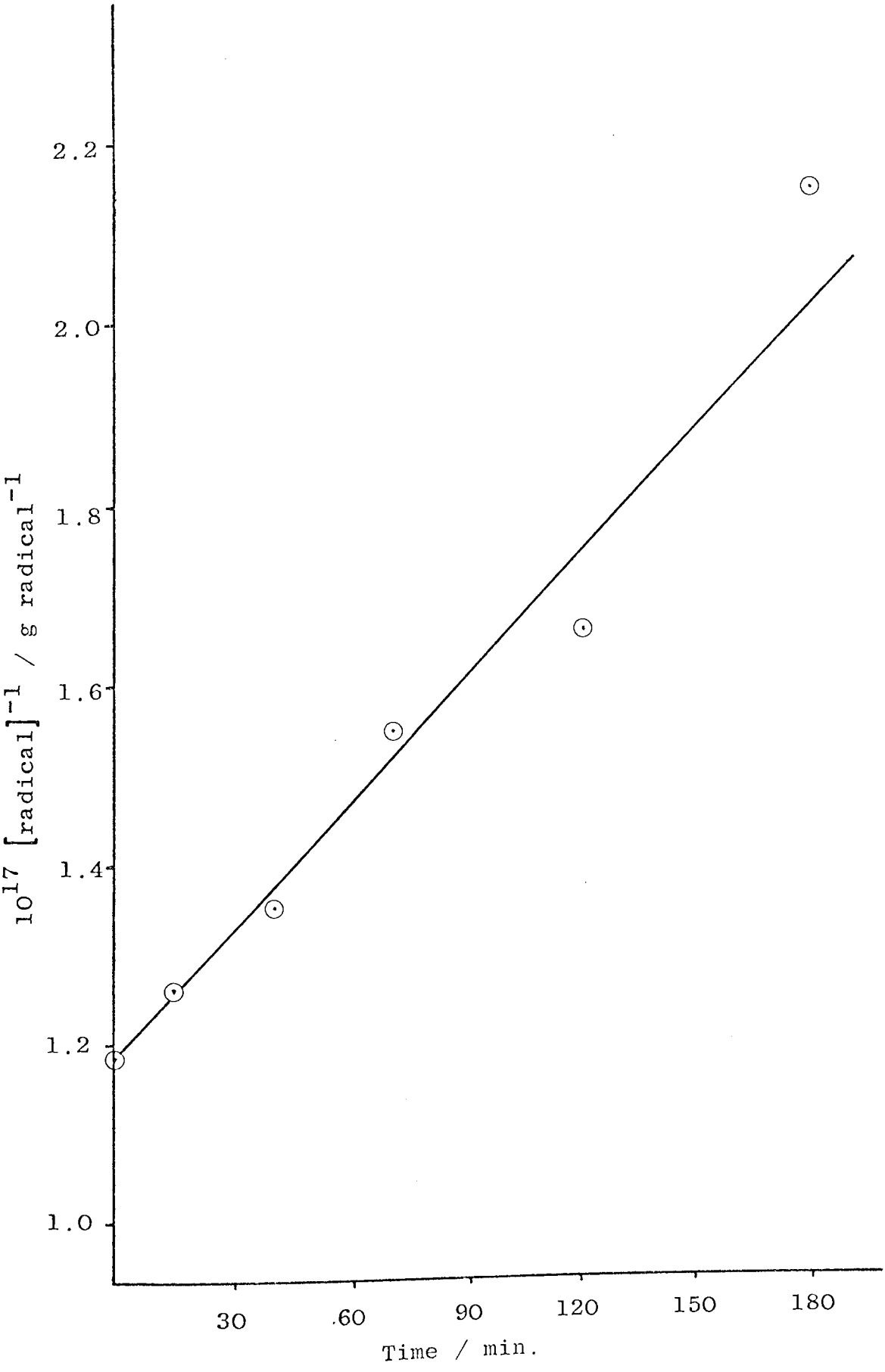

Fig. 4.22 Second-order plot of decay rate at 23°C of radicals produced in polypropylene by u-v irradiation.

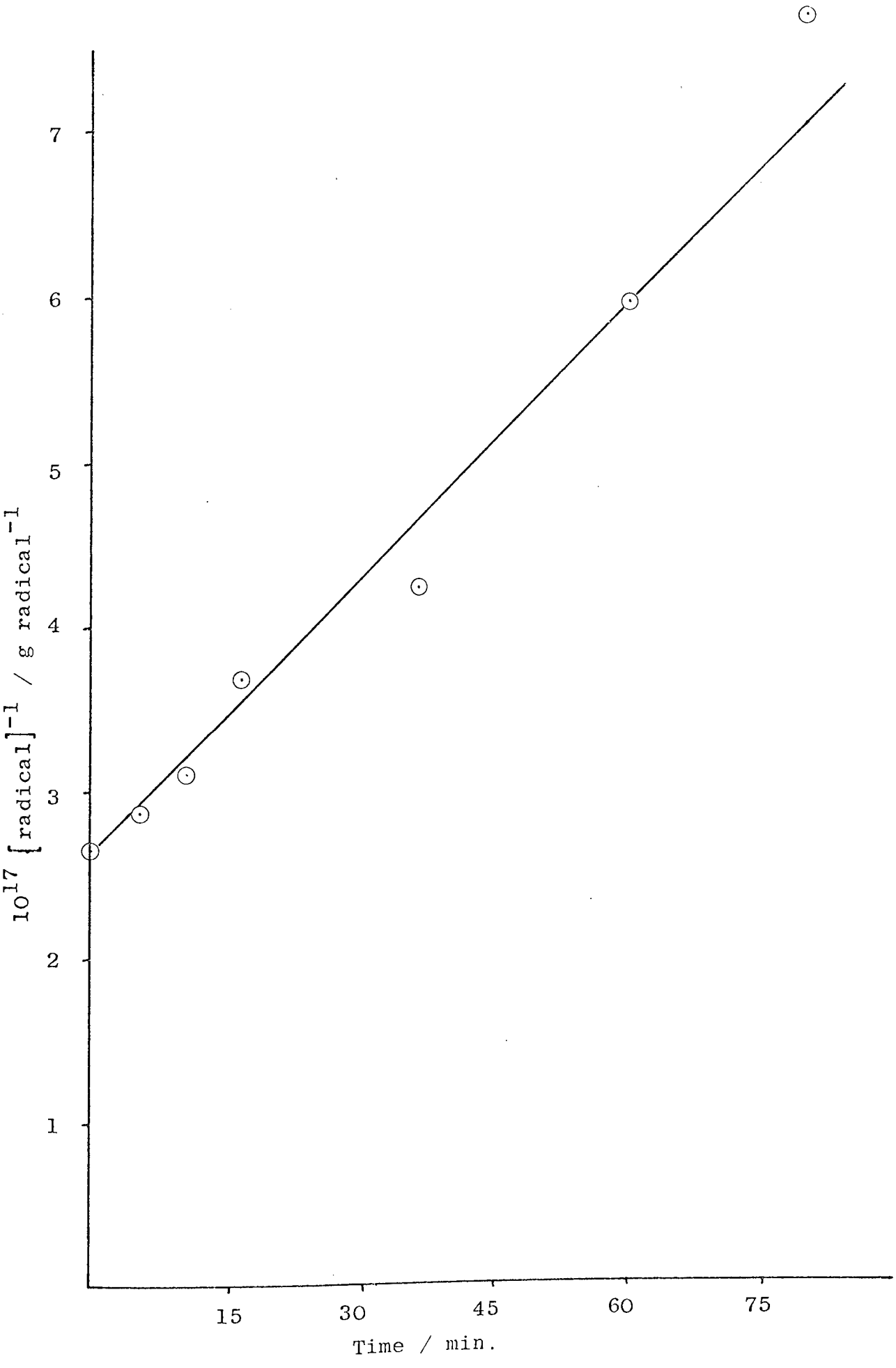

Fig. 4.23 Second-order plot of decay rate at 40°C of radical produced in polypropylene by u-v irradiation.

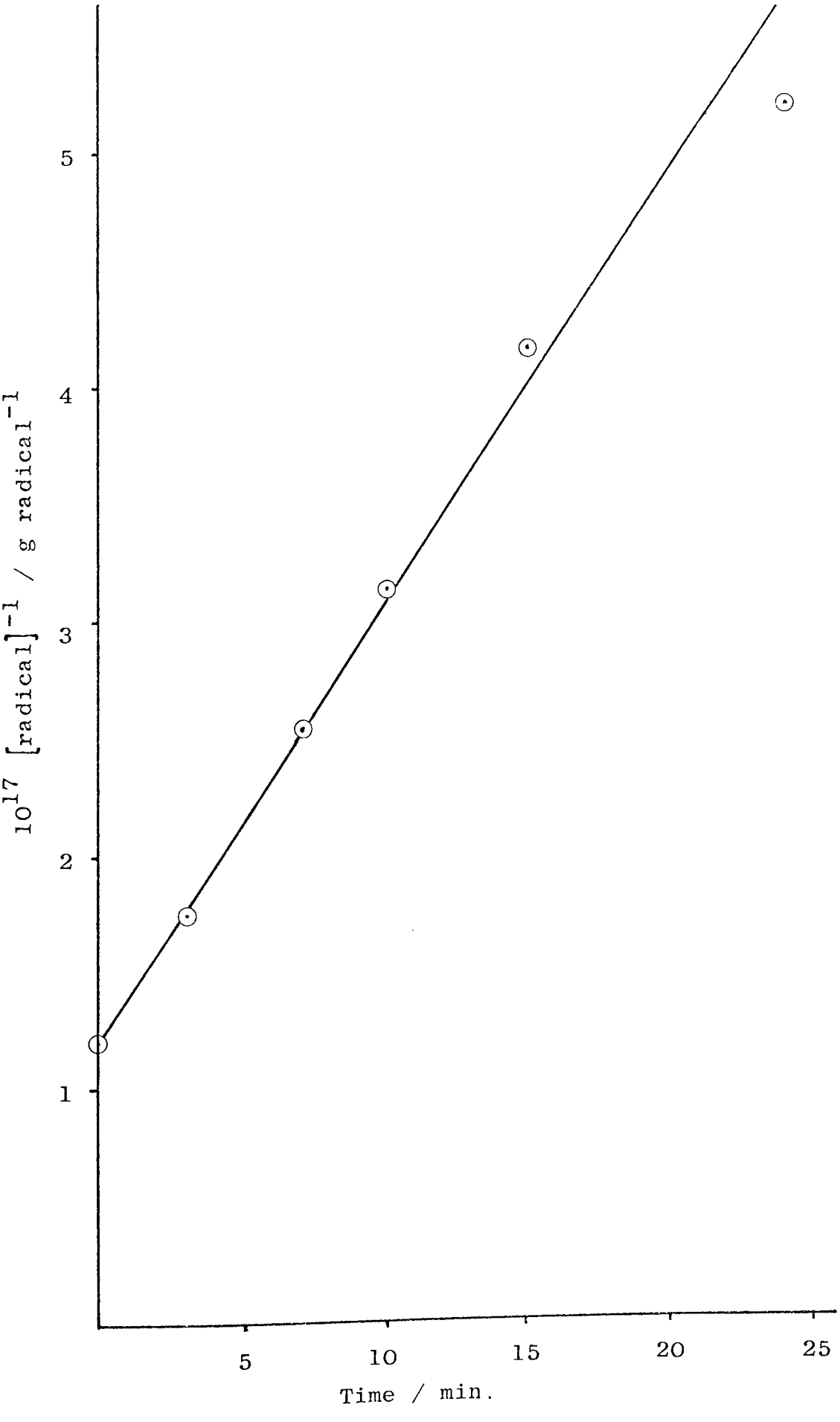

Fig. 4.24 Second-order plot of decay rate at 50°C of radical produced in polypropylene by u-v irradiation.

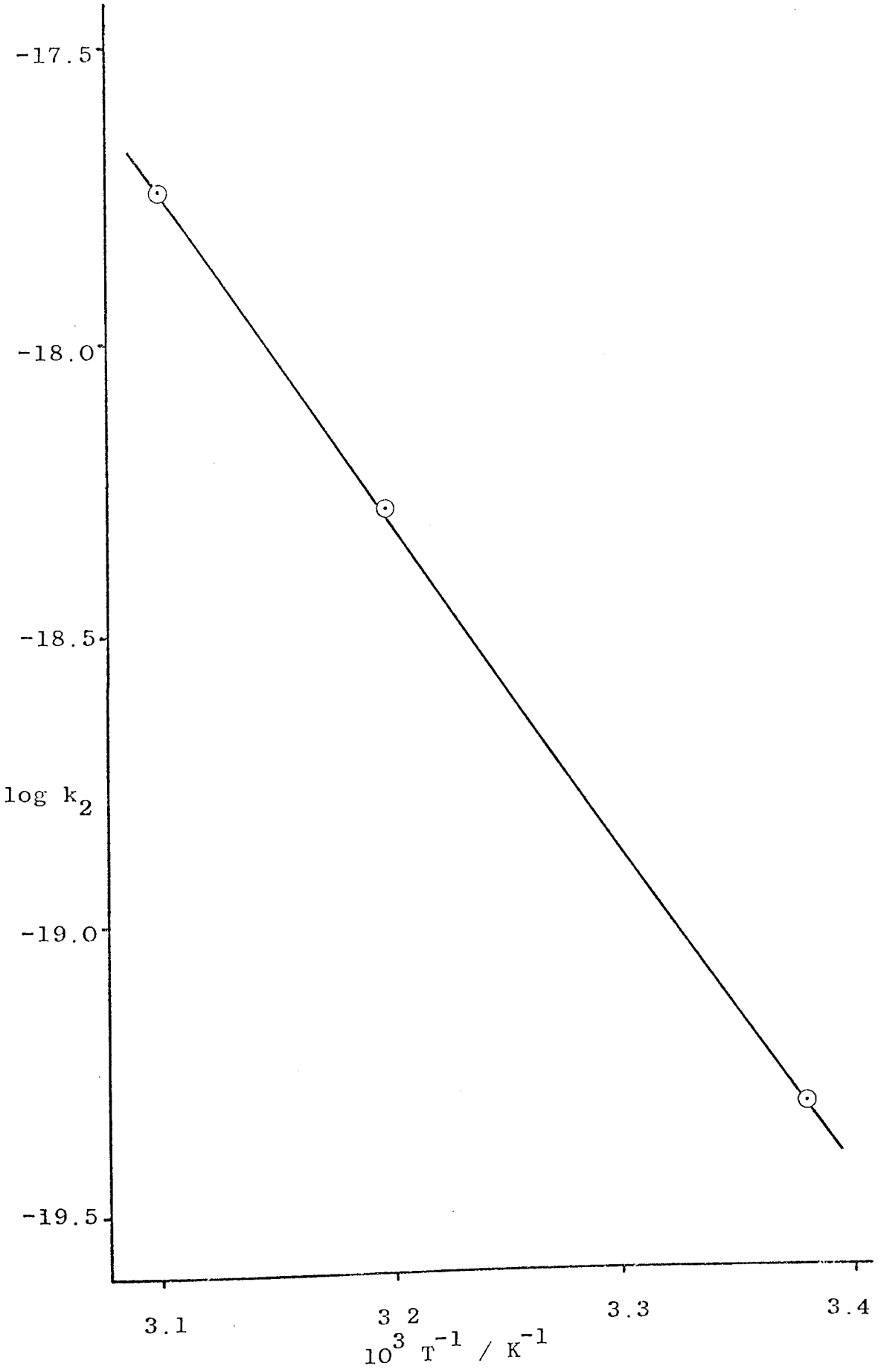

Fig. 4.25 Arrhenius plot of log k_2 vs. T^{-1} for radical produced in polypropylene by u-v irradiation

The pre-exponential factor may also be expressed as

$$A = 3.55 \times 10^{19} (\text{mol dm}^{-3})^{-1}\ \text{s}^{-1}$$

again assuming a polymer density of 0.9 g cm^{-3}. The activation energy of the decay process is quite close to that found for the peroxy radical recombination process. This observation suggests that the polymer matrix is the controlling factor in the radical decay process, as suggested by Lebedev(80).

Effect of ultra-violet light on pre-irradiated polypropylene

When polypropylene, that has been irradiated with high-energy radiation to produce peroxy radicals and then allowed to decay, is subjected to ultra-violet radiation, partial regeneration of the peroxy radicals occur. Figure 4.26 shows that there is a slight change in the E.S.R. spectrum under these conditions, an additional peak (arrowed) being formed, as well as an increase in intensity. The spectra in Figure 4.26 were obtained using a sample that had been irradiated to 15 megarad several months previously and allowed to decay at normal temperature. Although these spectra were obtained without the use of a calibration standard they show that at least 5 or 6-fold increase in the radical concentration has occurred. Another sample pre-irradiated to 10 megarad had decayed to a peroxy radical concentration of 0.54×10^{16} radical g^{-1} and following 10 minutes ultra-violet radiation this had increased to 4.75×10^{16} radical g^{-1}. This is 1.3% of the original radical concentration.

When freshly irradiated (electron) polypropylene is subjected to ultra-violet radiation there is no measurable

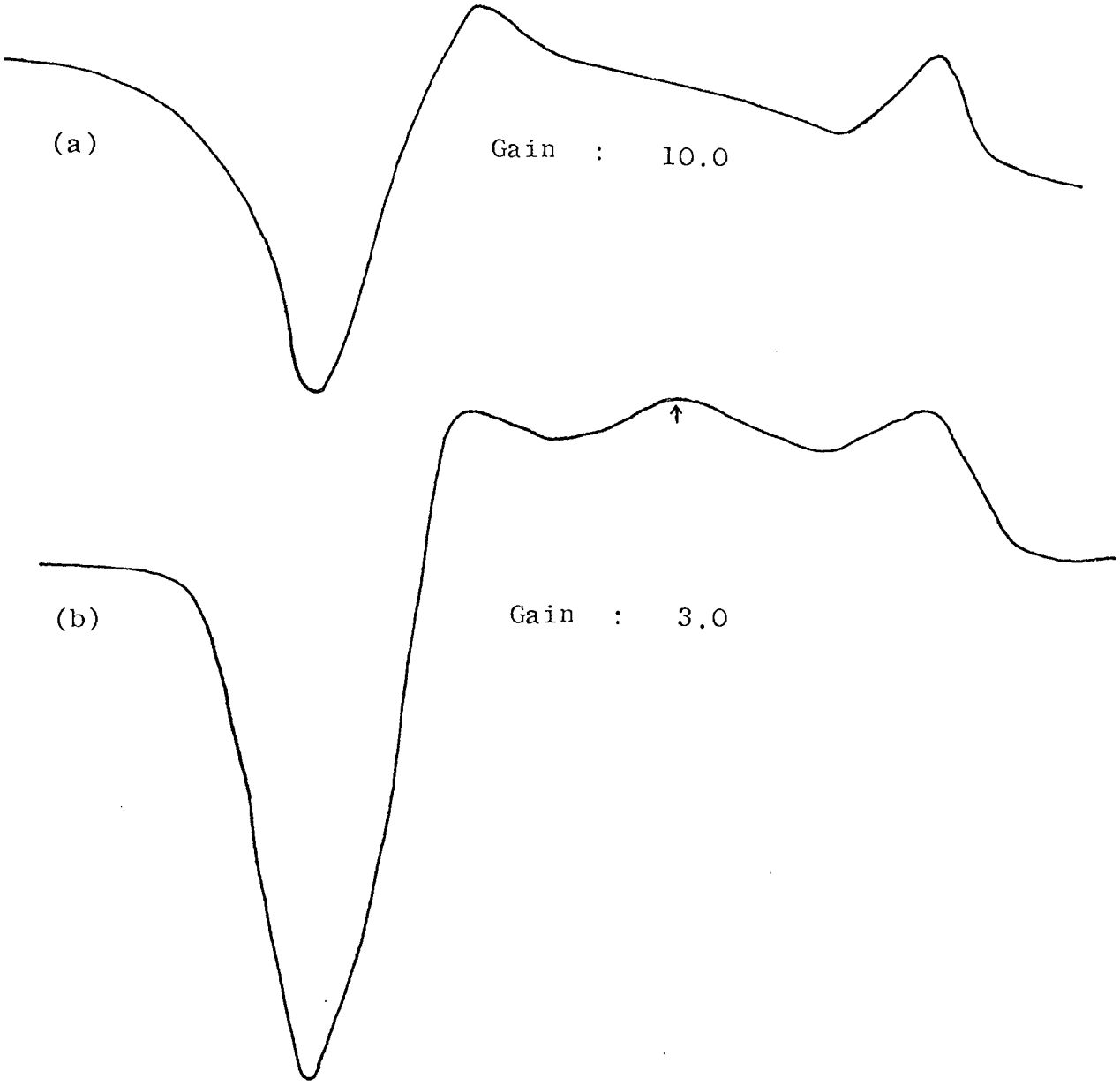

Fig. 4.26 E.S.R. spectra showing increase of $RO_2^{\bullet}$ caused by ultra-violet irradiation of pre-irradiated (γ) polypropylene.

increase in the number of radicals observed. Even with irradiated polymer samples that had decayed to undetectable levels of peroxy radical concentration, radical regeneration was possible. The maximum concentration of radicals that could be regenerated increased with the initial radiation dose and up to approximately 2.0% of the initial concentrations given in Table 4.1 could be regenerated.

4.3.7 Effect of Physical Form.

The radical produced on irradiation in air is dependent on the physical state of the polymer. Samples of polypropylene in the form of injection moulded discs, 1·8mm thick were γ-irradiated to a dose of 2.10 megarad at uncontrolled temperature, (approx. 325 K) and the radicals observed. The initial radical produced (Figure 4.27) is identical to that generated in vacuo (Figure 4.16) i.e. a mixture of hydrocarbon radicals but mainly

$$\sim\!\!\sim CH_2 - \underset{\displaystyle CH_3}{\overset{\displaystyle C^{\bullet}}{|}} - CH_2\!\sim\!\!\sim$$

On storage at room temperature the $RO_2^{\bullet}$ radical is only slowly formed and traces of the hydrocarbon radical are present for several days. At 55°C the formation of $RO_2^{\bullet}$ radical is more rapid, and Figure 4.27 illustrates the change in E.S.R. spectra with time. The hyperfine structure has completely disappeared within 40 mins, this change being considered to be controlled by the rate of diffusion of oxygen into the sample.

In view of the high temperature (50 - 55°C) and the considerable length of time in the irradiation unit, the lack of any evidence of the $RO_2^{\bullet}$ radical, immediately following irradiation is perhaps surprising. This would result if the

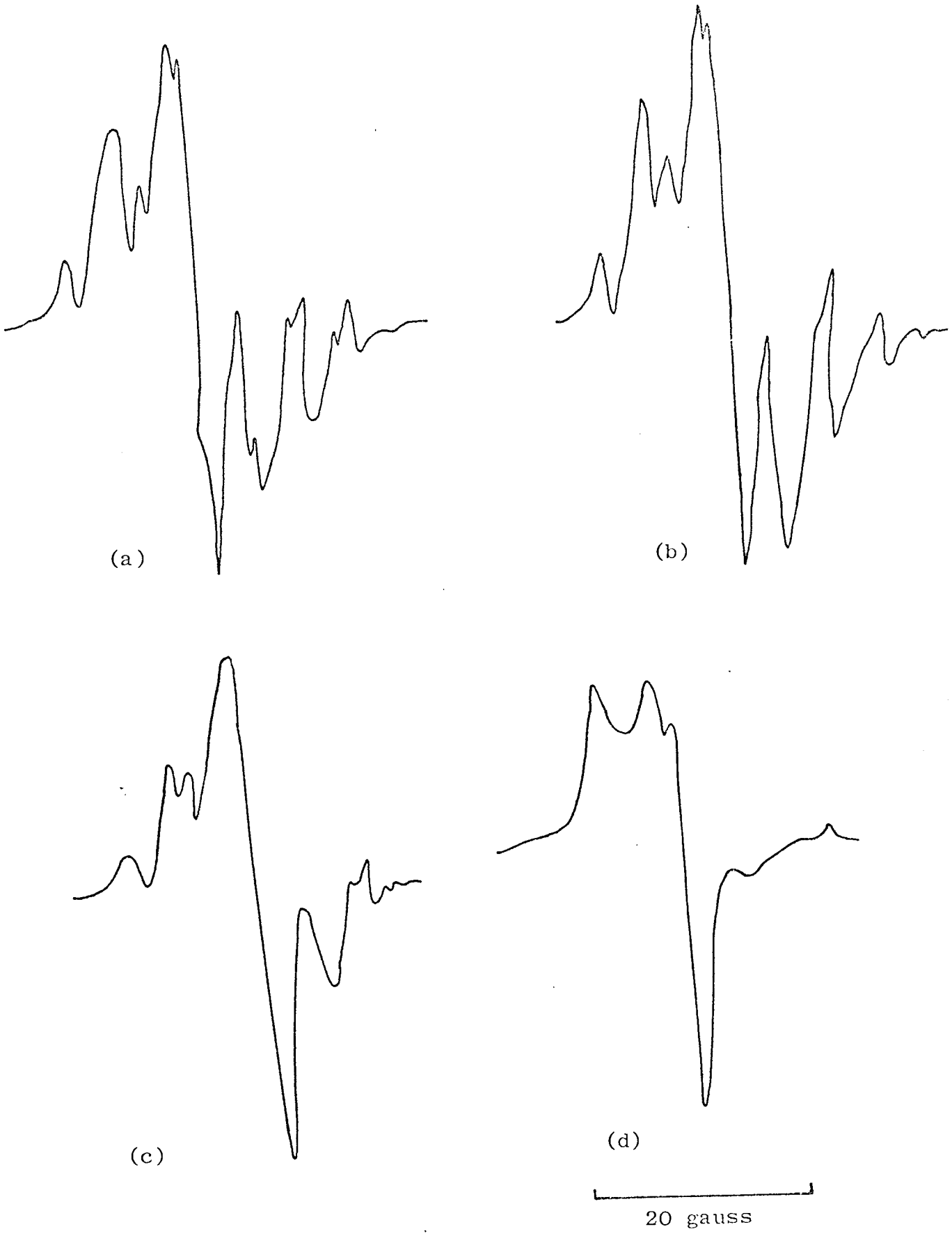

Fig. 4.27 E.S.R. spectra of γ-irradiated solid polypropylene; (a) initially, (b) after 2 min. at 55°C, (c) 11 min., (d) 30 min.

the reaction $R^{\bullet} + O_2 \longrightarrow RO_2^{\bullet}$ is reversed in the presence of high-energy radiation. In comparison, the polymer in powder form is much more rapidly converted to $RO_2^{\bullet}$ (4.3.2) occurring virtually instantaneously above -50°C. However, at temperatures low enough to minimise diffusion, the radical initially formed is also $R^{\bullet}$.

The initial concentration of hydrocarbon radicals produced in the solid polymer is the same as for the powder sample, if the irradiation temperature is low enough to prevent radical decay. The concentration of $RO_2^{\bullet}$ radicals eventually formed in the solid sample is considerably less than that found in the powder since considerable $R^{\bullet}$ radical recombination occurs before the oxygen can completely diffuse into the sample. Thus a solid sample, immediately following irradiation to 2.10 megarad had a radical concentration of 6.6×10^{17} radical g^{-1} which had fallen to 2.40×10^{17} radical g^{-1} when all trace of hyperfine structure had disappeared. Some measurements were also made with solid samples irradiated at 77 K in a stoppered tube containing air. The radical found on measurement at room temperature was the same mixture of hydrocarbon radicals found in vacuo (4.3.4) and the G-value of 0.96 agreed well with those for the polymer in powder form (G = 0.98 for $RO_2^{\bullet}$ and 1.03 for $R^{\bullet}$) .

4.4 Stereoblock Polypropylene

4.4.1 Irradiation with accelerated electrons

Irradiation of stereoblock polypropylene in air produced peroxy radicals, with an E.S.R. spectrum identical to that for isotactic

polymer (e.g. Figure 4.6). When irradiated to 2.5 megarad under uncontrolled temperature conditions the radical concentration found was 0.84×10^{18} radical g^{-1} compared with 0.97×10^{18} for isotactic polypropylene.

4.4.2 Decay Rate Measurement

The decay rate of the peroxy radical in stereoblock polypropylene in air was measured at 55°C, giving the results in Table 4.7.

Table 4.7

Time/min	Radical g^{-1}
0	8.43×10^{17}
75	2.05×10^{17}
127	1.34×10^{17}

The second-order rate constant for these data is found to be $4.95 \times 10^{-20}(\text{radical/g})^{-1}\ \text{min}^{-1}$ which is similar to that found for the isotactic polymer ($6.04 \times 10^{-20}(\text{radical/g})^{-1}\ \text{min}^{-1}$).

4.5 Atactic Polypropylene

4.5.1 Accelerated Electron Irradiation at Ambient Temperatures.

Attempts to produce stable free radicals by irradiation of atactic polypropylene in air or in vacuo at room temperature were unsuccessful. When irradiation was carried out at 195 K and maintained at this temperature until measurement at room

temperature, all radicals had disappeared during the short time necessary to set up the spectrometer.

4.5.2 γ-irradiation at 77 K

Irradiation and measurement in air at 77 K produced the E.S.R. spectrum shown in figure 4.28. The characteristic line-shape of the peroxy radical can be identified together with an additional broader species. Comparison to isotactic polypropylene irradiated at 77 K (Figure 4.9) and to atactic polypropylene irradiated in vacuo at 77 K (Figure 4.29) shows the same initial species is produced in each case. Although the outermost lines can be scarcely discerned, the spectrum is considered to be an 8-line one corresponding to the species

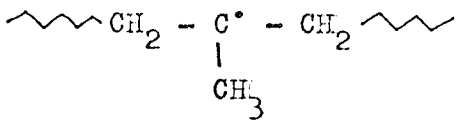

The partial formation of $RO_2^{\bullet}$ indicates that even at this temperature diffusion of oxygen and reaction with $R^{\bullet}$ can occur.

Figure 4.29 shows that in vacuo a more symmetrical spectrum is obtained, except in the region of 3260 gauss where a signal from the quartz tube is present. Quantitative measurements were not made using a copper ion standard, but the intensity of the signal was very similar to that obtained for the isotactic polymer under equivalent conditions.

4.5.3 Effect of Temperature

The γ-irradiated atactic polymer was increased in temperature using the variable temperature control facility on the Varian spectrometer. Measurements using a 2 minute scan were made at approximately 10 K intervals. Representative

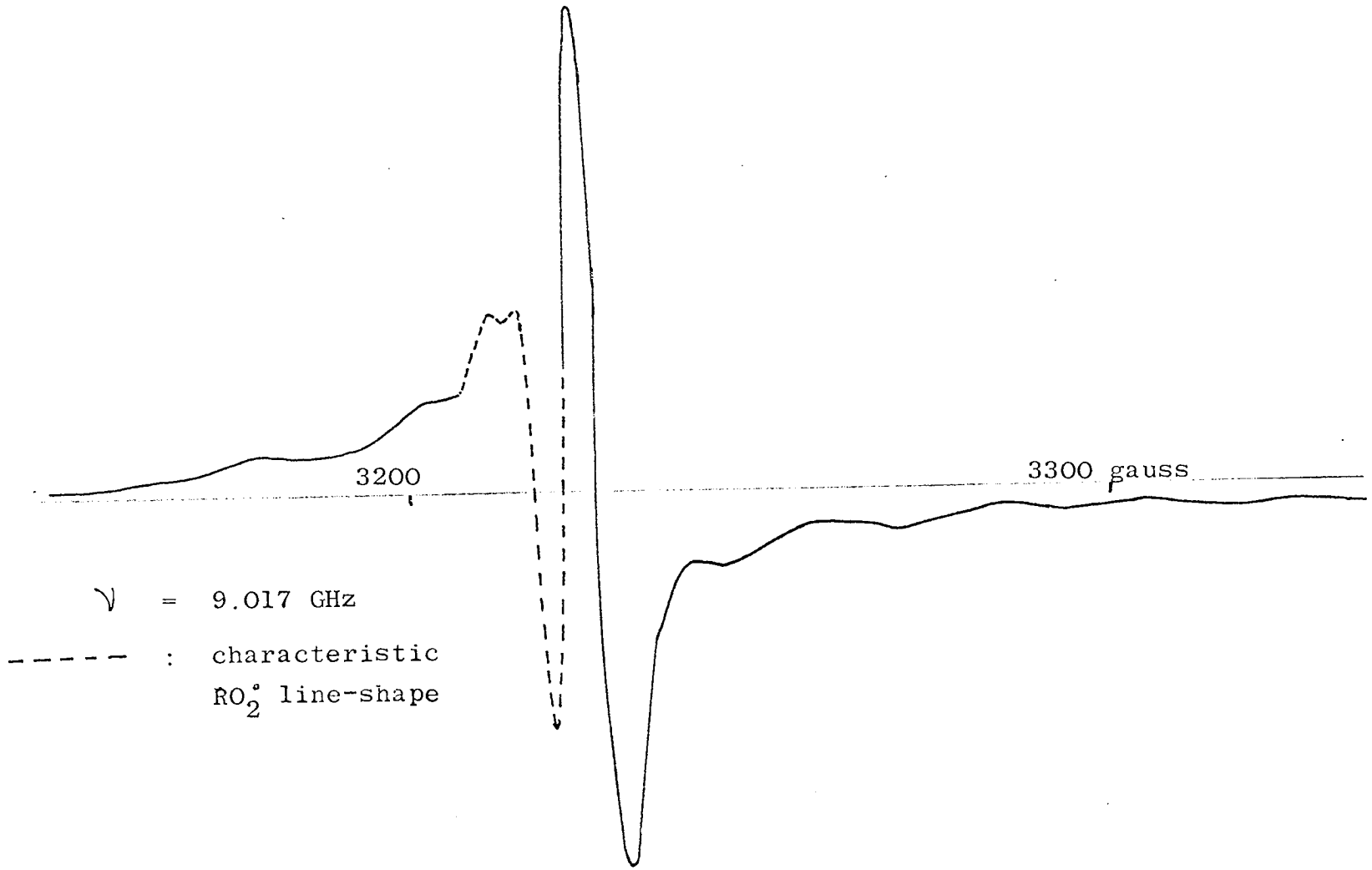

Fig. 4.28 E.S.R. spectrum of atactic polypropylene irradiated in air at 77 K.

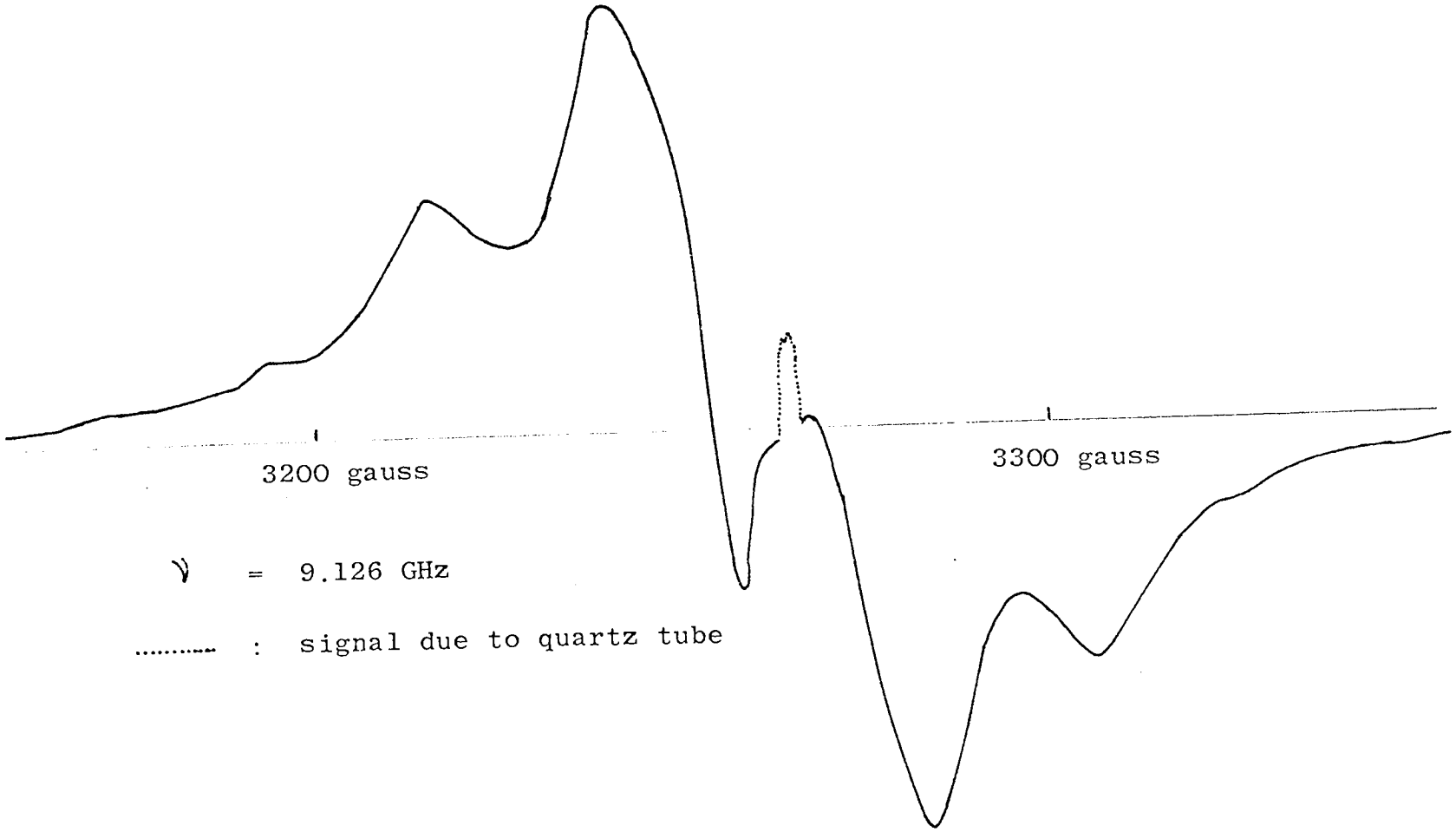

Fig 4.29 E.S.R. spectrum of γ-iradiated atactic polypropylene in vacuo at 77 K.

spectra are shown in Figure 4.30. These show that no additional radical is produced, but the intensity decreases as given in Table 4.8. All measurements were made at the same gain and magnetic field conditions and the time taken to stabilise the temperature between readings was approximately 1 minute.

Table 4.8 Effect of temperature on E.S.R. spectrum of γ-irradiated atactic polypropylene

Temperature / K	Peak-to-peak Signal Height (Arbitrary units)
134	55
141	53
150	49
160	46
170	43
180	40
190	38
200	35
210	32
220	28
230	25
240	22
250	20
260	10
270	-

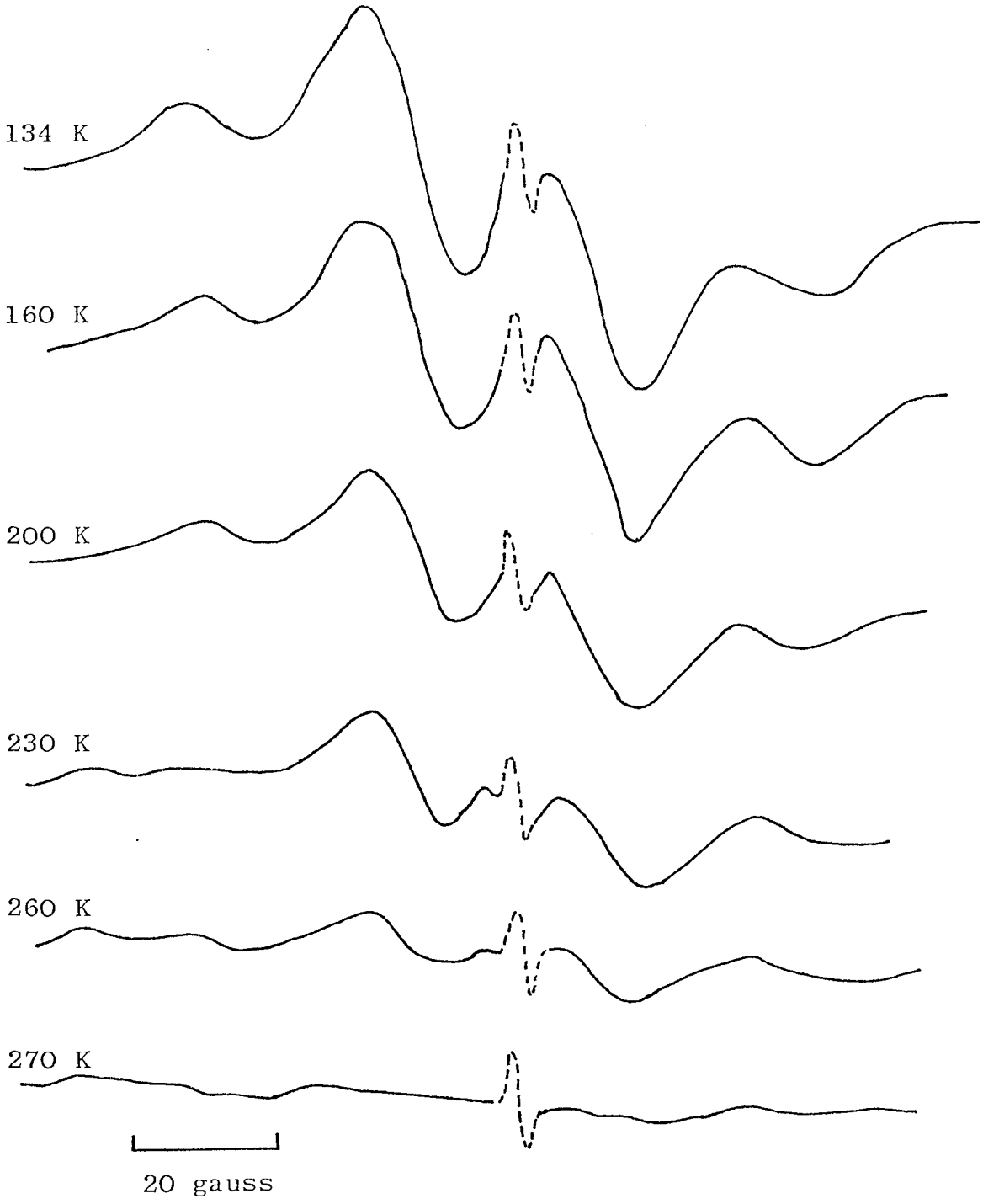

Fig. 4.30 Effect of increasing temperature on E.S.R. spectra of γ-irradiated atactic polypropylene.

(----- indicates spectrum resulting from quartz tube)

A steady decrease occurs over this range until the temperature approaches 250 K after which a rapid decrease occurs. This is shown in Figure 4.31. The final rapid decay takes place in the region of the glass transition (T_g = 255K) [132] above which the flexible polymer matrix and increased chain mobility would explain the accelerated decay. The relative constancy of the signal from the quartz tube, shown dotted in Figure 4.30 shows that the efficiency of radical detection by the instrument does not change with the temperature. The steady and relatively rapid decay up to T_g, shows that even in the glassy state the polymer radicals are much less stable than those trapped in the crystalline regions of the isotactic and sterco-block polymers.

4.6 Effect of Gaseous Environment

Table 4.9 shows the irradiation conditions that were used for the various gases.

Table 4.9

Gas	Irradiation	Dose/Megarad	Temperature
Nitrogen	Electron	2.50	195 K
Nitrogen	γ	2.10	77 K
Hydrogen	Electron	2.50	195 K
Hydrogen	γ	2.10	77 K
Oxygen	Electron	2.50	195 K
Oxygen	γ	1.19	77 K
Sulphur dioxide	Electron	2.50	273 K
Nitric oxide	Electron	2.50	195 K

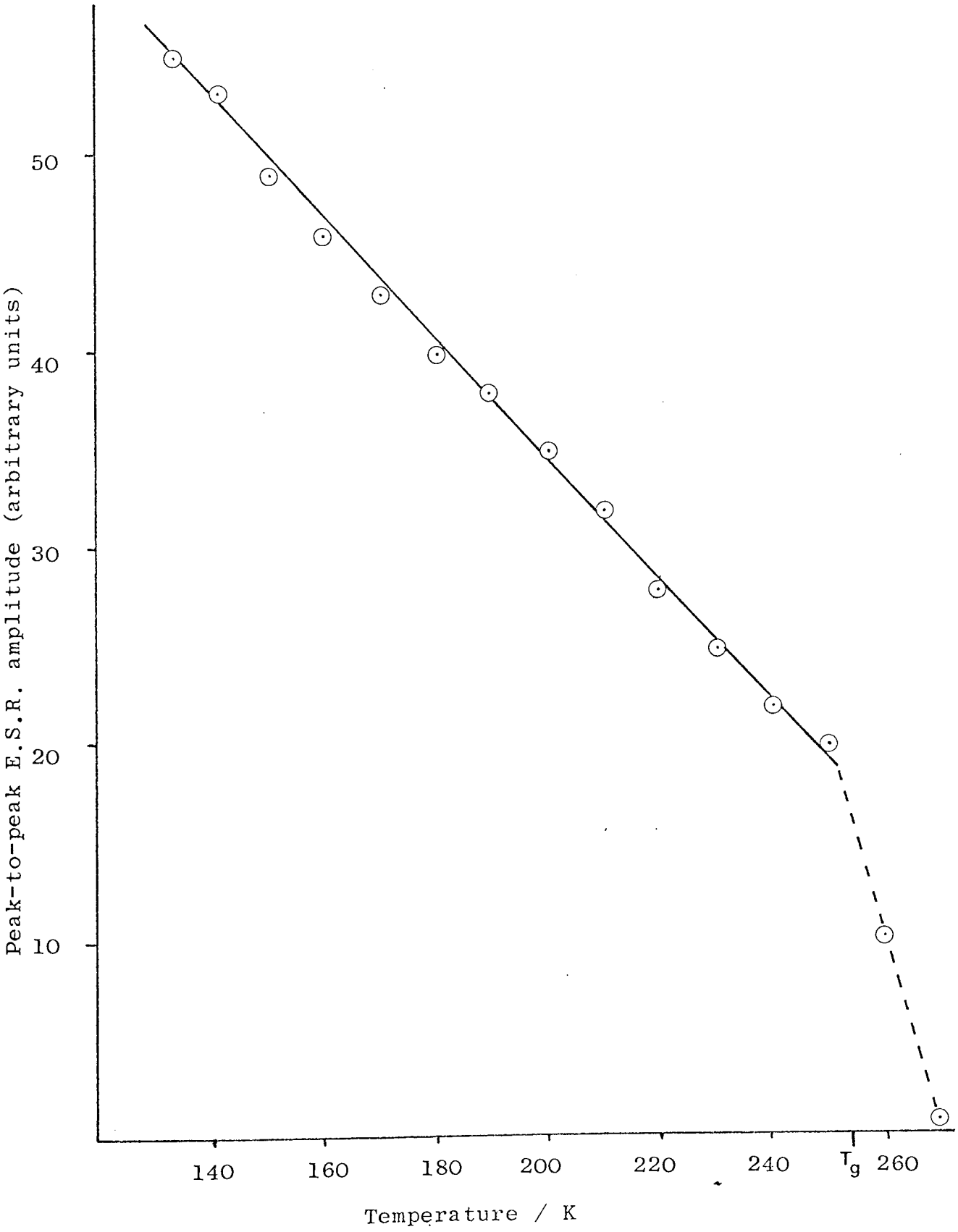

Fig. 4.31 Disappearance of free radicals in γ-irradiated atactic polypropylene with increase of temperature.

The electron-irradiated samples were measured at Aston on the Hilger Microspin instrument. The γ-irradiated samples were measured on the Varian E 3 spectrometer at Leicester.

4.6.1 Nitrogen

The radicals initially produced and the conversions on increasing the temperature and exposure to oxygen were identical to those produced in vacuo. Within experimental error the concentration of radicals was also the same as in vacuo.

4.6.2 Hydrogen

The initial radical produced on γ-irradiation at 77 K corresponded to that found in vacuo

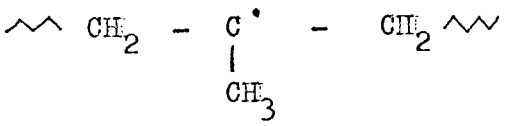

It was also found that irradiation with fast electrons at 195 K and measurement at room temperature again produced a simple 8-line spectrum corresponding to the above radical, whereas samples irradiated in nitrogen or in vacuo produced a complex spectrum at room temperature that was considered to be due to a mixture of radicals. The fact that such a mixture was not observed in a hydrogen atmosphere supports the conclusion that the secondary radical formed is an unsaturated species probably

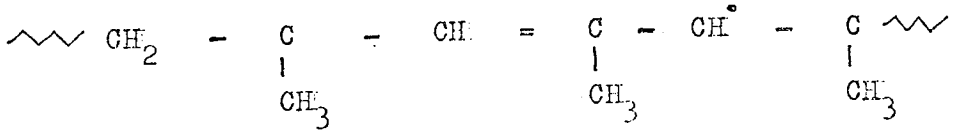

4.6.3 Oxygen

The E.S.R. spectrum obtained in oxygen is identical to that found in air (Figure 4.6). The concentration of $RO_2^\bullet$ was found to be 5.90×10^{19} radical g^{-1} for a dose of 1.19 megarad (γ) at 77 K. This may be expressed as a G-value of 0.79, while irradiation in air carried out simultaneously gave a G-value of 0.77. It can be concluded that irradiation in oxygen does not produce significantly more peroxy radicals than in air.

4.6.4 Sulphur Dioxide

Irradiation in sulphur dioxide at 273 K produced a radical, of which the E.S.R. spectrum was very similar to that of the peroxy radical but covering a magnetic field range of 60 gauss compared to 88 gauss for the latter. The radical was stable when exposed to air and was considered to be the sulphinyl radical $RSO_2^\bullet$. The same radical was also produced when the hydrocarbon radical produced by irradiation in vacuo was exposed to sulphur dioxide at room temperature, however exposure of the peroxy radical $RO_2^\bullet$ to sulphur dioxide did not cause production of $RSO_2^\bullet$.

The Z-factor found for this radical following manual integration of the E.S.R. spectrum was found to be

$$Z = 0.024 \pm 0.02$$

The initial concentration of radicals was found to be 0.70×10^{18} g^{-1} for a dose of 2.5 megarad, giving a G-value of 0.45.

Irradiation in vacuo followed by exposure to sulphur dioxide gave a radical concentration of 0.74×10^{18} g^{-1} ($G = 0.47$).

The rate of decay of the radical in air was measured at 40°C and 55°C giving the results in Table 4.10.

Table 4.10 Decay rate data for $RSO_2^\bullet$ radical in polypropylene.

	Time /min	$RSO_2^\bullet$ concentration / g^{-1}	$1/[RSO_2^\bullet]$
40°C	0	1.26×10^{17}	7.9×10^{-18}
	42	0.97×10^{17}	10.3×10^{-18}
	80	0.73×10^{17}	13.7×10^{-18}
	264	0.45×10^{17}	22.2×10^{-18}
55°C	0	3.80×10^{17}	2.6×10^{-18}
	26	1.21×10^{17}	8.3×10^{-18}
	66	0.62×10^{17}	16.1×10^{-18}

The second-order rate constants obtained were :

$$k_2 = 5.10 \times 10^{-20} \text{ (radical } g^{-1})^{-1} \text{ min}^{-1} \quad (40°C)$$

$$k_2 = 20.8 \times 10^{-20} \text{ (radical } g^{-1})^{-1} \text{ min}^{-1} \quad (55°C)$$

These rates of decay are slightly greater than those for $RO_2^\bullet$ in air. The approximate activation energy from these results is found to be 80 kJ mol^{-1}. Decay rates measured at 55°C in sulphur dioxide and in vacuo of the $RSO_2^\bullet$ radical gave more scattered data but indicated an initial rate similar to that found in air. In all cases there was no change in the shape of the E.S.R. spectrum during decay.

The effect of ultra-violet light on samples that had been pre-irradiated in sulphur dioxide and then allowed to decay was to regenerate the $RSO_2^{\bullet}$ radicals but only in very small amounts. When similar decayed samples were re-irradiated with fast electrons in air, only peroxy radicals could be observed but there was a strong smell of evolved sulphur dioxide. The concentration of $RO_2^{\bullet}$ produced in this way was 1.28×10^{18} radicals g^{-1} for a dose of 2.5 megarad at 195 K, which is almost the same as that obtained with polymer that had not been irradiated previously (1.27×10^{18} radical g^{-1}). It can be concluded that the sulphur dioxide is incorporated into the polymer after radical decay, presumably by hydrogen abstraction to produce a sulphinic acid species RSO_2H.

4.6.5 Nitric Oxide

No free radicals were detected when the polymer was irradiated in nitric oxide probably because of reaction of this gas with any initial radical formed to produce the diamagnetic species RNO. The E.S.R. measurements were made within one hour of the irradiation. On transferring the sample to an open tube, small amounts ($< 0.03 \times 10^{18}$ g^{-1}) of a fairly stable free radical were produced. The E.S.R. spectrum is an overlapping doublet covering 35 gauss and may be caused by the species $RNO_2^{\bullet}$.

4.7 Conclusions Obtained from E.S.R. Measurements.

4.7.1 Nature of Radicals Produced

(1) The initial radical produced at low temperatures is the alkyl radical

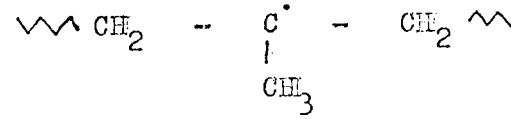

which produced an 8-line spectrum. The same radical is formed from isotactic and atactic polypropylene, using γ or electron irradiation. At 77 K oxygen does not react with this radical.

(2) On warming to room temperature, the E.S.R. spectrum becomes more complex, due to partial formation of a 9-line radical, thought to be an allyl radical

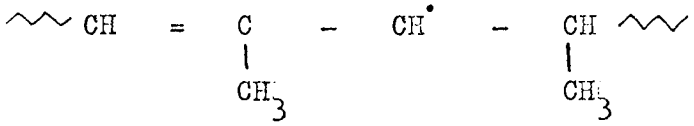

In a hydrogen atmosphere this spectrum is not observed.

(3) The peroxy radical $RO_2^{\bullet}$ is formed by irradiation in air, or by exposure of vacuum irradiated polypropylene to air. The exact site of the oxygen cannot be found from E.S.R. measurements but the initial radical is probably

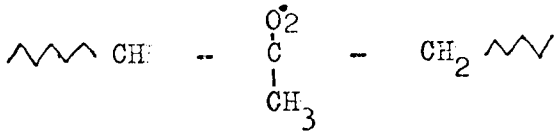

The radical $RO_2^{\bullet}$ was considered to be decomposed by high energy radiation, but unaffected by evacuation or photolysis. The radical $RO_2^{\bullet}$ was also formed by ultra-violet irradiation of pre-irradiated polypropylene containing hydroperoxide groups.

(4) The radical produced by ultra-violet irradiation of polypropylene was not identified, but appeared to be caused by the presence of carbonyl impurities in the polymer. Carlsson and Wiles[133] have shown that carbonyl impurities cause significant oxidation in the presence of molecular oxygen, and that the following reaction chiefly occurs :

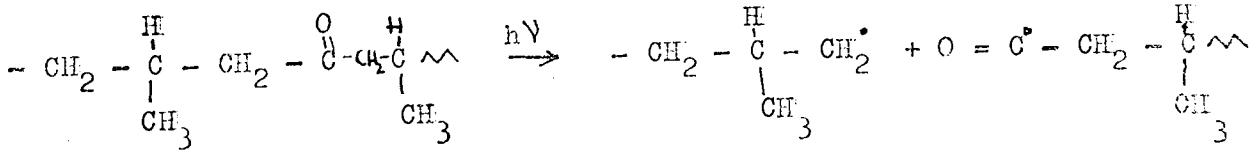

This mixture of alkyl and carbonyl radicals could be responsible for the complex spectrum illustrated in Figure 4.20.

(5) The polymer sulphinylradical $RSO_2^{\bullet}$ can be produced by irradiation in sulphur dioxide or by exposure of the hydrocarbon radicals to sulphur dioxide. The radical is stable on exposure to oxygen, and the method affords a simple way of incorporating sulphur into the polymer.

4.7.2 Radical Concentrations.

(1) The radiation yields of $R^{\bullet}$ and $RO_2^{\bullet}$ are very similar, 0.984 and 1.02 respectively. The values agree well with the values found by Libby [55]. A possible reason for obtaining similar radiation yields is that any peroxy radical produced in oxygen is decomposed by high energy radiation to reform alkyl radicals.

(2) The maximum concentration of free radicals is produced by irradiation at low temperatures. The peroxy radical however is not formed when irradiation is at 77 K.

(3) The radical yields from both γ and electron irradiation are the same.

4.7.3 Decay Rates.

(1) The decay rates and activation energies of all the radicals studied are similar, when the decomposition is in the presence of air. The decay processes are second-order and the rate is probably determined by the rigidity of the polymer matrix. The radicals were stable for several weeks at room temperature.

(2) The $RO_2^{\bullet}$ and $RSO_2^{\bullet}$ radicals are not altered during the decay but the hydrocarbon radical produces an increase of allyl radicals during the decay process.

4.7.4 Effects of Tacticity and Crystallinity.

(1) Amorphous polypropylene (atactic) can only trap free radicals at temperatures below T_g. Stereoblock and isotactic polypropylene show similar E.S.R. spectra and free radical concentrations. The ability to trap free radicals is thus determined by the physical form of the polymer and not by the chain structure (tacticity).

(2) The radical found in finely divided isotactic polypropylene irradiated in air is the peroxy radical $RO_2^{\bullet}$, whereas in solid samples the radical initially found is a hydrocarbon radical mixture that slowly changes to $RO_2^{\bullet}$ following irradiation.

CHAPTER FIVE : CRYSTALLISATION AND MELTING STUDIES

5.1 Melting Behaviour

5.1.1 Introduction

Polymer fusion may be treated as a first order phase transition (135). For many polymers however, a broad melting range that may be as large as 100°C, is frequently observed(136). A broad melting range occurs when the crystalline regions are small, causing surface free energies (between amorphous and crystalline phases) to be comparable to the free energy of fusion.

The broad range of melting causes problems in melting point determination, and in practice, the melting temperature is taken as the temperature at which the last trace of crystallinity disappears, when using the slowest practical heating rate. The methods for melting temperature determination include, dilatometry, specific heat, optical (polarised) microscopy, and differential thermal analysis (D.T.A.). The method of measurement, heating rate, and previous thermal history will each affect the observed melting temperature.

5.1.2 Experimental

Melting temperatures were determined by D.T.A., polarised microscopy and temperature - programmed microscopy. During melting evolution of gas was observed particularly for samples irradiated to high doses. This was caused by decomposition of hydroperoxide groups in the polymer.

Differential Thermal Analysis

The instrument used was a Du Pont 900 thermal analyser, which

basically consists of a temperature controller, D.C. amplifier, and X - Y recorder. Full details of its construction and operation are given in the instrument handbook[137]. The reference material was glass powder and the thermocouples were chromel/alumel. The cold junction of the thermocouple was maintained at 0°C in crushed ice. The polymer sample was placed in a slow stream of nitrogen at a nominal heating rate of 2°C/min (actual rate = 1.5°C/min). After melting the temperature was increased to 200°C, held for 10 minutes. and then cooled at a rate of 5°C/minute until the sample crystallised. The sample was again melted at a heating rate of 2°C/min. Multiple endotherms were obtained with the original and crystallised samples. The melting temperature was taken as the temperature of the larger peak. This occurred 7 - 8°C higher than a peak which was larger for the crystallised samples than the original ones.

Polarised microscopy (manual)

Melting temperatures were also determined on a Reichert-Kofler heating stage with manual temperature control. The sample, between microscope cover slips was pre-melted at 200°C for 10 minutes and then crystallised at 115 - 120°C on the heating stage. Using crossed polars and a final heating rate of about 1°C/min, the melting temperature was the temperature at which the last traces of birefringence could be observed.

Temperature - programmed microscopy

The Du Pont 900 thermal analyser accepts interchangeable modules for various aspects of thermal analysis. A hot-stage microscope module was designed and constructed by Harvey[138].

A Swift-polarising microscope was modified by the incorporation of an insulated stainless steel hot-stage. The temperature was controlled by the Du Pont 900 and recorded on the X-axis of the D.T.A. recorder. A Mullard cadmium sulphide photoresistor (ORP 12) was supported on a demonstration eyepiece and its output fed via a control circuit to the Y-axis of the recorder. Illumination was with a mains-stabilised 6V 15 watt lamp through crossed Nicol prisms.

Polymer samples, pre-melted and crystallised between 16mm cover slips were placed on the hot stage and heated at a nominal rate of $2^{\circ}C$/min. The graphs of depolarised light intensity (D.L.I.) vs. temperature were used to assess pre-melting changes, melting temperatures and crystallisation processes during cooling from the melt. Calibration using benzoic acid and ammonium nitrate, showed that the transition temperatures observed by D.L.I. occurred at the same temperature as the D.T.A. peaks and that no correction was necessary in the range 100° - $300^{\circ}C$, provided that heating rates of $2^{\circ}C$/min or less were used[138].

5.1.3 Results

The melting and crystallisation onset temperatures are given in Table 5.1. The melting temperatures obtained by the different methods are in good agreement and are considered accurate to $\pm$ $1^{\circ}C$. A series of temperature - programmed microscopy traces (D.L.I.) are shown in Figure 5.1. The melting temperature is taken as the temperature at which the trace joins the final baseline. Visual observation of the melting temperature on the Reichert-Kofler hot stage was aided by the large spherulite size and the low viscosity of the irradiated polymers when molten.

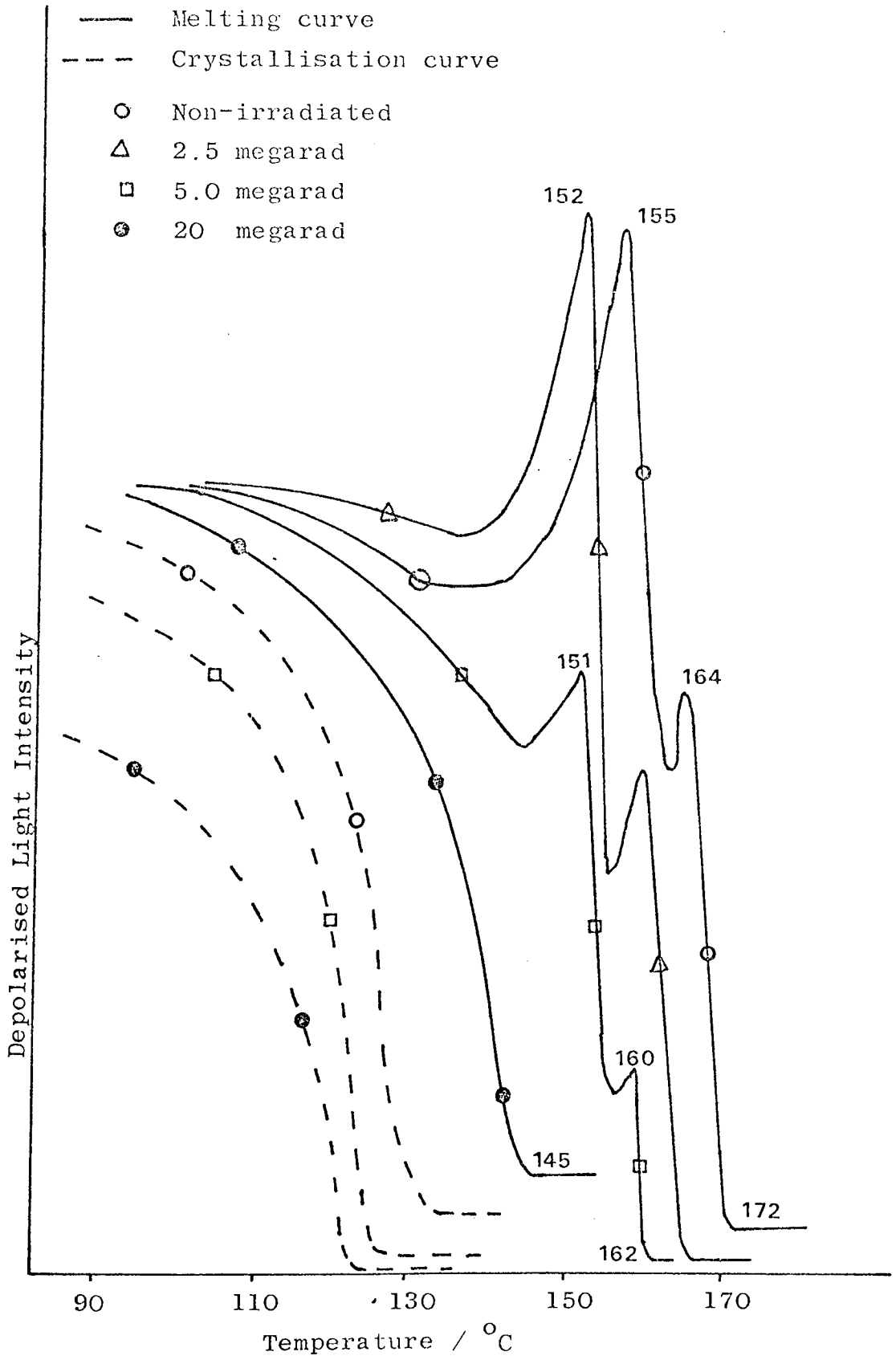

Fig. 5.1 Temperature programmed microscopy of polypropylene.

Table 5.1 Melting Temperatures.

Irradiations at 195 K		T_m / °C					
Dose/ megarad	Electron/γ radiation	Programmed Microscopy	D.T.A.	Kofler	Average	Crystalline fraction	Crystallisation onset/°C
0	-	172	172	172	172	1.00	134
2.5	E	170	170	170	170	0.96	132
3.25	E	169	-	170	169.5	0.95	
5.0	E	168	167	168	167.7	0.91	132
6.5	E	167	-	168	167.5	0.91	
9.75	E	164	-	164	164	0.85	
10.0	E	166	165	164	165	0.87	131
13.0	E	164	-	164	164	0.85	
16.25	E	162	-	163	162.5	0.83	
19.5	E	160	-	160	160	0.78	130
Irradiations at Room Temperature							
0	-	172	172	172	172	1.00	134
1.0	γ	169	169	-	169	0.94	134
2.5	γ	166	166	165	165.7	0.89	-
2.5	E	166	165	166	165.7	0.89	132
5.0	γ	161	160	161	160.7	0.79	-
5.0	E	162	-	159	106.5	0.79	130
10.0	γ	154	-	155	154.5	0.70	128
10.0	E	156	156	155	155.7	0.71	-
15.0	γ	149	151	150	150	0.63	123
20.0	γ	146	147	145	146	0.58	121
Stereoblock Polypropylene							
0	-	148		-	148	0.61	122
2.5	γ	142	-	-	142	0.53	116

The average melting temperature as a function of radiation dose is shown in Figure 5.2. Irradiation at 195K produces a much smaller decrease in melting temperature than does irradiation at room temperature. The crystallisation onset temperature under cooling conditions (5°C/min) also decreases with increasing radiation dose (Section 5.3.3).

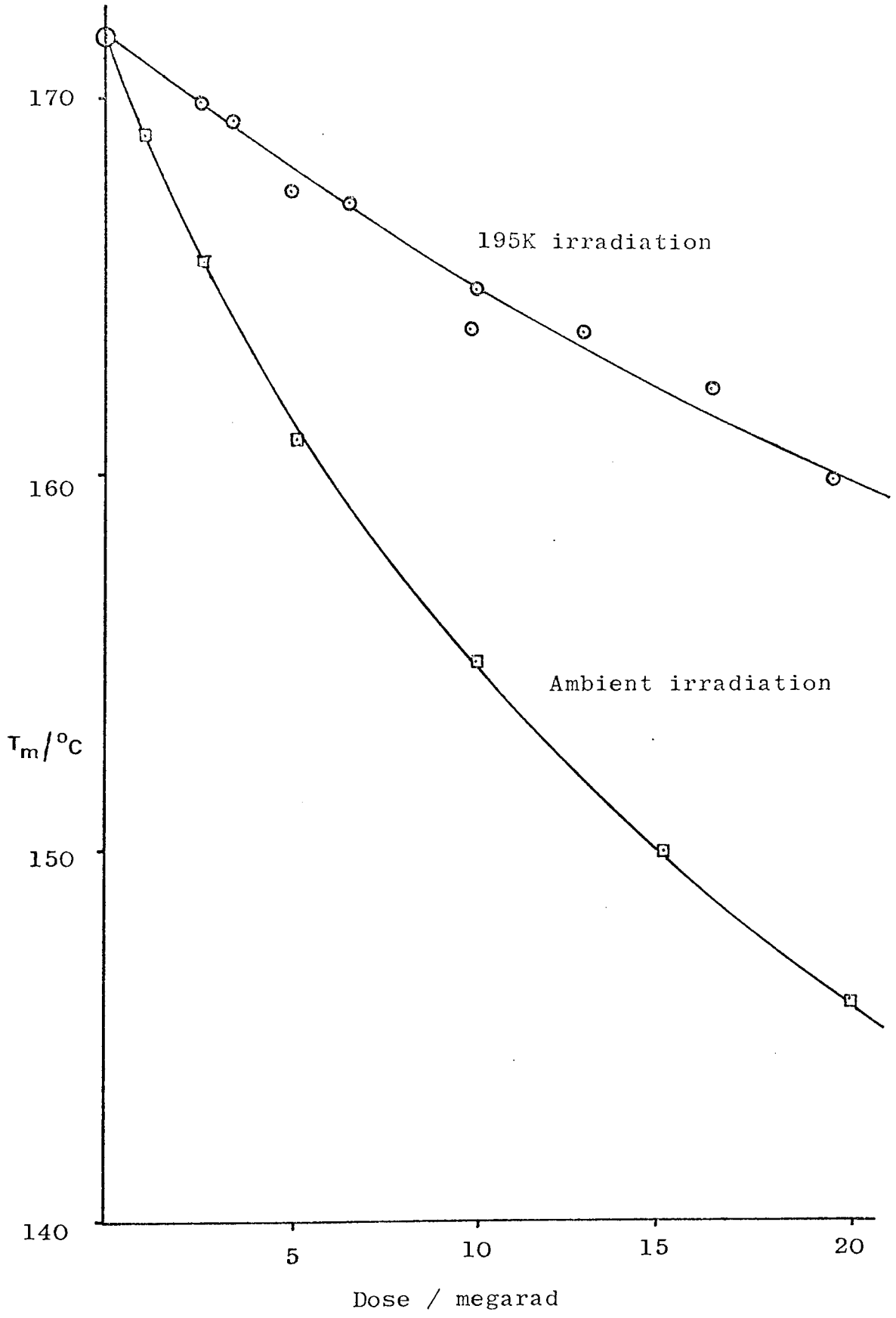

Fig 5.2 Melting temperatures of irradiated polypropylene as a function of radiation temperature and dose.

The temperature - programmed microscopy traces show an increase of D.L.I. preceding the melting temperature for some of the samples tested. This was not observed with samples irradiated to high doses (> 10 megarad) at room temperature. The D.L.I. curves of commercial (quenched) polypropylene film samples (Section 2.1.2) heated at $2^{\circ}C$/min are shown in Figure 5.3. The irradiated sample shows a much larger increase in D.L.I. prior to melting, than that exhibited by the non-irradiated film. Individual spherulites of these samples could not be observed at the magnifications used (200 x).

5.1.4 Discussion of Results

The melting temperature obtained by temperature - programmed microscopy was taken at the point at which the final baseline commenced. This produces a slightly higher melting temperature than in the method employed by Harvey [138] and Gilbert[139], who extrapolated the final steep portion of the D.L.I. curve to the continued baseline. This eliminated the final curvature thought to be caused by slow photocell response. However

(1) low molar mass compounds do not show this curvature;

(2) visual observation shows that spherulites are still present up to the higher temperature;

(3) the higher melting temperature agrees well with that microscopically observed and by D.T.A.

Figure 5.1 shows the melting to be a complex process beginning well below the final melting temperature. The melting curve of unirradiated and low dose - irradiated polypropylene can be divided into several sections :

(1) melting of imperfect crystals, beginning immediately

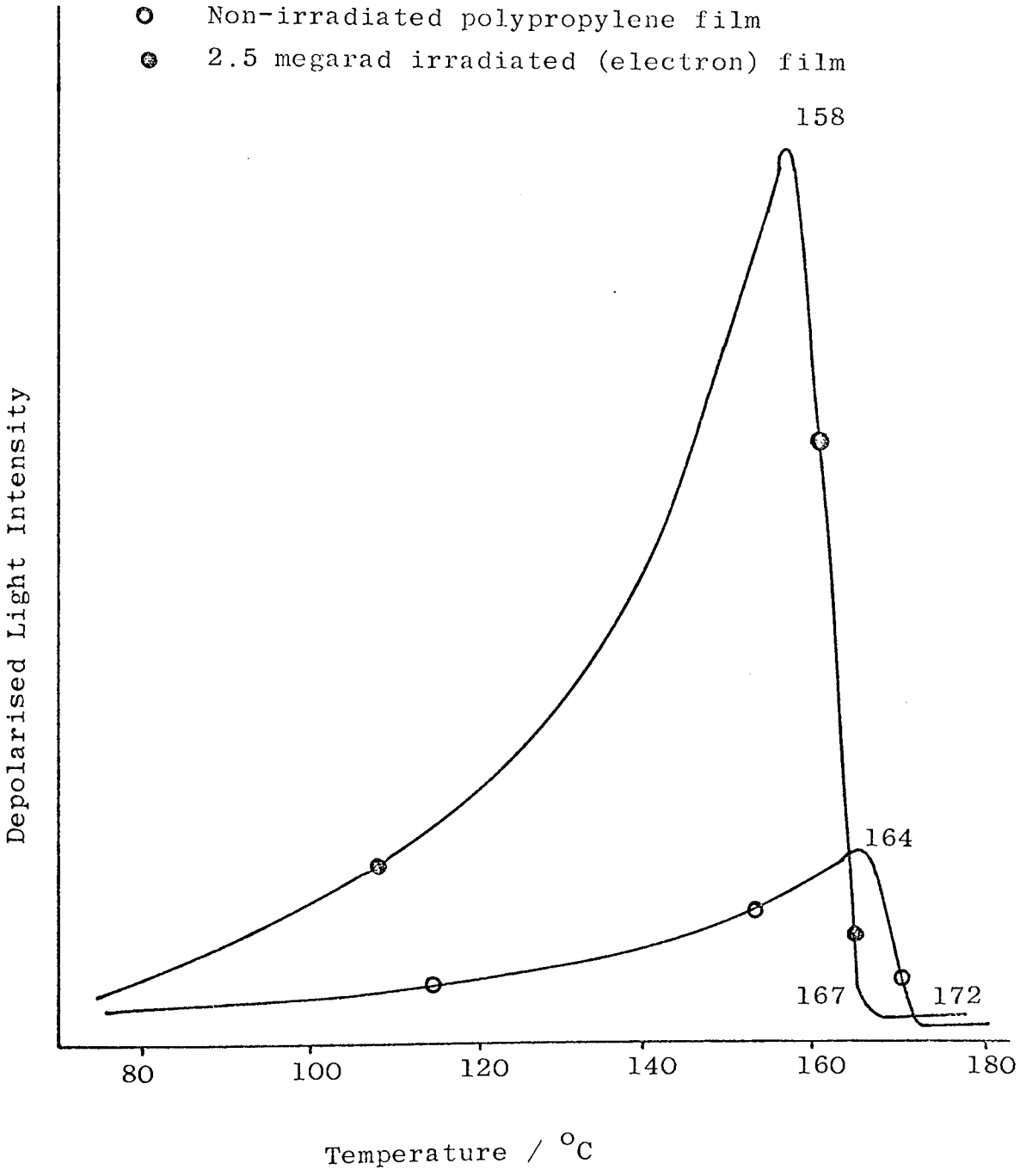

Fig. 5.3 Temperature programmed microscopy of irradiated and non-irradiated polypropylene film (quenched).

heating commences and causing a decrease in D.L.I. to approximately 140°C.

(2) an increase in D.L.I. probably caused by an increase in the perfection of existing crystals and reaching a maximum in the range 151 - 155°C. The peak temperatures were quite reproducible.

(3) a rapid decrease in D.L.I. as true melting commenced.

(4) a second increase in D.L.I. for which the reasons are uncertain. This may be caused by sample collapse bringing more spherulites into the field of view, but may be of more significance since the peak temperature coincides with the first peak observed by D.T.A. Interruption of the heating programme and holding at temperatures between the 'peaks' did not cause the second peak to be affected.

(5) a final decrease in D.L.I. with slow disappearance of the well-developed spherulites.

Samples irradiated to high doses showed only a regular gradual decrease in birefringence. This probably results from the imperfect structure of the spherulites (Figure 5.5 (d)).

The effect of irradiation temperature on melting temperature is surprisingly large. A possible reason for this is that considerable local melting, during irradiation, takes place in the uncooled polymer. In addition, the energy of the radiation is probably more evenly distributed when the amorphous regions of the polymer are in the glassy state. At higher temperatures the radiation damage is probably concentrated in the crystalline regions where the free radicals become trapped, and at the crystalline/amorphous interface.

The decreases in melting temperature are much larger than those reported by Kusy and Turner[112] and Rybnikar[109] but Natta et al[140] found similar decreases for thermally degraded polypropylene. This probably results from the smaller particle size of the polymer used in this study, causing larger extents of oxidative degradation. The crystalline fraction calculated from the Flory equation (1.13) assuming a heat of fusion of 32.6 kJ mol^{-1} [141], decreased to as low as 56% of the original crystallinity for a 20 megarad dose at room temperature. Calculated crystallinities are given in Table 5.1.

The intial G-values for loss of crystalline units, as defined in 1.3.5 are G(- cr) = 102 at 195 K and = 267 at room temperature. Such large values show that changes of chemical structure are taking place in addition to the simple thermodynamic effects on which the Flory equation is based. A plot of $1/T_m$ vs. radiation dose is shown in Figure 5.4. The change in slope of the room temperature series at high doses is thought to be caused by the change in spherulite structure for these samples. (Figure 5.5(d)).

The very large increase in D.L.I. of the irradiated quenched film (Figure 5.3) is caused by increased crystallinity occurring because of greatly reduced bulk viscosity of the polymer. At temperatures approaching the melting temperature the crystallinity is greatly increased compared to the small change in the non-irradiated film. It is probable that similar increases in crystallinity occur slowly at room temperature. For irradiated samples this probably plays an important part in the deterioration of mechanical properties on storage.

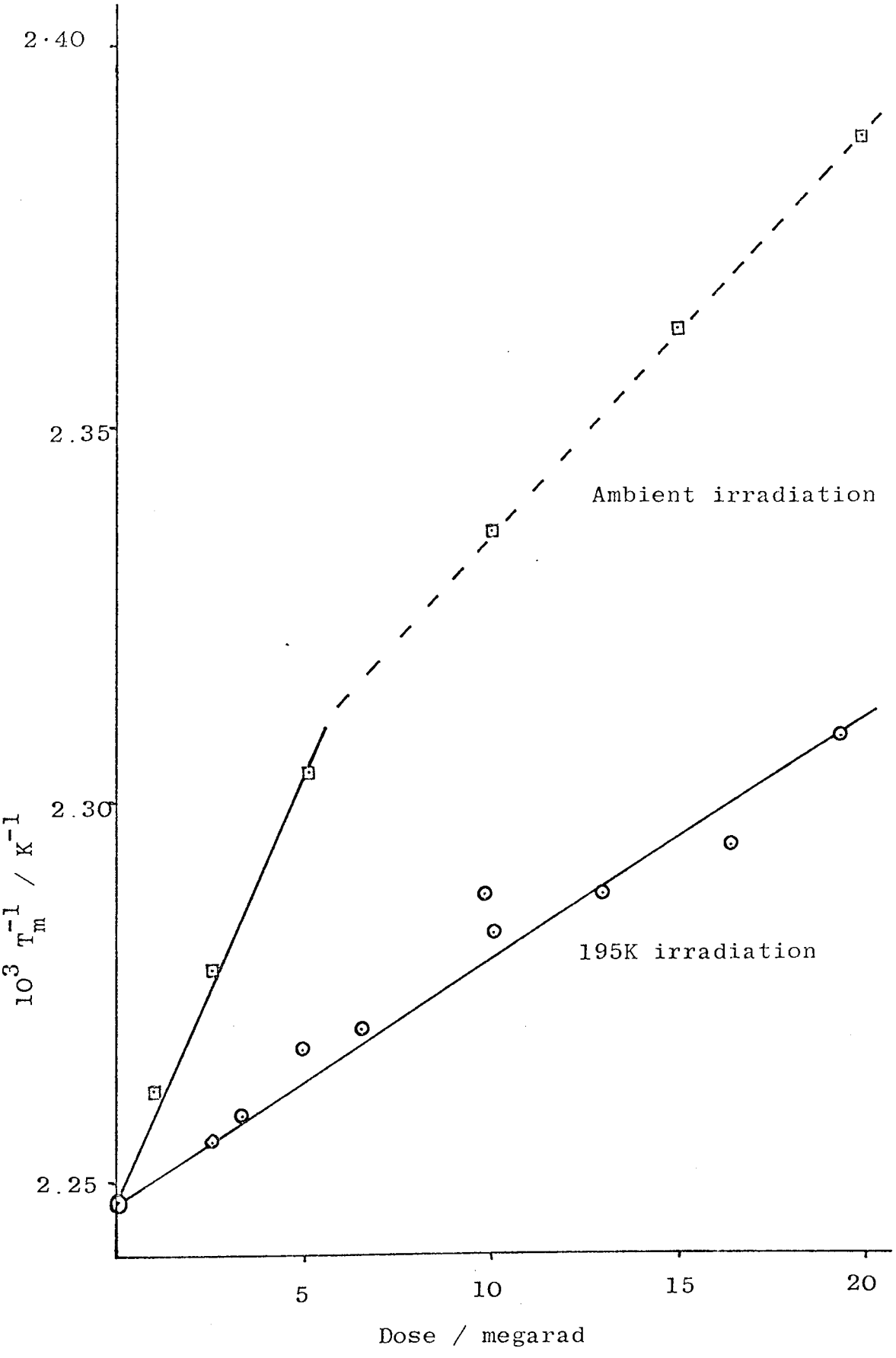

Fig. 5 4 Plots of 1 / T_m vs radiation dose .

5.2 Spherulite Studies

Isothermal growth rates of irradiated and non-irradiated polypropylene were measured and photographs taken of the spherulite appearance in a polarising microscope.

5.2.1 Experimental

A small quantity of polymer was placed between microscope slide and cover slip and melted at 200°C for 10 minutes on a hot plate. The cover slip was gently pressed to produce a thin uniform film. The slide was then rapidly transferred to a Reichert - Kofler microscope hot stage controlled at the required temperature in the range 130° - 135°C. The diameter of a single spherulite was measured with a calibrated micrometer eyepiece over a period of time until it impinged on another spherulite. The number of spherulites in the field of view were counted. Spherulite growth rates of samples irradiated to doses $>$ 2.5 megarad were not made, because at high doses the spherulite was non-symmetrical.

Photographs of the spherulite structure were taken on the Swift microscope used for temperature-programmed microscopy. The polymer samples were melted between cover slips at 200°C for 1 minute (10 minutes for unirradiated polymer) on a hot plate. The plate was then switched off and allowed to cool at room temperature. The cooling rate was initially 5°C/min and decreased to 3°C/min in the range 120 - 130°C. Photographs shown in Figure 5.5 were taken on a Beck reflex attachment camera, using Ilford HP 4 film with exposure times between 1 and 5 seconds.

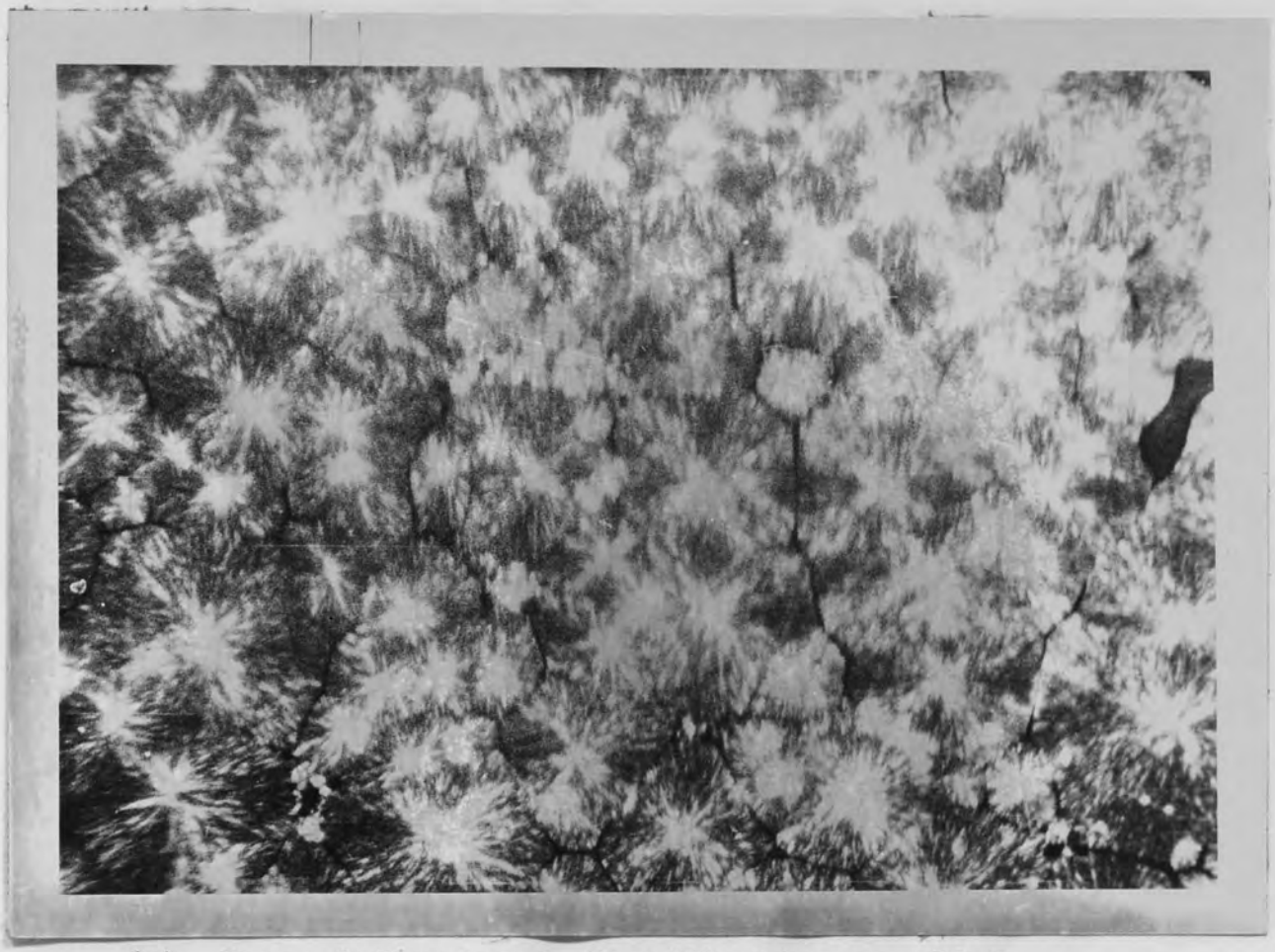

(a) Dose: 2.5 megarad; Magnification ca. 50 X

(b) Dose: 5.0 megarad; Magnification ca. 50 X

Fig. 5.5 Polypropylene spherulites

(c) Dose: 20 megarad; Magnification: ca. 50 X

(d) Dose: 20 megarad; Magnification: ca. 200 X

Fig. 5.5 Polypropylene spherulites

5.2.2 Results

The isothermal increase of spherulite diameter as a function of time is given in Table 5.3 and illustrated graphically in Figure 5.6.

Table 5.3 Spherulite diameter as a function of time at various temperatures for irradiated and non-irradiated polypropylene

	NON - IRRADIATED			IRRADIATED (2.5 Mrad, γ)		
	Time / Min	Diameter/ μm	Number in view	Time/ Min	Diameter/ μm	Number in view
130°C	4.25	131	9	3.75	108	2
	5.0	153	10	5.5	164	2
	6.0	186	11	6.5	195	3
	7.0	213	12	7	215	3
	8.0	244	12	8	248	3
	9.0	274	13	9	278	3
	11.0	321	13	10	311	3
132°C	4.0	84	18	4.75	89	4
	5.0	102	18	5.5	110	4
	6.5	132	19	7.0	138	4
	7.5	152	19	8.0	160	4
	9.0	180	20	9.0	183	4
	10.0	198	20	10.5	212	4
133.5°C	3.5	50	14	3.0	41	2
	5.5	78	14	5.0	63	2
	7.0	97	15	6.5	85	3
	9.0	124	15	7.5	97	3
	11.0	146	15	8.5	112	3
	13.0	182	16	9.5	123	3
				12.0	160	3

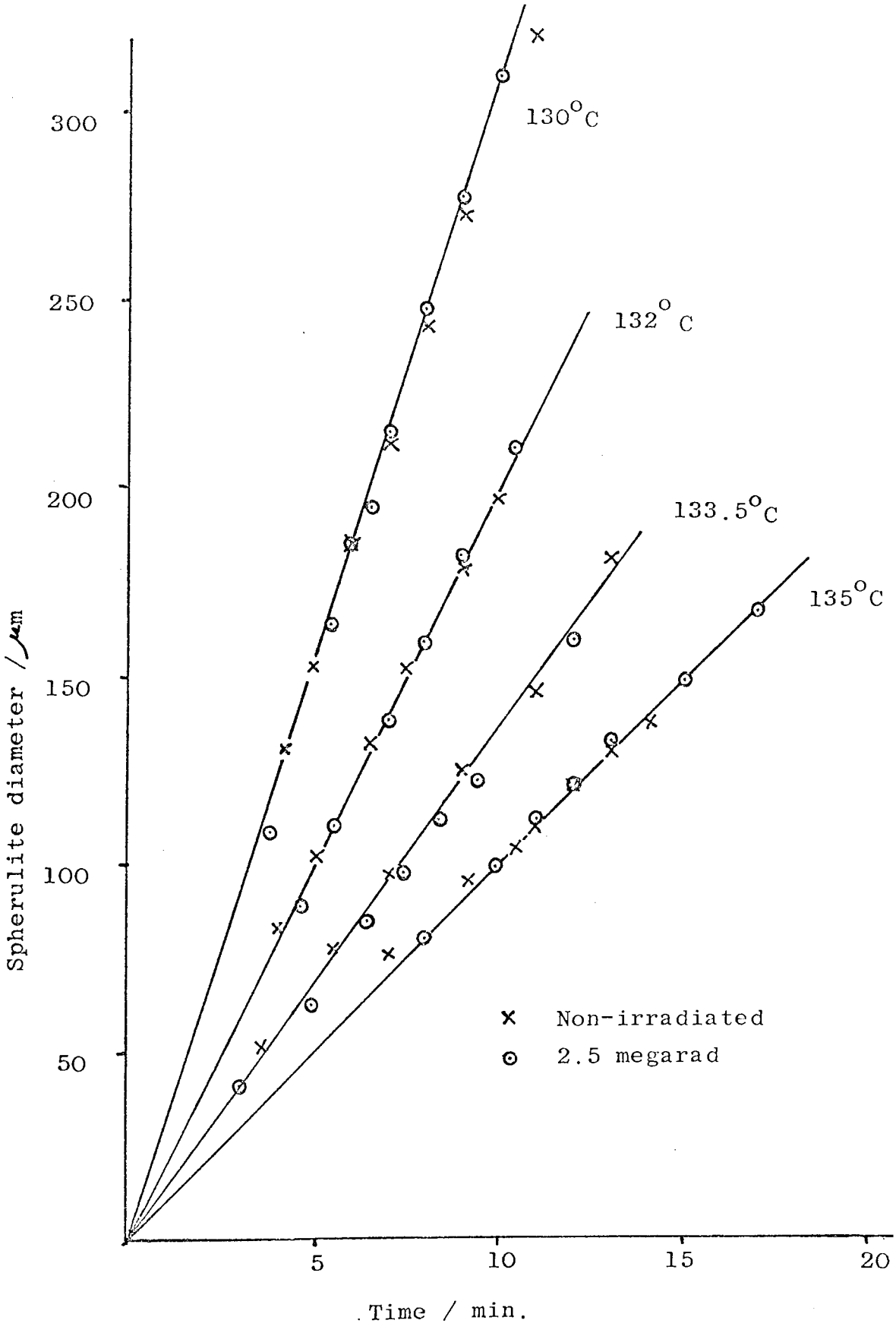

Fig 5.6 Plots of spherulite diameter vs. time for irradiated and non-irradiated polypropylene.

Table 5.3 continued .....

135°C	7.0	76	4	8.0	80	1
	9.25	96	4	10.0	99	1
	11.0	110	4	11.0	113	1
	12.0	121	4	12.0	121	1
	13.0	131	4	13.0	133	1
	14.0	139	4	15.0	149	1
	16.0	158	4	17.0	168	1

The growth rates of irradiated and non-irradiated polypropylene were found to be identical at each crystallisation temperature and are given in Table 5.4.

Table 5.4 Growth rates of spherulite radius for irradiated (2.5 Mrad) and non-irradiated polypropylene at various crystallisation temperatures.

Temperature /°C	Growth rate / μm min^{-1}
130	15.5
132	10.2
133.5	6.8
135	5.0

An estimate of the number of nuclei/unit volume was obtained by counting the average number of spherulites in films 0.1 mm thick, prepared using metal spacers. For irradiated polypropylene the nucleation density was 2×10^5 cm^{-3} and for non-irradiated polymer was 4×10^5 cm^{-3}, when crystallised at 132°C following melting at 200°C. These values must be regarded as approximate

because of (1) difficulty in obtaining a uniform film without excessive bubble formation, (2) large variations in the number of spherulites in the field of view. The spherulites appeared to nucleate at two levels in the film, which suggests nucleation was taking place at the glass surfaces.

5.2.3 Discussion

Figure 5.6 shows that nucleation of spherulite growth is predetermined with zero induction time, and that growth rates were not affected by a radiation dose of 2.5 megarad. The growth rates were faster than those observed by Falkai [142] who quotes growth rates of 4.3 and 1.6 $\mu m\ min^{-1}$ at 130° and 135°C respectively (of 15.5 and 5.0 $\mu m\ min^{-1}$ in Table 5.4). A probable explanation for this lies in the higher melting point of the polypropylene used in this study (172°C compared to 165°C). Limbert and Baer [143] have compared spherulite growth rates of several authors at equal levels of undercooling, $T_m - T_c$, and found good agreement. The results here also agree well when they are compared on this basis. Analysis of these results will be deferred to Section 5.3.3 following consideration of the overall rates of crystallisation.

The photographs of spherulite structure show that at 2.5 megarad (Figure 5.5 (a)) the spherulite appearance is similar to non-irradiated polypropylene, but with an increased tendency towards crack formation between spherulites. This probably results from the thinness of the irradiated film, but may be an important factor in causing brittleness of irradiated polypropylene. Spherulite cracking has also been observed in thermal oxidative degradation of polypropylene [144]. At higher

doses structural imperfection of the spherulites can be observed (Figure 5.5 (b - d)).

The spherulites in polypropylene irradiated at 20 megarad grew from elongated nuclei, producing oval or rectangular spherulites. The spherulites initially grew with an open fibrillar structure, of dendritic appearance. Degradation impurities probably concentrated in the interfibrillar regions and these crystallised at a later stage as the temperature was reduced. The final appearance is shown in Figures 5.5 (c) and (d). At low magnification the structure appears grainy, but at higher magnification the sheaf-like appearance can be seen. Keith and Padden have observed similar structures in thermally oxidised polypropylene [145] and in mixtures of isotactic and atactic polypropylene [146]. In the latter case however the interfibrillar material did not crystallise. Polypropylene irradiated to 5 megarad (Figure 5.5 (b)) shows an intermediate level of structural imperfection.

The smaller number of nucleating centres in the irradiated sample may be caused by the reduction in melting temperature T_m. At a given crystallisation temperature T_c, there will thus be a decrease in the extent of undercooling, $T_m - T_c$, which usually causes a reduction in the number of nucleating centres [135].

5.3 Isothermal Crystallisation

5.3.1 Introduction

The isothermal crystallisation of polymers is frequently described by the Avrami equation [147]

$$\theta = \exp (- kt^n) \quad \ldots\ldots\ldots 5.1$$

where θ is the volume fraction of polymer which has not crystallised at time t, k is the crystallisation rate constant and n is an integer. The equation assumed that nucleation occurs at randomly spaced locations in the crystallisation system and that crystal growth then occurs in one, two or three dimensions to form rods, discs or spheres. For instantaneous nucleation, as normally occurs in polypropylene, two dimensional growth corresponds theoretically to an Avrami exponent $n = 2$ and three dimensional growth to $n = 3$. When nucleation is not instantaneous but sporadic, these values are increased by 1. In practice, the value of n may not be an integer and may change during crystallisation.

Equation 5.2 can be written as

$$\ln 1/\theta = kt^n \qquad \ldots\ldots 5.2$$

or $$\log (\ln 1/\theta) = \log k + n \log t \qquad \ldots 5.3$$

and thus a plot of $\log (\ln 1/\theta)$ vs. $\log t$ may be used to evaluate k and n. Computer methods of analysis have also been developed [139] and are useful where n changes during crystallisation.

The half-time of crystallisation $t_{\frac{1}{2}}$ (when $\theta = \frac{1}{2}$) is widely used as a measure of the crystallisation rate. At $t_{\frac{1}{2}}$

$$\ln \theta = \ln \tfrac{1}{2} = - k t_{\frac{1}{2}}^{\,n} \qquad \ldots\ldots 5.4$$

whence $$t_{\frac{1}{2}} = (\ln 2 / k)^{1/n} \qquad \ldots\ldots 5.5$$

and $$k = \ln 2 / t_{\frac{1}{2}}^{\,n} \qquad \ldots\ldots 5.6$$

Crystallisation rate of polypropylene has been studied by dilatometry [142], differential scanning calorimetry [148] and microscopic investigations [149].

The effect of crystallisation temperature on rate of crystallisation has been the subject of several theories [135]. A series of equations have been derived of the general form

$$\ln k = \ln k_o - n\frac{E_D}{RT} - f\left[\frac{T_m^2}{T_c(\Delta T)^2}\right] \quad \ldots 5.7$$

in which T_m is the thermodynamic melting point, T_c is the crystallisation temperature, ΔT is $T_m - T_c$, k_o is a constant, E_D is the activation energy of segmental diffusion and f is dependent on the nature of nucleation and growth. In terms of crystallisation half-time

$$\ln \; 1/t_{\frac{1}{2}} = \frac{1}{n}\left(\ln k_o - \ln \ln 2\right) - \frac{E_D}{RT} - f'\frac{T_m^2}{T_c(\Delta T)^2} \quad \ldots 58$$

A plot of $\ln 1/t_{\frac{1}{2}}$ vs. $T_m^2 / T_c (\Delta T)^2$ should yield a straight line of slope f'

$$f' = \frac{8\pi\bar{\sigma}^3}{R(\Delta H_u)^2} \quad \ldots 5.9$$

in which $\bar{\sigma}$ is the mean interfacial free energy and ΔH_u the latent heat of fusion.

5.3.2 Experimental

Two techniques were used to measure isothermal crystallisation rates.

Differential scanning calorimetry

For this work the Du Pont D.S.C. cell was used with the Du Pont 900 thermal analyser. The temperature difference between sample and reference is recorded and is therefore a D.T.A. method rather than D.S.C. as conventionally defined. The Du Pont 900 was modified to improve the sensitivity, and the modifications amd technique are described in detail by Gilbert (139). The temperature difference T_d between sample and reference was in the range 0.02 - 0.1°C and this was displayed on a sensitive external recorder (Honeywell Electronik 19) fitted with a disc integrator (Model 352). The sensitivity range selected for all runs gave a recorder deflection of 1 inch for a temperature difference of 0.0153°C.

10 - 15 mg of polymer was placed in an aluminium sample pan and a similar weight of glass beads used as reference. The D.S.C. cell was rapidly heated to 200°C to melt the sample, which was then held at this temperature for 10 minutes (unirradiated) or 1 minute (irradiated). The short melt time for irradiated samples was to prevent excessive degradation but was sufficient to thoroughly melt the samples having very low melt viscosity. The cell was then rapidly cooled to the selected crystallisation temperature which could normally be controlled to $\pm$ 0.1°C.

As crystallisation proceeded T_d was observed to pass through a maximum before returning to the baseline. A typical crystallisation trace is shown in Figure 5.7 (a). The area beneath the crystallisation curve was obtained from the movement of the integrator pen. Figure 5 (b) shows the integrated crystallisation curve. When the recorder trace did not return to the original baseline, linear baseline-drift was assumed and allowed for. The integrated curve was

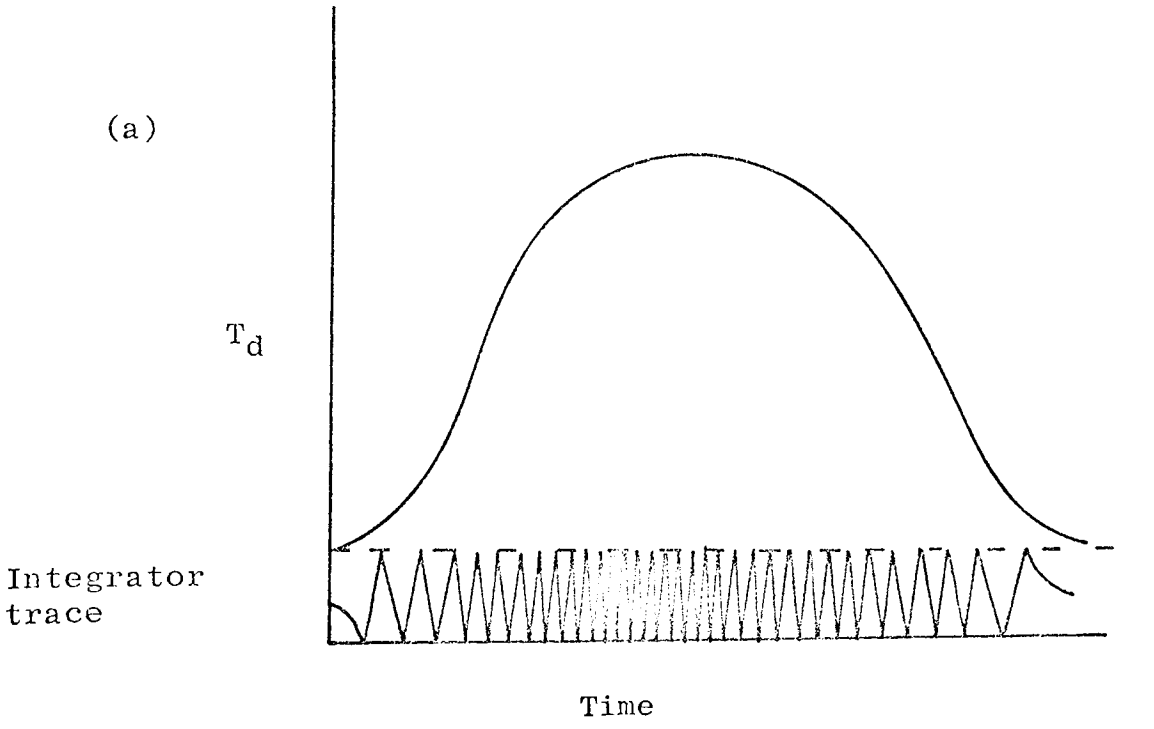

Fig. 5.7 Typical crystallisation curves

(a) T_d vs. time

(b) $A_t = \int_0^t T_d \cdot dt$ vs. time

used to obtain values of $t_{\frac{1}{2}}$, A_t and A_∞,

where

$$A_t = \int_0^t T_d \cdot dt \quad \ldots\ldots 5.10$$

and

$$A_\infty = \int_0^\infty T_d \cdot dt \quad \ldots\ldots 5.11$$

The Avrami equation may be written as

$$\frac{A_\infty - A_t}{A_\infty} = \theta = \exp\left[-k t^n\right] \quad \ldots\ldots 5.12$$

which can be rearranged to

$$n = t \frac{dA_t}{dt} \Big/ (A_\infty - A_t) \ln \frac{A_\infty}{A_\infty - A_t} \quad \ldots 5.13$$

A computer program [139] was used to evaluate n for each value of A_t. The program selected values of n within an arbitrary error limit of $\pm$ 0.2, from which an average value of n was computed, together with the crystallisation rate constant calculated from equation 5.6.

Isothermal microscopy

A Swift polarising microscope fitted with a double hot stage and photocell was also used for isothermal crystallisation rates. Its design, construction and use are described by Harvey [138]. Samples on dust-free cover slips were melted on one stage and then transferred with a push rod to the second stage held at the required crystallisation temperature.

The depolarised light intensity as a function of time was recorded and was of similar appearance to the integrated trace from D.S.C measurements (Figure 5.7 (b)). The results were analysed with the same computer program used for the D.S.C. results. The crystallisation half-time agreed well with that from D.S.C. measurement but the n values showed greater scatter.

The convenient limits of crystallisation were found to be 3 minutes and 40 minutes. Faster crystallisations could not be measured because of difficulty in rapidly obtaining the crystallisation temperature (D.S.C.) or relatively slow photocell response (microscopy). Slower crystallisations result in very flat crystallisation curves and difficulty was experienced in maintaining temperature control over a long period. In all cases induction period for crystallisation were absent.

5.3.3 Isothermal Crystallisation Results

Plots of $\ln 1/\theta$ vs time on log. log. paper were linear, over most of the crystallisation range, but computer analysis to obtain k and n was preferred. The values of n listed by the computer were constant (within $\pm$ 0.2) for $>$ 70% of the crystallisation range. The average value of n was found to be close to 2 for all samples studied up to radiation of 20 megarad. Corrected rate constants, assuming $n = 2$ are given in Table 5.5 together with other crystallisation data. The irradiated samples were electron irradiated at 195 K and stored at room temperature for several weeks before measurement. Figure 5.8 is a plot of crystallisation half-time as a function of crystallisation temperature for unirradiated and irradiated samples (2.5 and 5.0 megarad).

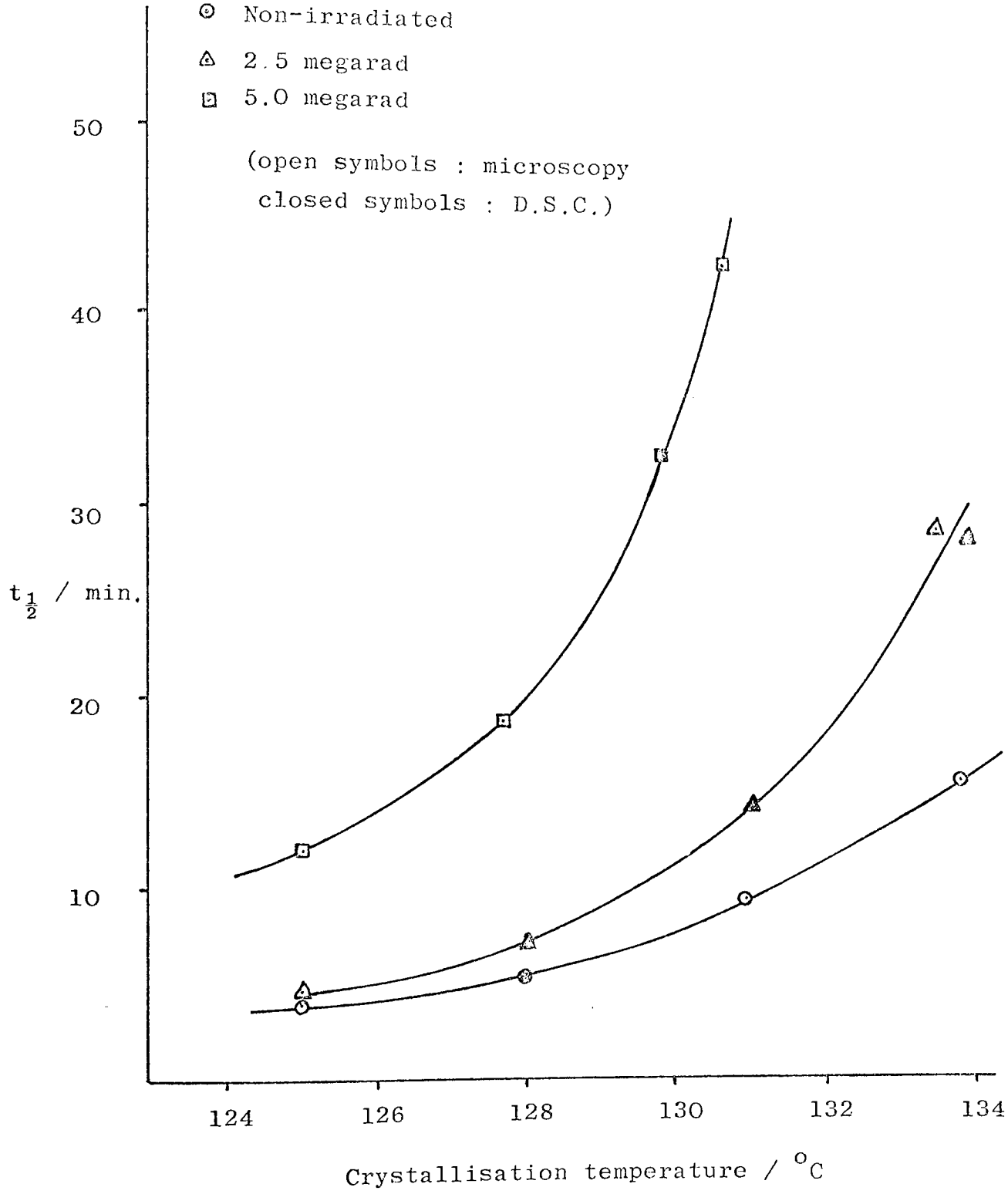

Fig. 5 8 Crystallisation half-times at various temperatures for non-irradiated and irradiated polypropylene.

Figure 5.9 shows the crystallisation half-time plotted against undercooling ΔT (= $T_m - T_c$), T_m was taken from Table 5.1 to be 172°C, 170°C and 168°C for the non-irradiated, 2.5 megarad and 5.0 megarad samples respectively.

Table 5.5 Crystallisation Kinetics Data

Dose/ Megarad	Technique	Temperature/ °C	$t_{\frac{1}{2}}$ /min	Average n	k x 10^3 /min $^{-n}$	Corrected k x 10^3 /min $^{-2}$
0	D.S.C.	133.8	15.5	2.16	1.96	2.88
0	D.S.C.	131.0	9.5	2.12	5.86	7.67
0	Mic	128.0	5.5	2.14	18.1	22.9
0	D.S.C	125.0	4.3	1.99	38.1	37.5
2.5	Mic	133.8	28.6	1.75	1.96	0.85
2.5	D.S.C.	133.4	29.0	2.11	0.57	0.82
2.5	Mic	131.0	14.5	2.08	2.67	3.30
2.5	Mic	127.8	7.2	2.03	12.6	13.4
2.5	Mic	125.0	4.65	1.84	41.1	32.0
5.0	D.S.C	130.6	43.0	2.10	0.25	0.37
5.0	Mic	129.8	33.0	2.26	0.23	0.63
5.0	D.S.C.	127.5	18.7	1.99	2.05	1.98
5.0	D.S.C.	125.0	12.0	1.86	6.82	4.81

5.3.4 Discussion

Figure 5.8 and Table 5.5 show that D.S.C. and microscopy produce similar results for the crystallisation rates of polypropylene. Secondary crystallisation causes a slow increase in the latter stage of the microscopy crystallisation curve but did not affect the D.S.C. curve.

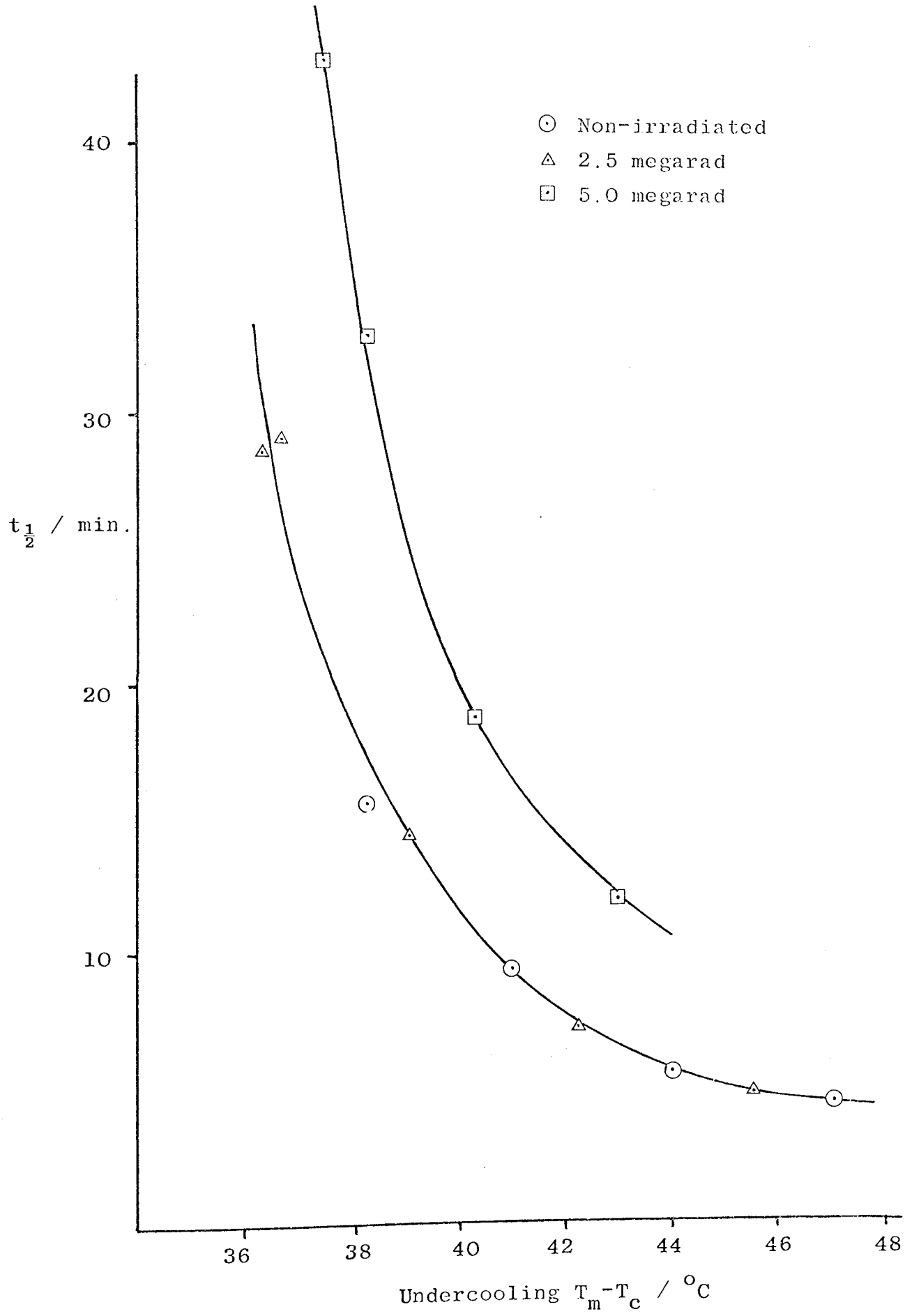

Fig. 5.9 Plot of crystallisation half-time $t_{\frac{1}{2}}$ vs. undercooling for irradiated and non-irradiated polypropylene.

When compared at equal temperatures, the crystallisation rates are found to decrease in the order : non-irradiated > 2.5 megarad > 5.0 megarad. Figure 5.9 shows however, that the crystallisation rates of the 2.5 megarad and non-irradiated polypropylene are almost equal when compared at equal levels of undercooling. This is not the case for the sample irradiated to 5 megarad, presumably because the imperfections in the crystalline structure, observable in Figure 5.5(b) causes additional reduction in the crystallisation rate.

The effect of temperature on crystallisation rate can also be assessed by plotting log crystallisation rate (as log $1/t_{\frac{1}{2}}$) vs $T_m^2 / \Delta T^2 T_c$ (Figure 5.10). T_m was taken as 445 K, 443 K and 441 K for the non-irradiated, 2.5 megarad and 5.0 megarad samples respectively. The linear plots suggest that these temperatures can satisfactorily be taken as the thermodynamic melting points. Linear graphs were also obtained when the temperature function $T_m / T_c \Delta T$ was used.

The slopes for irradiated polymers, -6.8 K are greater than for non-irradiated, -5.2K. The slope can be equated to $8\pi\bar{\sigma}^3 / R \Delta H_u^2$ (Equation 5.8) and thus the change of slope may be explained as an increase in the mean interfacial energy $\bar{\sigma}$, or a decrease in the heat of fusion ΔH_u following irradiation. The total area beneath the crystallisation curve, A_∞, measured by D.S.C. was found to be constant for each of the samples, suggesting that ΔH_u is unaffected by irradiation. Direct measurement of ΔH_u using a Perkin-Elmer differential scanning calorimeter (model 1B) confirmed this. Using the literature value of 10.9 kJ

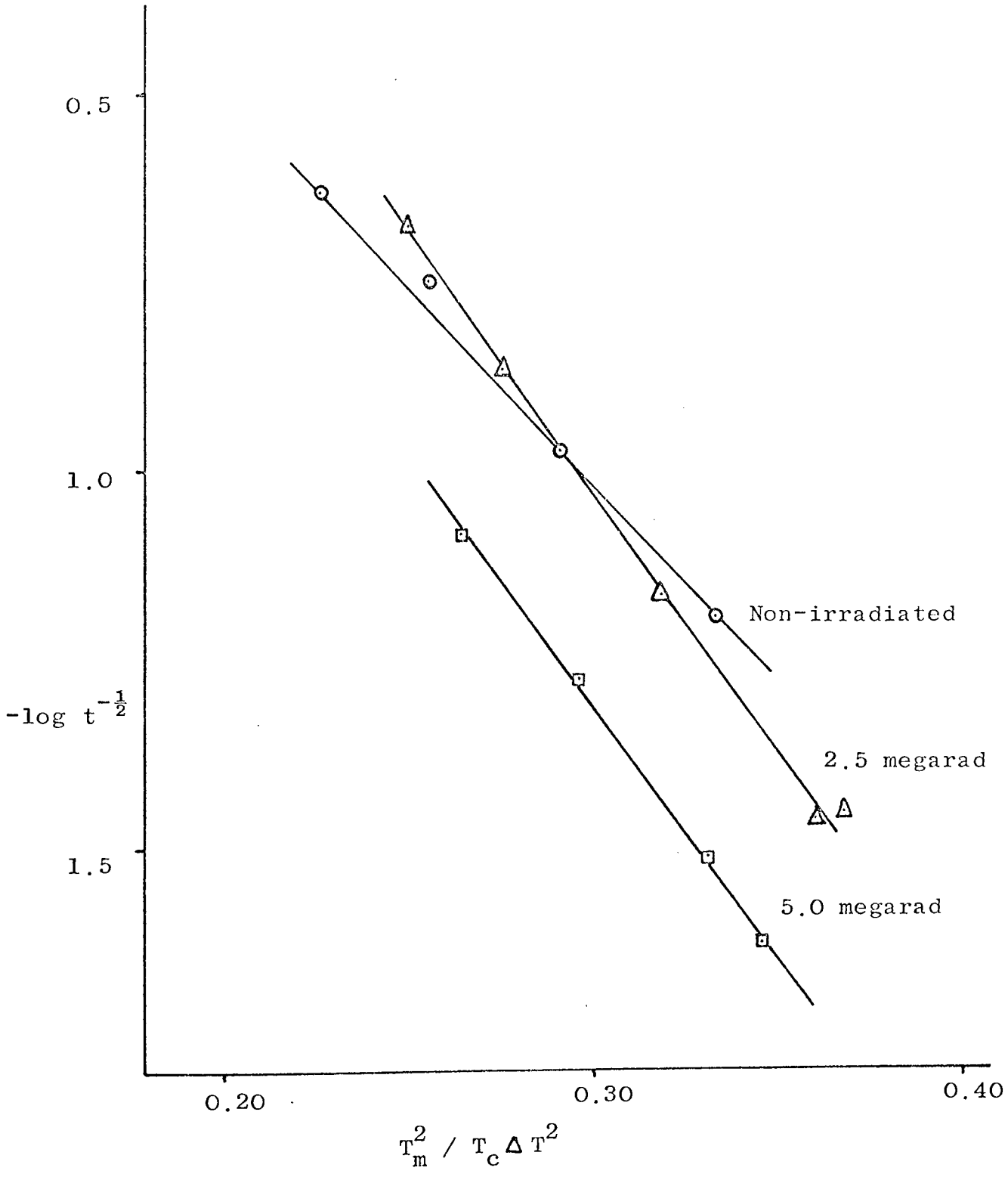

Fig. 5.10 Plot of log $t^{-\frac{1}{2}}$ vs. $T_m^2 / T_c \Delta T^2$ for irradiated and non-irradiated polypropylene.

mole repeat unit[141], σ may be calculated to be 5.4 x 10^{-3} J m^{-2} (5.4 erg cm^{-2}) for non-irradiated and 5.9 x 10^{-3} J m^{-2} for irradiated polypropylene. These values agree well with those found by Hamide et al [150] who obtained $\bar{\sigma}$ = 5 - 6 x 10^{-3} J m^{-2}.

At equivalent temperatures, the crystallisation half-times of the non-irradiatedpolymer are in good agreement with those obtained by Falkai[142] using dilatometry, Parrini et al [150] using microscopy, and Godivskii and Slonimskii using thermal methods [148]. The Avrami exponent n = 2 was also found by Godivskii and indicated 2-dimensional growth since pre-determined nucleation was observed (5.2). Dilatometric investigations by Falkai and other workers gave an Avrami value of n = 3, corresponding to volume growth on pre-determined nuclei. The explanation adopted by Godivskii to account for the discrepancy is that it results from the multi-stage character of the crystallisation process. The spherulites in polypropylene consist of fine ribbons or sheets with convoluted polymer chains [152]. Such planar structural elements are chiefly responsible for the heat evolution. In contrast, dilatometry detects the three-dimensional packing of these structural elements, by its effect on the overall polymer density. The Avrami value n = 2, obtained microscopically, may be due to birefringence of these planar structural elements, but an alternative and more likely explanation is that the film thickness is small in comparison to spherulite dimensions and this causes disc-like growth. Irradiation does not affect the Avrami exponent

and thus the same crystallisation mechanism can be assumed for the irradiated polymer.

5.3.5 Spherulite Growth Rate and Crystallisation

The spherulite growth rate S may be related to temperature by

$$S = S_o \exp\left[\frac{-E_D}{RT} - \frac{\Delta G^*}{RT} \right] \quad \ldots\ldots 5.14$$

in which S_o is a constant, E_D is the activation energy of viscous flow for transport of polymer segment across the liquid-spherulite interface and ΔG^* is the free energy barrier for formation of nuclei. Since E_D is certainly reduced by irradiation there must be an increase in ΔG^* to explain the unchanged spherulite growth rate. This increase in ΔG^* would cause a decrease in nucleation density and hence produce an overall lower crystallisation rate. The linearity of log S as a function of temperature is predicted by Equation 5.14 and is illustrated in Figure 5.11 using the data from Table 5.3.

Equation 5.14 may be developed as

$$S = S_o \exp\left[-\frac{E_D}{RT} - \frac{8 \pi \bar{\sigma}^3 T_m^2}{R \Delta H_u^2 T_c (\Delta T)^2} \right] \quad \ldots\ldots 5.15$$

A plot of log S vs $T_m^2 / T_c (\Delta T)^2$ in accordance with equation 5.15 is shown in Figure 5.11. The T_m values used were 445 K (non-irradiated) and 439 K (irradiated 2.5 M rad at room temperature). The slopes of the lines in Figure 5.12 are -4.6 K (non-irradiated) and -7.0 K (irradiated) giving respective values of $\bar{\sigma}$, 5.1 and 6.0 x 10^{-3} J m^{-2} in good

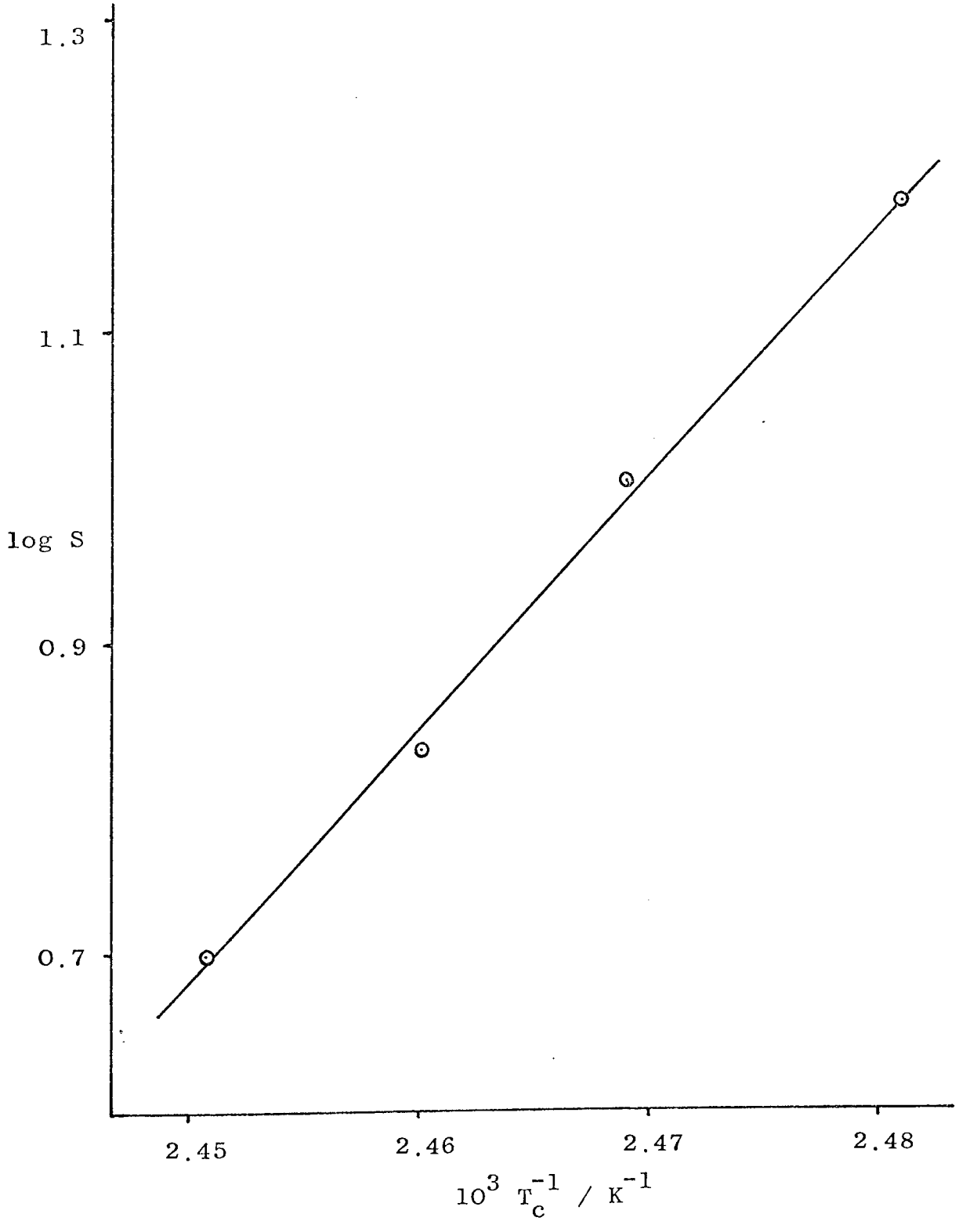

Fig. 5.11 Plot of log spherulite growth rate in polypropylene vs. T_c^{-1}.

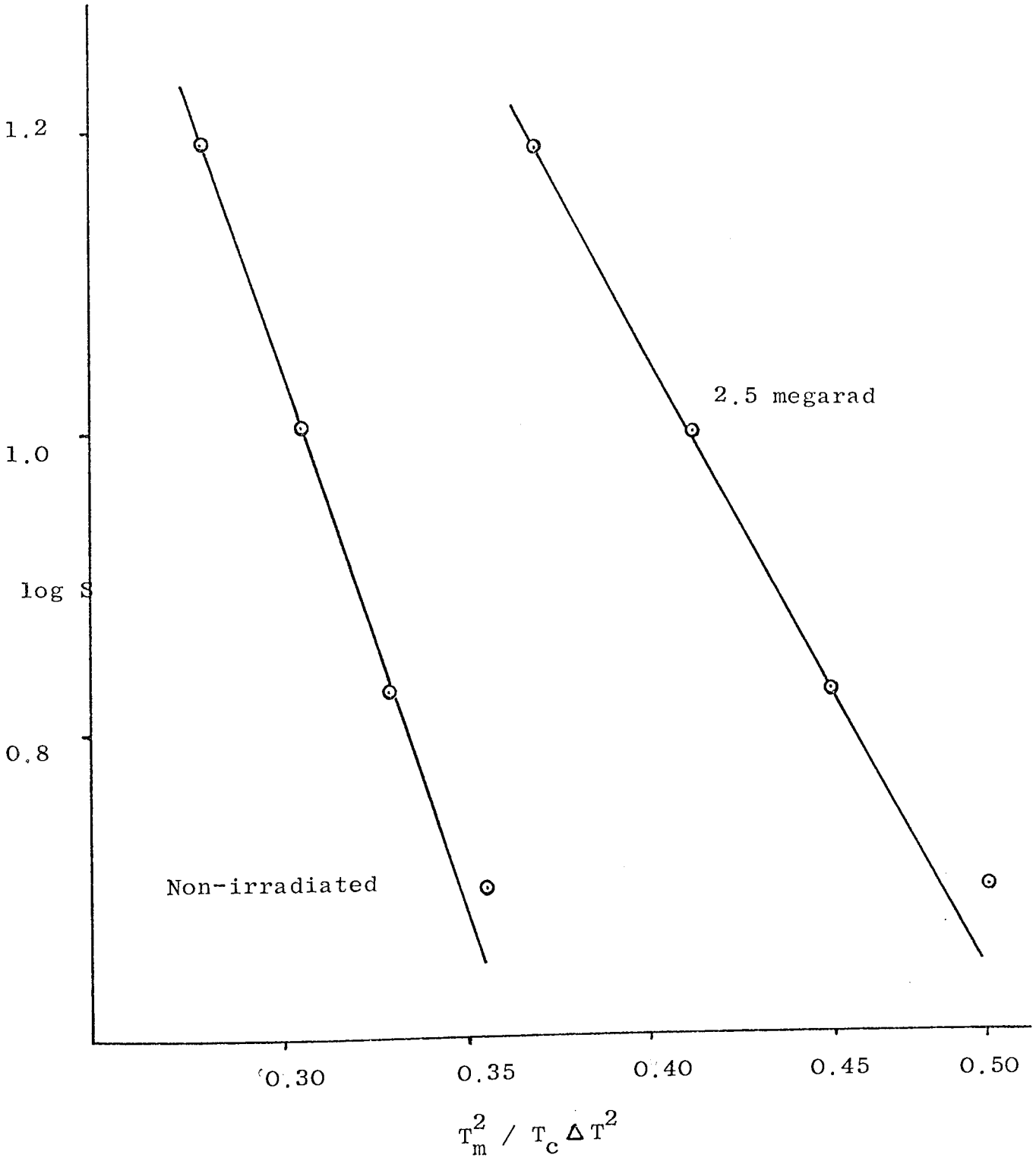

Fig. 5.12 Plot of log spherulite growth rate in polypropylene vs. $T_m^2 / T_c \Delta T^2$

agreement with those obtained from overall crystallisation rates (Figure 5.9).

The spherulite growth rate , S, can be related to the crystallisation rate constant k, by the equation derived by Morgan [153], for three-dimensional predetermined growth

$$k = \frac{4}{3} \pi S^3 N \quad \ldots\ldots 5.16$$

in which N is the number of nuclei/unit volume.

If the crystallisation half-times are used to calculate k, using equation 5.6 with n = 3, nucleation densities of 1.1 x 10^5 for non-irradiated and 0.3 x 10^5 for irradiated (2.5 M rad) polypropylene may be calculated. These are of the same order as those directly observed, but better agreement cannot be expected because of the inaccuracy of the observation method, and the use of rate constants calculated assuming n = 3, when this was not experimentally found.

5.4 Conclusions from Melting and Crystallisation Studies

5.4.1 Melting Studies

(1) Optical and thermal methods of melting point determination were in good agreement.

(2) A large decrease in melting temperature occurred as a result of irradiation of polypropylene in air. The temperature decrease, increased with radiation dose, and was much larger than that expected to result from chain scission only.

(3) The melting temperature decrease was smaller for irradiations at 195 K, compared to those at room temperature.

(4) Irradiated quenched polypropylene film shows a much

greater pre-melting crystallisation increase in depolarised light intensity than when non-irradiated.

5.4.2 Spherulite Studies

(1) Spherulites grow from pre-determined nuclei at identical rates for 2.5 megarad - and non-irradiated polypropylene.

(2) The nucleation density was reduced by irradiation.

(3) Polypropylene irradiated to moderate doses (2.5 and 5.0 megarad) shows a tendency towards crack formation between spherulites.

(4) At high doses, polypropylene spherulites grow in a distorted manner, and produce open sheaf-like structures.

5.4.3 Crystallisation Studies

(1) Isothermal crystallisation rates of polypropylene by D.S.C. and microscopy agree well, giving similar crystallisation half-times and an Avrami integer $n = 2$.

(2) At equal temperatures, irradiated polypropylene crystallises more slowly than non-irradiated polypropylene. At equal undercooling, 2.5 megarad and non-irradiated polypropylene crystallise at equal rates.

(3) Theories of the effects of crystallisation temperature on crystallisation rate can be applied to both non-irradiated and irradiated polypropylene.

CHAPTER SIX : THERMAL STABILITY AND HYDROPEROXIDE ANALYSIS

6.1 Thermal Stability

6.1.1 Introduction

The progress of pyrolytic decomposition reactions which produce volatile products can be determined by continuous weighing of the sample, the technique being known as thermogravimetric analysis or T.G.A. The fraction of the substance not yet decomposed, y, is related to the weight, W_t, at time t, by the equation

$$y = \frac{W_t - W_\infty}{W_o - W_\infty} \qquad \ldots. 6.1$$

where W_o and W_∞ are the initial and final weights.

For isothermal pyrolysis the reaction rate is given by

$$-\frac{dy}{dt} = k y^n \qquad \ldots. 6.2$$

in which n is the reaction order, which is frequently found to equal one.

Most T.G.A. measurements are made in a manner in which the temperature T is a linear function of t, i.e.

$$T = T_o + u t \qquad \ldots. 6.3$$

where u is the programmed heating rate.

If the rate constant k obeys the Arrhenius equation

$$k = A e^{-E/RT} \qquad \ldots. 6.4$$

then the equations can be combined to give (for a first order reaction)

$$-\frac{dy}{y} = \frac{A}{u} e^{-E/RT} . dt \qquad \ldots.. 6.5$$

Equation 6.5 may be integrated to

$$\ln \frac{1}{y} = \frac{A}{u} \int_{T_o}^{T} e^{-E/RT} .dt \quad \ldots\ldots 6.6$$

Various approximations for the integral in Equation 6.6 have been made, by Van Krevelen et al. [154], by Horowitz and Metzger [155] and by Broido [156]. Broido has made theoretical calculations which show that the relationship

$$\ln \ln \frac{1}{y} = \frac{-E}{0.960\ R} \left(\frac{1}{T} \right) + \text{const} \quad \ldots\ldots 6.7$$

is the most accurate of the three methods. For the range $0.999 > y > 0.001$ the error in E obtained from the slope of a plot of $\ln \ln {}^{1}/_{y}$ vs ${}^{1}/_{T}$ is less than 0.4%.

6.1.2 Experimental

The thermal decomposition of polypropylene was measured using the Dupont 950 thermogravimetric analyser module attached to the Dupont 900 thermal analyser. The weight of the sample is monitored as a function of temperature on the X - Y recorder of the Dupont 900. Isothermal operation is also possible in which the weight is measured as a function of time. Details of its construction are given in the instrument handbook[157].

The sample is held in a platinum boat attached to a balanced quartz rod. Change in weight causes a movement of the rod which is detected photoelectrically and recorded on the Y- axis of the recorder. A thermocouple in the vicinity of the sample boat measures the temperature which is displayed on the X-axis. The cold junction of thermocouple was maintained at $0^{o}C$ in crushed ice.

The following operation conditions were normally used :

Sample weight	:	10.0 mg
Temperature scale	:	50°C/inch
Initial weight scale	:	0.2 mg/inch
Inital suppression	:	9.0 mg
Final weight scale	:	2.0 mg/inch
Final suppression	:	0 mg
Heating rate	:	15°C/min
Atmosphere flow rate	:	1 SCFH (N_2, O_2, or Air)
Time constant	:	1 second.

For increased accuracy during the early stages of decomposition most runs were made using a 9.0 mg suppression and Y-axis scale of 0.2 mg/inch. This expanded the whole of the first 10% of the decomposition to cover the Y-axis span (5"). The suppression was removed and a sensitivity of 2 mg/inch used during the remaining 90% decomposition.

6.1.3 Results

Illustrative T.G.A. curves are shown in Figure 6.1 (nitrogen atmosphere) and Figure 6.2 (oxygen). Table 6.1 gives the temperatures at which degradation commences and at 10, 20 and 100% completion. The weight loss at 275°C increases on storage and is largely determined by the RO_2H concentration.

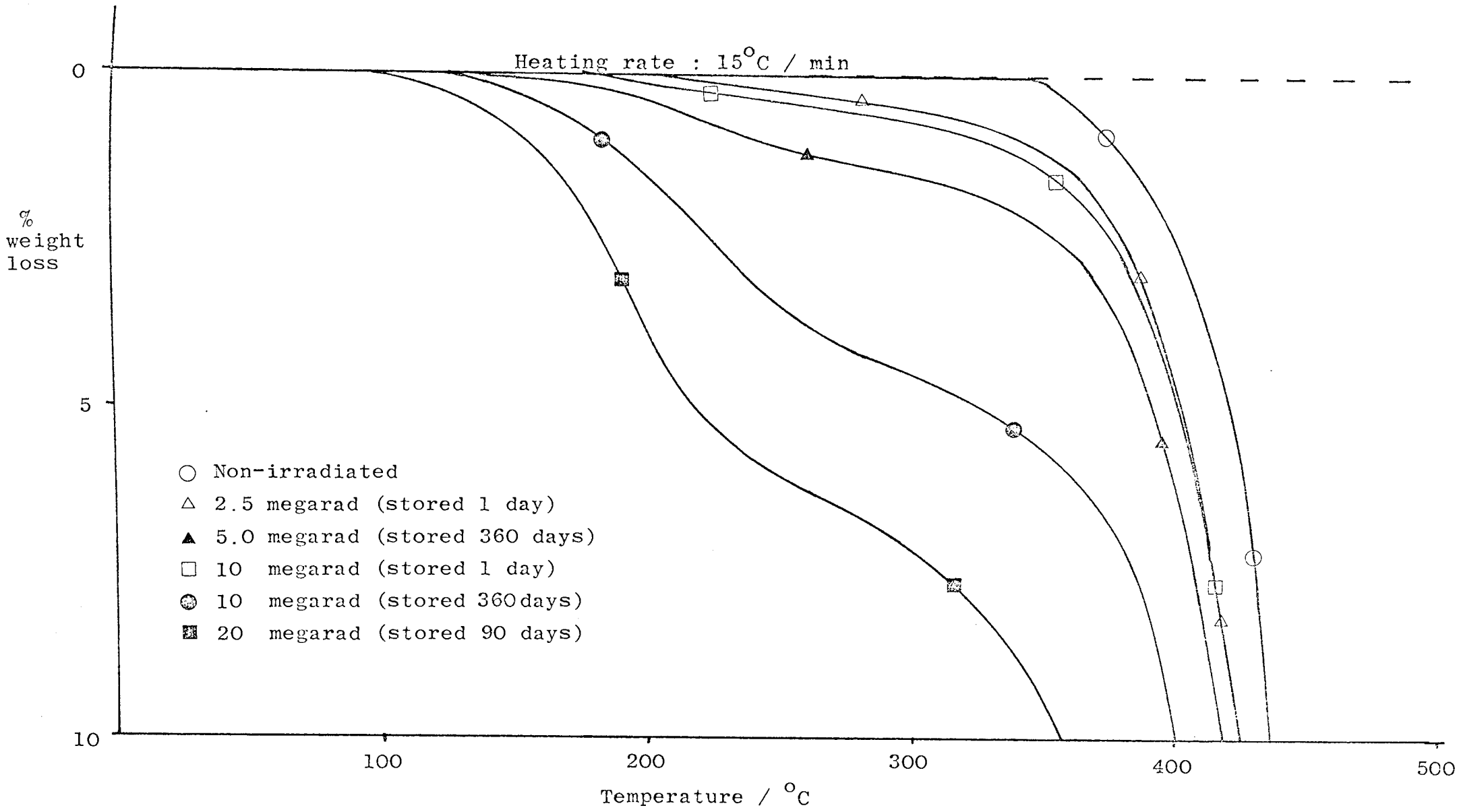

Fig. 6.1 T.G.A. curves of polypropylene in nitrogen (initial stages).

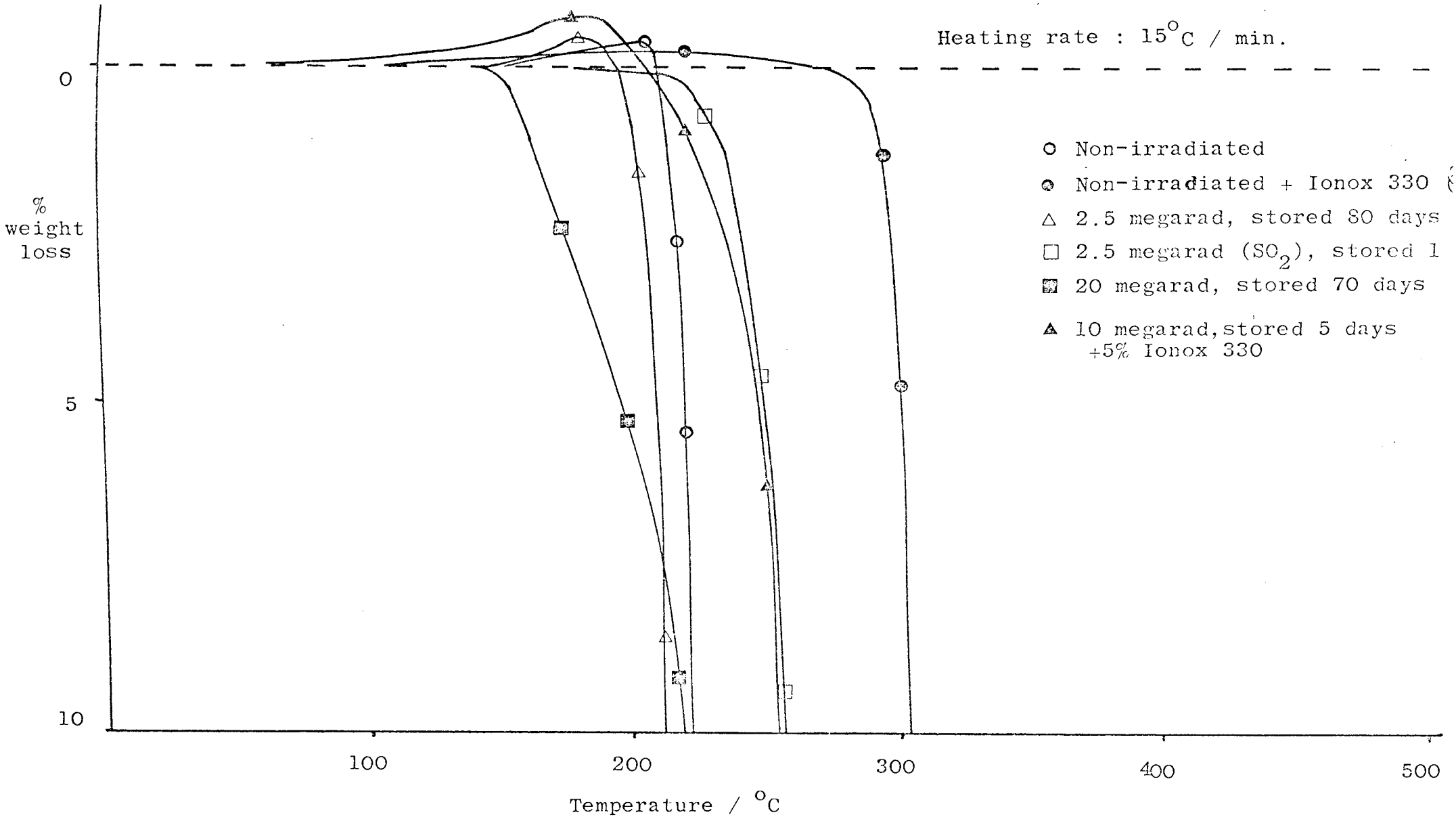

Fig. 6.2 T.G.A. curves of polypropylene in oxygen (initial stages).

Table 6.1 T.G.A. data, (Isotactic polymer unless stated)

NITROGEN ATMOSPHERE : Heating rate : 15°C/min

Polymer or radiation dose in megarad	Storage /day	Temperature /°C				% weight loss at 275°C
		0%	10%	20%	100%	
Isotactic (0)	-	340	435	455	505	0
" + 5% Ionox 330	-	325	470	495	530	0
Atactic (0)	-	95	430	460	500	1.5
Stereoblock(0)	-	280	425	440	490	0
2.5 (E)	1	200	430	460	500	0.4
2.5 (γ)	140	160	425	445	500	0.7
5.0 (E)	1	170	405	435	500	0.3
5.0 (E)	70	170	400	430	495	1.2
5.0 preheated at 260°C for 0 mins	70	330	405	430	510	-
10(E)	1	155	410	455	490	0.5
10 (E)	5	150	400	440	490	0.8
10 (E)	60	140	400	430	490	2.4
10 (E)	390	130	395	450	490	4.0
10 (E) + 5% Ionox	5	200	450	480	540	0.7
20 (γ)	7	150	380	430	500	2.0
20 (γ)	60	130	365	420	495	6.2
20 (γ)	140	110	375	400	495	6.9
20 (γ)	365	110	320	400	490	9.0
20 (γ)	700	105	260	385	470	12.0
20 (γ)+5% Ionox	60	80	330	405	495	7.9
2.5 in SO_2	1	335	420	440	490	0
2.5 in NO	1	280	440	455	490	0
2.5 in H_2	1	200	415	430	485	0.2
2.5 in N_2	1	210	405	430	490	0.3

Table 6.1 continued ....

AIR ATMOSPHERE

0	-	230	285	300	390	5.0
20 (Y)	60	155	235	265	400	26.0
2.5(E) in SO_2	1	250	300	325	385	3.5

OXYGEN ATMOSPHERE

0	-	205*	220	245(i)	245(i)	100
0 + 5% Ionox	-	230*	305	310(i)	310(i)	0
2.5 (Y)	140	190*	210	215	380	83
10 (E)	5	180*	235	245	340	56
10 (E) +5% Ionox	5	180*	250	265	420	28
20 (Y)	140	140*	190	205	320	80
2.5 (E) in SO_2	1	215	250	255(i)	255(i)	100

* Temperature at which maximum weight occurred prior to decomposition

(i) Ignition occurred

† Irradiation and storage was at room temperature

Isothermal decomposition rates at 180°C in oxygen were measured for polypropylene irradiated to a dose of 2.5 megarad and for non-irradiated polypropylene. Table 6.2 gives the results obtained and Figure 6.3 is a plot of $\log_{10} W_t$ vs time for each sample.

Table 6.2 Isothermal decomposition of polypropylene in oxygen at 180°C

Irradiated		Non irradiated	
Time/min	W_t/ mg	Time/min	W_t/ mg
0	10.00	0	10.00
4	9.55	10	9.97
8	9.02	16	9.88
12	8.44	20	9.76
15	8.04		
20	7.40	28	9.14
30	6.26	34	8.40
40	5.36	40	7.80
50	4.57	50	6.80
60	3.95	60	6.00

Figure 6.3 shows that the decomposition is first order but that for non-irradiated polypropylene there is an induction period of about 20 minutes. The rate constants obtained from the slope (= $-k_1/2.303$) of Figure 6.3 were

k_1 = 0.0157 min^{-1} (irradiated)

k_1 = 0.0130 min^{-1} (non-irradiated)

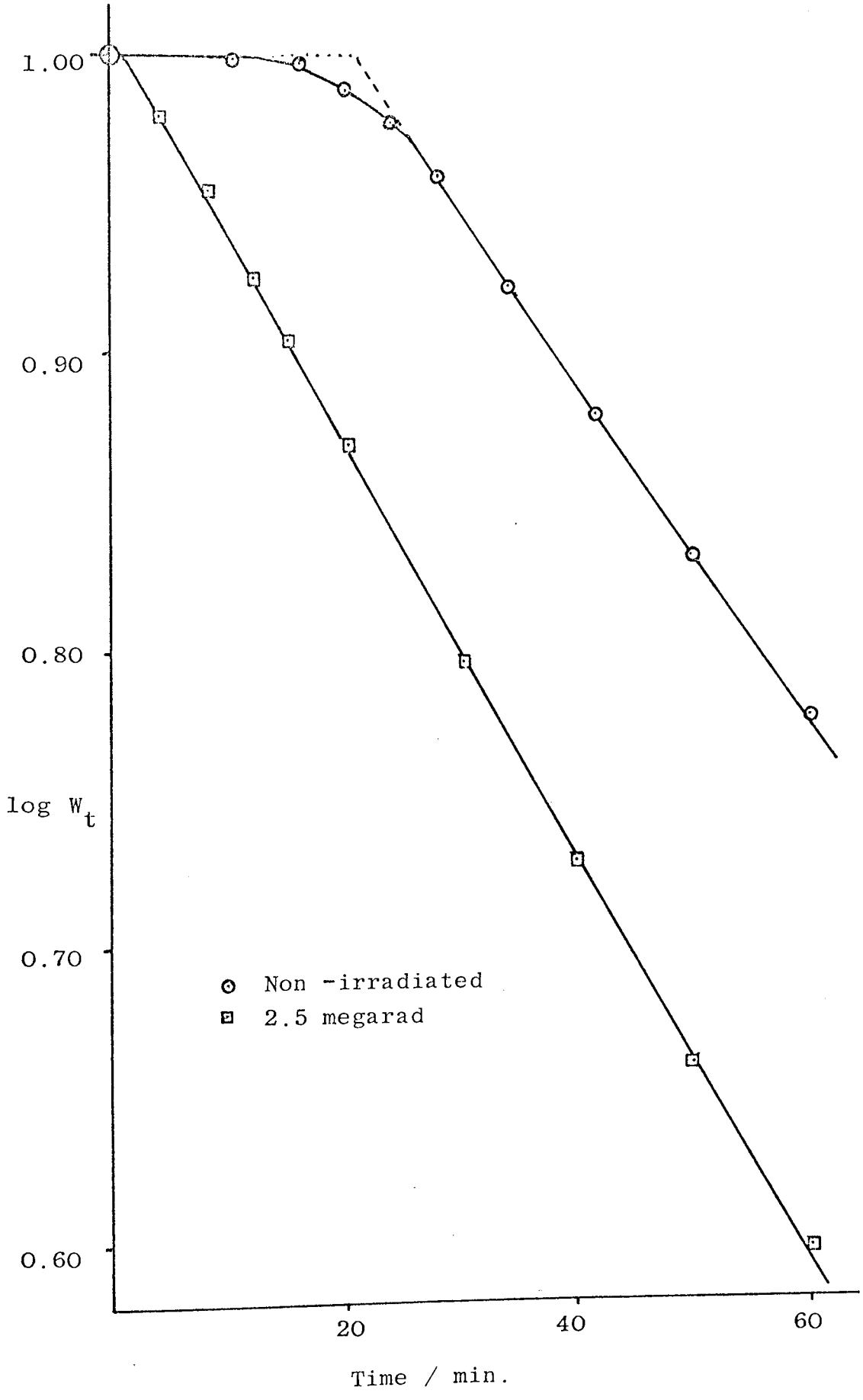

Fig. 6.3 Plot of log W_t vs. time for irradiated and non-irradiated polypropylene in oxygen at 180°C.

The decomposition of freshly irradiated polymer (2.5 megarad) was measured in a series of isothermal measurements to obtain the activation energy of the decomposition in nitrogen. The results given in Table 6.3 were obtained by increasing the temperature in steps and measuring the slope of the weight vs. time graph at each temperature.

Table 6.3 First-order decomposition rate constants of irradiated polypropylene in nitrogen

Temperature / °C	k_1 / min^{-1}
328	0.00065
357	0.00298
379	0.00724
398	0.0198
426	0.0600
449	0.195

An Arrhenius plot of $\log_{10} k_1$ vs $^1/_T$ is shown in Figure 6.4 from which the activation energy is found to be 157.0 kJ mol^{-1}.

6.1.4 Discussion

Irradiation decreases the temperature T_o at which weight loss commences. T_o occurs in the region of the melting point and decreases with radiation dose. Weight decrease in the initial stages, except for stored irradiated polymers of high hydroperoxide concentration is probably due to evaporation of low molar mass species rather than chemical degradation.

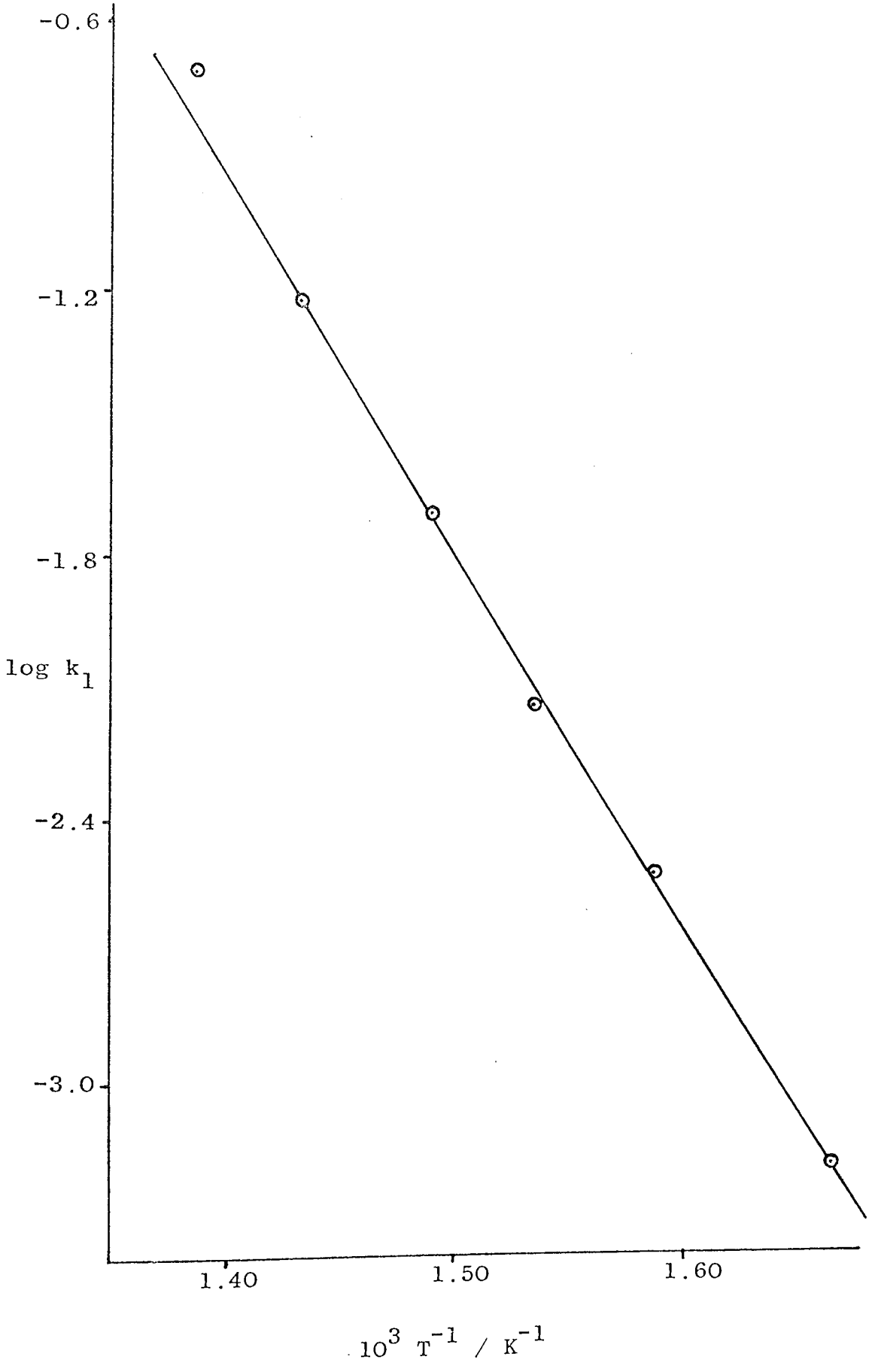

Fig. 6.4 Arrhenius plot of log k_1 vs. 1/T for thermal decomposition of irradiated polypropylene in nitrogen.

Analysis of the T.G.A. curves by plotting ln ln $\frac{1}{y}$ vs $\frac{1}{T}$ to obtain activation energies is shown in Figures 6.5, 6.6, 6.7, and the activation energies given in Table 6.4.

Freshly irradiated polypropylene was found to decompose with steadily increasing activation energy (Figure 6.5) but other decompositions could be divided into 1, 2 or 3 linear sections of the ln ln $\frac{1}{y}$ plot. Temperatures corresponding to 1, 2, 3, 5, 7, 10, 20, 30, 40, 50, 60, 70 and 80% weight loss were used in the construction of the plots. W_∞ was in all cases found to equal zero, i.e. with no solid residue. The stabiliser Ionox 330 was found to have a single activation energy over the decomposition range 1 - 90%. This showed that the method of analysis was applicable and that changes of apparent activation energy were not caused by instrumental effects such as non-linear heating rate. Linearity of the plot for freshly irradiated polypropylene was not improved by plotting the appropriate functions for zero and second order processes.

When the irradiated samples had been stored for a long period, the decomposition occurs in separate stages, shown in Figure 6.6 for a sample irradiated to 20 megarad. A moderately high activation energy, 70 kJ mol^{-1} is initially found ($< 215^{\circ}C$) followed by a stage ($215^{\circ}C$ - $377^{\circ}C$) with a very low apparent activation energy (12 kJ mol^{-1}) and slow decomposition rate. The low activation energy is however only an apparent effect reflecting the virtual lack of reaction in this temperature range. At temperatures $> 377^{\circ}C$, decomposition again becomes rapid with an activation energy of 104 kJ mol^{-1}. Figure 6.1 clearly shows the stepwise character of this decomposition.

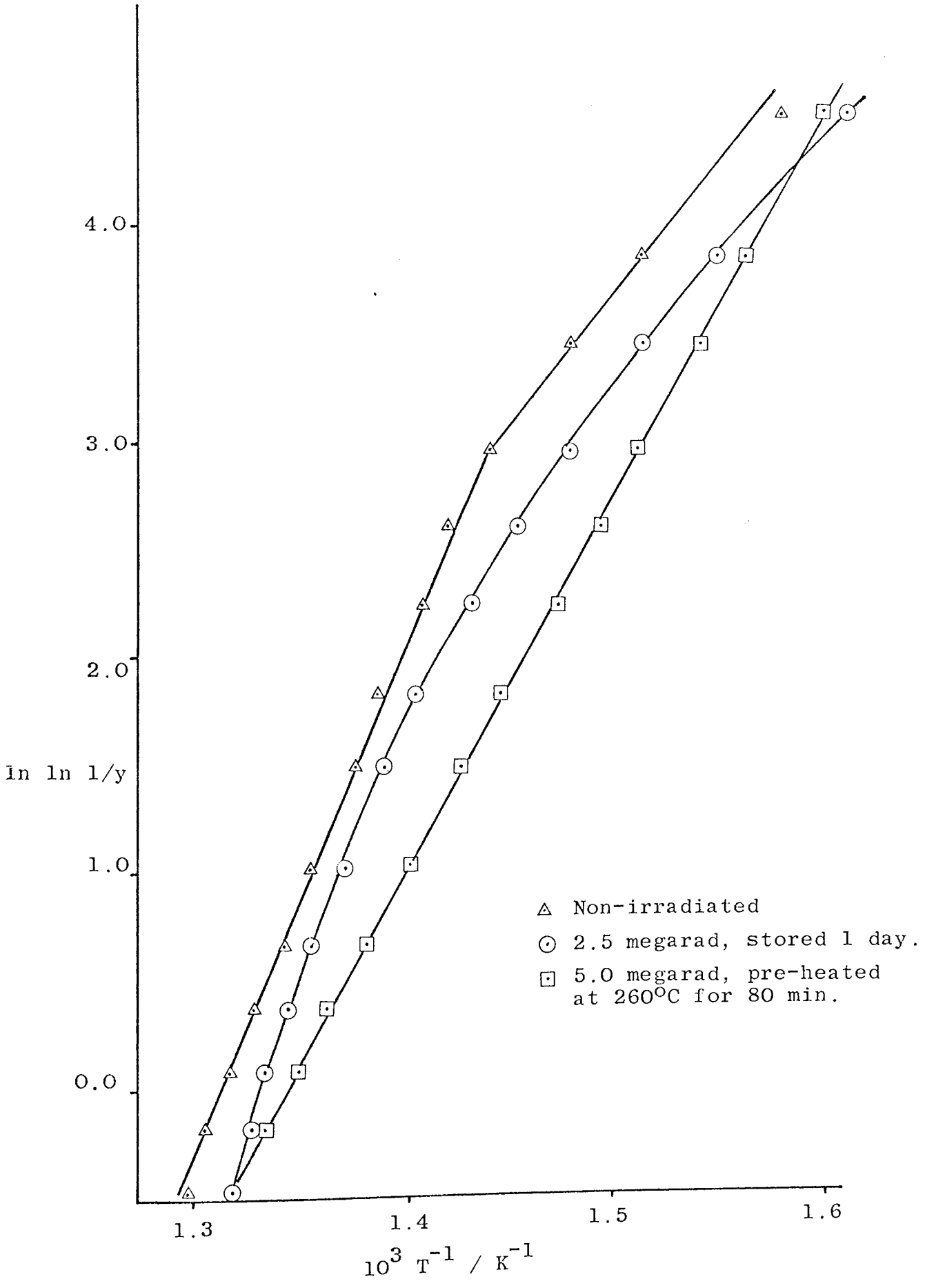

Fig 6.5 Plot of ln ln 1/y vs. 1/T for irradiated and non-irradiated polypropylene innitrogen.

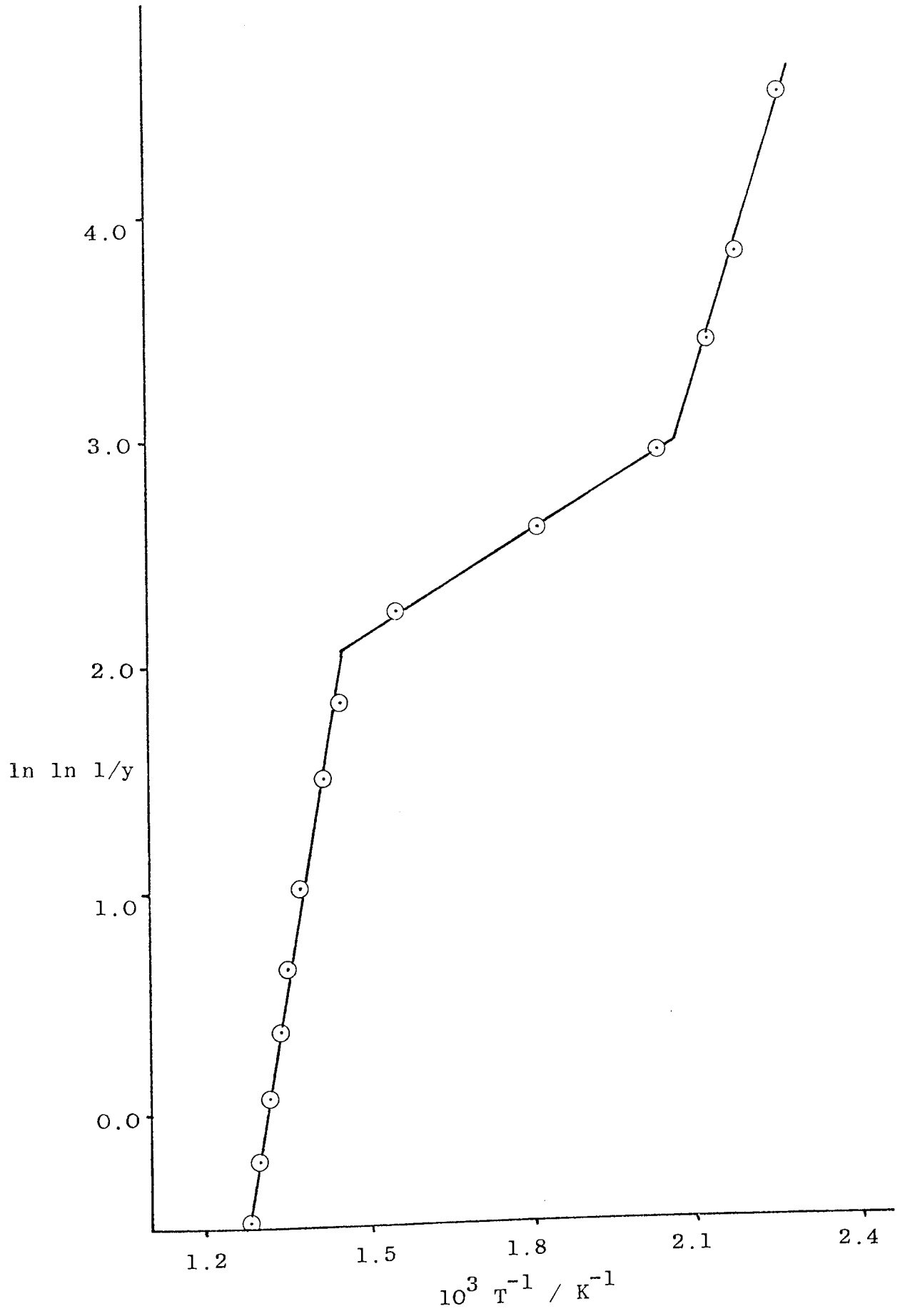

Fig 6.6 Plot of ln ln 1/y vs. 1/T in nitrogen, for polypropylene, irradiated to 20 megarad, stored 70 days.

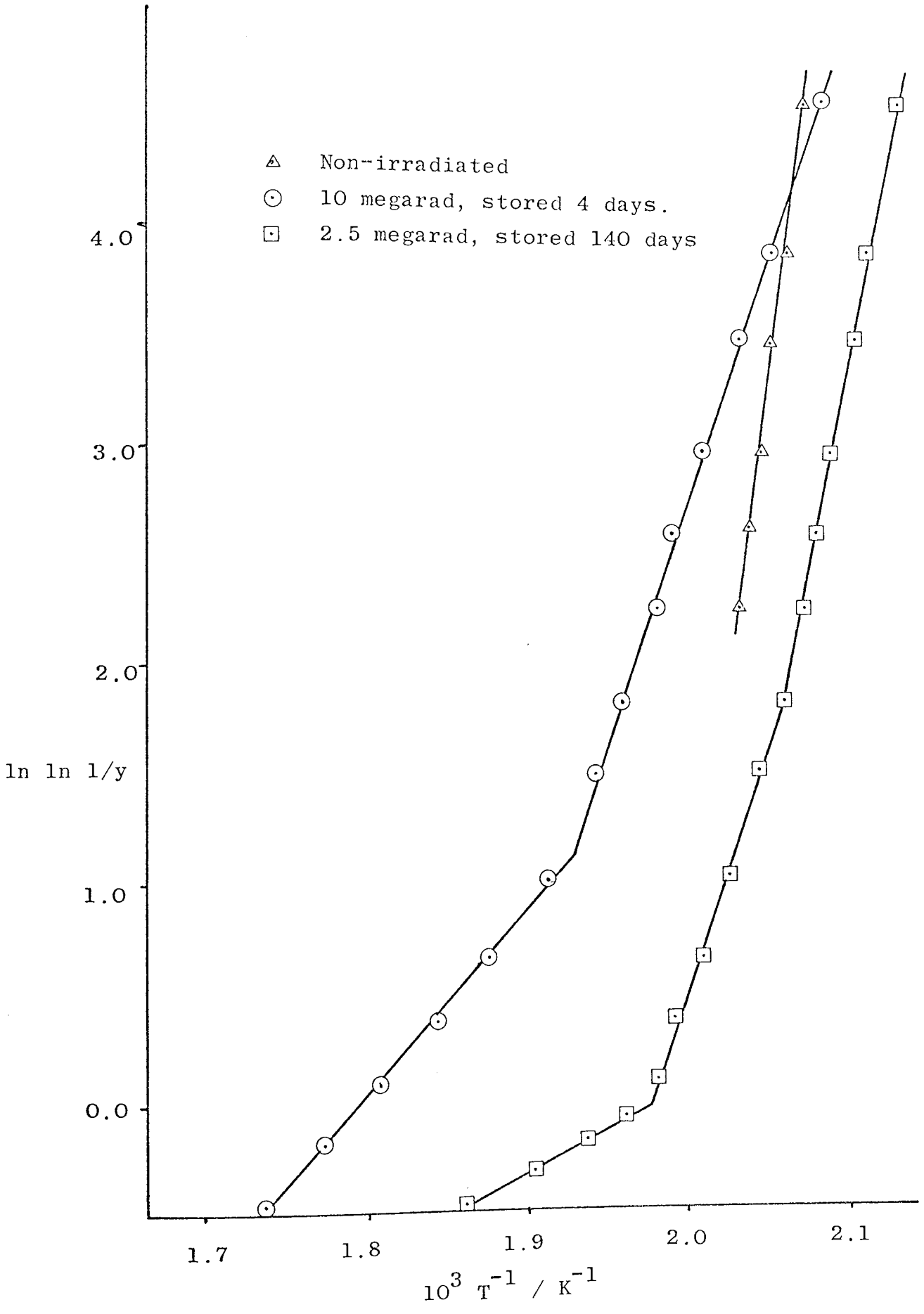

Fig. 6.7 Plot of ln ln 1/y vs. 1/T for irradiated and non-irradiated polypropylene in oxygen.

Table 6.4 Analysis of T.G.A. curves in nitrogen for polypropylene irradiated and stored in air.

Polymer or dose in megarad	Storage /day	E_A / kJ mol^{-1}	Temperature Range /°C	Decomposition Range / %
Isotactic (non-irr.)	-	102	346 - 398	1 - 7
Isotactic	-	190	398 - 447	7 - 80
Isotactic +5% Ionox	-	109	396 - 490	1 - 15
	-	400	490 - 523	15 - 70
Atactic (non-irr.)	-	144	285 - 451	1 - 15
	-	485	451 - 470	15 - 60
Stereoblock (non-irr.)	-	125	342 - 422	1 - 15
	-	190	422 - 471	15 - 80
Ionox 330	-	155	323 - 458	1 - 90
2.5 (E)	1	Variable	345 - 498	1 - 90
2.5 (γ)	140	96	348 - 423	1 - 10
	140	200	447 - 479	20 - 70
5 (E)	1	Variable	345 - 485	1 - 90
5 (E)	70	105	355 - 432	3 - 20
		190	432 - 463	20 - 60
10 (E)	1	Variable	337 - 485	1 - 90
10 (E)	390	39	186 - 240	1 - 3
		11.5	240 - 331	3 - 5
		116	400 - 465	10 - 60
20 (γ)	140	70	170 - 215	1 - 5
		12	215 - 377	5 - 12
		104	377 - 476	12 - 80
20 (γ) + 5% Ionox	60	78	156 - 198	1 - 5
		12	198 - 332	5 - 10
		181	332 - 484	10 - 80

Table 6.4 continued ....

2.5 (E) in SO_2	1	142	362 - 426	1 - 10
		188	426 - 474	10 - 70
2.5 (E) in NO	1	152	385 - 435	1 - 7
		243	435 - 475	7 - 60
2.5 (E) in H_2	1	100	327 - 414	1 - 10
		220	430 - 475	20 - 80

The initial weight loss is almost certainly caused by hydroperoxide decomposition. The weight loss that has occurred at 275°C (Table 6.1) is correlated with the hydroperoxide concentrations measured by iodine liberation in Table 6.8 (page 153). A sample irradiated to 5 megarad and stored for 140 days, was decomposed isothermally at 260°C. The sample lost weight rapidly until 1.2% had decomposed following which further weight loss was negligible. After heating at 260°C for 80 minutes the sample was heated at 15°C/min; no further weight loss occurred until 330°C but then decomposed with a uniform activation energy, of 141 kJ mol^{-1} This value may be compared to that of 157 kJ mol^{-1} obtained in the series of isothermal measurements (Table 6.2).

It may be concluded that following decomposition of the hydroperoxide, the irradiated polymer is relatively stable and that further decomposition is purely thermal similar to non-irradiated polypropylene. The latter stages of the T.G.A. traces were quite similar for most samples measured. Attempts

were made to identify the products of the hydroperoxide decomposition by gas chromatography of samples heated to 160 - 180°C. The gas chromatogram proved to be complex however showing 3 major peaks and at least 24 minor peaks. Mass spectrometry confirmed this observation.

The presence of antioxidant, Ionox 330, encouraged the decomposition of hydroperoxides as may be observed by the reduction in T_o from 130°C to 80°C for a stored 20 megarad sample. For freshly irradiated and non-irradiated polymer there is however an increase in the temperature at which weight loss occurs.

Samples irradiated in gases in which peroxy radicals are not formed on exposure to air (nitric oxide and sulphur dioxide) show degradation similar to the non-irradiated polymer i.e. high T_o and no weight loss at 275°C. The T.G.A. curves of samples irradiated in nitrogen and hydrogen are very similar to those irradiated to the same dose in air. This is due to the immediate conversion of the hydrocarbon radicals to peroxy radicals on exposure to air during the initial weighing.

Air and oxygen atmospheres

The T.G.A curves in oxygen frequently showed small initial increases in weight ($< 1\%$) due to absorption of oxygen. This was followed by a rapid weight loss. The rate of weight loss and activation energy was largest for the non-irradiated polymer and ignition occurred at a weight loss of 12% at 240°C. The irradiated polymer began to decompose at lower temperature but

did so more steadily and without ignition. The $\ln \ln \frac{1}{y}$ vs. $^1/_T$ plots are given in Figure 6.7 and corresponding activation energies in Table 6.5.

Table 6.5 Analysis of T.G.A. curves in air and oxygen

Polymer or dose in megarad	Storage / day	E_A / kJ mol^{-1}	Temperature Range / °C	Decomposition Range / %
	AIR			
Isotactic (non-irr.)	-	259	243 - 281	1 - 10
	-	100	281 - 363	10 - 90
20 (γ)	60	66	151 - 193	1 - 5
		31	193 - 242	5 - 15
		64	242 - 361	15 - 90
2.5 (E) in SO_2	1	275	261 - 274	1 - 3
	1	96	274 - 375	3 - 70
	OXYGEN			
Isotactic (non-irr)	-	482	210 - 220	1 - 10 (i)
+ 5% Ionox	-	428	290 - 301	1 - 7 (i)
2.5 (E)	140	341	197 - 210	1 - 10
		200	210 - 243	10 - 70
		25	243 - 305	70 - 90
10 (E)	5	190	208 - 252	1 - 20
	5	72	250 - 310	30 - 80
20 (γ)	140	100	165 - 235	2 - 60
2.5 (E) in SO_2	1	208	227 - 251	1 - 7 (i)

N.B. samples were irradiated and stored in air, unless stated

(i) = ignition

The antioxidant, Ionox 330, was effective in increasing T_o for irradiated and non-irradiated samples. Polypropylene irradiated in sulphur dioxide showed much greater thermal stability than when irradiated in air. The T.G.A. curve (SO_2 sample) was similar to that of non-irradiated polypropylene but without an initial weight increase.

The lower decomposition temperature of irradiated polypropylene is probably because there is no induction period preceding decomposition, whereas such an induction is found for non-irradiated polypropylene (Figure 6.3). This was also confirmed by direct measurement of the volume of oxygen absorbed in the temperature range 100° - $130^{\circ}C$. The non-irradiated polymer showed an induction period before absorption steadily occurred, whereas none was present with irradiated polypropylene.

T.G.A. curves in air were broadly similar to those in oxygen, but decomposition temperature were higher and rates of degradation less. Polypropylene irradiated in sulphur dioxide showed slightly greater thermal stability than non-irradiated polypropylene.

6.2 Hydroperoxide Analysis

6.2.1 Experimental

After some attempts to measure hydroperoxide concentration by infra-red spectroscopy, it was found more suitable to use a technique of iodine liberation under acidic conditions, in which the reaction

$$RO_2H + 2I^- + 2H^+ \rightarrow I_2 + ROH + H_2O$$

took place.

0.100 g of polymer was refluxed in 5 cm^3 of spectroscopic grade methanol with 2cm^3 of aqueous potassium iodide (1 mol dm^{-3}) and 0.6 cm^3 of purified glacial acetic acid for 10 minutes under nitrogen. 5 cm^3 of aqueous potassium hydroxide (1 mol dm^{-3}) were added and the mixture cooled. Addition of the base, which buffered the mixture at pH = 5, eliminated oxidation of the iodide during measurement. The solution was filtered to remove the polymer and the solution analysed spectroscopically. An absorption maximum was found to occur at 370 nm. The absorbance was measured at this wavelength using a Unicam SP 600 with 5 mm silica cells, using standard dilutions if necessary. Distilled water was used in the reference beam and blank runs without polymer gave zero absorbance. Duplicate analyses were made and found to be reproducible to $\pm$ 4%. It is possible that not all of the hydroperoxide in the polymer reacted, but prolonged reflux for 2 hours gave only a slight increase in absorbance and may have been due in part to atmospheric oxidation.

The iodine concentration was calibrated by the use of potassium iodate solution (10^{-3} mol dm^{-3}) which was added to acidified methanolic potassium iodide using the same total volume as in the polymer analysis. The iodine concentrations were calculated from the following reaction equation :

$$IO_3^- + 5\,I^- + 6\,H^+ \rightarrow 3\,I_2 + 3H_2O$$

6.2.2 Results

Table 6.6 Calibration Data for hydroperoxide analysis

Volume of 10^{-3} mol dm^{-3} KIO_3/ cm^3	Moles of I_2 liberated x 10^6	Absorbance at 370 nm in 5mmcells	Absorbance x 10^{-6}/ I_2 moles
0	0	0	-
0.05	0.15	0.12	0.80
0.10	0.30	0.225	0.75
0.15	0.45	0.355	0.79
0.20	0.60	0.47	0.78
0.25	0.75	0.59	0.79
0.30	0.90	0.70	0.78
0.45	1.05	0.83	0.79
0.40	1.20	0.925	0.77

The iodine and hence hydroperoxide concentrations were calculated from the absorbance using the average value of 0.78 / μ mole, (from the last column of Table 6.6).

Table 6.7 Hydroperoxide concentrations for polypropylene irradiated and stored at room temperature

Dose/ Megarad	Storage/day	Absorbance	Hydroperoxide conc^{n} / μmol g^{-1}
0	-	0.015	0.19
2.5	0	0.04	0.51
	7	0.06	0.77
	28	0.11	1.40
	56	0.145	1.85
	90	0.19	2.45
	130	0.225	2.80
	190	0.29	3.70
	315	0.42	5.40
	365	0.45	5.75
10	0	0.07	0.90
	7	0.11	1.4
	21	0.175	2.25
	30	0.26	3.35
	49	0.32	4.10
	119	0.84	11.0
	210	1.06	13.6
	315	1.37	17.6
	365	1.57	20.1
15	365	2.30	
20	0	0.095	1.20
	365	3.15	40.4

The effect of storage time on hydroperoxide concentration is shown in Figure 6.8 for polypropylene irradiated to 2.5 and 10 megarad. The hydroperoxide concentration as a function of radiation dose for samples stored for 365 days is shown in Figure 6.9.

6.2.3 Discussion.

The concentration of species that liberates iodine from iodide, assumed to be accessible hydroperoxide groups, can be seen to be very small immediately following irradiation. This suggests that the peroxy radical itself is either not capable of oxidising iodide ions or is trapped within crystalline regions not penetrated by the reflux mixture. The hydroperoxide concentration increases steadily following irradiation and is still increasing more than one year after irradiation.

The hydroperoxide concentrations may be compared to the initial $RO_2^{\cdot}$ concentration measured by E.S.R. which for room temperature irradiation were 1.67 μmol g^{-1} and 4.83 μmol g^{-1} for 2.5 and 10 megarad reppectively. It can be seen from Table 6.7 that after storage the hydroperoxide concentrations are several times greater than the radical concentration. Williams (159) has similarly observed that polyethylene consumes more than 4 oxygen molecules per free radical in post irradiation oxidation. It is evident that the chain process

$$RO_2^{\cdot} + RH \rightarrow R^{\cdot} + RO_2H$$

$$R^{\cdot} + O_2 \rightarrow RO_2^{\cdot}$$

is repeated several times before recombination of radicals occurs.

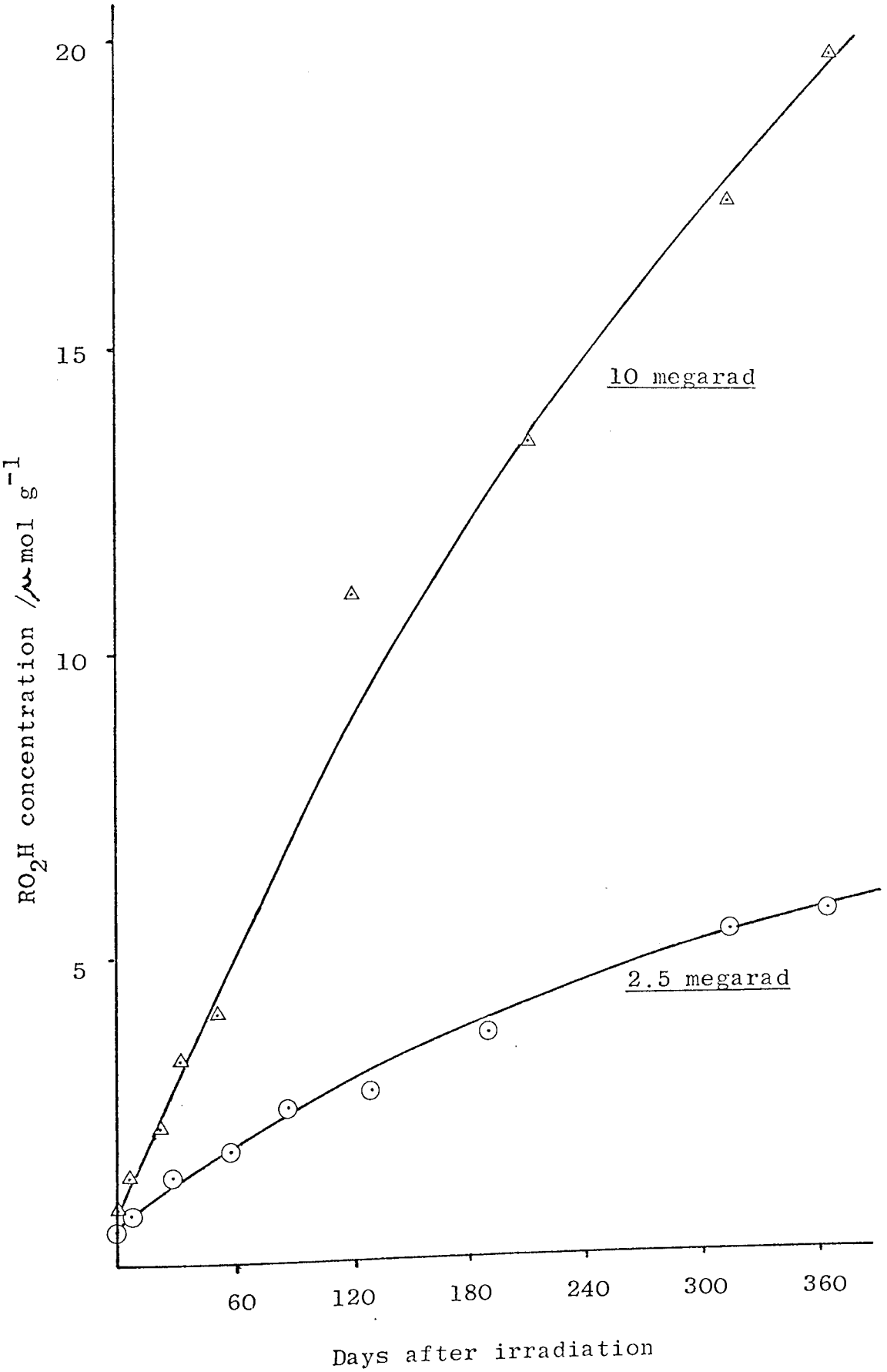

Fig. 6.8 Hydroperoxide concentration in irradiated polypropylene, as a function of storage time.

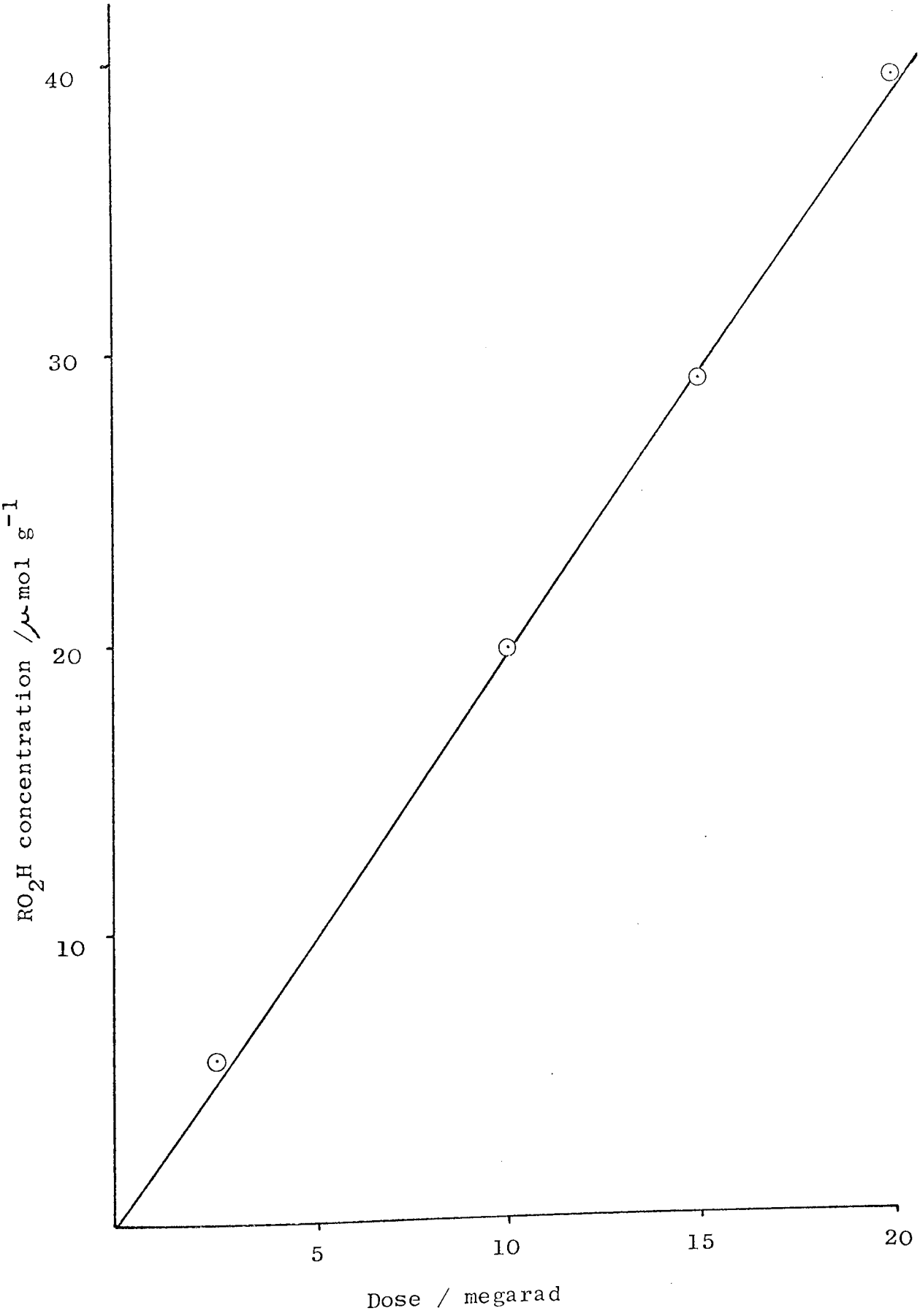

Fig. 6.9 Hydroperoxide concentration vs. radiation dose in polypropylene, 1 year after irradiation.

The time scale over which the hydroperoxide concentration increases is perhaps surprising when the free radical concentrations and their decay rates are considered. Assuming an average laboratory temperature of 18°C, for which the radical decay rate constant (section 4.3.3) is calculated to be 2.52×10^{-22} $(\text{radical}/g)^{-1}\ \text{min}^{-1}$, the remaining radical concentration after 365 days would be $7.6 \times 10^{-15}\ g^{-1}$. ($1.26 \times 10^{-2}$ μ mol g^{-1}) and would be $< 1\%$ of the original concentration after 10 weeks. This should cause only very slow reaction rates. The hydroperoxide growth may therefore involve processes in which some existing hydroperoxides decompose to produce radical sites from which further chain reaction develops.

The hydroperoxide concentration may also be compared to the weight loss in the initial stages of T.G.A. in nitrogen (Table 6.1). Table 6.8 compares the weight loss at 275°C to the hydroperoxide concentrations interpolated from Figure 6.8 for the 10 megarad sample. The number of repeat units lost, for each hydroperoxide group is also given.

Table 6.8 Comparison of hydroperoxide concentration and % weight loss at 275°C in irradiated (10 megarad) polypropylene.

Days after irradiation	Hydroperoxide / μ mol g^{-1}	% weight loss	No of repeat units lost / hydroperoxide group
1	0.90	0.5	132
5	1.30	0.8	146
60	5.2	2.4	109
390	20.8	4.0	46

The data in Table 6.8 show that the initial weight loss in the thermal decomposition of irradiated polypropylene is caused by the presence of hydroperoxide groups. Each hydroperoxide group causes the loss of many repeat units from the polymer chain.

CHAPTER SEVEN : GENERAL DISCUSSION AND CONCLUSIONS

Detailed discussion and conclusions of each area of measurement or study, has been given in the appropriate chapter. This chapter considers the general conclusions that may be made concerning the effects of ionising radiation on polypropylene.

7.1 Discussion and Conclusions

7.1.1 Effect of Radiation Type

In all areas of study both γ and electron irradiation produced identical effects in polypropylene for a given radiation dose. This is perhaps surprising when the duration of irradiation is taken into account, since the length of time in contact with γ-irradiation was more than 1000x greater than with electron irradiation. In this study the use of finely divided polypropylene powder has eliminated the effects of diffusion-controlled oxidative processes, but with bulk specimens such processes are expected to cause differences to be observed with the different types of radiation.

7.1.2 Effect of Radiation Temperature

Large differences were observed in the G-values at 195K and at room temperature, for both chain scission (from $\bar{M}_v$) and loss of crystalline units (from T_m). In contrast, the E.S.R. results of free radical concentration, show only a slight temperature effect. Table 7.1 illustrates this.

Table 7.1 G-values for electron-irradiated polypropylene at 195K and at room temperature

G-value	195K	Room Temp	G_{RTemp}/G_{195}
*G(s)	2.00	5.52	2.76
G(-cr)	102	267	2.61
$G(RO_2^{\bullet})$	0.78	0.63	0.81

*Assuming random molar mass distributions.

The smaller free radical formation ($G(RO_2^{\bullet})$ at room temperature is explained by the bimolecular decay of radicals during irradiation and before measurement. The initial process in radical formation is loss of a hydrogen atom from the 'cage' in which recombination with the parent radical can take place. A small hydrogen atom can presumably escape from this cage even at low temperatures.

Molar mass decrease, however, will only be observed when there is movement of newly-formed chain ends away from one another so that scission becomes permanent. This will undoubtedly be favoured by the additional mobility that the polymer has, when above the glass transition temperature. The radiation temperature effect on melting temperature can be seen from the G-value ratio in Table 7.1. Increased mobility of the polymer matrix can thus be considered to assist loss of crystalline units in addition to chain scission.

Although the decrease in molar mass and melting temperature occur simultaneously, the large melting temperature decrease is not explicable solely in terms of decreasing molar mass.

For example, reduction in $\bar{M}_v$ from 368,000 (non-irradiated polymer) to 31,000 (caused by a 10 megarad dose at room temperature) would not be expected, in itself, to cause the reduction in T_m from 172°C to 154°C that is found. Considerable changes in chemical structure (viz. hydroperoxide formation) are additionally responsible for the decrease in T_m and the consequent large values of G (-cr).

Irradiation temperature effects have previously been observed with polyethylene [160], where those properties determined by crosslinking, show a marked temperature effect, while hydrogen evolution shows little change with temperature. Charlesby [6] has suggested that the temperature effect is a characteristic feature of certain types of radiation induced reaction, which may serve as a method of classifying chemical reactions in terms of fast and slow radicals. Because of the limitation of the irradiation facilities employed in this study, it is not possible to say whether the temperature effect on $\bar{M}_v$ and T_m is gradual or stepwise.

7.1.3 Effect of Storage

The major effects of storing polypropylene after irradiation in air, are a decrease in peroxy radical concentration and an increase in hydroperoxide concentration. However, the process is not a simple equimolar conversion and comparison of the two concentrations show that 1 year after irradiation approximately 4 hydroperoxide groups are formed for each initial radical. The hydroperoxide concentration increases for many months after irradiation, while the free radical concentration is less than

1% of the original, a few weeks after irradiation.

The failure of freshly irradiated polypropylene to cause quantitative oxidation of iodide ions indicates that the peroxy radicals are trapped within crystalline regions, which the ions do not penetrate. The readiness, with which the hydroperoxide groups react with iodide ions, suggest that they are much more accessible and probably are not contained within the crystalline regions. The rejection of hydroperoxide groups from the crystalline regions may account for some of the changes of mechanical properties on storage.

7.2. Post - irradiation Degradation and Possible Remedies

7.2.1 Post-irradiation Degradation

The two most important effects of irradiation of polypropylene in air, in relation to service of irradiated polypropylene articles are :

(1) reduction in molar mass,

(2) increase in hydroperoxide concentration.

The deterioration of mechanical properties is largely caused by the molar mass decrease, with the consequent large reduction in bulk viscosity. Cracking around spherulites as a result of the large viscosity decrease is thought to be chiefly responsible for post-irradiation embrittlement. The large hydroperoxide concentration in irradiated, stored polypropylene will cause problems in use at elevated temperatures, or if exposed to sunlight.

7.2.2 Suggestions for Overcoming Post-irradiation Degradation

The problems of post-irradiation embrittlement as a result of molar mass decrease can be alleviated in the following ways :

(1) Use higher molar mass polypropylene.

(2) Irradiate at low temperatures.

(3) Irradiate in inert atmospheres.

(4) Use anti-radiation or antioxidant additive.

Suggestion (4) however may cause formation of unacceptable colour in the irradiated articles, and may also present possible toxicity problems.

The problems of hydroperoxide build-up may be reduced in the following ways :

(1) Irradiate and store in an inert atmosphere.

(2) Irradiate in sulphur dioxide.

(3) Expose to free radical scavenger e.g nitric oxide or methyl mercaptan, following irradiation.

(4) Heat to around 70°C for 1 day or more in nitrogen, to cause accelerated free radical decay.

Suggestion (4) however may cause weakening by favouring crystallisation and crack formation.

Possibly the most convenient way of minimising post-irradiation damage is to carry out the irradiation under an inert atmosphere in air-tight containers. The irradiated articles could then be stored and supplied in such containers. If kept for some weeks prior to use then the free radical concentration would be minimal, and eventual oxidative degradation only very small.

7.3 Suggestions for Further Work

Following the work described in this thesis a number of points have arisen which may warrant further investigation.

(1) An investigation of the effects or radiation temperature on $\bar{M}_v$ and T_m, to cover a wide and continuous temperature range.

(2) Identification of the initial products of thermal decomposition or irradiated polypropylene by the simultaneous use of gas chromatography and/or mass spectrometry with thermogravimetric analysis.

(3) Effects of irradiation in other gaseous media. Irradiation in sulphur-containing gases e.g. sulphur monochloride, may prove to be effective in stabilising polypropylene to oxidation.

(4) Investigation of the effect of sample size and shape, with respect to the importance of diffusion processes in post-irradiation changes.

(5) An investigation of the effects of ozone on irradiations in air; the presence of ozone cannot be avoided in air irradiation, since it is continuously formed. In irradiation units that do not have enforced air circulation, the concentration of ozone can become quite high and may considerably affect oxidation processes.

REFERENCES

1 Roentgen, W.C. Annal.Phys., 64, 1, (1896).

2 Becquerel, H.C. Seanc. Acad Sci.(Paris) 122, 420, (1896).

3 Mund, W., and Koch, W., Bull. Soc. Chim. Belg. 34,119 (1925).

4 Dole, M., and Rose, D., 114th A.C.S. Symposium,(1948).

5 Charlesby, A., Proc. Roy.Soc.(London) 215A, 187,(1952).

6 Charlesby, A., Atomic Radiation and Polymers, Pergamon Press : Oxford 1960.

7 Hochanadel, C.J. Comparative effects of radiation, Chap.8 J. Wiley and Sons, N.Y., (1960).

8 O'Donnell, J.H. and Sangster, D.F. Principles of Radiation Chemistry, E Arnold (publ.) (1970).

9 Dewhurst, H.A., J. Phys. Chem. 62, 15, (1958).

10 Kevan, L., and Libby, W.F. J. Chem. Phys.39, 1288, (1964).

11 Dewhurst, H.A., J. Am. Chem. Soc. 83, 1050, (1961).

12 Magat, M., and Villard, R., J. Chem. Phys. 48, 385, (1951).

13 Wall, L.A., J. Polymer-Sci., 17, 141, (1955).

14 Alexander, P., Charlesby, A., and Ross, M., Proc. Roy.Soc. (London), 223A , 392 (1954).

15 Williams, T.F., Trans Farady Soc. 57, 755, (1961).

16 Dole, M., Milner, D.C. and Williams, T.F., J.Am. Chem. Soc. 80, 1580, (1958).

17 Charlesby, A., and Pinner, S.H., Proc. Roy. Soc. (London) 249A, 367, (1959).

18 Inokuti, M., J. Chem. Phys. 38, 2999, (1963).

19 Scott, G., Atmospheric Oxidation and Antioxidants, Elsevier Amsterdam, (1965).

20 Bolland, J.L., Quart. Rev. (London) 3, 1, (1949).

21 Reich, L., and Stivala, S.S.,Rev. Macromol.Chem. 1, 249, (1966).

22 Bolland, J.L., and Gee, G., Trans. Farad. Soc. 42, 236, (1946).

23 Miller, A.A., Lawton, E.J., and Balwitt, J.S., J. Polymer Sci. 14, 503, (1954).

24 Black, R.M., and Lyons, B.J., Nature, 180, 1346, (1957).

25 Waddington, F.B., J. Polymer Sco. 31, 221, (1958).

26 Charlesby ,A., and Pinner, S.H., Proc. Roy. Soc. (London), 249A, 367, (1959).

27 Dole, M., and Schnabel, W., J. Phys. Chem. 67, 295, (1963).

28 Salovey, R., and Dammont, F.R., J. Polymer Sci., 1A, 2155,(1963).

29 Geymer, D.O., Makromol. Chem., 99, 152, (1966).

30 Odian, G., Lamparella, D., and Canamare, J., J. Polymer Sci., C. 16, 3619, (1968).

31 Sobue, H., Tajima, Y., and Tabata, Y., Kogyu Kag. Zasshi, 62, 1774, (1959).

32 Sobue, H., and Tajima, Y., Nature, 188, 315, (1960).

33 Kondo, M., and Dole, M., J. Phys. Chem. 70, 883, (1966).

34 Staren'kii, A.G., Lavrentovich, Y.I., and Kabakchi, A.M., Polymer Sci. U.S.S.R., 12, 2806, (1970).

35 Inokuti, M., J. Chem. Phys. 38 3006, (1963).

36 Woodward, A.E., J. Polymer Sci., B1, 621, (1963).

37 Veselovskii, R.A., Leschenko, S.S., and Karpov, V.L., Polymer Sci. U.S.S.R. 10, 881, (1968).

38 Black, R.M., and Lyons, B.J., Proc. Roy. Soc. (London), 253A, 322, (1959).

39 Jellinek, H., 'Stereochemistry of Macromolecules', Vol. III. Chap. 10. ed. A.D. Ketley, Edward Arnold (publ.) (1969).

40 Keyser, R.W., Clegg, B., and Dole, M., J. Phys. Chem. 67,300,(1963)

41 Dole, M., Trans. Am. Nucl. Soc. 3, 356, (1960).

42 Lyons, B.J., J. Polymer Sci., A3, 777, (1965).

43 Marans, N.S., and Zapas, L.J., J. App. Polymer Sci., 11, 705, (1967).

44 G.E.C. Patent No. 831 914 (Britain) (1960).

45 Chappell, S.A., Sauer, J.A., and Woodward, A.E. J. Polymer Sci., 1A, 2805, (1963).

46 Charlesby, A., Von Arnim, E., and Callaghan, L., Int. J. Appl. Rad. Isotopes, 3, 226, (1958).

47 Slovokhotova, N.A., Zenlyanski, N.N., Ilchieva, Z.F., Vasileev, L.A., and Kargin, V.A., Polymer Sci. U.S.S.R. 6, 608, (1964).

48 Sobue, H., Tajima, Y., and Tabata, Y., Kogyu. Kag. Zasshi, 62, 1777, (1959).

49 Dole, M., in Crystalline Olefin Polymers, ed. R. Raff and W.K. Doak, Interscience 1964.

50 Alexander, P., Black, R.M. and Charlesby, A., Proc. Roy. Soc. 232 A, 31, (1955).

51 Schultz, A.R., J. Polymer Sci., 35, 369 (1959)

52 Williams, T.F., Trans. Faraday Soc. 57, 755, (1961)

53 Campbell, D., J. Polymer Sci. D., 4, 91, (1970)

54 Tsvetkov, I.D., Polymer Sci., U.S.S.R., 2, 165, (1961)

55 Libby, D., Ormerod, M.G., and Charlesby, A., Polymer, 1, 212, (1960)

56 Charlesby, A., and Ormerod, M.G., Uppsala Symposium, Paper 11 (1961)

57 Ohnishi, S., Ikeda, Y., Kashiwagi, M., and Nitta, I., Polymer, 2, 119, (1961)

58 Ohnishi, S., Sugimoto, S., and Nitta, I., J. Polymer Sci. 1 A, 625, (1963)

59 Fischer, H., and Hellwege, K., J. Polymer Sci. 56, 33, (1962)

60 Yoshida, H., Ranby, B., Acta. Chem. Scand. 19, 72, (1965)

61 Loy, B.R., J. Polymer Sci., 1A, 2251, (1963)

62 Forrestal, L.J., and Hodgson, W.G., J. Polymer Sci, 2A, 1275, (1964)

63 Milinchuk, V.K., Pshezetskii, S., Kotov, A.G., Tupikov, V.I., and Tsivenko, V.I., Polymer Sci., U.S.S.R., 4, 679, (1963)

64 Iwasaki, M., and Toriyama, K., J. Chem. Phys. 46, 2852,(1967)

65 Milinchuk, V.K., and Pshezetskii, S.Y., Dokl Akad. Nauk. U.S.S.R., 152, 655, (1963)

66 Aycough, P.B., and Munari, S., Polymer Letters, 4, 503, (1966)

67 Butiagin, P.J. 'Polmer Reactions' - Prague Symposium 1971 also in Pure Appl. Chem., 30, 57, (1972)

68 Nara, S., Shimada, S., Kashiwabara, H., and Sohma, J., J. Polymer Sci., A 2 6, 1435, (1968)

69 Kusimoto, N., J. Polymer Sci., C 23, 837, (1968)

70 Lawton, E.J., Balwit, J.S., and Powell, R.S., J. Chem. Phys. 33, 395, (1966)

71 Geymer, D.O., and Wagner, C.D., Nature, 208, 72, (1965)

72 Klinshpont, E.R., Milinchuk, V.K., and Pshezetskii, S.Y., Polymer Sci. U.S.S.R., 12, 1715, (1970)

73 Sohma, J., Chem. High Polymers Japan, 27, 289,(1970).

74 Milinchuk, V.K., and Pshezetskii, S.Y., Chem. Abs. 65, 10686,(1966)

75 Waite, T.R., J. Chem. Phys. 28, 103, (1958)
Physical Review 107, 463, (1957)

76 Lebedev, J.S., Kinetics and Catalysis, 8, 245, (1967)

77 Smith, W.V., and Jacobs, B.E., J. Chem. Phys. 37, 141, (1962)

78 Ohnishi, S., Bull. Chem. Soc. Japan, 35, 254, (1962)

79 Ohnishi, S.I., and Nitta, I., J. Polymer Sci., 38,451, (1959)

80 Lebedev, Y.S., Tsvetkov,Y.D., and Voevodskii, V.V., Kinetics and Catlysis, 1, 464, (1960)

81 Bresler, S.E., Kazbekov, E.N., Fomichev, V.N., Sech, F., and Smeitek, P., Soviet Physics - Solid State, 5, 491,(1963)

82 Pudov, V.S., Vysokomol, Soed, B14, 714, (1973)

83 Milinchuk, V.K., and Pshezetskii, S.Y., Polymer Sci. U.S.S.R., 6, 733, (1965)

84 Vale, R.L., Rediation Damage in Polypropylene A.E.R.E. R 4725 Publ. by H.M.S.O., (1964)

85 Ferse, V.A., Wuckel, L., and Kich, W., Koll. Zeit., 224,33, (1968)

86 Matveev, V.K., Vaisberg, S.E., Karpev, V.L., Polymer Sci., U.S.S.R., 11, 3032, (1968)

87 Bohm, G.G., J. Polymer Sci., A-2 5, 639, (1967)

88 Matsuo, K., and Dole, M., J. Phys. Chem., 63, 837, (1959)

89 Fischer, H., Hellwege , K.H., and Neudorfl, P., J. Polymer Sci., A-11, 2109, (1963)

90 Gupta, R.P., J. Phys. Chem. 68, 1229, (1964)

91 Tanaka, H., Bull. Chem. Soc. Japan, 37, 1128, (1964)

92 Eda, B., Nunome, K., and Iwasaki, M., Polymer Letters, 7,91,(1969)

93 Nechitailo, N., Polak, L.S., and Sanin, P.I., Soviet Plastics, No.7, 3, (1962)

94 Neudorfl, P., Koll. Seit. 224, 132, (1968)

95 Chien, J.C. J. Polymer Sci. A - 1 6, 393 (1968)

96 Ershov, Y.A., Lukovnikov, A.F. and Boturina, A.A., Kinetica i Kataliz, 5, 752, (1964)

97 Neiman, M.B., 'Ageing and Stabilisation of Polymers' Chap. 1, Consultants Bureau, New York, 1965. 'The Ageing and Stabilisation of Polymers' (Ed. A.S. Kuzminskii) Chap.1. Elseveir 1971

98 Pudov, V.S., and Neiman, M.B., Neftekhimiya, 3, 750,(1963)

99 Chien, J.C., Vandenberg, E.J., and Jabloner, H., J. Polymer Sci. A - 1, 6, 381, (1968)

100 Boak, P., Chem. Prumysl, 17, 439,(1967)

Ibid. 17, 216,(1967)

101 Aneli, D.N., Nechitailo, N.A., and Sanin, P.I., Soviet Plastics,No. 6, 17, (1967)

102 Geymer, D.O., Makromol. Chem. 100, 186 (1967)

103 Kaurkova, G.K., Kachan,O.O., Korner, K.A., and Chervyatsova,L.L. Chem. Abs. 64, 1406 c (1966)

104 Ayscough, P.B., Ivin,K.J., and O'Donnell, J.H., Proc. Chem. Soc. 71 (1961)

105 Kuri, Z. and Ueda, H., J. Polymer Sci. 50, 349,(1962)

106 Filippov, M.T., Dzaghatspanyan, R.V., Kordev, B.M., and Zetkin, V.I., Polymer Sci. U.S.S.R., 8, 1934, (1968)

107 U.S. Patent 3,156,636 (1959)

108 Kozlov, P.V., Polymer Sci., U.S.S.R., 2, 196, (1961)

109 Rybnikar, F., Plasta Kautschuk, 10, 324, (1963)

110 Tikhomirov,V.S, Byalynitskaye,O.I., Serenkov,V.I., and Abramova, I.M., Soviet Plastics, No 10, 20, (1971)

111 Nechitailo, N.A., Polak, S.L., and Sanin,P., Soviet Plastics No 7, 4(1962)

112 Kusy, R.P., and Turner, D., Macromolecules 4, 337,(1971)

113 Flory P.J. J. Chem. Phys. 15, 684 (1947). 17, 223, (1949)

114 I.C.I. Information Service Note 1088. 'The Effects of Atomic Radiation on Plastics Materials'(1965)

115 Houdret, C., and Lamm, A., Rev. Gen. Caout,40,323,(1963)

116 Sauer, J.A., Merrill, L.J., and Woodward, A.E., J. Polymer Sci., 58, 19 (1963)

117 Hybart, F.J., Private Communication

118 Luongo, J.P., J. App. Polymer Sci. 3, 302, (1960)

119 Chell Chemical Company Information Sheet, IE/152/2/66

120 Brandrup, J., and Immergut, E., 'Polymer Handbook', Interscience, London (1966)

121 Henson, J.L., Ph.D. Thesis, University of Aston (1970)

122 Chinai, S.N., Matlack, J.D., Resnick, A.L. and Samuels, R.J., J. Polymer Sci., 17, 391 (1955)

123 Allen, G., Booth, A.C., and Jones, M.N., Polymer, 5, 195, (1964)

124 Carter, W.C., Scott, R.L., and Magat, M., J. Am. Chem. Soc. 68, 1480 (1946)

125 Moraglio, G., Chim. e Ind. 41, 879 (1959)

126 Chien, J.C.W., J. Polymer Sci, PtA, 1, 1839, (1963)

127 Huggins, M.L., Ind. Eng. Chem. 35, 980, (1943)

128 Danusso, F., and Moraglio, G., J.Polymer Sci. 24, 161 (1957)

129 Boden, G.F., M.Sc. Thesis, University of Manchester (1964)

130 Instruction Manual. Vapour Pressure Osmometer, Model 301A, Mechrolab Inc. California

131 Fox, T.G., Gratch, S., and Loshaek, S., 'Rheology - Theory and Application', Chap. 12. Acad. Press., New York, (1956)

132 Ayscough, P.B., 'Electron Spin Resonance in Chemistry', Appendix V, Methuen Press, London (1967)

133 Carlsson, D.J., and Wiles, D.M., Macromolecules, 2, 587, (1969)

134 Reding, F.P., J. Polymer Sci., 21, 548, (1956)

135 Mandelkern, L., 'Crystallisation of Polymers'. McGraw-Hill Inc. New York (1964)

136 Sharples, A., 'Introduction to polymer crystallisation.' Edward Arnold (publishers) Ltd., London, (1966)

137 Instruction Manual. Du ont 900 differential Thermal analyser. Du Pont, Delaware.

138 Harvey, E.D., Ph.D. Thesis, University of Aston (1970)

139 Gilbert, M., Ph.D. Thesis, University of Aston (1970)

140 Natta, G., Pasquor, I., Zambelli, A., and Gatt, G., Makromol. Chem. 70, 191, (1964)

141 Natta, G., et al, Atti. Acad. Nazl. Lincei, 25, 498, (1958)

142 Falkai, B.V., Makromol. Chem. 4, 86, (1960)

143 Limbert, F.J. and Baer, E., J. Polymer Sci.

144 Van Schooten, J., J. App. Polymer Sci. 4, 122 , (1960)

145 Keith, H.D., and Padden, F.J., J. App. Phys. 35, 1270, (1964)

146 Keith, H.D., and Padden, F.J., J. App. Phys. 35, 1286, (1964)

147 Avrami, M., J. Chem. Phys. 7, 1103 (1939)

148 Godovskii, Yu.K., and Slonimskii, G.L., Polymer Sci., U.S.S.R. 8, 441, (1966)

149 Rybnikar, F., J. Polymer Sci. Pt C, 16, 129 (1967)

150 Kamide, K.J., Inamoto, Y., and Ohno, K., Chem. High Polymers (Japan) 22, 597, (1965)

151 Parrini, P., and Corrieri, G., Makromol. Chem. 62, 83, (1963)

152 Griffith, J.H., and Ranby, B.G. J. Polymer Sci. 38, 107, (1959)

153 Morgan, L.B., Phil. Trans. A.247, 13, (1954)

154 Van Krevelen, D.W., Van Heerden, C., and Huntjens, F.J., Fuel 30, 253, (1951)

155 Horowitz. H.H., and Metzger, G., Anal. Chem. 35, 1464, (1963)

156 Broido, A. J. Polymer Sc. Pt. A-2, 7, 1761, (1969)

157 Instruction Manual. Du Pont 950 thermogravimetric analyser, Du Pont Delaware.

158 Klinshpont, E.R., Milinchuk, V.K., and Dmitriev, S.N., Vysokomol. Soedin,. Ser. A 14, 1596 (1972)

159 Williams, T.F., Ph.D. Thesis, University of London (1960)

160 Charlesby, A., and Davison, W.H.T., Chem. and Ind. (Rev.), 232 (1957)

161 Assenheim, H.M., Introduction to Electron Spin Resonance, Hilger and Watts Ltd. (Publ.), London. (1966)

ACKNOWLEDGEMENTS

The author wishes to express his gratitude to Dr. F.J. Hybart and Professor G. Scott for their supervision and guidance of this work.

To the technicians and research colleagues of the Chemistry Department for their helpful assistance and discussion.

To Professor M. Symons and Dr. A.R. Lyons for the use of the irradiation and E.S.R. facilities of the Physical Chemistry Department of the University of Leicester.

To the authorities of the Polytechnic, Wolverhampton for their permission and assistance to carry out this work.

Finally I should like to thank my wife for her patience and encouragement throughout the course of this work.